CONTENTS

Regular contribution

ISSRNS 2016

13th International School and Symposium on Synchrotron Radiation in Natural Science

13-18 June 2016, Ustroń, Poland

Organized by Polish Synchrotron Radiation Society
in cooperation with Adam Mickiewicz University, Poznań, Poland

Advisory Board

- **Sine Larsen**, Department of Chemistry, University of Copenhagen, Denmark
- **Mariusz Jaskólski**, Center for Biocrystallographic Research, Polish Academy of Sciences, Poznań, Poland
- **Dmitri I. Svergun**, EMBL-Outstation c/o DESY Hamburg, Germany
- **Marek Stankiewicz**, NCPS Solaris, Jagiellonian University, Kraków, Poland
- **John R. Helliwell**, School of Chemistry, University of Manchester, UK
- **Andrea Di Cicco**, School of Science and Technology, University of Camerino, Italy
- **Federico Boscherini**, Department of Physics and Astronomy, University of Bologna, Italy
- **Christoph Quitmann**, MAX IV Laboratory, Lund University, Sweden
- **Andrzej Joachimiak**, Structural Biology Center & Midwest Center for Structural Genomics Biosciences Division, Argonne National Laboratory, Argonne, IL, USA
- **Krystyna Jablonska**, Institute of Physics, Polish Academy of Sciences, Warszawa, Poland

Organizing Committee

- **Maciej Kozak** (Chairman) - Adam Mickiewicz University, Poznań, Poland
- **Wojciech Kwiatek** (Treasurer) - Institute of Nuclear Physics, Polish Academy of Sciences, Kraków, Poland
- **Paweł Piszora** (Co-Chairman, Editor) - Adam Mickiewicz University, Poznań, Poland
- **Damian Paliwoda** (Editor) - ESRF, Grenoble, France
- **Zuzanna Pietralik** - Adam Mickiewicz University, Poznań, Poland
- **Michał Taube** - Adam Mickiewicz University, Poznań, Poland
- **Żaneta Kołodziejska** - Adam Mickiewicz University, Poznań, Poland
- **Maciej Gielnik** - Adam Mickiewicz University, Poznań, Poland
- **Weronika Andrzejewska** - Adam Mickiewicz University, Poznań, Poland
- **Michalina Skupin** - Adam Mickiewicz University, Poznań, Poland
- **Julia Jakubowska-Ludwiczak** - Adam Mickiewicz University, Poznań, Poland
- **Jolanta Darul** - Adam Mickiewicz University, Poznań, Poland

SPONSORS:

Ministry of Science and Higher Education
Republic of Poland

PREVAC

UAM
Adam Mickiewicz University in Poznań

MeasLine

SPECS™

IRtech®

ABL&E-JASCO® Polska Sp. z o.o.

Welcome to the 13th International School and Symposium on Synchrotron Radiation in Natural Science

On behalf of the Organizing Committee and International Scientific Advisory Committee we are pleased to welcome you to the 13th International School and Symposium on Synchrotron Radiation in Natural Science (ISSRNS 2016) organized by the Polish Synchrotron Radiation Society (PTPS) in cooperation with the A. Mickiewicz University in Poznań in Ustroń-Jaszowiec (Poland). The aim of this interdisciplinary meeting, organized as a biennial event from 1992, is to bring together scientists and students working with synchrotron radiation and new comers interested in using SR based techniques.

This year we celebrating 25th anniversary of Polish Synchrotron Radiation Society therefore our conference is organized in GWAREK hotel (Ustroń-Jaszowiec), in the place, where the first ISSRNS meeting took place in 1992. This beautiful place is located in Silesian Beskids mountain range (Beskidy mountains, southern part of Poland), and is an excellent place for sports and recreation activities. Since the first conference, ISSRNS is a traditional forum for presentation and discussion of recent developments in the field of the synchrotron radiation instrumentation and applications of SR in fundamental research as well as material studies and life sciences. The topics of ISSRNS 2016 cover main areas of applications of synchrotron radiation:

- X-ray diffraction studies of materials at extreme conditions,
- in situ synchrotron studies of materials,
- scattering techniques in structural analysis of new materials and biological macromolecules,
- X-ray imaging, nanoimaging and nanotomography,
- macromolecular crystallography of complex systems,
- design and development of instrumentation for synchrotrons and free electron lasers,
- applications of X-ray fluorescence, X-ray absorption, and photoelectron spectroscopies in material science and biophysics,
- X-ray magnetic dichroism,
- other applications of synchrotron radiation in nanosciences and soft matter physics.

We would like to thank all lecturers for accepting our invitations to show the results of their exciting studies. We also thank all the participants for preparing oral and poster presentations. We wish you fruitful and stimulating conference.

Organizers

PROGRAMME

Monday, 13 June 2016

14^{00}-19^{00}	Registration and Reception		
15^{00}-15^{10}	Opening Address		
15^{10}-15^{50}	L-01	Mariusz Jaskólski	Crystal pathologies in macromolecular crystallography, their detection and handling
15^{50}-16^{30}	L-02	Anders Mikkelsen	Synchrotron based imaging and spectroscopy of nanostructures for electronics and photonics – growth, geometry and function
16^{30}-17^{00}	Coffee Break		
17^{00}-17^{40}	L-03	Armin Wagner	Long-wavelength macromolecular crystallography – MAD or SAD?
17^{40}-18^{20}	L-04	Christian Pettenkofer	Unusual observation of image potential states of nanosized Ag clusters, observed by direct photo emission
18^{20}-18^{40}	O-01	Witold Gospodarczyk	A role of microfluidic flow and gemini surfactants in amyloid aggregation of lysozyme and other proteins
19^{00}-	Barbecue		

Tuesday, 14 June 2016

8^{00}-9^{00}	Registration and Reception		
Session A			
9^{00}-9^{40}	L-05	Wojciech Roseker	Double pulse X-ray Photon Correlation spectroscopy using hard X-ray delay line
9^{40}-10^{00}	O-02	Malgorzata Sowinska	Atomic layer deposition of Al_2O_3 on $CH_3NH_3PbI_3$ for enhancement of perovskite solar cells stability
10^{00}-10^{20}	O-03	Marcin Sikora	Local structure of transition metal dopants into 3D topological insulators probed with angular dependent XAFS
10^{20}-10^{40}	O-04	Dieter Schmeisser	The Cu2p-edge of superconducting BiSrCu-Oxides studied by resonant Photoelectron Spectroscopy
10^{40}-11^{00}	O-05	Edyta Piskorska-Hommel	EXAFS and DAFS from particles of phase ω in β-Ti(Mo) single crystals
11^{00}-11^{40}	Coffee Break		
11^{40}-12^{20}	L-06	Marie-Emmanuelle Couprie	Towards compact short wavelength Free Electron Laser using laser plasma acceleration
12^{20}-12^{40}	O-06	Mesfin Ayele	Development and characterization of a compact laboratory laser-plasma soft X-ray source and its usage for contact microscopy
12^{40}-13^{00}	O-07	Alfio Torrisi	Development of EUV and SXR nanoscale imaging systems based on double stream gas puff target sources
Session B			
9^{00}-9^{40}	L-07	Andrei V. Petukhov	Structure and long-range-order in colloidal self-assembly
9^{40}-10^{20}	L-08	Jan Dreiser	Molecular single-ion magnets: Harnessing molecule-surface interactions

10^{20}-11^{00}	L-09	Jung Ho Je	Ultrafast/nanoscale dynamics studied by X-ray imaging
11^{00}-11^{40}	Coffee Break		
11^{40}-12^{20}	L-10	Czesław Kapusta	Study of oxide materials for energy applications with X-ray spectroscopies
12^{20}-12^{40}	O-08	Joanna Kowalska	Fe X-ray Absorption and X-ray Magnetic Circular Dichroism Studies on FeMo cofactor of Nitrogenase and Related Models
12^{40}-13^{00}	O-09	Iwanna Jacyna	Synchrotron radiation studies of ultrathin Pt/Co/Pt trilayers irradiated by nanosecond pulses from EUV plasma
13^{00}-14^{20}	Lunch		
15^{00} - 19^{00}	Excursion		
19^{00}-20^{00}	Dinner		

Wednesday, 15 June 2016

Session A

9^{00}-9^{40}	L-11	Andrzej Joachimiak	Structural Biology Using Light Sources Helps Combat Infectious Diseases and Antibiotic Resistance
9^{40}-10^{20}	L-12	Banaszak Michal	Monte Carlo structure factors for self-assembling polymers
10^{20}-10^{40}	O-10	Tomasz Wasowicz	Photo-induced fragmentation of biomolecules in the gas phase
10^{40}-11^{00}	O-11	Monika Basiura-Cembala	Polyamide 6 – the trouble with crystal polymorphism
11^{00}-11^{40}	Coffee Break		
11^{40}-12^{20}	L-13	Wojciech Rypniewski	Structural studies of chitinases from extremophiles
12^{20}-12^{40}	O-12	Joanna Czapla-Masztafiak	DNA UV-damage investigated by X-ray spectroscopy
12^{40}-13^{00}	O-13	Anna Wolska	XAFS study on the ultrathin Pt/Co/Pt trilayers modified with short light pulses

Session B

9^{00}-9^{40}	L-14	Marcin Klepka	Structural studies of bioactive metalo-organic ligand complexes using XAFS
9^{40}-10^{20}	L-15	Grochulski Pawel	Review of biological application facilities at the Canadian Light Source
10^{20}-10^{40}	O-14	Michał Taube	Structural studies of *Pseudomonas syringae* effector protein HOPQ1 and its complex with plant 14-3-3 protein
10^{40}-11^{00}	O-15	Jakub Szlachetko	Establishing nonlinearity thresholds with ultraintense X-ray pulses
11^{00}-11^{40}	Coffee Break		
11^{40}-12^{20}	L-16	Marcello Coreno	Photoionization of atoms molecules and clusters with novel XUV light sources

12^{20}-12^{40}	O-16	Ismail Saber	Study of photoionized plasmas emission spectra of atomic and molecular gases excited by intense EUV pulses
12^{40}-13^{00}	O-17	Matthias Girod	CERIC-ERIC, the new multi-technique research infrastructure for materials research in Central-Eastern Europe
13^{00}-14^{20}	Lunch		
15^{00}-15^{40}	L-17	Hiromitsu Tomizawa	Status of the petawatt-class twin optical laser facility for the synergy experiments with XFEL (SACLA)
15^{40}-16^{20}	L-18	Wojciech Gawelda	Scientific opportunities and challenges for time-resolved studies using X-ray Free Electron Lasers
16^{20}-16^{40}	O-18	Sergio Rodrigues	Latest developments in laboratory SAXS/WAXS instruments
16^{40}-17^{00}	O-19	Violeta Simic-Milosevic	New developments in Near Ambient Pressure XPS –EnviroESCA, Small Spot and Imaging NAP-XPS Solutions
17^{00}-17^{15}	Coffee Break		
17^{15}-19^{00}	General Assembly of the Polish Synchrotron Radiation Society		
19^{00}-20^{00}	Dinner		
20^{00}- …	Poster Session		

Thursday, 16 June 2016

9^{00}-9^{40}	L-19	Thomas Tschentscher	Preparing for first science experiments at European XFEL
9^{40}-10^{20}	L-20	Yoshiharu Sakurai	Understanding a lithium ion battery using high-energy synchrotron X-rays
10^{20}-11^{00}	L-21	Christopher Chantler	The Hybrid XAS technique for dilute [1-10 mM] solutions at high accuracy
11^{00}-11^{40}	Coffee Break		
11^{40}-12^{20}	L-22	Koichi Matsuo	New developments in the structure analysis of biomolecules using synchrotron-radiation vacuum-ultraviolet circular dichroism
12^{20}-13^{00}	L-23	Miguel Ángel García Aranda	Applied crystallography at ALBA synchrotron
13^{00}-14^{20}	Lunch		
14^{20}-19^{00}	Conference Excursion		
19^{00}-22^{00}	Conference Dinner		

Friday, 17 June 2016

9^{00}-9^{40}	L-24	Manfred Rößle	High Brilliance SAXS on synchrotrons
9^{40}-10^{20}	L-25	Tobias Madl	Integration of SAXS with Complementary Techniques for Structural Characterization of Large Biomolecular Complexes
10^{20}-11^{00}	L-26	Augusto Marcelli	Mineral dust iron geochemistry of the last 160 kyears

11^{00}-11^{40}	Coffee Break		
11^{40}-12^{20}	L-27	Adriana Wawrzyniak	Solaris as a new class of low energy high brightness light source
12^{20}-12^{40}	O-20	Marcin Zając	The status of the PEEM/XAS beamline at Solaris
12^{40}-13^{00}	O-21	Karolina Szamota-Leandersson	Commissioning of ARPES beamline at the Polish National Synchrotron Solaris
13^{00}-14^{20}	Lunch		
15^{00}-15^{40}	L-28	Andrew Beale	Chemical imaging of functional materials under process conditions
15^{40}-16^{20}	L-29	Davide Ferri	Enhancing the sensitivity of X-ray based techniques by pulse experiments
16^{20}-16^{50}	Coffee Break		
16^{50}-17^{30}	L-30	Ewa Banachowicz	The protein structure by the combination of SAXS, light scattering and simulations
17^{30}-18^{10}	L-31	Bart Goderis	An in-situ synchrotron X-ray view on the crystallization of synthetic polymers for 3D printing under Fast Scanning Calorimetry conditions
18^{10}-18^{30}	O-22	Wojciech Błachucki	Self-absorption free HEROS method applied to a time-resolved study following oxidation of single site Ta catalysts
18^{30}-18^{50}	O-23	Michał Nowakowski	Determination of electronic structure of iron compounds using resonant X-ray emission spectroscopy
19^{00}-20^{00}	Dinner		

Saturday, 18 June 2016

9^{00}-9^{40}	L-32	Angela Trapananti	Investigating the structure of liquid metals at extreme conditions by X-ray absorption spectroscopy
9^{40}-10^{20}	L-33	Michael Hanfland	Crystallography at high pressures using synchrotron radiation
10^{20}-10^{40}	O-24	Joanna Stępień	Local atomic structure evolution around dopant ions in YSZ+Mn solid solution
10^{40}-11^{00}	Coffee Break		
11^{00}-11^{30}	Closing Remarks		
12^{00}-13^{00}	Lunch		
13^{00}-14^{00}	Return to……		

L-01 **Monday, 13.06., 15^{10} - 15^{50}**

Crystal pathologies in macromolecular crystallography, their detection and handling

M. Jaskolski[1]* and Z. Dauter[2]

[1] *Center for Biocrystallographic Research, Institute of Bioorganic Chemistry, Polish Academy of Sciences and Department of Crystallography, Faculty of Chemistry, A. Mickiewicz University, Poznan, Poland*
[2] *Macromolecular Crystallography Laboratory, National Cancer Institute, Argonne National Laboratory, Argonne IL, USA*

Keywords: pseudosymmetry, non-crystallographic symmetry (NCS), translational NCS, crystal twinning, merohedry, lattice-translocation defects, order-disorder twinning, OD-twinning, aperiodic crystals, superstructure, modulated structure, commensurate modulation, incommensurate modulation, quasicrystals, diffraction anisotropy, diffuse scattering, mosaicity

*e-mail: mariuszj@amu.edu.pl

Crystals formed by macromolecules, such as proteins or nucleic acids, contain a huge volume fraction (20-90%) of water, which envelopes the macromolecules in an ordered hydration shell, to become totally disordered as bulk solvent farther away. The macromolecules form, therefore, only sporadic, weak direct contacts and the degree of crystalline order is often less than perfect. Apart from typical physical defects and rather trivial poor quality/habit/growth or mosaicity problems, macromolecular crystals can also suffer from several kinds of pathologies, in which everything seems to be perfect, except that from the structural point of view the interpretation may be very difficult or even impossible. For some time it was believed that certain types of pathologies are not found in macromolecular crystals and, when encountered, such cases were discarded as rare curiosities. Today we have to admit that such pathologies are actually quite common. The simplest case is pseudosymmetry, or non-crystallographic symmetry (NCS), when two or more molecules are related locally by some kind of symmetry transformation, which is not propagated further. Translational NCS (tNCS) is particularly nasty as it leads to a strong bias of reflection intensity distribution and makes molecular replacement very difficult. Lattice-translocation defects, also called order-disorder twinning (OD-twinning), occur when molecules are packed regularly in layers but the layers are stacked (without rotation) in two or more discrete modes, with a unique translocation vector. When solved, such a structure will consist of two (or more) shifted, possibly overlapping, identical models. Crystal twinning arises when small crystallites, called twin domains, have different orientation dictated by a symmetry operation that is not part of the space group symmetry of the crystal structure. When the extra symmetry belongs to the same crystal system, the alignment of the twin domains, and of the overlapping reflections, is perfect and this case is termed merohedry. Pseudomerohedral twins arise when a low-symmetry unit cell has parameters with higher metric symmetry (e.g. the monoclinic angle β=90°). When the twin domains adopt two orientations the twinning is hemihedral, when four - tetartohedral, eight - ogdohedral. The separate twin domains scatter X-rays independently (incoherently) and therefore twin detection is based on intensity data statistics. The tests are complicated by the fact that some other pathologies (e.g. tNCS) have the opposite effect on intensity statistics. There are also crystals in which the periodic (lattice) order is broken or absent. When strict short-range translational order from one unit cell to the next is lost but the long-range order is restored by a periodic Atomic Modulation Function (AMF), we have a modulated crystal structure. If the period of AMF runs over an integral number of unit cells, the modulation is commensurate and can be interpreted as a case of tNCS. Otherwise the modulation is incommensurate and such a structure is very difficult to solve, refine and interpret. In quasicrystals, the periodic order in 3D space is lost completely and the diffraction pattern, which is still discrete, cannot be even indexed using three *hkl* indices. Among the presented cases only the fully aperiodic quasicrystals have not been reported yet for macromolecules. But this may be only a matter of time.

L-02 **Monday, 13.06., 15^{50} - 16^{30}**

Synchrotron based imaging and spectroscopy of nanostructures for electronics and photonics – growth, geometry and function

A. Mikkelsen[1]*

[1] *Department of Physics and NanoLund, Lund University, Professorgatan 1, 22362 Lund, Sweden*

Keywords: synchrotron radiation, spectromicroscopy, nanostructures, electronics, photonics

*e-mail: anders.mikkelsen@sljus.lu.se

Already today, the circuits in the chips driving our computers and mobile devices have reached the nanoscale. This development is only accelerating, and in the future nanoscale electronic and photonic components will be ubiquitous in consumer electronics, renewable energy devices, energy storage, LEDs and much more. Synchrotron based techniques are playing a significant role in the development of future electronics as it is possible to directly investigate many aspects of device growth, operation and structure that is not available by laboratory based techniques.

In this presentation three prominent examples will be given demonstrating the use of different synchrotron based techniques, often in combination with complementary lab based methods. All these methods will be available at the highest level at the next generation synchrotron [1] MAX IV currently under construction in Lund (inauguration 21st of June 2016), which will also briefly be introduced.

Firstly we present studies of free-standing III-V nanowires. These have the potential to become central components in future electronics and photonics with applications in IT, life-science and energy[2]. The atomic scale structure and morphology of semiconductor nanowire surfaces are central in determining both growth and function of the wires [3]. Using synchrotron based Spectroscopic Photo Emission and Low Energy Electron Microscopy (SPELEEM) we have characterized III-V nanowire surface chemistry and electronic properties, investigated ultra-thin dielectrics, native oxides and epitaxial shells [4-6]. Combining this with several types of Scanning Probe Microscopy a complete picture of surface chemistry, effects on bandbending and information on axial and radial doping is obtained [3,7-11]. We demonstrate a complete control of their surface chemistry and structure to the atomic scale can be obtained. We show how full III-V nanowire devices can be imaged in SPELEEM – the devices are specially designed to avoid image distortions and to enable display of clean surfaces.

Secondly we will discuss dynamic studies of surface chemistry and dynamics using SPELEEM and ambient pressure X-ray Photoelectron Spectroscopy (AP-XPS). Using *in situ* SPELEEM performed in real time, we explore the dynamics of micron-sized Ga self-propelled droplets on GaP(111). The motion of these droplets can be further manipulated using Au nanoparticles. We establish the equations of motion that can generally describe the Ga droplet dynamics and demonstrate how several nanoscale and atomic scale mechanisms act together to control the motion of the droplets [12,13]. We then go on to show how the chemistry of technologically important processes such as Atomic Layer Deposition (ALD) of HfO_2 can be directly investigated using AP-XPS. This gives us new insights into the growth processes and demonstrate that the simple picture of the ALD growth is not quite true when the process can be explored while it is happening.

Thirdly, we discuss nanofocused hard X-ray beams as nondestructive probes that uniquely allow direct measurements of the nanoscale strain distribution and composition inside the micrometer thick layered structures found in many electronic device architectures. While the method has generally been considered time consuming, we demonstrate that by special design of X-ray nanobeam diffraction experiment we can (in a single 2D scan with no sample rotation) measure the individual strain and composition profiles of many structures in an array of upright standing nanowires [14]. Additionally the use of the coherence of the X-ray beam allows for considerable gains in resolution without tightly focusing the X-ray beam. In the present case, we image complex nanowires for nanoLED fabrication and compare to theoretical simulations [14,15]. We then go on to discuss the use of the new highly coherent synchrotrons such as MAX IV for microscopy [16].

---

[1] *Ultimate upgrade for US synchrotron*, *Nature* **501** (2013) 148.
[2] E. Lind *et al.*, *IEEE J. El. Dev. Soc.* **3** (2015) 96; J. Wallentin *et al.*, *Science* **339** (2013) 1057; B. Monemar *et al*, *Semiconductors and Semimetals* (Elsevier), Vol **94**, Chapter 7.
[3] A. Mikkelsen, E. Lundgren, Surface Science **607** (2013) 97-105.
[4] R. Timm *et al.*, *Appl. Phys. Lett.* **99** (2011) 222907.
[5] R. Timm *el al.*, *Microelectron. Eng.* **88** (2011) 1091.
[6] M. Hjort *et al*, *Appl. Phys. Lett.* **99** (2011) 233113.
[7] M. Hjort *et al*, *ACS Nano* **6** (2012) 9679.
[8] E. Hilner *et al.*, *Nano Lett.* **8** (2008) 3978.
[9] M. Hjort *et al.*, *Nano Lett.* **13** (2013) 4492.
[10] M. Hjort *et al.*, *ACS Nano* **8** (2014) 12346.
[11] J. L. Webb *et al.*, *Nano Lett.* **15** (2015) 4865.
[12] E. Hilner *et al.*, *Nano Lett.* **9** (2009) 2710.
[13] A.A. Zakharov *et al.*, *ACS Nano* **9** (2015) 5422.
[14] T. Stankevic *et al.*, *ACS Nano* **9** (2015) 6978.
[15] T. Stankevic *et al.*, *Appl. Phys. Lett.* **107** (2015) 103101.
[16] U. Johansson, U. Vogt, A. Mikkelsen, Proc. SPIE 8851, X-Ray Nanoimaging: Instruments and Methods, 88510L (September 26, 2013); doi:10.1117/12.2026609.

L-03 **Monday, 13.06., 17^{00} - 17^{40}**

Long-wavelength macromolecular crystallography – MAD or SAD?

A. Wagner [1*], O. Aurelius[1], R. Duman[1], K. el Omari[1] and V. Mykhaylyk[1]

[1]*Diamond Light Source, Harwell Science and Innovation Campus, Didcot OX11 0DE, United Kingdom*

Keywords: macromolecular crystallography, experimental phasing

*e-mail: armin.wagner@diamond.ac.uk

Over the past years technical developments such as single-photon counting detectors and improved stability from synchrotron sources and Beamline equipment have led to an increased number of protein and nucleic acid structures being solved by experimental phasing techniques at longer wavelengths around λ = 2 Å [1]. Single wavelength anomalous diffraction (SAD) utilizes therein the increase of the anomalous signal from sulphur or phosphorus towards their K absorption edges which are around 5 Å and 6 Å, respectively. Solving the crystallographic phase problem directly in the absence of a know protein model similar to the one under investigation and without additional labelling of the protein or nucleic acid has the potential to become the method of choice for phasing macromolecular crystals.

At Diamond Light Source, over the past years, the long-wavelength MX Beamline I23 [2] has been designed, constructed and is currently being commissioned. The Beamline differs radically from the existing well developed and established MX beamlines. To eliminate air absorption, the complete Beamline is operated in vacuum, including the sample environment and the detector.

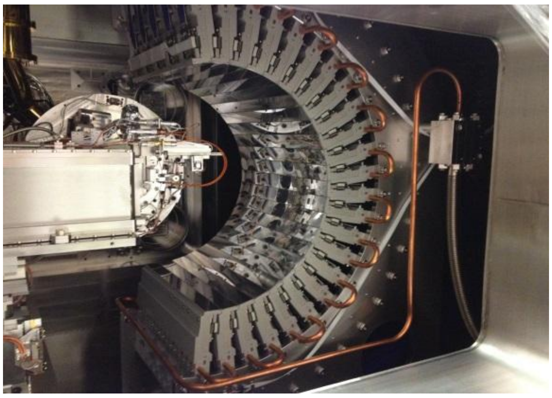

Figure 1: Pilatus 12M detector in I23 vacuum vessel.

Several technical issues had to be addressed, leading to a variety of pioneering new developments, like the large in-vacuum semi-cylindrical Pilatus 12M detector (Fig.1) and the dedicated kappa goniometer. The Beamline covers a wavelength range from 1.1 to 5.9 Å (2.1 – 11.5 keV) which allows accessing several K absorption edges of biological relevance like phosphorus, sulphur, chlorine, potassium and calcium, elusive on other MX beamlines. Apart from experimental phasing experiments, anomalous contrast can be used to identify and distinguish these light atoms in the electron density and use their positions to help model building at low resolution.

First data has been successfully collected and several structures have been solved using SAD phasing based on phasing information from phosphorus, sulphur and calcium. At the moment the data quality at wavelengths larger than 3.1 Å is affected by the increased sample absorption and most of the experiments have been performed around this wavelength with an anomalous signal approximately twice as high as at 2 Å. Significant amount of work will be needed to correct for the absorption effects to obtain data quality of similar quality as obtained at shorter wavelengths.

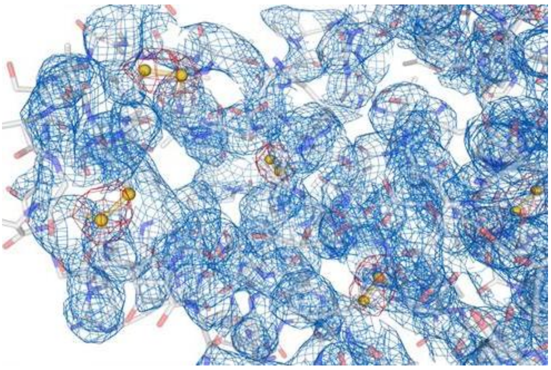

Figure 2: Electron density map (blue $2F_o$-F_c, 1 sigma) and anomalous difference Fourier map (red, 5 sigma). Thaumatin model (PDB code 4ZG3) superimposed.

Nevertheless, first data around the sulphur K-edge from the test protein thaumatin could be collected and processed with subsequent successful structure determination based on anomalous differences. Figure 2 shows the electron density map after experimental phasing from data collected at a wavelength of 4.96 Å (E = 2.5 keV) at a maximum resolution of 3.2 Å, limited by the size of the detector.

The presentation will focus on the underlying design ideas of the new long-wavelength in-vacuum Beamline, discuss first results and give an outlook on potential MAD experiments around the edges of sulphur and phosphorus.

---

[1] J. Rose, B.-C. Wang, M. Weiss, *IUCrJ* **2** (2015) 431.
[2] A. Wagner, R. Duman, K. Henderson. V. Mykhaylyk, *Acta Cryst.* D**72** (2016) 430.

L-04 **Monday, 13.06., 17^{40} - 18^{20}**

Unusual observation of image potential states of nanosized Ag clusters, observed by direct photo emission

C. Pettenkofer[1]*

[1]*Helmholtz-Zentrum Berlin, Albert-Einstein str 15,*
12489 Berlin, Germany

*e-mail: pettenkofer@helmholtz-berlin.de

Ag films are grown by Van der Waals epitaxy on cleaved WSe_2 (0001) surfaces. For low coverage the growth mode is Volmer-Weber type leading to (111) oriented islands as demonstrated by LEED. Islands of about 70 nm diameter for a nominal 3 Å film grow in registry with the substrate. For p-type substrates a surface photovoltage is generated at the Schotky barrier between substrate and film, which can be easily followed by the position of the Schockley type surface state S1 of the Ag(111) surface exposed to vacuum. For low photon energies an emission out of image potential states belonging to the Ag(111) surface are observed directly in normal photoemission: These emissions are lost for thicker films when a continously closed film is prepared. Normally image state emissions are only observed by inverse photoemission or two photon photo emission experiments. Here the emission is explained by a roughness induced lowering of the potential barrier at the sides of the clusters leading to a direct photoemission below the nominal workfunction of the (111) surface.

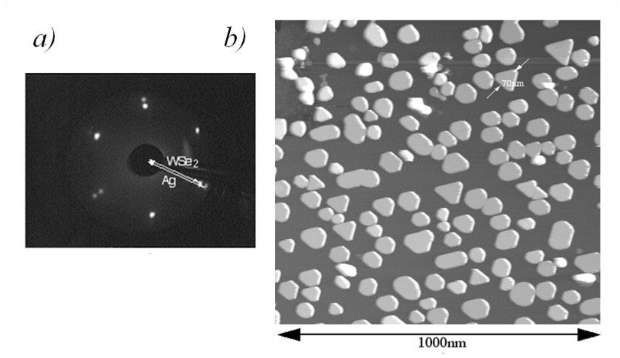

Figure 1: a) LEED pattern of 12 Å Ag on WSe_2, 66 eV; b) STM image of 10 Å Ag on WSe_2.

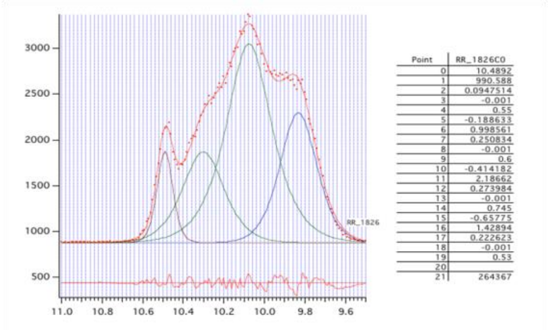

Point	RR_1826C0
0	10.4892
1	990.588
2	0.0947514
3	-0.001
4	0.55
5	-0.188633
6	0.998561
7	0.250834
8	-0.001
9	0.6
10	-0.414182
11	2.18662
12	0.273984
13	-0.001
14	0.745
15	-0.65775
16	1.42894
17	0.222623
18	-0.001
19	0.53
20	
21	264367

Figure 2: Spectrum taken with 4.6 eV E_{phot} for 6 Å Ag film.

L-05 **Session A, Tuesday, 14.06., 9^{00} - 9^{40}**

Double pulse X-ray Photon Correlation Spectroscopy using hard X-ray delay line

W. Roseker[1]*, S. Hruszkewycz[2], R. Rysov[1],
F. Lehmkühler[1,3], S. Lee[4], M.Walther[1], T. Osaka[5],
P.H. Fuoss[2], G. B. Stephenson[2], M. Sikorski[6], S. Song[6],
A. Robert[6] and G. Grübel[1,3]

[1]*Deutsches Elektronen-Synchrotron (DESY), Notkestr 85,*
22607 Hamburg, Germany
[2]*Materials Science Division, Argonne National Laboratory,*
Argonne, Illinois 60439, USA
[3]*The Hamburg Centre for Ultrafast Imaging, Hamburg,*
Germany
[4]*Korea Research Institute of Standards and Science, Daejeon*
305-340, Rep. of Korea
[5]*Theory Team, Beamline Research and Development Group,*
XFEL Research and Development Division, RIKEN SPring-8
Center
1-1-1 Kouto, Sayo-cho, Sayo-gun, Hyogo 679-5148, Japan
[6]*SLAC National Accelerator Laboratory, 2575 Sand Hill Road,*
Menlo Park, CA 94025, USA.

Keywords: hard x-ray delayline, free-electron laser, coherence

*e-mail: wojciech.roseker@desy.de

The conventional X-ray Photon Correlation Spectroscopy (XPCS) [1] technique at 3rd generation synchrotron sources is routinely probing nanoscale dynamics of condensed matter systems (e.g. capillary wave flucutations, magnetic domain fluctuations, rheological properties of soft matter, dynamics in glass-forming systems) at time scales between milliseconds to hours. X-ray Free Electron Lasers (XFEL) based on Self Amplified Spontaneous Emission (SASE) deliver ultra-fast and spatially highly coherent hard X-ray radiation with extreme peak brightness

($\approx 10^{12}$ photons in a single pulse) making it an ideal probe for studying atomic-scale dynamics in various condensed matter systems whose characteristic times can be considerably shorter than time resolutions provided at storage rings (≈100 ps). At the existing X-ray FEL sources, the time resolution of XPCS measurements is defined by the repetition rates of the X-ray pulses to few milliseconds. Moreover due to severe fluctuations in intensity and position of the FEL pulses [2], it is difficult to obtain proper photon correlation between successive scattering signals. In principle, these obstacles can be overcome by employing the "split-delay" approach i.e using hard X-ray delaylines [3].

Here, we report on successful implementation of the hard X-ray delayline [4,5] at the Linac Coherent Light Source. The device is capable of providing two X-ray pulses with controllable time delays ranging from a few femtoseconds to nanoseconds, which is sufficient for probing ultrafast phenomena in versatile choices of condensed matter systems. The measured throughput of the device within 1.47×10^{-5} energy bandwidth of the exit beam at 7.9 keV is 30% [5]. The X-ray FEL pulses after the X-ray delayline are used to generate high (69%) contrast speckle patterns from nanoparticles (as shown in Figure 1), which is only possible due to the well-preserved transverse coherence. Measuring intensity fluctuations also reveals that only a single or double temporal modes remain in the beam, indicating the delivery of near Fourier transform limited pulses. We also successfully performed a proof of principle Split Pulse XPCS experiment on a model system of small (R = 1 nm) gold nanoparticles dispersed in hexane solvent with hard x-rays and obtained the first time autocorrelation function in the ns time domain.

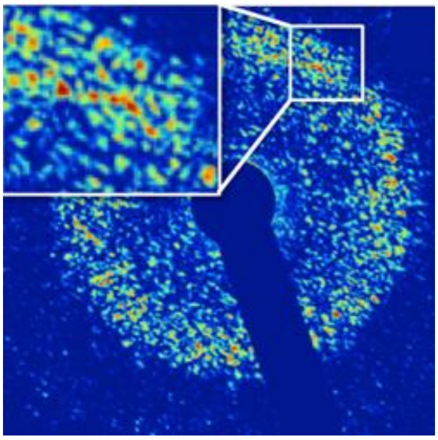

Figure 1. Typical pattern showing randomly oriented speckles.

Acknowledgments: We thank the Hamburg Centre for Ultrafast Imaging (CUI) for financial support. The Linac Coherent Light Source (LCLS) at SLAC National Accelerator Laboratory, is an Office of Science User Facility operated for the U.S. Department of Energy Office of Science by Stanford University. S. Lee was supported by the Converging Research Center Program through the Ministry of Science, ICT and Future Planning, South Korea (NRF-2014M3C1A8048818, NRF-2014M1A7A1A01030128).

[1] G. Grübel, F.Zontone, *J. Alloys. Compd.* **362** (2004) 3.

[2] F. Lehmkuehler, P. Kwasniewski, W. Roseker, B. Fischer, M. A. Schroer, K. Tono, T. Katayama, M. Sprung, M. Sikorski, S. Song, J. Glownia, M. Chollet, S. Nelson, A. Robert, C. Gutt, M. Yabashi, T. Ishikawa, G. Grübel, *Sci. Rep.* (2015) 5.

[3] W. Roseker, H. Franz, H. Schulte-Schrepping, A. Ehnes, O. Leupold, F. Zontone, A. Robert, G. Grübel, *Opt. Lett.* **34** (2009) 1768.

[4] W. Roseker, H. Franz, H. Schulte-Schrepping, A. Ehnes, O. Leupold, F. Zontone, S. Lee, A. Robert, G. Grübel, *J. Synchrotr. Rad.* **18** (2011) 481.

[5] W. Roseker *et al.*, *Proc. SPIE* 8504, X-Ray Free-Electron Lasers: Beam Diagnostics, Beamline Instrumentation and Applications, 85040I (2012).

L-06 **Session A, Tuesday, 14.06., 11^{40} - 12^{20}**

Towards compact short wavelength Free Electron Laser using laser plasma acceleration

M. E. Couprie[1]*

[1] *Synchrotron SOLEIL, Saint-Aubin, 91 192 Gif-sur-Yvette France*

Keywords: free-electron laser, laser wakefield acceleration, undulator

*e-mail: couprie@synchrotron-soleil.fr

More than 50 years after the lasers discovery [1] and more than 30 years after the first Free Electron Laser (FEL) using relativistic electrons in a periodic magnetic field as a gain medium [2], the advent of X-ray free elctrons lasers open new paths for investigation of matter for imaging, ultra-short phenomena for example. The emergence of the femtosecond, high power (typically GW), peak and average brilliance, tunable X-ray FELs constitutes a major scientific revolution, after the one brought by the laser invention. FEL user facilities (FLASH [3], FERMI@ELETTRA in the seeded configure tion [4], LCLS [5] and SACLA [6] in the hard X-ray) enable to harvest new scientific results in unexplored scientific areas. Present X-ray FEL are usually built on linear accelerators of high beam quality, delivering nC charge, with 0.01 % energy spread and 1 µm.rad emittance.

While additional X-ray FEL centers are under construction, new directions are also taken, such as operation at high repetition with multiplexed FEL beamlines with FELs relying on superconducting linear accelerators, advanced seeding, and compactness in considering reducing the size of each constituting components. Besides advanced seeding schemes [7] and compact undulators [8]. Besides, one also considers replacing the conventional linear accelerator by a compact one system relying on an alternative concept, such as dielectric acceleration, inverse FEL and Laser Plasma Acceleration (LPA) [9]. In LPA, a short multi-TW laser pulse in focus in a gas jet (cell, capillary) and drives strong plasma waves in its wake [10, 11] which can drive the electron acceleration to GeV on a mm scale. Synchrotron radiation has been already observed with LPA [12-15]. But the present electron divergence (1 mrad) and energy spread (of the order of 1 %) does not match the present performance of conventional linear accelerators used for short wavelength FELs. In consequence, an adequate beam manipulation through the transport to the undulator is needed for FEL amplification. One first strategy is to use a demixing chicane to sort out the electrons in energy and reduce the slice energy spread by typically one order of magnitude [16, 17]. One can even take advantage of this introduced correlation to focus the electron slices in synchronization with the progress of the optical wave in the undulator for higher effective electronic density [18, 19] in the so-called chromatic matching scheme. An alternative strategy is to use a transverse gradient undulator [20].

Tests experiments will be reviewed, such as the COXINEL one [21].

Acknowledgments: This work is supported by the COXINEL ERC Grant.

---

[1] A. L. Schawlow, C. H. Townes, *Phys. Rev.* **112** (1958) 1940.
[2] D.A.G. Deacon *et al., Phys. Rev. Lett.* **38** (1977) 892.
[3] W. Ackermann *et al., Nature Photonics* **1** (2007) 336.
[4] E. Allaria *et al., N. Jour. Phys.* **14** (2012) 113009.
[5] P. Emma *et al., Nature Photonics* **4** (2010) 641.
[6] T. Ishikawa *et al., Nature Photonics* **6** (2012) 540.
[7] G. Lambert *et al., Nature Physics* **4** (2008) 296.
[8] M. E. Couprie *et al.*, Cryogenic undulators, Proceeding SPIE, Prague, April (2015)
[9] T. Tajima *et al., Phys. Rev. Lett.* **43** (1979) 267.
[10] E. Esarey, C. Schroeder, W. Leemans, *Reviews of Modern Physics*, **81** (3) (2009) 1229, 2009.
[11] V. Malka, J. Faure, C. Rechatin, A. Ben-Ismail, J. Lim, X. Davoine, and E. Lefebvre, *Physics of Plasmas* **16** (5) (2009)056703.
[12] H.-P. Schlenvoigtet *et al., Nature Physics* **4** (2008) 130.
[13] M. Fuchs *et al., Nature Physics* **5** (2009) 826.
[14] G. Lambert *et al*, Proced. FEL conf., Nara, Japan, Aug. 2012
[15] M. P. Anania *et al., Appl. Phys. Lett.* **104** (2014) 264102.
[16] A. Maier, A. Meseck, S. Reiche, C. Schroeder, T. Seggebrock, F. Gruener, *Physical Review X*, **2** (3) (2012) 031019.
[17] M. E. Couprie, A. Loulergue, M. Labat, R. Léhé, V. Malka, *J. Physics B : At., Mol. Opt. Phys.* **47**, 234001.
[18] A. Loulergue, M. Labat, C. Benabderrahmane, V. Malka, M. E. Couprie, *New J. Phys.* **17** (2015) 023028.
[19] M. Khojoyan, F .Briquez, M. Labat, A. Loulergue, O. Marcouillé, F. Marteau, G. Sharma, M. Couprie, "Transport studies of LPA electron beam towards the fel amplification at COXINEL," Nuclear Instruments and Methods in Physics Research Section A: Accelerators, Spectrometers, Detectors and Associated Equipment, 2016.
[20] Z. Huang *et al., Phys. Rev. Lett.* **109** (2012) 204801.
[21] M. Couprie, M. Labat, C. Evain, F. Marteau, F. Briquez, M. Khojoyan, C. Benabderrahmane, L. Chapuis, N. Hubert, C. Bourassin-Bouchet, *et al., Plasma Physics and Controlled Fusion* **58** (2016) 034020.

L-07 **Session B, Tuesday, 14.06., 9^{00} - 9^{40}**

Structure and long-range-order in colloidal self-assembly

A. V. Petukhov[1;2]*

[1] *van 't Hoff laboratory for physical and colloid chemistry, Debye Institute for nanomaterials science, Utrecht University, the Netherlands*
[2] *Laboratory of physical chemistry, Eindhoven University of Technology, the Netherlands*

Keywords: self-assembly, colloidal crystals, SAXS, microradian resolution

*e-mail: a.v.petukhov@uu.nl

Colloids are able to self-assemle into various structures with periodicity on the scales ranging from nanometres to about a micron. They are widely recognized as an important model system to study nucleation phenomena in freezing, melting and solid-solid phase transitions, jamming and glass formation. In addition, colloidal crystals are attractive for multiple applications since they can be used as large-scale low-cost templates to fabricate novel materials with unique optical properties such as the full photonic bandgap, 'slow' photons and negative refraction, as well as materials for application in catalysis, biomaterials and sensorics.

Nowadays small-angle X-ray scattering (SAXS) is widely recognised as an indispensable structure characterisation tool at the mesoscopic scales. Recent developments of synchrotron sources and X-ray detectors provide a very fast and effective tool to study colloidal crystals and their real-time development. The high penetration power of X-rays makes SAXS applicable to almost all system types. In addition, the intrinsically low contrast of all materials for X-rays ensures, in the vast majority of cases, a high quality of the scattering data that is free of multiple scattering contributions. SAXS also gives access to a broad range of spatial scales from a nanometre to microns. Moreover, as will be discussed in more detail in the lecture, microradian resolution can be achieved using synchrotron sources and refractive optics [1]. This provides access to periodicities up to several microns. Moreover, positional correlations on distances up to submillimetre can be accessed from the width of diffraction peaks measured with microradian resolution.

The results will be illustrated by a number of examples. In particular, the structure of rhombic crystals spontaneously formed by cubic colloids with rounded corners will be discussed [2,3]. Another example will be the transition to a lower-symmetry body-centred tetragonal structure in a system of magnetic core-shell spherical colloids, which is induced by dipole-dipole interactions between colloids [4]. A short overview of some of our studies of lyotropic colloidal liquid crystals spontaneously formed by highly anisometric colloidal particles [5,6] will be given. Finally, in-situ studies of the self-ogranization of semiconductor quantum dots of different shape at a liquid interface [7-9] using grazing-incidence SAXS will be illustrated.

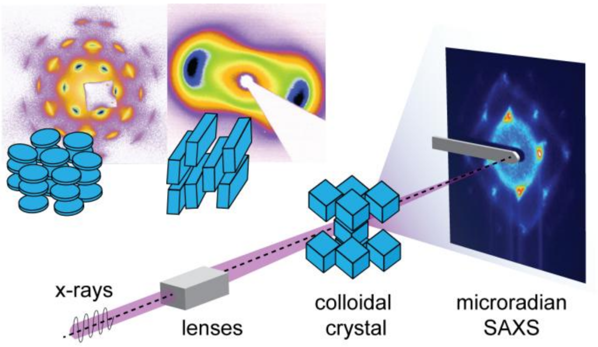

Figure 1. Schematic principle of microradian x-ray diffraction setup and examples of diffraction patterns measured in (from left to right) columnar crystals of colloidal gibbsite platelets, biaxial nematic phace of goethite boards, and crystals of hematite colloidal superballs (=cubes with rounded esges).

Acknowledgments: The author gratefully acknowledges crucial contributions of many colleagues, students and postdocs from Utrecht University, which cannot be all listed here. Synchrotron experiments are made possible thanks to support and developments by the personnel of the Dutch-Belgian beamline BM-26 DUBBLE and beamlines ID-10, ID-6, ID-2, and ID-1 of the European Synchrotron (ESRF) in Grenoble, France. This work was financially supported by the Netherlands Organization for Scientific Research (NWO). NWO and ESRF are acknowledged for for granting beamtime.

---

[1] A.V. Petukhov *et al.*, *Curr. Opin. Coll. & Interf. Sci*. **20** (2015) 272.
[2] J.-M. Meijer, PhD thesis, Utrecht University, 2015; J.-M. Meijer *et al.*, to be published.
[3] J.-M. Meijer *et al.*, *Soft Matter* **9** (2013) 10729.
[4] A. Pal *et al.*, *Angew. Chem. Int. Ed.* **54** (2015) 1803.
[5] A.V. Petukhov *et al.*, *Phys. Rev. Lett.* **95** (2005) 077801.
[6] E. van den Pol *et al.*, *Phys. Rev. Lett.* **103** (2009) 258301.
[7] F. Pietra *et al.*, *Nano Letters* **12** (2012) 5515.
[8] M.P. Boneschanscher *et al.*, *Science* **344** (2014) 1377.
[9] W. van der Stam *et al.*, *Nano Letters* **16** (2016) 2608.

L-08 **Session B, Tuesday, 14.06., 9^{40} - 10^{20}**

Molecular single-ion magnets: Harnessing molecule-surface interactions

J. Dreiser[1]*

[1]*Swiss Light Source, Paul Scherrer Institute, CH-5232 Villigen PSI, Switzerland*

Keywords: molecular magnets, surfaces, x-ray absorption spectroscopy, x-ray magnetic circular dichroism, scanning tunneling microscopy

*e-mail: jan.dreiser@psi.ch

Single-molecule magnets (SMMs) [1,2] are molecular complexes containing transition metal or lanthanide ions, which exhibit slow relaxation of their magnetization. SMMs and their mononuclear counterparts, molecular single-ion magnets (SIMs) [3,4] are attractive building blocks for potential molecular spintronics and quantum information processing devices. One route toward construction of such devices is the deposition of SMMs and SIMs on flat surfaces [4–6].

In this contribution I will show several examples of such molecule-inorganic hybrid structures studied by low-temperature, high-field x-ray magnetic circular dichroism (XMCD) as well as by scanning tunneling microscopy (STM). I will point out possible caveats that can occur when SMMs and SIMs are removed from their native molecular crystal environment and put into the hostile environment of an inorganic surface. I will highlight the importance of the molecule-surface interaction for the magnetic properties of the surface deposited molecules. Furthermore, I will demonstrate that by careful choice of the surface a significant improvement of the magnetic properties compared to the bulk molecular crystal can be achieved.

---

[1] D. Gatteschi, R. Sessoli, J. Villain, *Molecular Nanomagnets* (Oxford University Press, 2006).
[2] R. Sessoli, D. Gatteschi, A. Caneschi, M. A. Novak, *Nature* **365** (1993) 141.
[3] S.-D. Jiang, B.-W. Wang, S. Gao, *Molecular Nanomagnets and Related Phenomena* (Springer, Berlin, Heidelberg 2014), pp. 111–141.
[4] J. Dreiser, *J. Phys. Condens. Matter* **27** (2015) 183203.
[5] N. Domingo, E. Bellido, D. Ruiz-Molina, *Chem. Soc. Rev.* **41** (2011) 258.
[6] A. Cornia, M. Mannini, *Molecular Nanomagnets and Related Phenomena* (Springer, Berlin, Heidelberg 2014), pp. 293–330.

L-09 **Session B, Tuesday, 14.06., 10^{20} - 11^{00}**

Ultrafast/nanoscale dynamics studied by X-ray imaging

J. H. Je[1]*

[1]*Pohang University of Science and Technology,*
San 31 Hyoja-dong, Pohang 790-784, Korea

Keywords: X-ray imaging, interface dynamics

*e-mail: jhje@postech.ac.kr

Fluid/fluid flow is very commonly encountered in nature such as in rain drops, ink-jet printing, winds surrounding a hurricane or a tornado, whirlpools in the wake of boats, wetting, etc. The flow phenomena are important in understanding physical, chemical, and biological processes occurring at their interfaces. Despite recent advanced science and technology, the *visualization* of interface dynamics, which is an essential gateway to understanding the flow phenomena, is however a challenge because interface dynamics mostly happens in extreme conditions of ultrafast time domains (~μs) and/or nanoscale regimes in bulk systems.

Here we apply *phase contrast x-ray imaging* to visualize the *micro/nano and/or ultrafast* interface dynamics, especially, in '*drop impact*' and '*wetting'*. Phase contrast X-ray imaging in this study is mostly based on refraction enhanced phase contrast.

First, we discover that intense irradiation by hard X-rays decreases the effects of natural *surface tension* of water, as directly evidenced by phase contrast X-ray imaging [1]. A model based on ionization and surface charging explains this so far undetected phenomenon. This is an example of the largely unexplored effects that can be produced by extreme intense x-ray irradiation – an important issue due to current development of x-ray free-electron-lasers with unprecedented brilliance.

When a liquid drop impacts a solid surface, air is generally entrapped underneath. Using ultrafast phase-contrast x-ray imaging, we directly visualize the profile of an extracted air film and its evolution into a bubble during drop impact. We identify a complicated evolution process that consists of three stages: i) inertial retraction of the air film, ii) contraction of the top air surface into a bubble, and iii) pinch-off of a daughter droplet inside the bubble [2]. Energy transfer during retractin drives the contraction and pinch-off of a daughter droplet. The wettability of the solid surface affects the detachment of the bubble, suggesting a method for bubble elimination in many drop-impact applications.

A bubble reaching an air-liquid interface usually bursts and forms a liquid jet. Jetting is relevant to climate and health as it is a source of aerosol droplets from breaking waves. Jetting has been observed for large bubbles (R >> 100μm). However, few studies have been devoted to small bubbles (R < 100μm) despite the entrainment of a large number of such bubbles in sea water. Here we show that jet formation is inhibited by bubble size; a jet is not formed during bursting for bubbles smaller than a critical size [3]. Using ultrafast X-ray imaging, we build a phase diagram for jetting and the absence of jetting.

A vortex is a flow phenomenon that is very commonly observed in nature. Despite long studies more than a century, the origin of the vortices and their dynamics remain unclear, mostly due to the lack of appropriate visualization methods. With ultrafast X-ray phase-contrast imaging, we show that the formation of vortex rings originates from the energy transfer by capillary waves generated at the moment of the drop impact [4]. Interestingly, we find a row of vortex rings along the drop wall with different power-law dependencies of the angular velocities on the Reynolds number.

One of the most questionable issues in wetting is the force balance that includes the vertical component of liquid surface tension. On soft solids, the vertical component leads to a microscopic protrusion of the contact line, that is, a '*wetting ridge*'. The wetting principle determining the tip geometry of the ridge is at the heart of the issues over the past half century. Here we reveal a universal wetting principle from the ridge tips directly visualized with high spatio-temporal resolution of x-ray imaging. We find that the cusp of the ridge is bent with an asymmetric tip (Fig. 1), whose geometry is invariant during ridge growth or by surface softness [5]. The singular asymmetry is deduced by linking the macroscopic and microscopic contact angles to Young and Neuman laws, respectively.

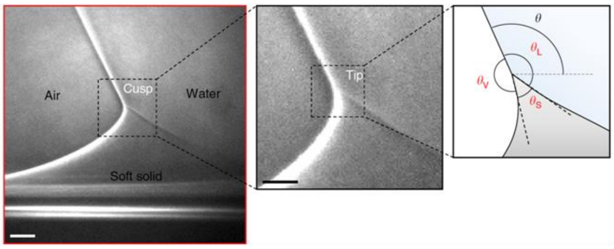

Figure 1. High-resolution X-ray imaging of a wetting ridge (left) with a bent cusp (middle) and an asymmetric tip (dashed square in middle). Extraction of three interfaces from the ridge tip (right) enables us to measure the macroscopic (θ) and the microscopic (θ_S, θ_V, *and* θ_L) contact angles. Scale bars, 2 and 1 μm, respectively.

Ultrafast/nanoscale dynamics based on using phase-contrast X-ray imaging will significantly contribute to resolve various unsolved puzzling problems in nature.

Acknowledgments: This work was supported by the Ministry of Trade, Industry and Energy (MOTIE) and Korea Institute for Advancement of Technology (KIAT) through the International Cooperative R&D Program.

---

[1] B.M. Weon *et al., Phys. Rev. Lett,* **100** (2008) 217403.
[2] J.S. Lee *et al., Phys. Rev. Lett,* **109** (2012) 204501.
[3] J.S. Lee *et al., Nat. Comm.* **2** (2011) 367.
[4] J.S. Lee *et al., Nat. Comm.* **6** (2015) 8187.
[5] S.J. Park *et al., Nat. Comm.* **5** (2014) 4369.

L-10 **Session B, Tuesday, 14.06., 11^{40} - 12^{20}**

Study of oxide materials for energy applications with X-ray spectroscopies

Cz. Kapusta[1*], K. Kollbek[1,2], J. Stępień[1], M. Sikora[1,2], K. Schneider[3], K. Zakrzewska[3] and J. Szlachetko[4,5]

[1]*AGH University of Science and Technology, Faculty of Physics and Applied Computer Science, Kraków, Poland*
[2]*AGH University of Science and Technology, Academic Centre for Materials and Nanotechnology, Kraków, Poland*
[3]*AGH University of Science and Technology, Faculty of Computer Sciences, Electronics and Telecommunications, Kraków, Poland*
[4]*Paul Scherrer Institute, Swiss Light Source, Villigen-PSI, Switzerland*
[5]*Institute of Physics, Jan Kochanowski University, Kielce, Poland*

Keywords: titania nanomaterials, doped zirconia, perovskites, photoelectrolysis, fuel cells, XAS, XES, RIXS

*e-mail: kapusta@agh.edu.pl

In the lecture selected applications of X-ray spectroscopies for the study of materials for energy conversion are to be presented. Three groups of materials are discussed: titania nanofilms/ nanopowders, yttria stabilized/doped zirconia and the lanthanide – 3d element perovskites. The titania based materials attract nuch interest due to their applications in photovoltaics and catalysis. Yttria stabilized zirconia and perovskites are the materials used for fuel cells. Results obtained with the following X-ray spectroscopic methods will be presented: High Resolution XAS/XES (X-ray Absorption Spectroscopy / X-ray Emission Spectroscopy) derived from RIXS (Resonant Inelastic X-ray Scattering) measurements, as well as a conventional XAS in the XANES (Near Edge Absorption Structure) and EXAFS (Extended X-ray Absorption Structure).

For the study of doped titania nanopowders and nanofilms of various oxygen stoichiometry, crystal structure and the cation and anion sites doping, two dimensional RIXS dependences have been measured at the Ti:K edge. They delivered HR-XES and HR-XANES spectra which provided information on e.g. band gap (Fig. 1, [1]) or the location of dopants in the next neighborhood of the Ti site.

The yttria stabilized zirconia doped with manganese, of the formula $Mn_x(Y_{0,148}Zr_{0,852})_{1-x}O_{2-\delta}$, has been studied with conventional XAS spectroscopy in the XANES and EXAFS range at the Mn:K, Zr:K and Y:K edges [2]. The Mn spectra, Fig. 2, show a considerable change of the edge energy and shape corresponding to changes of Mn average valence and symmetry of its local environment with x, in contrast to Zr (Fig. 2) and Y, where slight changes in the spectra are observed only.

A combination of XANES and XES methods was applied to $LaMn_{1-x}Co_xO_3$ system [3]. It provided the information on the charge and spin evolution of manganese and cobalt on x.

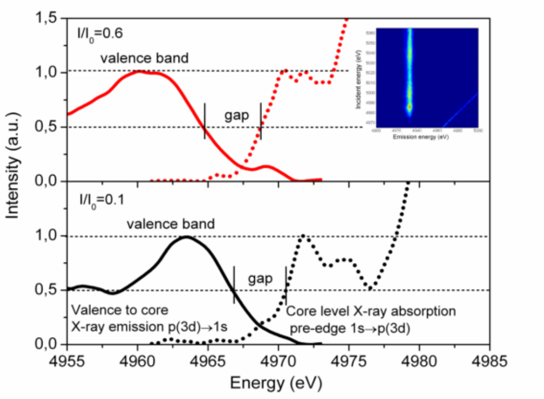

Figure 1. Pre-peak of Ti-K-edge HR-XANES (dashed) and Kβ lines of XES spectra (solid) of TiO_{2-x} for different x (I/I_0), after [1]. The extracted band gap energy is marked. Inset - the RIXS plane, from which XES and XANES spectra were derived.

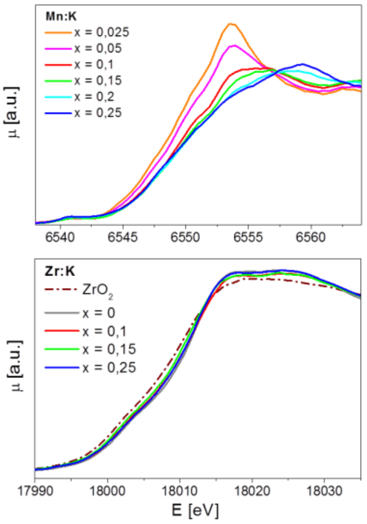

Figure 2. XANES spectra of $Mn_x(Y_{0,148}Zr_{0,852})_{1-x}O_{2-\delta}$ at the Mn:K and Zr:K edges (after [2]).

The results are analysed in terms of unique information on the individual element valencies, projected bands, site symmetries, charge and spin states provided by the synchrotron radiation exploiting X-ray spectroscopies. The relation of these data to those obtained by other methods, e.g. magnetometry, and to the crucial applied properties and parameters of the materials is discussed.

---

[1] K.Kollbek, M.Sikora, Cz.Kapusta, J.Szlachetko, K.Zakrzewska, K.Kowalski, M. Radecka, *Appl. Surf. Sci.* **281** (2013) 100.
[2] J. Stępień, *PhD Thesis*, AGH University of Science and Technology, Kraków, 2015.
[3] M. Sikora, K. Knizek, Cz. Kapusta, P. Glatzel, *J. Appl. Phys.* **103** (2008) 07C907.

L-11 **Session A, Wednesday, 15.06., 9^{00} - 9^{40}**

Structural Biology Using Light Sources Helps Combat Infectious Diseases and Antibiotic Resistance

A. Joachimiak[1]*

[1]*Structural Biology Center, Midwest Center for Structural Genomics, Biosciences, Argonne National Laboratory, Argonne, IL, 60439 and Center for Structural Genomics of Infectious Diseases, Computational Institute, University of Chicago, Chicago, Illinois 60667*

*e-mail: andrzejj@anl.gov

Many aspects of protein function, including molecular recognition, assembly and catalysis, depend on the 3D atomic structure. X-ray crystallography remains the most powerful method capable of providing atomic information on interactions of proteins with other macromolecules and small ligands. Modern light sources and dedicated macromolecular crystallography (MX) beamlines have expanded our competence in determining macromolecular structures. New strategies developed allow data collection from highly demanding crystals using mini-beams and reduce radiation damage. Genome sequencing projects have accelerated significantly and now include studies of many human pathogens. Expanded protein sequence space allows comprehensive approaches to studies of the entire cellular systems. Structural Genomics efforts took advantage of these innovations and contributed a complementary array of the rapid, highly integrated and cost effective methods in molecular and structural biology and created structure determination pipelines. When combined with MX synchrotron facilities, advanced software and computing resources, these pipelines resulted in significant acceleration of protein structure determination and expanded the range of projects. Structure determination pipelines can be applied to emerging diseases. Several examples of application of light sources to important biology challenges will be discussed. Structures obtained through X-ray crystallography combined with biochemical assays and numerical simulation can help to construct a model of the enzymes catalytic pathways. Structures of complexes with ligands in combination with *in vitro* and *in vivo* inhibition studies can provide important insights into the interactions that modulate selectivity and potency of inhibitors that could serve as lead compounds for drug development.

Acknowledgments: This work was supported by NIH Grant GM094585, the NIAID/DHHS Contracts [HHSN272200700058C and HHSN272201200026C]. The use of SBC beamlines was supported by the U.S. DOE, BER [DE-AC02-06CH11357].

L-12 **Session A, Wednesday, 15.06., 9^{40} - 10^{20}**

Monte Carlo structure factors for self-assembling polymers

M. Banaszak[1]*

[1]*Faculty of Physics, Adam Mickiewicz University,*
Umultowska 85, 61614 Poznań, Poland

*e-mail: mbanasz@amu.edu.pl

We present Monte Carlo data for self-assembling multiblock copolymer melts and solutions.

We use experimentally determined Flory–Huggins interaction parameters, χ, to quantify the interactions between ionic and nonionic monomers. Analysis of the experimental data indicate that χ between poly(styrenesulfonate) and polystyrene is about 5, a value that is orders of magnitude larger than that obtained in mixtures of nonionic polymers. Our model predicts that clustering of ionic monomers in the disordered state results in stabilization of the disordered phase and the product $p2\chi N$ is well above the mean-field value of 10.5 at the order–disorder transition (N is the total number of monomers per chain). Network morphologies and hexagonally packed cylinders are observed in the ordered state at large p values while more traditional lamellar phases are found at small values of p. Simulations indicate that complex morphologies such as gyroid and perforated lamellae are obtained in symmetric block copolymers wherein the volume fraction of the B block, ϕB, is about 0.5, while simple unperforated lamellae are obtained in asymmetric block copolymers wherein ϕB is about 0.25. This result is very different from the well-established phase behavior of nonionic block copolymers but consistent with experimental results. We also make a number of additional predictions, still awaiting an experimental verification, such as the emergence of the hexagonal phase in the weak segregation limit, and a remarkable insensitivity of the product p^2χN (N is the total number of segments in a copolymer chain) at the order–disorder transition to ϕB.

L-13 **Session A, Wednesday, 15.06., 11^{40} - 12^{20}**

Structural studies of chitinases from extremophiles

W. Rypniewski[1]*

[1]*Institute of Bioorganic Chemistry, Polish Academy of Sciences, Center for Biocrystallographic Research, Noskowskiego 12/14, 61-704, Poznań, Poland*

*e-mail: wojtekr@ibch.poznan.pl

Proteins from extremophiles hold the secret of protein stability and enzymatic efficiency. We have analysed chitinases from cold-adapted and thermophilic bacteria, compared them and looked for the features that give those ezymes their special characteristics.

L-14 **Session B, Wednesday, 15.06., 9^{00} - 9^{40}**

Structural studies of bioactive metal-organic ligand complexes using XAFS

M. T. Klepka[1*], A. Drzewiecka-Antonik[1] and A. Wolska[1]

[1]*Institute of Physics, Polish Academy of Sciences,*
Al. Lotnikow 32/46, 02-668 Warsaw, Poland

Keywords: XAFS, metal-organic ligand complex, coordination geometry

*e-mail: mklepka@ifpan.edu.pl

Biologically active metal complexes of organic ligands are being widely investigated. However, very often among reports about biological activity there is little information concerning metal – organic ligand binding mechanism. This lack is a result of a fact that for coordination compounds it is difficult to obtain crystals. In such a case diffraction techniques are inapplicable and any structural information can only be speculated. Detailed knowledge about structure is extremely important in studies of bioactive coordination complexes. Without it planning the chemical reactions to properly modify chemical or physical properties of final product is ineffective.

X-ray absorption fine structure (XAFS) technique is not commonly applied to study metal-organic ligand interactions. The great advantage of XAFS over other experimental techniques is that it can be used for crystal as well as amorphous materials at different states: (i) solid, (ii) liquid or (iii) gaseous. XAFS provides information about the local atomic order, coordination number, kind of atoms, oxidation state, relative disorder and even angles between central atom and near neighbours. Such information is essential to study structure-activity relationship for the disordered complexes.

Goal of our studies is to get information about binding mechanism of organic ligand to metallic center. In order to achieve that we perform analysis in several steps. First, infrared spectroscopy is used to monitor whether complexation reaction was successful. In parallel elemental and thermal analyses are being performed. In the second step Cambridge Structural Database (CSD) is being searched to find initial model for DFT calculations and EXAFS analysis. Third step is refining model using XANES analysis. The last step is confirmation of the final model using EXAFS analysis.

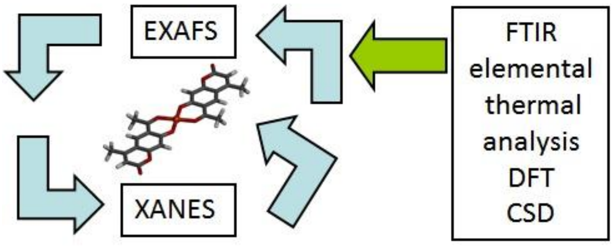

Figure 1. Scheme of the analysis steps

During presentation examples of performed studies with e.g.:

(i) phenoxyacetic and benzoic acids [1],
(ii) benzo[*b*]furan derivatives [2],
(iii) methylohydantoin [3],
(iv) coumarin derivatives [4]

and future perspectives will be presented and discussed.

Acknowledgments: Experimental research was funded from the Polish National Science Centre (Grant No. UMO-2012/07/D/ST5/02251). This research was supported in part by PL-Grid Infrastructure. Financial support from the EU FP7 EAgLE project under the grant agreement REGPOT-CT-2013-316014 is gratefully acknowledged.

---

[1] M.T. Klepka, A. Drzewiecka, A. Wolska, W. Ferenc *Chem. Phys. Lett.* **553** (2012) 59.
[2] A. Drzewiecka, A. E. Koziol, M. T. Klepka, A. Wolska, S. B. Jimenez-Pulido, M. Struga *Chem. Phys. Lett.* **575** (2013) 40.
[3] M. Puszynska-Tuszkanow, Z. Staszak, T. Misiaszek, M.T. Klepka, A. Wolska, A. Drzewiecka-Antonik, H. Faltynowicz, M. Cieslak-Golonka *Chem. Phys. Lett.* **597** (2014) 94.
[4] M.T. Klepka, A. Drzewiecka-Antonik, A. Wolska *et al., J. Inorg. Biochem.* **145** (2015) 94.

L-15 **Session B, Wednesday, 15.06., 9^{40} - 10^{20}**

Extended Abstract

Review of biological application facilities at the Canadian Light Source

P. Grochulski[1,2]* M. Fodje[1], S. Labiuk[1],
T. W. Wysokinski[1], G. Belev[1], G. Korbas[1]
and S. M. Rosendahl[1]

[1]*Canadian Light Source Inc., 44 Innovation Boulevard, Saskatoon, SK S7N 2V3, Canada*
[2]*College of Pharmacy and Nutrition, University of Saskatchewan, Saskatoon, SK S7N 5E5, Canada*

Keywords: synchrotron radiation, macromolecular crystallography, medical imaging, infrared spectroscopy, X-ray absorption spectroscopy

*e-mail: pawel.grochulski@lightsource.ca

The Canadian Light Source Inc. (CLS) is a mid-size 3rd generation 2.9 GeV synchrotron located on the campus of the University of Saskatchewan in Saskatoon (www.lightsource.ca). Last year, the CLS celebrated its 10th anniversary of operation. Currently there are 15 beamlines operating at the facility, with an additional two being commissioned and five under construction. A current summary of Bio/Life Sciences department publication activity is shown in Figure 1.

The Bio/Life Science department at the CLS was created one year ago to facilitate support and research in the biological and health related fields. It is composed of the following facilities: Canadian Macromolecular Crystallography Facility (CMCF), Mid Infrared Spectromicroscopy (Mid-IR), Biomedical Imaging and Therapy (BMIT) and, recently built, Biological X-ray Absorption Spectroscopy (BioXAS) which is currently being commissioned.

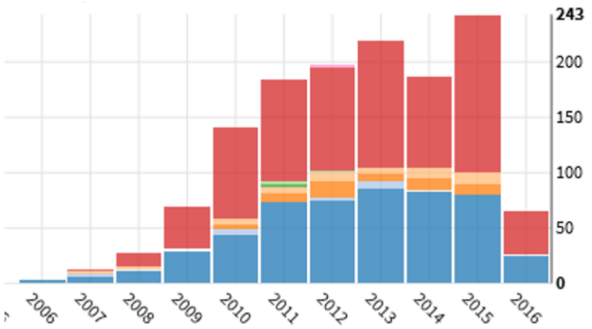

Figure 1. CLS Bio/Life Sciences department activity summary. Number of publications containing data from associated beamlines by year, including: peer-reviewed articles (blue), conference proceedings (light blue), doctoral theses (orange), masters theses (light orange), magazine articles (green), book/chapter sections (light green), PDB depositions (red) and patents (pink).

The sector is well equipped to study biological objects ranging from atomic resolution (CMCF and BioXAS) to cells and tissues (BioXAS and Mid-IR) through to larger samples such as organs, live animals and plants (BMIT). Since 2006, researches acquired data at the Bio/Life Sciences beamlines to produce a total of 516 peer-reviewed articles, 59 doctoral theses and 49 masters theses making use of data acquired at the associated beamlines.

The CMCF is composed of two beamlines (08ID-1 and 08B1-1) and it serves more than 65 Canadian and some international labs. The main techniques available at the CMCF are as follows; high resolution macromolecular X-ray crystallography, Multi/Single wavelength Anomalous Dispersion (MAD/SAD), small molecule crystallography and EXAFS on crystals. Since its inception 10 years ago, 390 peer reviewed papers were published with data collected at the CMCF and more than 720 structures deposited in the PDB. Drug development is an important area of Canadian research and we outline here an example of a successful path from a high-resolution crystal structure to a therapeutic antibody. About 2 in 5 Canadians will develop cancer in their lifetime, and about 1 in 4 Canadians will die of cancer. In 2015, it is estimated that 196,900 Canadians developed cancer, and 78,000 died of cancer. More than half of new cancer cases (51%) are lung cancers. Netrin-1 is a protein involved in neuronal navigation, immune cell migration and cell survival. Its interaction with receptor (UNC5) is responsible for cell proliferation, therefore finding a molecule that would interrupt this interaction would trigger tumor cell death. Using the high-resolution capabilities of the CMCF beamlines at the CLS, a Canadian-European collaboration was able to identify the part of Netrin-1`s structure that actually performs this function [1]. Using this information the researchers were able to design an antibody to target that area of Netrin-1, and showed it triggers death of cancer cells under laboratory conditions. The antibody, now named NP137, is currently in clinical trials.

BMIT is composed of two beamlines (05ID-2 and 05B1-1). The following techniques are available at BMIT; conventional absorption imaging, Diffraction Enhanced Imaging (DEI), K-edge Subtraction (KES), Multiple Image Radiography (MIR) and Phase Contrast Imaging both in planar and Computed Tomography (CT) mode [2]. The research conducted at BMIT over the last 5 years has been described in 68 publications and contributed to 23 theses. Ongoing core research programs include; bone and cartilage growth and deterioration, cardiovascular and lung imaging and disease, human and animal reproduction, cancer imaging and therapy, spinal cord injury and repair, developmental biology, as well as the introduction of new imaging methods. A recent example of work done at BMIT is related to arthritis. Arthritis is the leading cause of long-term disability in Canada, with osteoarthritis being the most common form of the disease. Unfortunately, most cases of osteoarthritis are identified only once the disease is well advanced and irreversible damage has occurred. To better understand the causes of osteoarthritis, investigators introduced a strontium tracer into joints developing osteoarthritis, and spatially mapped the temporal changes in bone, using K-edge subtraction synchrotron micro-CT [3]. 3D imaging indicated clear differences between healthy bone, which showed a uniform distribution of strontium, and subjects developing osteoarthritis, which showed pathological changes occurring in the bone microstructure. In particular, tracer was found beneath the cartilage and at bone margins, which eventually develop into bone spurs and limit normal joint movement. New X-ray optical instrumentation projects are being pursued at the BMIT beamlines to address the needs for various imaging programs, for example, an expander for dynamic real life imaging (Figure 2) [4] which allows the imaging of larger objects using a single frame.

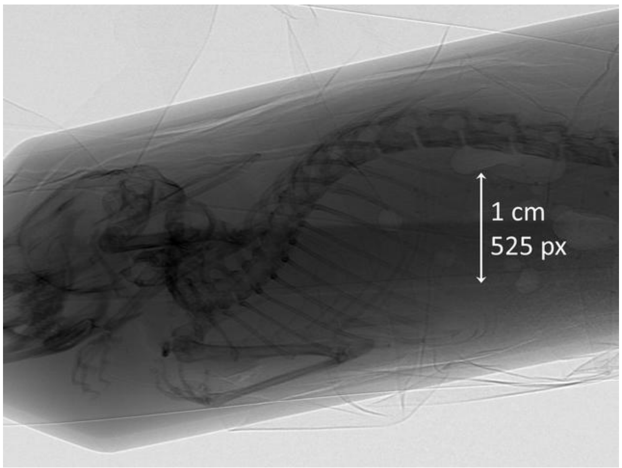

Figure 2. Full field phase image of euthanized mouse.

At the Mid-IR beamline, the following experiments are performed; full field spectromicroscopy at diffraction-limited spatial resolutions (single point mapping and large area mapping utilizing a Focal Plane Array detector), Photoacoustic Spectroscopy, Polarization Modulation IR Spectromicroscopy and Time-Resolved measurements. Since 2006, Mid-IR users have published 68 peer-reviewed articles, while 7 doctoral theses and 8 masters theses were defended using data from the beamline. Mid-IR can be used to obtain biochemical, structural and dynamical information about biological systems. Since normal and cancerous cells differ in their biochemical and/or structural natures, Fourier transform infrared spectroscopy (FTIR) can be utilized to differentiate them. Using this method one can detect chemical changes in the very early stages of cancer, before any morphological changes occur. At the CLS, FTIR was successfully applied to samples from breast and skin cells [5].

BioXAS is composed of 3 beamlines. Two of them are dedicated to X-ray absorption spectroscopy and are being commissioned, while one will be a multi-mode X-ray fluorescence imaging line. Techniques include X-ray Fluorescence (XRF), X-ray Absorption Spectroscopy (XAS) Imaging, multi-mode X-ray fluorescence imaging & micro-XAS. The beamlines are tailored for biological and health-related studies of metals in living systems using X-ray absorption spectroscopy (XAS) and XAS-imaging. These techniques allow determination of molecular form and location of metals in almost any type of material, including purified metal-containing proteins, intact biological tissues and living organisms [6].

Acknowledgments: This work was supported by The Canadian Light Source is supported by the Canada Foundation for Innovation, Natural Sciences and Engineering Research Council of Canada, the University of Saskatchewan, the Government of Saskatchewan, Western Economic Diversification Canada, the National Research Council Canada, and the Canadian Institutes of Health Research.

---

[1] M. Gradin *et al., Cancer Cell* **29**(2) (2016) 173.

[2] S. Wiebe *et al., Synchrotron Radiation News* **28**(5) (2015) 16.

[3] P. Arash, D. Cooper, M. Doschak, *Journal of Orthopedic Research* **33**(11) (2015) 1655.

[4] M. Martinson *et al., J. Synchr. Rad.* **22** (2015) 1.

[5] H. Ukkonen *et al., Vibr. Spectroscopy* **79** (2015) 24.

[6] M. Korbas *et al., ACS Chem. Biol.* **8** (2013) 22.

L-16 **Session B, Wednesday, 15.06., 11^{40} - 12^{20}**

Photoionization of atoms molecules and clusters with novel XUV light sources

M. Coreno[1,2]*

[1]*CNR-ISM, Basovizza Area Science Park, 34149 Trieste, Italy*
[2]*Elettra-Sincrotrone Trieste, Italy*

Keywords: synchrotron radiation, free-electron laser, laser HHG source; electron spectroscopy

*e-mail: marcello.coreno@elettra.eu

XUV spectroscopic investigations on the electronic structure of matter continuously profit from advances in laser and synchrotron radiation instrumentation. Photon flux and energy resolution achievable at third generation facilities, such as the Gas Phase beamline of the Elettra storage ring (Trieste, Italy) [1], have enabled for the last 2 decades thorough studies of inner-shell electron photoionization even with low density targets such as metal-organic vapours [2], clusters [3], as well as of thermolabile organic radicals [4] or biotic molecules [5].

More recently the interest of the physical chemistry-chemical physics community has been attracted by the opportunity of exploring also the temporal dynamics of isolated systems by means of novel state-of-the-art light ultrafast vacuum ultraviolet light sources. For this purpose two new beamlines capable of delivering fs- VUV photon pulses have recently been commissioned in the framework of the FERMI Free Electron Laser (FEL) facility [6]: the Low Density Matter beamline at FERMI [7, 8] and CITIUS [9], a state-of-the-art laboratory source, based on laser High Harmonic Generation on rare gases.

I will illustrate the different facilities, available to the Atomic and Molecular Physics Users' community of Elettra (Trieste, Italy) for the study of spectroscopy and dynamics of isolated systems, as well as recent developments in the instrumentation.

I will then present experiments where synchrotron radiation photoionization techniques have been applied to gas phase molecular targets of increasing complexity, ranging from molecules of biological interest, to metal containing molecules and clusters. The high resolution photoemission set-up for molecular vapours recently assembled in our collaboration with the group of prof. Carla Puglia (Uppsala University, Sweden) will be described. Data on aromatic and heteroaromatic systems of interest for organic electronics will be reported, in order to highlight the relevance of high quality XUV spectroscopic investigations for a thorough description of the electronic structure of oligothiophenes and polyaromatic hydrocarbons (PAH), such as biphenylene (fig.1) [10] and coronene (fig.2) [11, 12].

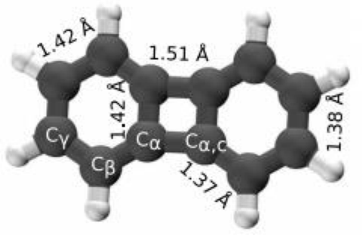

Figure 1. Biphenylene molecule.

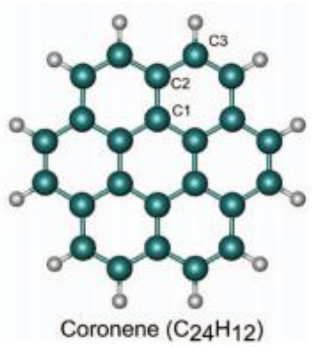

Figure 2. Coronene, with nonequivalent carbon atoms labeled.

Finally, I will also outline research opportunities opened in the field of atomic and molecular physics by the novel ultrafast light sources developed at Elettra. In particular I will discuss recent pump-probe experiments, which on one side are used for characterizing our novel VUV light sources [13], and on the other side are also paving the way for thorough investigations of electron dynamics in molecular excited states and for femtochemistry application of ultrafast VUV radiation.

Acknowledgements: this work was supported by the Carl Tygger Foundation (Sweden), for making available the VG-Scienta SES-200 photoelectron analyser at the GasPhase beamline, Elettra, Italy.

---

[1] K.C. Prince, *et al, J. Synch. Rad*. **5** (1998) 565; see also http://www.elettra.eu/elettra-beamlines/gasphase.html.
[2] M. Coreno, *et al., Dalton Trans*. **43** (2014) 513.
[3] T. Mazza, M. Devetta, P. Milani, G. Bongiorno, M. Coreno, P. Piseri, *New J. Phys.* **13** (2011) 023009.
[4] B. Kovac, Kovač, I. Ljubić, A. Kivimäki, M. Coreno, I. Novak, *PCCP* **17** (2015) 10656.
[5] O. Plekan *et al., J.Phys. Chem. A* **116** (2012) 5653.
[6] E. Allaria, *et al., Nature Photonics* **6** (2012) 699.
[7] V. Lyamayev *et al., J. Phys. B* **46** (2013) 164007.
[8] C. Svetina, *et al., J. Synchrotron Rad*. **22** (2015) 538.
[9] C. Grazioli, *et al. , Rev. Sci. Instr*. **85** (2014) 23104.
[10] J. Lüder, *et al., J. Chem. Phys.,* **141** (2015) 074305.
[11] G. Fronzoni, *et al., J. Chem. Phys.* **141** (2015) 44313.
[12] A. Acocella, *et al., PCCP* (2016) ***asap***;
DOI: 10.1039/C5CP06455D.
[13] E. Allaria, *et al., Phys. Rev.* X **4** (2014) 41040.
.

L-17 **Wednesday, 15.06., 15^{00} - 15^{40}**

Status of the petawatt-class twin optical laser facility for the synergy experiments with XFEL (SACLA)

H. Tomizawa[1,2]*

[1] *Japan Synchrotron Radiation Research Institute, Kouto 1-1-1, Sayo, Hyogo 679 – 5198, Japan*
[2] *RIKEN, SPring-8 Center, Kouto 1-1-1, Sayo, Hyogo 679 – 5148, Japan*

Keywords: petawatt-class laser, synchrotron radiation, x-ray free-electron laser

*e-mail: hiro@spring8.or.jp

SACLA [1] X-ray Free Electron Laser (XFEL) has been constructed and operated next to the largest 3rd-generation synchrotron radiation source at SPring-8. Recently, the XFEL was upgraded to a seeded FEL scheme as one of the options to improve the longitudinal (temporal) coherency. There is the synergy experimental facility at the meeting point of both SACLA and SPring-8 (see Figure 1). The synergy experiment uses can utilize both x-ray sources at this facility.

We are preparing the third "extreme" light source in this facility: petawatt-class optical laser systems synchronized to the 3rd-generation synchrotron radiation source and full-coherent seeded XFEL. These light sources are a complementary trinity to discover the dynamical nature of a variety of materials under different conditions. Experimental research using high power optical lasers combined with XFELs open new frontiers in high energy density (HED) sciences. The capabilities of pump/probe methods are dramatically improved due to the brightness of the XFEL pulses with ultrafast duration.

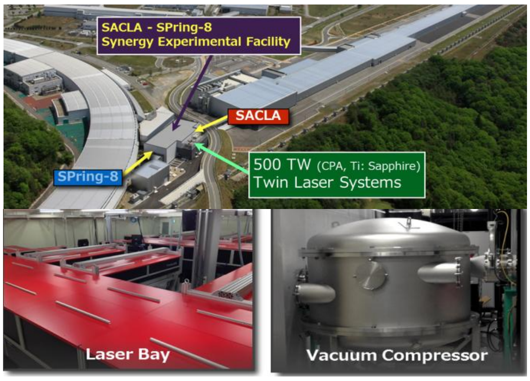

Figure 1. The synergy experimental facility with a pettawatt-class laser systems (500 TW x2.).

Currently, an experimental platform for HED sciences with a twin 500 TW Ti:Sapphire laser system is under beam commissioning for experiments combined with the XFEL for research objectives that require high peak power in the optical laser pulses. Thanks to alternative seeding from one of the common front ends, two optical laser pulses are delivered simultaneously with the maximum power of 500 TW in each into a target chamber located in an experimental hutch 6 (EH6) at BL 2, which was recently commissioned as a SACLA's 2nd hard x-ray beamline. A focusing capability using sets of compound refractive lenses will be applied to increase the x-ray fluences on the sample. One of the most key issues for the integrated experimental platform is the development of diagnostics that meet requirements both from the high power optical laser and XFEL.

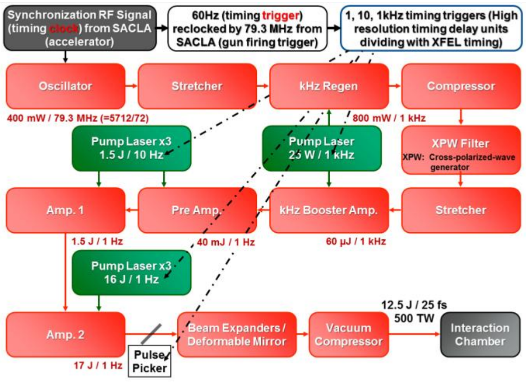

Figure 2. The petawatt-class twin optical laser system synchronized to XFEL (SACLA).

One of the most important key technologies for pump/probe methods is high-resolution timing delay units between the petawatt laser pulses and XFEL pulses (see Figure 2). The laser timing system consists of timing clock and re-clocked trigger delay systems. The laser oscillator is synchro-locked to RF clock of 79.3 MHz, which is a divided-by-72 frequency of the SACLA accelerator basic RF (C-band: 5712 MHz).

The optimizations of laser pulse characteristics are strongly required for user experiments. Hitherto, laboratory lasers have been tuned and aligned for each requirement manually by laser experts. Automatic laser tuning requires sophisticated algorithms, and the metaheuristic algorithm is one of the best solutions. The metaheuristic laser tuning system is expected to reduce the human resources and time required for laser preparations. I demonstrated some successful results on a metaheuristic algorithm based on a genetic algorithm to optimize spatial (transverse) laser profiles, and a hill-climbing method extended with a fuzzy set theory to align the laser path automatically [2]. I have developed an auto-aligner for a large laser system together with Photo-Physics Laboratory Inc. since 2007 [3]. It was named the Advanced Tactical Aligner (ATA). We are installing the ATA system based on a metaheuristic algorithm in the front ends of this petawatt laser system.

The status and future perspective of the developments of this facility will be reported in the presentation. The synergy user experiments utilizing extreme light sources will be openly discussed.

---

[1] T. Ishikawa, *et. al.*, *Nat. Photonics.* **6** (2012) 540.
[2] H. Tomizawa, *Rad. Phys. Chem.***80** (2011) 1145.
[3] H. Tomizawa and T. Kojima, Application Date: March 3 2010; Japanese Patent No.5545830.

L-18 **Wednesday, 15.06., 15^{40} - 16^{20}**

Scientific opportunities and challenges for time-resolved studies using X-ray Free Electron Lasers

W. Gawelda[1,2]*

[1]European XFEL, Albert-Einstein-Ring 19, 22761 Hamburg, Germany
[2]Institute of Physics, Jan Kochanowski University, Świętokrzyska 15, 25-406 Kielce, Poland

Keywords: X-ray free-electron laser, pump-probe, femtosecond

*e-mail: wojciech.gawelda@xfel.eu

With the advent of soft- and hard X-ray Free Electron Lasers (XFEL) sources, entirely new scientific opportunities and prospects have been become available in the field of time-resolved X-ray spectroscopy and X-ray scattering. One of the most unprecedented features of XFELs is their ability to produce high intensity pulsed X-ray beams with single pulse duration well below 100 femtoseconds (1 fs = 10^{-15} s). This property allows dynamical studies of light-matter interactions virtually in any medium on the very fundamental timescales of interatomic motions, i.e. intra- and intermolecular vibrations, from gas-phase to complex strongly correlated solids, i.e. high-temperature superconductors, and biomolecules. However, this unique feature of XFEL beams permits also to snapshot static structures of nanometer-sized protein crystals before the ionization and electrostatic forces “destroy” the crystal. These developments led to establishing new methodologies in structural biology, such as serial femtosecond crystallography (SFX) and very rapid development of new sample delivery methods.

In this talk I will present a state-of-the-art overview of the abovementioned research venues, which highly benefit from the progress in the field of XFEL technology, and in particular, I will focus on those aspects, which profit most from the temporal properties of the XFEL beams.

L-19 **Thursday, 16.06., 9^{00} - 9^{40}**

Preparing for First Science Experiments at European XFEL

T. Tschentscher[1]*

[1]European XFEL, Holzkoppel 4, 22869 Schenefeld, Germany

*e-mail: thomas.tschentscher@xfel.eu

The European X-Ray Free-Electron Laser (European XFEL) in the Hamburg area, Germany, is presently entering its commissioning phase and prepares for first scientific user experiments. Following successful first commissioning of the main electron accelerator, the first undulator, and the x-ray beam transport and instrumentation at the Femtosecond X-ray Experiments (FXE) and (SPB/SFX) instruments an early user experiment program shall start in summer 2017. In the talk I will briefly summarize the status of the European XFEL project and provide details about the start of user operation. Using examples of recent scientific applications, using other x-ray FEL facilities, and the available instrumentation at the science instruments at European XFEL then will be used to discuss classes of experiments that will be possible to be conducted in the early user program.

L-20 **Thursday, 16.06., 9^{40} - 10^{20}**

Understanding a lithium ion battery using high-energy synchrotron X-rays

Y. Sakurai[1]*

[1]*Japan Synchrotron Radiation Research Institute, 1-1-1 Kouto, Sayo, Hyogo 679-5198, Japan*

Keywords: high-energy X-rays, Compton scattering, redox orbitals, operando observation

*e-mail: sakurai@spring8.or.jp

Lithium ion battery is one of the popular energy storage devices and its lifetime and safety are central issues in battery manufacturing. For this purposes, extensive and intensive studies have been carried out by various synchrotron X-ray techniques, including XRD, XAFS, XES, HAXPES, RIXS, Compton scattering and others. Among them, high-energy X-ray scattering, i.e Compton scattering, is better placed to measure disordered materials under various sample conditions. The electron momentum density observed by this technique is a ground-state property of an electron system, which allows us to interpret the experimental results straightforwardly with electronic structure calculations. Moreover, it can also probe materials inside a metal container, such as a commercial battery. Therefore, high-energy X-ray Compton scattering is a unique tool to investigate a battery at the quantum and product levels under in situ and operando conditions.

In this talk, we present our recent works: quantum-scale characterization of redox orbitals in an electrode material [1] and product-scale mapping of lithium distributions in a commercial battery (see Fig. 1) [2, 3].

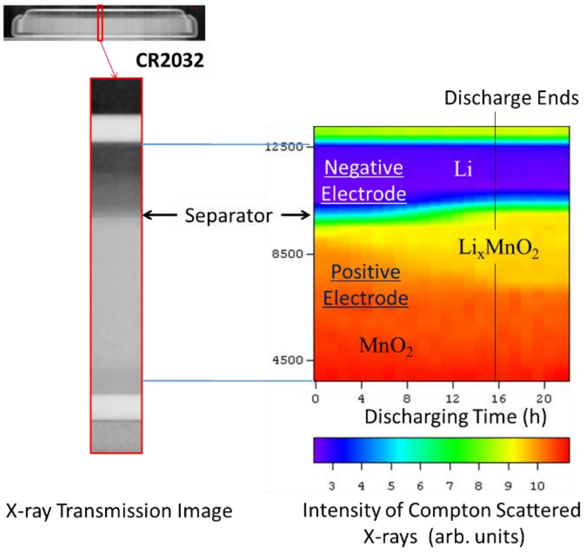

Figure 1. Intensity map of Compton-scattered X-rays as a function of vertical position and discharge time of the battery (CR2032) [2]. Lithium migration and internal structure change are clearly observed.

Acknowledgments: This work was supported by Japan Science and Technology Agency.

---

[1] K. Suzuki, B. Barbiellini, Y. Orikasa, H. Go, H. Sakurai, S. Kaprzyk, M. Itou, K. Yamamoto, Y. Uchimoto, Y. J. Wang, H. Hafiz, A. Bansil, Y. Sakurai, *Phys. Rev. Lett.* **114** (2015) 087401.

[2] M. Itou, Y. Orikasa, Y. Gogyo, K. Suzuki, H. Sakurai, Y. Uchimoto, Y. Sakurai, *J. Synchrotron Rad.* **25** (2015) 161.

[3] K. Suzuki, B. Barbiellini, Y. Orikasa, S. Kaprzyk, M. Itou, K. Yamamoto, Y. J. Wang, H. Hafiz, Y. Uchimoto, A. Bansil, Y. Sakurai, H. Sakurai, *J. Appl. Phys.*, **119** (2016) 025103.

L-21 **Thursday, 16.06., 10^{20} – 11^{00}**

The Hybrid XAS technique for dilute [1-10 mM] solutions at high accuracy

C. T. Chantler[1]*

[1]*School of Physic, University of Melbourne, Victoria 3010, Australia*

Keywords: synchrotron radiation, XAFS, Hybrid

*e-mail: chantler@unimelb.edu.au

XAFS can now be used to investigate electron inelastic mean free paths, dynamical and thermal bonding, to measure nanoroughness and most importantly to assess the significance of alternate hypotheses with derived experimental uncertainty.

A new approach is introduced for determining XAS spectra on absolute and relative scales using multiple solutions with different concentrations by the characterisation and correction for experimental systematics. This Hybrid technique is a development of standard XAFS along the lines of high-accuracy XERT but with applicability to solutions, dilute systems and cold cell environments. We have applied this methodology to determining absolute XAS of [bis(N-n-propyl-salicylaldiminato)] nickel(II) and [bis(N-i-propyl-salicylaldiminato)] nickel(II) complexes with square planar and tetrahedral structures in 15 mM and 1.5 mM dilute solutions. Dilute systems provide excellent XANES and XAFS spectra by transmission, and we confirm that transmission measurements can be superior to conventional fluorescence measurements even for dilute systems. For the first time, we have determined XAS of the isomers from low concentration solutions on an absolute scale with a 1%-5% accuracy, and with relative precision to 0.1% to 0.2% in the active XANES and XAFS regions after inclusion of systematic corrections. This allows a range of new insights for multi-phase systems, for going beyond fingerprinting to theoretical validation and for species identification in dilute systems using XAFS.

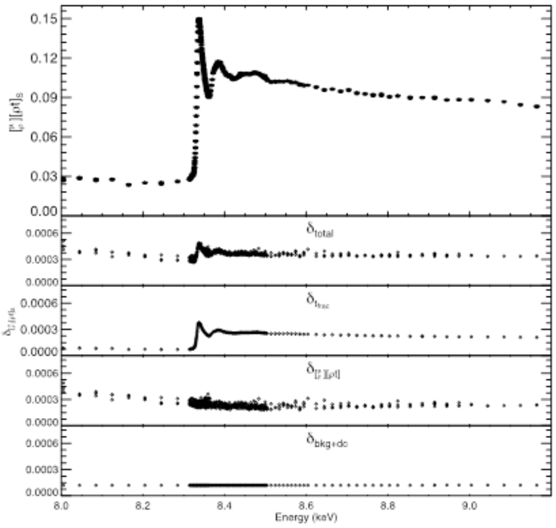

Figure 1. Corrected and normalised XAS of the (i-pr Ni) isomer determined from the attenuations of 15 mM solutions following the solvent subtraction. The modelled background was subtracted from the corrected (dark-current and scatting effect) attenuations of the solutions (shown by the ◇ symbols; sample detail). The corresponding uncertainty was propagated from the uncertainty contributions of experimental systematics, and from the variance of repeated measurements with both the solution and the solvent. The defined accuracy will allow the reliable structural analysis of (i-pr Ni) using XAFS. At each of the energies, three aperture dependent measurements are in excellent agreement.

---

[1] C. T. Chantler, M. T. Islam, S. P. Best, L. J. Tantau, C. Q. Tran, M. H. Cheah, A. T. Payne, *J. Synchr. Rad.* **22** (2015) 1008.

[2] M. T. Islam, C. T. Chantler, L. J. Tantau, C. Q. Tran, M. H. Cheah, A. T. Payne, S. P. Best, *J. Synchr. Rad.* **22** (2015) 1475.

[3] M. T. Islam, J. D. Bourke, S. P. Best, L. J. Tantau, C. Q. Tran, F Wang, C. T. Chantler, *J. Phys. Chem. C,* **120**(17) (2016) 9399–9418.

L-22 **Thursday, 16.06., 11^{40} - 12^{20}**

New developments in the structure analysis of biomolecules using synchrotron-radiation vacuum-ultraviolet circular dichroism

K. Matsuo[1]*

[1] *Hiroshima Synchrotron Radiation Center, Hiroshima University, Higashi-Hiroshima, 739-0046, Japan*

Keywords: amyloid fibrils, hydration, membrane-bound protein, monosaccharide, structural dynamics, secondary structure, vacuum-ultraviolet circular dichroism

*e-mail: pika@hiroshima-u.ac.jp

Circular dichroism (CD) is defined as the difference between the absorption of left- and right-circularly polarized light and is very sensitive to the steric structures of optically active materials such as biomolecules. The CD spectra of biomolecules are measurable at low concentrations under various solvent conditions, which makes CD spectroscopy a powerful technique for analyzing the structures of proteins, saccharides, and DNA in aqueous solution. However, the structural information obtainable from this technique has been limited because a conventional CD instrument using an experimental light source is generally not capable of measuring the CD in the vacuum-ultraviolet (VUV) region below 190nm. Synchrotron radiation (SR) is an excellent high-flux source of photons in the VUV region, and VUVCD spectrophotometers have been constructed using SR to extend the short-wavelength limit of CD spectra. Recently techniques for analyzing the biomolecule VUVCD spectra have been largely developed by the combination with theoretical analysis and bioinformatics, which allowed us to obtain novel structural information of biomolecules based on the high-energy transitions such as acetal and hydroxy groups. In this paper, we show recent progress of SR-VUVCD spectroscopy in the structural analysis of saccharides and proteins.

Monosaccharaides such as D-glucose exhibited the characteristic VUVCD spectra below 190 nm depending on the complicated equilibrium structures between the gauche and trans conformations of hydroxyl-methyl group and between the α-/β-anomer configurations of hydroxy group. These spectra were theoretically calculated using a molecular dynamics (MD) simulation and a time-dependent density functional theory. From the comparisons between experimental and theoretical spectra, we revealed the dynamics-structure-hydration relationships of these monosaccharides, which are important factors for understanding their functions such as the molecular recognition and stabilization of proteins. [1, 2] The VUVCD analysis of globular proteins coupled with bioinformatics such as neural-network method allowed us to accurately estimate the contents, numbers of segments, and sequences of α-helix and β-strand structures of proteins. This spectroscopy was applied to the structural analysis of membrane-bound proteins, showing that the numbers of helical segments of the proteins largely increased due to the membrane interaction. The orientations of the helix segments on the membrane surface were determined by the flow linear dichroism apparatus installed in the VUVCD instrument [3] The CD spectrum of amyloid fibrils of β_2-microglobulin core fragments were theoretically calculated using a CD theory and MD simulation, disclosing that the conformations of these fibrils were composed of amyloid accumulations in which the parallel β-sheets stack in an antiparallel manner. [4] These results demonstrate that VUVCD spectroscopy can provide crucial structural information of biomolecules in aqueous solution to open a new field in the structural biology and chemistry.

Acknowledgments: This work was supported by JSPS KAKENHI Grant Number 23687020, 40403620, and 15KK0260, and by a grant from Kurata Memorial Hitachi Science and Technology Foundation

---

[1] K. Matsuo, H. Namatame, M. Taniguchi, K. Gekko *J. Phys. Chem. A* **40** (2012) 9996.

[2] K. Matsuo, H. Namatame, M. Taniguchi, K. Gekko *Biomedical Spectroscopy and Imaging* **4** (2015) 269.

[3] K. Matsuo, H. Namatame, M. Taniguchi, K. Gekko *Proteins* **84** (2016) 349.

[4] K. Matsuo, H. Hiramatsu, K. Gekko, H. Namatame, M. Taniguchi, R. W. Woody *J. Phys. Chem. B* **118** (2014) 2785.

L-23 **Thursday, 16.06., 12^{20} - 13^{00}**

Applied crystallography at ALBA Synchrotron

M. A. G. Aranda[1]*

[1]*ALBA synchrotron, Carrer de la Lum, 2-26, 08290 Cerdanyola del Vallès, Barcelona, Spain*

Keywords: synchrotron radiation, diffraction, scattering

e-mail: migarcia@cells.es

ALBA is a third generation synchrotron facility constructed and managed by the consortium CELLS (www.cells.es) and it includes a 3 GeV storage ring with a relatively low horizontal emittance, 4.6 nm×rad. ALBA synchrotron is the largest Spanish research infrastructure that started operation with official users in May 2012.

I will divide the talk in three parts: i) a succinct general description of the facility; ii) a brief overview of the operating beamlines and those under construction; and iii) a summary of applied crystallographic studies that are being carried out at our synchrotron.

I will start with a very brief description of our facility including milestones, staff structure, general parameters, and our accelerator complex: linac, booster and the store ring.

Secondly, I will introduce our seven operating beamlines. 1) BL13-XALOC: macromolecular crystallography, 2) BL04-MSPD: high-resolution and high pressure powder diffraction, 3) BL11-NCD: non-crystalline diffraction for small (and wide) angle X-ray scattering experiments (SAXS/WAXS), 4) BL29-BOREAS: soft X-ray magnetic circular dichroism and scattering; 5) BL24-CIRCE: photoemission spectroscopy (with near ambient pressure capabilities, NAPP) and microscopy (PEEM), 6) BL22-CLAESS: X-ray absorption and emission spectroscopies, and 7) BL09-MISTRAL: soft X-ray full-field cryo-microscopy.

Three additional beamlines are being currently built. 8) BL01-MIRAS: infrared micro-spectroscopy, to become operational in November 2016; 9) BL20-LOREA: angle resolved photo-emission spectroscopy, to become operational in December 2018; and 10) BL-MICROFOCUS-MX: microfocus for macromolecular crystallography, which will become operational in 2020. A scheme of the ten beamlines are given in Figure 1.

Thirdly, I will describe selected crystallographic works that are being carried out at our beamlines. These studies range from single crystal investigations of macromolecules at BL13-XALOC, to powder diffraction studies at BL04-MSPD, or bio- small angle scattering at BL11-NCD.

BL13-XALOC has an optics design based on an in-vacuum undulator, a Si(111) channel-cut crystal monochromator and a pair of mechanically bendable KB mirrors. This allows several operation modes including a focused configuration, where both mirrors can focus the beam at the sample position to 52 μm × 5.5 μm FWHM (H×V) and a defocused configuration that can match the size of the beam to the dimensions of the crystals. The endstation includes a high-accuracy single-axis diffractometer, a removable minikappa stage, an automated sample-mounting robot and a photon-counting detector that allows shutterless operation. Several examples of data collections and crystal structures will be presented.

BL04-MSPD powder diffraction beamline has a superconducting wiggler as photon source which allows a very broad energy range, 8-50 keV. The energy of the photons are selected using a Si(111) double crystal monochromator. Furthermore, MSPD has two endstations. The first endstation is devoted to high-resolution and high-speed powder diffraction. The detector system for high-resolution is a multycrystal analyzer setup coupled to point detectors, whereas the detector for high-speed data collection is a Mythen-II. Several examples of *in-situ* experiments will be presented. The second endstation is a microcrystal diffraction setup based on a KB mirror which results in a beam size close to 15 μm and a CCD detector system. Several types of experiments can be carried out including single-microcrystal like data collection in thin samples. However, this endstation is optimized for high-pressure powder diffraction studies in diamond-anvil-cells, DACs, where heating and cooling equipments are available (electrical resistance heating!). Examples of high-pressure studies using DACs will be presented.

Finally the capabilities of BL11-NCD for bio-SAXS will be presented. Here, it is possible to corroborate the structures determined by macromolecular crystallography of crystals for the same system(s) in solution. Aggregation effects as well as flexibility behavior, etc., may be characterized.

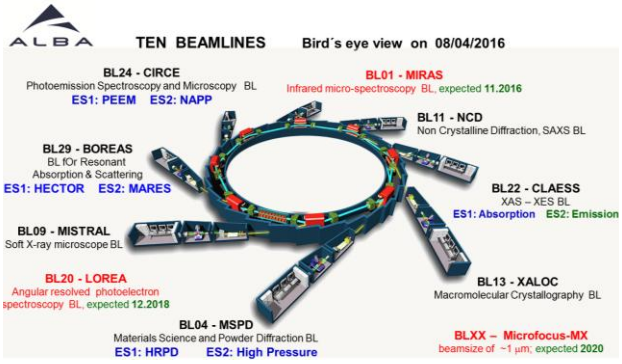

Figure 1. Overview of ALBA synchrotron beamlines as 08th of April, 2016.

L-24 **Friday, 17.06., 9^{00} - 9^{40}**

High Brilliance SAXS on synchrotrons

M. Roessle[1]*

[1]Luebeck University of Applied Science; Laboratory of X-Ray Engineering; Mönkhofer Weg 239; Lübeck; Germany

e-mail: manfred.roessle@fh-luebeck.de

The brilliance of the X-ray beam is the important quality parameter of X-ray sources. Brilliance sums up the beam parameters such as beam intensity, opening angle of the beam, size of the beam and the proportion of monochromaticity of the X-ray radiation. With existing modern X-ray optics many of these beam parameter can be altered, however beam focusing and the opening angle dependent strongly on the source. Because of the special arrangements of the beamline components SAXS relies on the high brilliance of the X-ray beam delivered by modern synchrotrons. At such state-of-the-art high brilliance beamlines high quality SAXS data are collected within several milliseconds on very small sample volumes. On the other hand, high brilliance X-rays are causing radiation damage especially to biological samples, which has to be treated by counteractions.

New developed, advanced sample environments based on microfluidic devices allows handling sample volumes of several pico-liters. Such devices are used for SAXS high throughput screening of hundreds of different sample conditions. If such a screening campaign includes as well automated data analysis procedures up to final model building, SAXS will be the method of choice for e.g. ligand screening in pharmaceutical industries.

Since microfluidic devices can operate on low flow rates on small channels, effects of low Reynolds numbers provide different types of SAXS experiments. For instance fast mixing of liquids is used for time resolved scattering experiments. Further applications are online sample preparation by applying mechanical and physical stress to the sample. While such techniques allow analyzing the kinetics of chemical or biochemical reactions, need investigations on the dynamics of a system a more sophisticated approach.

At high brilliance X-ray sources classical pump-probe experiments facilitates the analysis of reaction dynamics. For these investigations, for instance an ultra-short laser pulse is triggering the reaction in the sample. The high flux synchrotron beam is used for investigated the structural response of the system. Such experiments need, beside the brilliance of a synchrotron beam suitable fast detector system for recording the data in short time frames.

This lecture introduces the brilliance parameter and describe modern X-ray optics. The fields of applications are discussed and some experimental highlights shown. Possible strategies for handling radiation damage will be presented and future directions of SAXS introduced.

L-25 **Friday, 17.06., 9^{40} - 10^{20}**

Integration of SAXS with Complementary Techniques for Structural Characterization of Large Biomolecular Complexes

T. Madl[1,2,3,4]*, S. Rüdiger[5], M. Sattler[1,2] and J. Buchner[1,2]

[1]Department of Chemistry, Technical University Munich, Lichtenbergstraße 4, 85748 Garching, Germany
[2]Institute of Structural Biology, Helmholtz Zentrum München, Ingolstädter Landstraße 1, 85764 Neuherberg, Germany
[3]Institute of Molecular Biology & Biochemistry, Medical University of Graz, Harrachgasse 21/III, 8010 Graz, Austria
[4]Omics Center Graz, BioTechMed Graz, 8010 Graz, Austria
[5]Bijvoet Center for Biomolecular Research, Utrecht University, Padualaan 8, 3584 CH Utrecht, The Netherlands

Keywords: Integrative Structural Biology, SAXS, NMR, EM

*e-mail: tobias.madl@medunigraz.at

Structural analysis of multi-domain protein complexes is a key challenge in current biology and a prerequisite for understanding the molecular basis of essential cellular processes. The use of solution techniques is important for characterizing the quaternary arrangements and dynamics of domains and subunits of these complexes. As experimental data for large protein complexes are sparse, it is advantageous to combine these data with additional information from other solution techniques.

In my presentation I will show our recent achievements in integrating Small-Angle X-ray Scattering (SAXS) data with complementary data from Nuclear Magnetic Resonance Spectroscopy, X-ray crystallography, electron microscopy, and mass spectrometry to study structure and dynamics of large disease-related proteins and protein complexes [1-9]. By using our integrated approach we were able to provide a comprehensive and accurate description of protein complex structure and dynamics in a native-like environment. This underscores the central role of SAXS for structure determination of protein complexes and ensures its unique role and contributions in integrated structural biology approaches in the future.

Acknowledgments: This work was supported by the Bavarian Ministry of Sciences, Research and the Arts (Bavarian Molecular Biosystems Research Network), the German Research Foundation (Emmy Noether program MA 5703/1-1), the Center for Integrated Protein Science Munich (CIPSM), and the Austrian Science Fund (FWF: P28854).

---

[1] M. Gersch, K. Famulla, M. Dahmen, C. Gobl, I. Malik, K. Richter, V. S. Korotkov, P. Sass, H. Rubsamen-Schaeff, T. Madl, H. Brotz-Oesterhelt, S. A. Sieber, *Nat. Comm.* **6** (2015) 6320.

[2] C. Gobl, T. Madl, B. Simon, M. Sattler, *Prog Nucl Magn Reson Spectrosc* **80** (2014) 26.

[3] V. Haslbeck, J. M. Eckl, A. Drazic, D. A. Rutz, O. R. Lorenz, K. Zimmermann, T. Kriehuber, C. Lindemann, T. Madl, K. Richter, *Sci Rep* **5** (2015) 17058.

[4] J. R. Huang, L. R. Warner, C. Sanchez, F. Gabel, T. Madl, C. D. Mackereth, M. Sattler, M. Blackledge, *J Am Chem Soc* **136** (2014) 7068.

[5] G. E. Karagoz, A. M. Duarte, E. Akoury, H. Ippel, J. Biernat, T. Moran Luengo, M. Radli, T. Didenko, B. A. Nordhues, D. B. Veprintsev, C. A. Dickey, E. Mandelkow, M. Zweckstetter, R. Boelens, T. Madl, S. G. Rudiger, *Cell* **156** (2014) 963.

[6] O. R. Lorenz, L. Freiburger, D. A. Rutz, M. Krause, B. K. Zierer, S. Alvira, J. Cuellar, J. M. Valpuesta, T. Madl, M. Sattler, J. Buchner, *Mol Cell* **53** (2014) 941.

[7] R. Muller, M. A. Grawert, T. Kern, T. Madl, J. Peschek, M. Sattler, M. Groll, J. Buchner, *Proc Natl Acad Sci U S A* **110** (2013) 10183.

[8] A. Rohl, F. Tippel, E. Bender, A. B. Schmid, K. Richter, T. Madl, J. Buchner, *EMBO Rep* **16** (2015) 240.

[9] A. Rohl, D. Wengler, T. Madl, S. Lagleder, F. Tippel, M. Herrmann, J. Hendrix, K. Richter, G. Hack, A. B. Schmid, H. Kessler, D. C. Lamb, J. Buchner, *Nat Commun* **6** (2015) 6655.

L-26 **Friday, 17.06., 10^{20} - 11^{00}**

Mineral dust iron geochemistry of the last 160 kyears

A. Marcelli[1,2]*

[1] *INFN - Laboratori Nazionali di Frascati, Via E. Fermi 40, I-00044 Frascati, Italy*

[2] *RICMASS, Rome International Center for Materials Science Superstripes, Via dei Sabelli 119A, 00185 Rome, Italy*

*e-mail: marcelli@lnf.infn.it

Windblown mineral particles (dust) plays a key role in the climate system and many challenging studies allowed the quantitative estimation of direct and indirect effects on climate and environmental phenomena. Dusts are naturally stored in glaciers and ice sheets from polar areas represent unique natural archives of the particulate present in the atmosphere. Among the many challenging researches on aerosols/dust the current emergency determined by the global warming is triggering scientists to carefully look for signs of past climate changes. Indeed, the reconstruction of past climate trends may be useful to understand the Earth's climate and, eventually, paleoclimatic data could help to understand the balance between positive feedback components such as greenhouse gases and negative feedback components like mineral dust. The most precise information on Earth's climate variation can be extracted from ice cores drilled both in polar and mid-latitude-high-altitude glaciers. Within this framework, the characterization of low concentration of airborne particles in natural ice is fundamental. TALDICE (*Talos Dome* Ice Core) is a 1620 m long ice core, retrieved from *Talos Dome*, a peripheral dome of the *East Antarctic* plateau. The proximity to the sea influences the moisture budget and guarantees a high snow accumulation rate and thus a high time resolution of the climatic record. The TALDICE atmospheric dust record presents peculiar features, related to the influence of local *Antarctic* dust sources and to the regional atmospheric circulation, which affects the *Ross Sea* region [1,2].

The reconstruction of undisturbed stratigraphic sequences of dusty ice layers from shallow and deep ice cores provides information on the temporal variability of atmospheric dust loads and allows investigating the dust-climate coupling on different timescales. In addition, characterization of dust dispersed in the ice cores to correlate past environmental and climatic conditions with particles source areas is now possible. Cutting-edge synchrotron radiation-based spectroscopic techniques such as Total-Reflection X-Ray Fluorescence (TXRF) and X-ray Absorption Near Edge Structure (XANES) have been used to investigate in a non-destructive way the microparticle mineralogy. However, experiments are extremely challenging for *Antarctic* ice core samples, where mineral concentrations are extremely reduced and dust is often mixed with poorly crystalline material such as volcanic glasses. Experiments performed at the *Stanford Synchrotron Radiation Laboratory* (SSRL) and at the *Diamond* facility in *Oxford*, allowed to identify and to compare the mineral composition. XANES spectra combined with TXRF results not only demonstrate the feasibility of such kind of analysis but also that it may usefully complement other techniques commonly used in the ice core analysis [3,4].

I will show that the application of techniques usually applied in the field of materials science, mineralogy and crystallography can give an important contribution to ice core science, with new and original information. The interpretation of data and the extraction of useful climatic proxy is still in progress but premises are extremely encouraging. Preliminary results point out that the atmospheric dust deposited at *Talos Dome* during the last 160 kyr is not uniform, pointing out a clear and significant variability. The analysis could be a first step toward the comprehension of this and other unsolved climatic issues.

---

[1] B. Delmonte *et al., J Quat Sci.,* **25** (2008) 1327.

[2] S. Albani *et al., Clim. Past,* **8** (2012) 741.

[3] G. Cibin, *et al., Spectr. Acta B* **63** (2008) 1503.

[4] A. Marcelli, *et al., J. Anal. At. Spectrom.* **27** (2012) 33.

L-27 **Friday, 17.06., 11^{40} - 12^{20}**

Solaris as a new class of low energy and high brightness light source

A. I. Wawrzyniak[1]* on behalf of the Solaris Team

[1]*Solaris National Synchrotron Radiation Centre, Jagiellonian University Czewone Maki 98, 30-392 Kraków, Poland*

Keywords: low emittance, doble bend achromat, synchrotron radiation, tune, chromaticity

*e-mail: adriana.wawrzyniak@uj.edu.pl

In the light sources the main figure of merit for users is a high brightness of the synchrotron radiation. However, the brightness strongly depends on the horizontal and vertical emittance of the circulating electron beam in a storage ring. Over decades the lattice design of the storage rings has evolved and the natural emittance has been significantly reduced up to few nanometers. Recently the new generation of diffraction limited light sources has been considered [1-7] and designed [8-11] allowing for further reduction of the emittance up to picometers. One of such an example is the MAX IV 3.0 GeV storage ring in Lund, Sweden [4,8], that is now under commissioning. The concept of diffraction limited lattice design uses the multi bend achromat (MBA) cells, since the natural emittance decreases with the increase of dipole magnets number to the third power. Other way to achieve the natural emittance reduction is to increase damping partition number. This can be achieved by designing combined function magnets with strong focusing.

Solaris, which is a replica of the MAX IV 1.5 GeV storage ring, although is not using the MBA lattice, has many of the technological innovative concepts used for ultra-low emittance storage rings. As such, Solaris uses a single solid iron block containing all the multipole magnets of the double bend achromat [12]. The iron block has accurately machined pole profiles of the gradient bending magnets, the quadrupole/sextuple magnets and multipole corrector elements. The magnet is its own girder allowing for very fast and smooth installation. The use of small magnet gaps brings the benefit of high fields but requires vacuum chambers of high mechanical accuracy and distributed pumping. Recently, Solaris light source was constructed in Krakow, Poland and the commissioning of the storage ring has started in May 2015 [13,14]. After 2 weeks of optimisation the first light at the bending magnet beamline front end was observed. After 7 months of commissioning good performance of Solaris synchrotron has been achieved. The injection to the storage ring occurs at 525 MeV and the beam is ramped up to the final energy of 1.5 GeV. The optics has been corrected close to the design one. Solaris is operating at the working point of (11.22, 3.15) and the corrected chromaticity of (+0.89, +0.9). The stored electron current in the storage ring is increasing (Fig1). Recently, 511 mA of current was possible to store at the injection energy.

The vacuum system of storage ring is still under conditioning. After 28 Ah of beam cleaning the lifetime at 100 mA is 3h. In April 2016 the UARPES undulator has been tested and put into operation, which required some optics adjustment. The UARPES beamline commissioning has started. Within this presentation the current status of Solaris facility and the commissioning results will be presented.

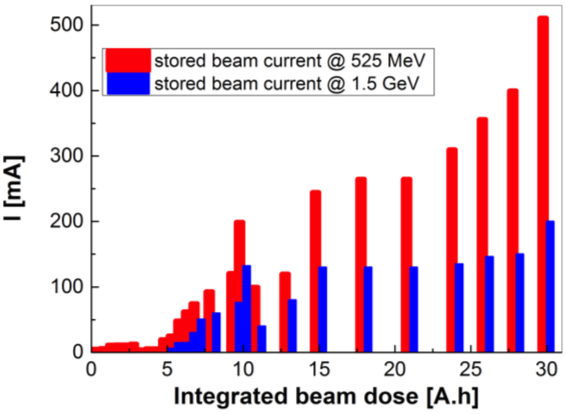

Figure 1. The stored beam current vs. integrated beam dose.

Acknowledgments: Authors would like to thank the MAXIV and Elettra teams and D. Einfeld (ESRF) for providing necessary support during design, installation and commissioning phases. Acknowledgments to F. Perez (ALBA) and G. Rehm (Diamond) for help and fruitful discussions in the Solaris control room.

---

[1] D. Einfeld, M. Plesko, *Nucl. Instrum. Methods Phys. Res., Sect. A* **335** (1993) 402.
[2] W. Joho, P. Marchand, L. Rivkin, A. Streun, *Proc. Of EPAC 94*, London, England (World Scientific, River Edge, NJ), (1994) 627.
[3] D. Einfeld, J. Schaper, M. Plesko, *Proc. of PAC1995*, Dallas, TX, (1995) 177.
[4] S.C. Leemann, Å. Andersson, M. Eriksson, L.-J. Lindgren, E. Wallén, J. Bengtsson, A. Streun, *Phys. Rev. ST Accel. Beams* **12** (2009) 120701.
[5] M. Borland, V. Sajaev, Y. Sun, *Proc. of PAC2013*, Pasadena, CA, (2013) 249.
[6] Y. Sun, M. Borlnad, *Proc. of IPAC2015*, Richmond, VA, USA TUPJE071, (2015) 1803.
[7] H. Tarawneh *et al.*, *Proc. of PAC2013*, Pasadena, CA, 2013 (IEEE, New York, 2013), MOPHO23, (2013) 288.
[8] MAXIV Detailed Design Report, https://www.maxlab.lu.se/node/113
[9] L. Farvacque *et al.*, *Proc. of IPAC2013*, Shanghai, China, MOPEA008 (2013) 79.
[10] J-L. Revol, *et al.*, *Proc. Of IPAC2014*, Dresden, Germany, MOPRO055 (2014) 209.
[11] L.Liu *et al.*, *Proc. of IPAC2013*, Shanghai, China, (2013) 1874.
[12] M.R. Bartosik *et al.*, *Radiat. Phys. Chem.* **93**, (2013) 4.
[13] A.I. Wawrzyniak *et al.*, *Proc. of IBIC2015*, Melbourne, Australia, WEDLA01, (2015) 602; http://www.JACoW.org
[14] A.I. Wawrzyniak *et al.*, to be published in *Proc. of IPAC2016*, WEPOW029 (2016).

L-28 **Friday, 17.06., 15^{00} - 15^{40}**

Chemical imaging of functional materials under process conditions

A. M. Beale[1,2]*, S. D. M. Jacques[2,3], M. Di Michiel[4], J. F. W. Mosselmans[5], S. W. T. Price[5], P. Senecal[1,2] and A. Vamvakeros[1,2]

[1] *Department of Chemistry, UCL, 20 Gordon Street, London, WC1H 0AJ*
[2] *Research Complex at Harwell, Didcot OX11 0FA*
[3] *School of Materials, Manchester University, Oxford Road, Manchester, M13 9PL*
[4] *ESRF, BP 220, F-38043 Grenoble, France*
[5] *Diamond Light Source, Harwell Science and Innovation Campus, Didcot, OX11 0DE*

*e-mail: andrew.beale@ucl.ac.uk

The imaging of catalysts and other functional materials under reaction conditions has advanced significantly in recent years [1,2]. The combination of the computed tomography (CT) approach with methods such as X-ray diffraction (XRD), X-ray fluorescence (XRF), and X-ray absorption near edge spectroscopy (XANES) [3-5] now enables local chemical and physical state information to be extracted from within the interiors of intact materials which are, by accident or design, commonly inhomogeneous. The spatially resolved signals obtained can reveal information that would otherwise be lost in bulk measurement. Such local signals are simpler to interpret since they are highly likely to contain fewer phases. Studying intact materials rather than idealised powders allows for behaviour under industrially relevant conditions to be observed. Furthermore the background signal from in situ apparatus / cell can be readily separated.

We show how such methods have been applied to understanding the behaviour of a number of catalytic systems at a range of length scales. Crucially we demonstrate that the obtained chemical and physical information can be correlated to catalytic activity and selectivity. At the small length scales, sample size and density allow for transmission of comparatively low energy signals allowing combination of XRF-CT and XANES-CT in conjunction with XRD-CT, enabling simultaneous multi-technique imaging. This combined approach has been used to characterise intact single catalytic particles (a 100 μm Mo promoted Pt/C catalyst under liquid phase hydrogenation operating conditions [3,4]) and packed bed micro-reactors (500 μm reactor containing Co/SiO_2 Fischer Tropsch catalysts under methanation conditions), enabling identification of active species and correlation to performance. High energy XRD-CT enables large/dense objects to be studied. We show how this has been used to study the behaviour of industrial pellets (e.g. following the evolution of the cobalt phases in 3 mm diameter $Co/\gamma\text{-}Al_2O_3$ catalyst under industrial conditions) and also to see inside working bulk reactors (6 mm catalytic membrane reactor device used for the oxidative coupling of methane; the reactor consists of a dense ceramic oxygen transport membrane containing a packed bed of $Mn\text{-}Na\text{-}W/SiO_2$)[5]. In the latter case the active state is captured and material is observed to form that is likely to impact on the long term performance of the reactor. Such information is vital to rational catalyst and reactor design that cannot be obtained by conventional bulk measurements.

Acknowledgments: This work was supported by EPSRC (UK), BP, Diamond Light Source Ltd and ESRF.

---

[1] A. M. Beale, *et al., Coord Chem Rev* **277** (2014) 208.
[2] J. D. Grunwaldt *et al., Chem Cat Chem* **5** (2013) 62.
[3] S. W. T. Price, *et al., PCCP* **17** (2015) 521.
[4] S. W. T. Price, *et al., Angew. Chem. Int. Ed.* **54** (2015) 9886.
[5] A. Vamvakeros, *et al., Chem Comm* **51** (2015) 12752.

L-29 **Friday, 17.06., 15^{40} - 16^{20}**

Enhancing the sensitivity of X-ray based techniques by pulse experiments

D. Ferri[1]*

[1]*Paul Scherrer Institut, 5232 Villigen, Switzerland*

Keywords: synchrotron radiation, modulation experiments

*e-mail: davide.ferri@psi.ch

X-ray based synchrotron methods are invaluable tools for materials characterization under relevant process conditions. In the particular case of heterogeneous catalysis, these methods have become indispensable to obtain key structural information on catalytic materials under in situ and operando conditions. High energy X-rays further enable larger cross sections and sufficient time-resolution to follow rapid structural changes in the sub-second regime.

Despite the enormous advantages over traditional characterization methods, the large majority of the X-ray based techniques remain bulk-sensitive. Thus subtle structural changes, which could be associated to near surface variations, are obscured by bulk structural changes. This issue is further hampered by the fact that typical experiments are carried out at steady state under static conditions. Pulse experiments offer a possibility of improvement because the catalyst is stimulated to perform a specific event and to exhibit the structural changes associated with that event. Repetition of the event, thus repeated pulses (modulation), already improve the signal-to-noise ratio of any spectroscopic/diffraction method. Further enhancement can be achieved by filtering out the static signals, e.g. the unresponsive bulk, by phase sensitive analysis (Figure 1) [1]. It should be emphasized that this approach is valid irrespective of spectroscopy/diffraction method. Pulse experiments not only represent a powerful analytical method to increase sensitivity of a given characterization technique to small changes. From a catalytic view point, they can also simulate the operation of some specific automotive catalysts but also the regeneration of catalysts in large scale industrial plants.

The potential of pulse experiments is demonstrated in the specific cases of X-ray absorption spectroscopy (XAS) and high energy X-ray diffraction (XRD) of catalysts based on precious metals (Pd, Rh) used in automotive catalysis. In the case of XAS, pre-reduced 2 wt% Pd/Al_2O_3 and 2 wt% Rh/Al_2O_3 are compared during repeated CO-NO pulses at 300°C [2]. Partial re-oxidation of both metals in the presence of NO can be followed only after phase sensitive analysis of the time-resolved spectra. Moreover, generation of carbidic species, which are necessarily formed at the surface of Pd nanoparticles, is also enhanced by analysis of the phase-resolved data and by the EXAFS fit of Pd/Al_2O_3.

In the case of high energy XRD, the advantage of using this approach is emphasized in the case of 2 wt% Pd/$CeZrO_2$ (Pd/CZ) [3] that is typically silent in the XRD with respect to the Pd-PdO phase. The time-resolved high energy XRD data collected during CO-O_2 experiments at 300°C display the reflections of the bulk material but hardly display any tangible change. Given the fine dispersion of PdO induced by CZ, no information is available about the state of Pd. The XRD data after phase sensitive analysis exhibit only the very subtle changes associated with the signals responding to the modulation experiment. Besides providing information on the dynamics of reduction and re-oxidation of the Ce^{3+}/Ce^{4+} pair, the data also shows additional broad features corresponding to reflections of Pd nanoparticles of 2 nm. The sole intensity change is associated with the relative increase of long range order attributed to PdO reduction. Therefore, the modulation data can capture simultaneously the dynamic reduction and re-oxidation of PdO and CZ.

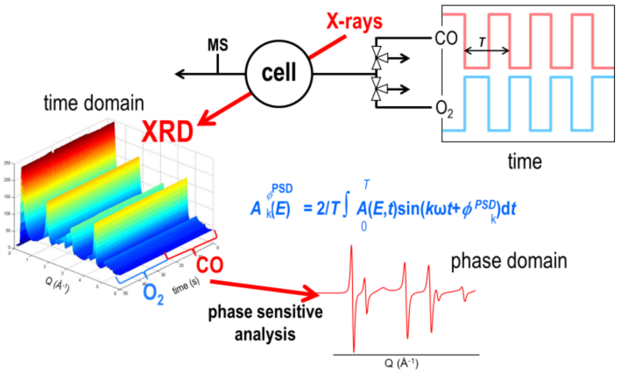

Figure 1. Layout of a high energy XRD modulation experiment.

In conclusion, subtle structural changes in XAS spectra and XRD patterns can be captured and their temporal response precisely assessed by performing modulation experiments. This provides access to detailed structural-dynamic behaviour of catalytic systems.

Acknowledgments: This work was supported by the Swiss National Science Foundation (SNF) and the Competence Center for Materials Science and Technology (CCMX).

---

[1] D. Baurecht, U. P. Fringeli, *Rev. Sci. Instrum.* **72** (2001) 3782.

[2] D. Ferri, S. K. Matam, R. Wirz, A. Eyssler, O. Korsak, P. Hug, A. Weidenkaff, M. A. Newton, *PCCP* **12** (2010) 5634.

[3] D. Ferri, M. A. Newton, M. Di Michiel, G. L. Chiarello, S. Yoon, Y. Lu, J. Andrieux, *Angew. Chem.* **53** (2014) 8890.

L-30 **Friday, 17.06., 16^{50} - 17^{30}**

The protein structure by the combination of SAXS, light scattering and simulations

E. M. Banachowicz[1]* and A. Patkowski[1]

[1] *Faculty of Physics, Adam Mickiewicz University of Poznan, Umultowska Street 85, 61-614 Poznań, Poland*

Keywords: gyration radius, form factor, hydrodynamic parameters, overall shape

*e-mail: ewas@amu.edu.pl

The knowledge of the proteins and the nucleic acids structure is crucial to understanding how these molecules are involved in a extremely complex network of interactions related to the life processes of all living organisms. Therefore for decades the high-resolution experimental techniques determining the spatial arrangement of all elements of the biological molecules with a precision of individual atoms have been developed. Despite the fact that in 30 years of existence Protein Data Bank nearly 120,000 of the spatial structures were solved, the number of known and predicted protein is many times greater. Many of these structures cannot be solved either by conventional diffraction techniques or NMR spectroscopy. Sometimes, however, even general information about the shape of the molecule is sufficient to reproduce a more detailed picture of its construction. Sufficient information can provided by low-resolution techniques based on small angle scattering like for example SAXS or hydrodynamic techniques like dynamic light scattering (DLS), fluorescence correlation spectroscopy (FCS), viscosimetry and analytical ultracentrifugation (AUC).

The techniques classified as low-resolution allow only to determine the overall shape and size of molecules in solution. However, a combination of these techniques can significantly extend the interpretation of the experimental results. This statement was tested on protein with known three-dimensional structure as well as wide set of hydrodynamic and structural parameters. As a simple example the combination of hydrodynamic radius of lysozyme with data on hydration and partial specific volume is presented. The partial specific volume, thickness and density of hydration layer determine the radius of the spherical model of the molecule, R_h. The ratio of hydrodynamic radius, R_H, to R_h evaluates a sphericity of lysozyme and the spherical model can be replacement by the model of ellipsoid. The length of semi-axis, a and b, of "dry" prolate ellipsoid corresponded with the dimensions known from the crystallographic structure of lysozyme. Afterwards the combination of hydrodynamic radius, partial specific volume, hydration with crystallographic structure of lysozyme was chosen to clarify possible changes in the protein structure under elevated pressure. The R_H of lysozyme was measured at an elevated pressure and information on the density of hydration layer in these conditions were find. The compilation of collected parameters showed decrease in dimensions of ellipsoid describing particle at pressure of 150 MPa in comparison to the structure under ambient conditions. A significant reduction concerned the major semi-axes. The most likely explanation assumes the collapse of a deep crevice known from 3D-structure, which divides the protein into two domains.

The radius of gyration, R_G, and hydrodynamic radius, R_H, are associated with shape and dimension of biological molecule in a similar manner. Both the measurement of radius of gyration and hydrodynamic radius of small molecules in solution require high precision and often are marred by an error resulting from interpartical interactions (impact of the structure factor). In addition, for a single radius a whole family of divers models can be offered. However, the use of the relation linking R_H, R_G and ratio b/a, can significantly reduce the number of solutions and cross-check the dimensions designated by different experimental techniques (Fig.1).

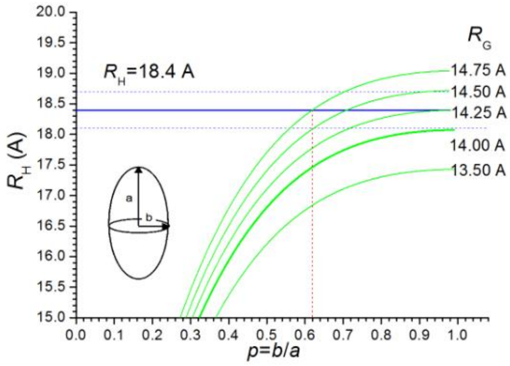

Figure 1. The dependence of hydrodynamic radius vs. ratio of semi-axis for constant values of gyration radius of prolate ellipsoid. The horizontal line indicates the experimental value of R_H.

At present a variety of methods for design of more specific structural models of the molecules in solution are developed. The starting point for more complex models are experimental form factors and/or hydrodynamic parameters in combination with either the high-resolution structure or an *ab initio* modeling [1-3]

The easiest way to build a detailed model of the protein is the distribution of its elements in a space defined by the coordinates of atoms of the experimentally solved or predicted structure. This type of model can be used among other to investigate the structure associates and the polydispersity of experimentally tested solution. While coupling model simulation of the internal dynamics of the protein chain allows to recognize conformational changes, for example, at different conditions of solvent.

The algorithms allowing to random motions of model of the polypeptide chain are the basis for modeling the structure of the intrinsically disordered proteins. This group of proteins discovered nearly 20 years ago constitutes a serious challenge for all known experimental techniques of the spatial structure determination. One of the tactics used for analysis of the structure of random coil is coupling simulation of the free movement of the chain with the measurements of its overall structural parameters (Fig. 2).

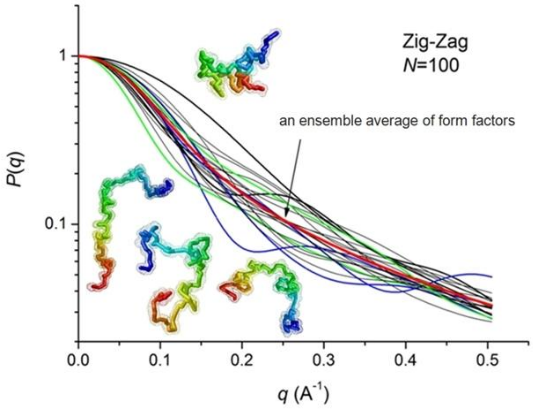

Figure 2. Experimentally measured form factor of the unfolded protein chains corresponds to the ensemble average of all conformations. The ensamble average – indicated by the arrow, at the same time all form factors corresponding to particular chain conformations are obtained - all other lines.

For example based on a large population of equilibrium conformations generated by the simulations the hydrodynamic parameters, the gyration radii and the form factors of the protein chains can be determined. The result of the simulations is an ensemble averaged set of values that could be compared with the experimental data. The population of positively verified models can be used chain by chain for the analysis of chains' local trends.

---

[1] J. Blobel, P. Bernadó, D.I. Svergun, R. Tauler, M. Pons, *J. Am. Chem. Soc.* **131** (2009) 4378.

[2] M. H. J. Koch, P. Vachette, D. I. Svergun, *Quarterly Reviews of Biophysics* **36** (2003)147.

[3] P. Chacón, J. F. Díaz , F. Morán, J. M. Andreu, *J. Mol. Biol.* **299** (2000) 1289.

L-31 **Friday, 17.06., 17^{30} - 18^{10}**

An in-situ synchrotron X-ray view on the crystallization of synthetic polymers for 3D printing under Fast Scanning Calorimetry conditions

B. Goderis[1]*, D. Baeten[1], O. Verkinderen[1], G. Portale[2], P. Van Puyvelde[1] and V.B.F. Mathot[1]

[1]KU Leuven, Celestijnenlaan 200F, 3001 Heverlee, Belgium
[2]Zernike Institute for Advanced Materials, Nijenborgh 4, 9747 AG Groningen, The Netherlands

Keywords: fast calorimetry, synchrotron WAXD and SAXS, polyamides

*e-mail: bart.goderis@chem.kuleuven.be

Nowadays fast scanning chip calorimeters (FSC) are commercially available, allowing to study the thermal behavior of sub microgram samples at heating rates up to 40000 °Cs^{-1} and cooling rates up to 5000 °Cs^{-1} [1-2]. In fact, for maintaining thermal control, minute sample amounts are mandatory rather than optional. Besides downscaling in sample mass, the availability of fast rates opens the possibility to create and study metastable structures that otherwise remain inaccessible. However, although the thermal behavior reveals the presence of such structures, the calorimeter on its own cannot identify their nature or morphology. Moreover, some of these phases are short living or only existing at temperatures other than room temperature by which morphological investigations of the material conditioned on the chip – after having been detached from the calorimeter - are not possible. There is therefore a need for methodologies that provide morphological information at the scanning rates comparable to those of such chip calorimeters.

We recently modified an existing Mettler Flash DSC 1 in such a way that the chip can be controlled outside the machine. The chip in action can therefore be presented in front of an X-ray beam.

Experiments were conducted at DUBBLE, the Dutch Belgian Beam Line at the ESRF. The setup and the measuring protocol (stroboscopic data acquisition) were optimized by using high-density polyethylene (HDPE). WAXD patterns at every degree during the crystallization and melting at FSC typical scanning rates from 20 up to 200 °C s^{-1} were analyzed in terms of the temperature and scanning rate dependent material crystallinities and crystal densities. Interestingly, the combined approach revealed FSC thermal lag issues, for which can be corrected [3].

In a second set of experiments the high-rate crystallization and melting behavior of polyamide 12 (PA12) and polyamide 11 (PA11) was considered. These polymers are used in 3D printing via the selective laser sintering (SLS) of 50 μm grains. High rate crystallization and melting is inherent to this sintering process. The isothermal crystallization of PA11 and PA12 were studied over the entire temperature range between the glass transition temperature and the melting temperature. Using coooling rates of 1000 °Cs^{-1} allowed bypassing crystallization on cooling which enabled studying the isothermal crystallization at large supercooling. Similar to other polymers reported in literature [4], a bimodal crystallization rate dependence on temperature is observed for PA11and PA12 (Figure 1).

Isothermal solidification at high supercooling yields a mesomorphic phase in less than a second, whereas at very low supercooling crystals are obtained. At intermediate supercooling, mixtures of mesomorphic and crystalline material are generated at a ratio proportional to the supercooling. This ratio is constant over the isothermal solidification time [3]. The obtained data lead to the hypothesis that the two maxima in the crystallization rate are due to a crystallization retardation at the minimum in the crystallization rate curve. This retardation results from the competition between mesomorphic and crystalline phase formation and is referred to as 'self-poisoning'.

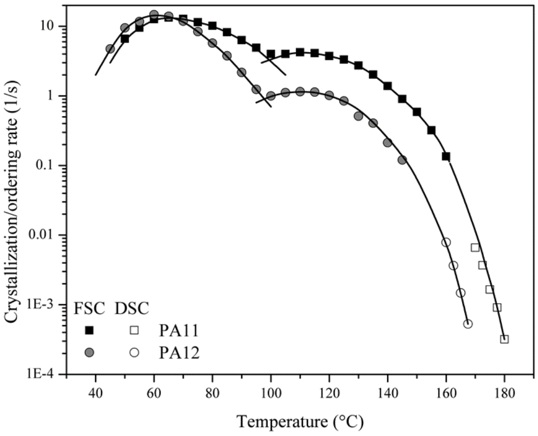

Figure 1. FSC-based crystallization rate of PA11 and PA12.

Acknowledgments: This work was supported by the research fund of the KU Leuven (IDO), FWO Vlaanderen (Project No. G.0495.10N), the SIM Stream Program, and by SciTe B.V. (The Netherlands).

[1] E. Zhuravlev, C. Schick, *Thermochim. Acta*, **505**(1-2) (2010) 1 and ditto 14

[2] V. Mathot, M. Pyda, T. Pijpers, G. Vanden Poel, E. van de Kerkhof, S. van Herwaarden, F. van Herwaarden, A. Leenaers, *Thermochim. Acta* **522**(1-2) (2011) 36.

[3] D. Baeten, V. B. F. Mathot, T. F. J. Pijpers, O. Verkinderen, G. Portale, P. Van Puyvelde, B. Goderis, *Macromol. Rapid Commun*. **36**(12) (2015) 1184.

[4] R. Androsch, A. M. Rhoades, I. Stolte, C. Schick, *Eur. Polym. J.* **66** (2015) 180.

L-32 **Saturday, 18.06., 9^{00} - 9^{40}**

Investigating the structure of liquid metals at extreme conditions by X-ray absorption spectroscopy

A. Trapananti[1]*, F. Iesari[2], G. Aquilanti[3]
and A. Di Cicco[2]

[1]*CNR-Istituto Officina dei Materiali, c/o Department of Physics, University of Perugia, Perugia, Italy*
[2]*School of Science and Technology, Physics Division, University of Camerino, Camerino (MC), Italy*
[3]*Elettra–Sincrotrone Trieste S.C.p.A., Trieste (Italy)*

Keywords: liquid metals, x-ray absorption spectroscopy, high-temperature, high-pressure

*e-mail: trapananti@iom.cnr.it

Investigating the structure of stable and undercooled liquids over a wide pressure range is an important issue in fundamental physics and represents an extraordinary experimental challenge with large implications in other fields, such as materials science and geophysics.

X-ray absorption spectroscopy (XAS) has the capability to provide atom specific information concerning interatomic distances and coordination numbers and, in favourable cases, beyond the pair correlations, on higher order distributions. For the analysis of liquids and disordered systems, a combination of molecular modelling methods and experimental data is essential to move beyond the traditional peak-fitting approach. For our studies, Reverse Monte Carlo (RMC) modelling has been implemented into XAS data analysis codes (RMC-GNXAS) [1] and provides realistic three dimensional models of the structure of disordered systems compatible with data sets from both XAS and diffraction experiments. Such models can then be analysed in terms of pair distribution functions, coordination numbers and bond angle distributions to obtain a complete insight into the atomic correlations at the microscopic level.

Within this contribution, some applications of XAS and Reverse Monte Carlo for the investigation of elemental liquid metals at ambient and high pressure conditions will be reviewed.

For liquid and undercooled Cu and Ni [2,3] at ambient pressure, signatures of short-range fivefold ordering have been investigated and estimates of the fraction of nearly-icosahedral configurations were obtained.

In the case of liquid Sn [4], the local coordination and geometry have been investigated up to moderate pressure (< 5 GPa) and related to the possible occurrence of pressure induced transitions between two different liquid phases (polyamorphism), largely debated for such metals involving directional and open coordination environments.

Recent experiments for the determination of the melting temperature of Fe at extreme pressure (up to the megabar) by XAS [5] will be also reported.

---

[1] A. Di Cicco, A. Trapananti, *J. Phys. Condens. Matter* **17** (2005) S135.

[2] A. Di Cicco, A. Trapananti, S. Faggioni, A. Filipponi, *Phys. Rev. Letters* **91** (2003) 135505.

[3] A. Di Cicco, F. Iesari, S. De Panfilis, M. Celino, S. Giusepponi, A. Filipponi, *Physical Rev. B* **89** (2014) 060102.

[4] A. Di Cicco, A. Trapananti, E. Principi S. De Panfilis, A. Filipponi, *Appl. Phys. Lett.* **89** (2006) 221912.

[5] G. Aquilanti, A. Trapananti, A. Karandikar, I. Kantor, C. Marini, O. Mathon, S. Pascarelli, R. Boehler, *PNAS* **112** (2015) 12042.

L-33 **Saturday, 18.06., 9^{40} - 10^{20}**

Extended Abstract

Crystallography at high pressure using synchrotron radiation

M. Hanfland[1]*

[1]*European Synchrotron Radiation Facility, 71, avenue des Martyrs, CS 40220, 38043 Grenoble, France*

Keywords: high pressure, crystallography

*e-mail: hanfland@esrf.fr

ID09A was a state of the art high pressure diffraction beamline at the ESRF, carrying out monochromatic diffraction experiments with large area detectors. Powder and single crystal diffraction experiments could be performed at high pressures in diamond anvil cells, permitting accurate determination of crystallographic properties of the investigated samples. After more than 20 years of successful operation, ID09A has been closed in November 2015. It will be replaced by a new and improved beamline, ID15B.

X-ray source for ID15B will be the U20 in vacuum undulator from ID09A. The monochromator will be a horizontally diffracting nitrogen cooled Si (111) single bounce Bragg monochromator. ID15B will operate at a fixed angle with an energy of 30 keV. Experience with ID09A has shown, that 30 keV is well matched for high pressure diffraction experiments in DACs. Two transfocators with 200 μm diameter linear (1-D) beryllium compound refractive lenses for vertical and horizontal focussing, respectively, will provide a highly variable and very clean beam with an expected minimum spot size on the sample of less than 5 x 5 μm^2. The expected flux will be comparable to ID09A. The experimental setup, build mostly from components already in use on ID09A, will be located on an extremely stable granite table. Data will be collected with a MAR555 flat panel detector.

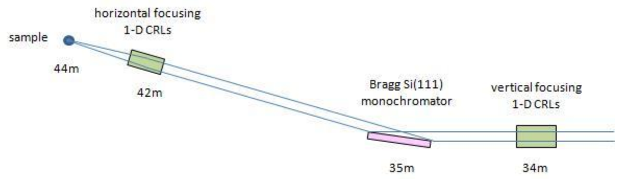

Figure 1. Optical layout of ID15B.

Recent technical advances have significantly added to the utility of single crystal X-ray diffraction experiments at high pressures [1]. New ways of supporting diamond anvils, like Boehler Almax anvils [2], have considerably increased the volume of accessible reciprocal space. Use of Helium or Neon as pressure transmitting medium extends substantially the practicable pressure range. Flat panel detectors have noticeably decreased the data collection time and increased the accuracy. Data can be collected at low and high temperatures. Even single crystal diffraction experiments with laser heating have become possible [3].

One system extensively studied with single crystal diffraction is arsenolite (As_4O_6) and its interaction with Helium. During a first experiment [4] we discovered that Helium can enter the molecular arsonolite crystal forming an intercalation compound with the stoichiometry As_4O_6 + 2He. The same type of reaction was observed independently in powder diffraction experiments [5]. To better understand the transformation more diffraction experiments on single crystals with ~25 μm diameter were performed. He penetration starts between 3 and 4 GPa and is complete after 2 days. Split reflections and changing intensity ratios indicate, that He is slowly infiltrating the crystal from the outside. During pressure release He leaves the arsenolite crystal at 3 GPa. The He discharge is fast.

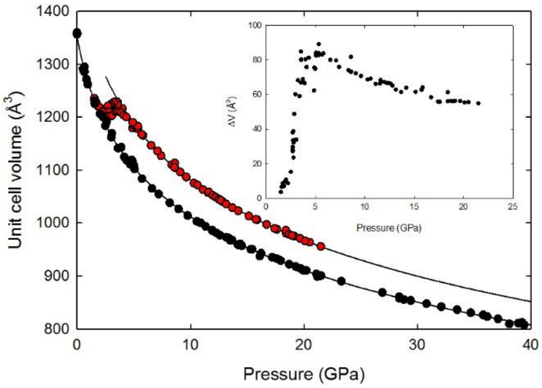

Figure 2. Volume of As_4O_6 (black dots) and As_4O_6 + 2He (red dots) as function of pressure. The insert shows the volume difference, decreasing from 80 Å^3 after complete intercalation at 5 GPa to 60 Å^3 at 20 GPa.

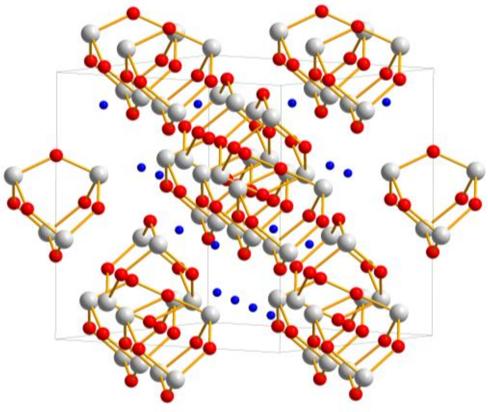

Figure 3. Structure of As_4O_6 + 2He at 11.6 GPa. The Helium atoms (blue) are in the 16c positions (origin choice 1, centre of the As_4O_6-molecules in the 8*b* positions).

The structure of the He intercalated arsenolite was determined from the single crystal data. He intercalated As_4O_6 remains cubic (S.G.: *Fd*-3*m*). Difference Fourier maps show, that the He atoms are located in the 16c positions. Refinement indicates, that the 16c positions are probably fully occupied confirming the As_4O_6 + 2He stoichiometry.

No penetration is observed with Neon as pressure transmitting medium. He infiltration can also be avoided by increasing the pressure rapidly to over 10 GPa permitting us to study the structural properties of arsenolite under quasi hydrostatic conditions to very high compressions. No structural transitions or signs of amorphisation were observed for pressures approaching 40 GPa.

Other systems extensively studied are superconducting radical cation salts derived from the donor molecule bis(ethylenedithio)-tetrathiafulvalene (BEDT-TTF, or ET for short) [6]. They constitute an important class of materials in the burgeoning field of molecular organic conductors. ET and iodine form a plethora of polymorphic phases, denoted by small Greek letters, the electrical conductivities of which range from semiconducting to metallic to superconducting.

One polymorphic phase is α-$(ET)_2I_3$, a prototypical organic metal, known to undergo a metal-insulator transition at 135 K. The transition can be suppressed by pressure. At ambient temperature we discovered a structural phase transition at ~13 GPa. The structure of the high pressure phase was determined from the single crystal data. During the transition α-ET_2I_3 remains triclinic (S.G.: R-1). The unit cell volume doubles. A small discontinuity indicates a first order phase transition. The most remarkable change is in the configuration of the triiodide molecules. Before the transition both I – I distances are equal and the molecule is straight. After the transition both I – I distances are considerably larger, they are no longer equal and the molecule is at an angle. No additional transitions or signs of amorphisation were found for pressures approaching 30 GPa.

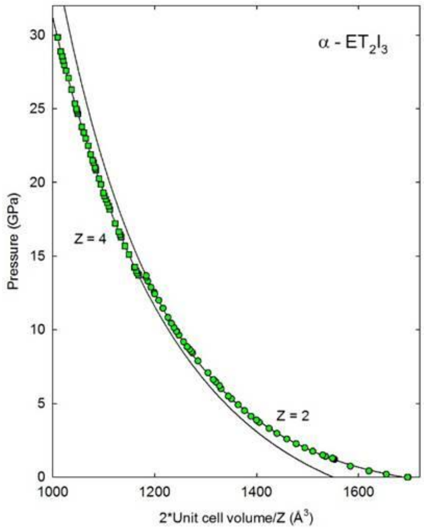

Figure 4. Equation of state of α-ET_2I_3. α-ET_2I_3 undergoes a structural phase transition at ~13 GPa with a doubling of the unit cell volume.

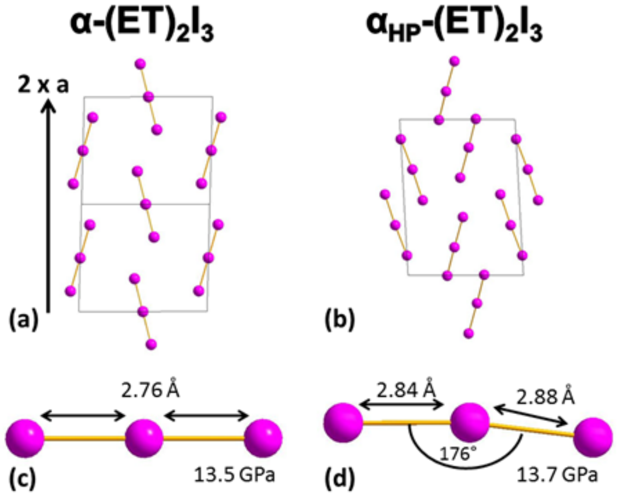

Figure 5. I_3 molecule before and after the phase transition. In the high pressure phase I – I bond lengths increase and the molecule is no longer symmetric.

Single crystal diffraction permits an exhaustive characterization of the structural changes under pressure. Molecules in certain molecular solids compressed with a quasihydrostatic pressure transmitting medium as shown here for As_4O_6 and bis(ethylenedithio)-tetrathiafulvalene can be surprisingly stable up to exceptionally high compressions.

Acknowledgments: Work done in collaboration with S. Brun and H. Müller. Arsenolite single crystals from P.A. Gunka.

---

[1] M. Merlini, M. Hanfland, *High Pressure Research* **33** (2013) 511.

[2] R. Boehler, K. DeHantsetters, *High Pressure Research* **24** (2004) 391.

[3] I. Kupenko, *et al, Review of Scientific Instruments* **83** (2012) 124501.

[4] P.A. Gunka, *et al., Crystal Growth & Design* **15** (2015) 3740.

[5] J.A. Sans, *et al.*, Physical Review B **93**, (2016) 054102.

[6] S. Brun - Études structurales des conducteurs organiques bidimensionnels à haute pression, PhD-thesis, Grenoble (2013).

O-01 **Monday, 13.06., 18^{20} - 18^{40}**

A role of microfluidic flow and gemini surfactants in amyloid aggregation of lysozyme and other proteins

W. Gospodarczyk[1]* and M. Kozak[1,2]

[1]Department of Macromolecular Physics, Faculty of Physics, Adam Mickiewicz University, ul. Umultowska 85, 61-614 Poznań, Poland
[2]Joint Laboratory for SAXS studies, Faculty of Physics, Adam Mickiewicz University, Umultowska 85, 61–614 Poznań, Poland

Keywords: amyloid aggregation, microfluidics, protein-surfactant interaction, gemini surfactants

*e-mail: 1kamien@amu.edu.pl

There is a number of different proteins known, to undergo amyloid aggregation, a specific kind of aggregation being responsible for several severe human diseases. There are neurodegenerative disorders among these diseases, such as Huntington's disease, Parkinson disease, prion diseases, as well as other, like liver cirrhosis or type II diabetes. All amyloid-prone proteins misfold in a similar way, following a common pathway of conformational changes. In quest for an effective drug it is vital to understand the molecular mechanism underlying the process of amyloidogenesis. Parallelly, it is also crucial to screen prospective drugs among various molecules which can inhibit this aggregation.

Microfluidics, an experimental technique dealing with flow of small volumes of samples in channels of small cross sections, has been eagerly used to enhance the scope of traditional research, including amyloid-related studies. Microfluidics offers, among others, low sample consumption, fast analysis, effective mixing of reagents, small droplets formation and their movement control, single nucleation sites tracking, creation of specific flow environment. On the other hand, gemini (dimeric) surfactants, used in our study, are a promising group of compounds in search for substances hampering amyloid aggregation. Their molecules consist of two polar heads linked with a spacer and two hydrophobic tails bound to the heads. Gemini surfactants exhibit good physico-chemical properties, as compared to their monomeric counterparts, such as lower critical micellisation concentration, better solubility, higher surface activity. They are biocompatible and biodegradable, what makes them interesting candidates for testing their inhibitory influence on amyloidogenesis.

In our study we aimed at determining the influence of microfluidic flow, mimicking the flow of proteins in blood vessels, solely on the pace of amyloid aggregation of different proteins, including lysozyme and amyloid beta 1-42 peptide, the latter linked with Alzheimer disorder, in order to coming closer to understanding the molecular mechanism of amyloid aggregation. To reach this aim, we employed a microfluidic system to induce such flow in a glass microchip having one 5-metre long channel and synchrotron radiation small angle X-ray scattering (SR-SAXS), circular dichroism (CD) spectroscopy and transmission electron microscopy (TEM). We also checked how pH and temperature can influence this process. Moreover, we investigated the influence of a number of gemini surfactants on amyloid aggregation of proteins under study. The results of these analysis will be presented on the conference.

Acknowledgments: These experiments were supported by a research grant (DEC-2013/09/N/ST5/02444) from National Science Centre (Poland).

O-02 **Session A, Tuesday, 14.06., 9^{40} - 10^{00}**

Atomic layer deposition of Al_2O_3 on $CH_3NH_3PbI_3$ for enhancement of perovskite solar cells stability

M. Sowinska[1]*, C. Das[1], K. Wojciechowski[2], Z. Rouissi[1], H. J. Snaith[2] and D. Schmeisser[1]

[1] *BTU Cottbus-Senftenberg, Konrad-Wachsmann-Allee 17, 03046 Cottbus, Germany*
[2] *Clarendon Laboratory, University of Oxford, Parks Road, Oxford OX13PU, United Kingdom*

Keywords: synchrotron-based X-ray photoelectron spectroscopy, perovskite solar cells, atomic layer deposition

*e-mail: malgorzata.sowinska@b-tu.de

Organic-inorganic perovskites like methylammonium lead triiodide ($CH_3NH_3PbI_3$) films represent a new paradigm for photovoltaics, which have the potential to overcome the performance limits of current technologies and achieve low cost and high versatility.[1-5] Although the power conversion efficiency of the $CH_3NH_3PbI_3$-based perovskite solar cells exceeded already 21 %, a number of key issues must be solved before the wide-spread commercialization will be possible.

Typically, when exposed to the air or moisture hybrid perovskite films degrade within a couple of hours or days.[1,2] Moreover, the $CH_3NH_3PbI_3$ perovskite cannot sustain prolonged annealing at temperatures higher than around 85°C.[3,4] It also undergoes degradation upon applying electric field with the presence of moisture.[5] Improving and controlling perovskite stability along with understanding of degradation pathways are now deeply studied. By understanding how the material properties affect the performance of perovskite solar cells, further improvements for future applications will be possible.

The conformal coverage of the $CH_3NH_3PbI_3$ perovskite film at low temperature with a thin metal oxide layer is very promising to protect it against degradation. The perfectly matching method to fulfill both requirements is the atomic layer deposition (ALD) [6]. In order to prevent thermal degradation of the perovskite a deposition at temperatures lower than 80°C is desirable.

In this paper, we present our X-ray photoelectron spectroscopy (XPS) and atomic force microscopy (AFM) studies on the ALD growth of Al_2O_3 on the $CH_3NH_3PbI_3$ perovskite film at room temperature. TMA and H_2O were used as aluminium and oxygen precursors for ALD. The chemical and electronic changes occurred at the $Al_2O_3/CH_3NH_3PbI_3$ interface were firstly investigated using synchrotron radiation source XPS (SR-XPS) at the undulator beamline U49/2-PGM2 at BESSY-II in Berlin/Adlershof with the ASAM end-station. The photoelectrons were excited by X-rays with energies of 640 eV and recorded by the PHOIBOS-150 (SPECS GmbH) hemispherical electron analyzer equipped with a 1D delay line detector at take-off angle (α) of 45°. The topography measurements were performed at room temperature by AFM using the Veeco CP-II AFM system operated in a contact mode.

The SR-XPS and AFM results of the $Al_2O_3/CH_3NH_3PbI_3$ interface indicate that Al_2O_3 initially grows layer by layer up to approximately 12 ALD cycles (~0.6 nm) and then 3D islands start to form (see Fig. 1). After 50 ALD cycles the 2D Al_2O_3 film is covered with approximately 86 % of Al_2O_3 islands.

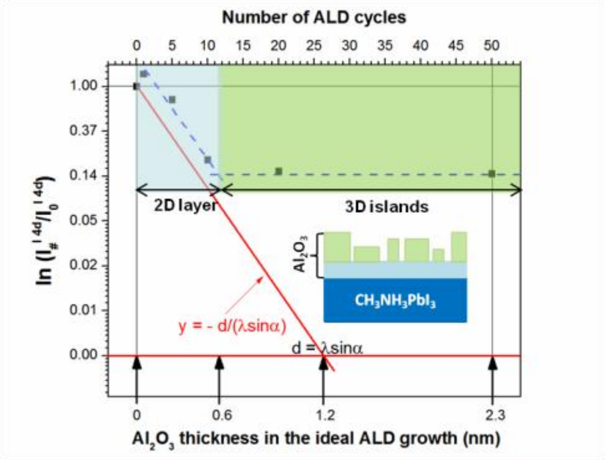

Figure 1. Growth model of Al_2O_3 on $CH_3NH_3PbI_3$ perovskite at room temperature based on analysis of the I4d XPS signal attenuation versus number of complete TMA and H_2O ALD cycles.

Moreover, XPS results have shown that oxygen is initially present in the perovskite film most probably due to not fully removed DMF solvent and it participates in the reaction with TMA precursor through adsorption on active sites during the few first ALD cycles.

The stability test upon air exposure of the alumina/perovskite system has shown that coating the perovskite film with an ultra thin Al_2O_3 layer enhances its lifetime. This finding opens new possibilities to increase the stability of the perovskite solar cells where the low temperature processing is mandatory to protect the perovskite film against degradation.

Acknowledgments: Authors would like to acknowledge the support of Guido Beuckert from BTU. This work was partially supported by the German Federal Ministry of Education and Research (BMBF, 03IN2V4A, 03IN2V4B), German Research Foundation (DFG, SCHM 745/31-1) and EPSRC, UK.

---

[1] T. Leijtens, G. E. Eperon, S. Pathak, A. Abate, M. M. Lee, H. J. Snaith, *Nat. Commun.* **4** (2013) 2885.
[2] J. A. Christians, P. A. Miranda Herrera, P. V. Kamat, *J. Am. Chem. Soc.* **137** (2015) 1530.
[3] B. Conings, J. Drijkoningen, N. Gauquelin, A. Babayigit, J. D'Haen, L. D'Olieslaeger, A. Ethirajan, J. Verbeeck, J. Manca, E. Mosconi, F. D. Angelis, H.-G. Boyen, *Adv. Energy Mater.* **5** (2015) 1500477.
[4] L.-C. Chen, C.-C. Chen, J.-C. Chen, C.-G. Wu, *Solar Energy* **122** (2015) 1047.
[5] T. Leijtens, T. T. Hoke, G. Grancini, D. J. Slotcavage, G. E. Eperon, J. M. Ball, M. D. Bastiani, A. R. Bowring, N. Martino, K. Wojciechowski, M. D. McGehee, H. J. Snaith, A. Petrozza, *Adv. Energy Mater.* **5** (2015) 1500962.
[6] G. Niu, W. Li, F. Meng, L. Wang, H. Dong, Y. Qiu, *J. Mater. Chem. A* **2** (2014) 705.

O-03 **Session A, Tuesday, 14.06., 10^{00} - 10^{20}**

Local structure of transition metal dopants into 3D topological insulators probed with angular dependent XAFS

M. Sikora[1]*, A. Kozłowski[2], M. Waśniowska[3],
K. Maćkosz[2], M. Dobrzański[2], I. Miotkowski[4],
M. Nachtegaal[5] and Z. Kąkol[2]

[1]*AGH University of Science and Technology, Academic Centre for Materials and Nanotechnology, Krakow, Poland*
[2]*AGH University of Science and Technology, Faculty of Physics and Applied Computer Science, Krakow, Poland*
[3]*Institut für Experimentelle und Angewandte Physik, Christian-Albrechts-Universität zu Kiel, Germany*
[4]*Department of Physics, Purdue University,West Lafayette, Indiana, USA*
[5]*Swiss Light Source, Paul Scherrer Institute, Villigen, Switzerland*

Keywords: XAS, XNLD, topological insulators, transition metal dopants,

*e-mail: marcin.sikora@agh.edu.pl

A new state of quantum matter which has a topologically nontrivial electronic structure characterized by a bulk energy gap but gapless chiral edge states, leading to the quantized Hall effect without an external magnetic field is among most intriguing physical phenomena discovered in the last decade. Quantum anomalous Hall effect has been observed in thin films of V and Cr doped topological insulators (TIs), i.e. magnetic topological insulators, where robust bulk ferromagnetic (FM) ordering is spontaneously developed. The ability to externally control the magnetic properties of Tis could be important both for fundamental and technological interest, particularly in view of recent developments in magnetoelectrics and spintronics [1].

Among crystalline TI the long range magnetic order is established only in the Mn-doped Bi_2Te_3 in the temperature range below T_C = 12 K. On the other hand, in iron and cobalt doped bismuth chalcogenides, long range magnetic order has not been observed, while magnetic susceptibility reveal intriguing anizotropy, that is tentatively ascribed to non-uniform distribution of transition metal dopants between cation sites of Bi and interstitial position within Van der Walls gap.

In this contribution we present results of systematic investigations of local structure around transition metal dopants into single crystals of bismuth chalcogenides by means of K-edge EXAFS and angular dependent XANES spectra. The measurements performed at room temperature at SuperXAS beamline show e.g. a systematic angular dependence in Mn doped Bi_2Te_3, while the evolution of respective spectra in Mn doped Bi_2Se_3 is negligible. A significant difference between these systems is also visible in EXAFS spectra that reveal considerable evolution in local crystal structure around Mn dopants in both systems. Supported by theoretical modeling of angular dependent XANES by means of FDMNESS code and double shell analysis of EXAFS spectra, we will assess the preferential sites for transition metal doping of TI crystals and discuss its influence on magnetic properties of magnetic crystalline TIs.

Acknowledgments: Support from the grant of National Science Center of Poland (2015/17/B/ST3/00128) is acknowledged.

---

[1] J.G. Checkelsky, J. Ye, Y. Onose, Y. Iwasa, Y. Tokura, *Nat. Phys.* **8** (2012) 729.
[2] M. Waśniowska, M. Sikora, M. Dobrzański, T. Eelbo, M. M. Soares, M. Rams, I. Miotkowski, R. Wiesendanger, R. Berndt, Z. Kąkol, A. Kozłowski, *Phys. Rev. B* **92** (2015) 115412.

O-04 **Session A, Tuesday, 14.06., 10^{20} - 10^{40}**

The Cu2p-edge of superconducting BiSrCu-Oxides studied by resonant Photoelectron Spectroscopy

D. Schmeißer[1]* and C. Janowitz [2]

[1]*Angewandte Physik-Sensorik, BTU Cottbus,*
Konrad Wachsmann Allee 17, 03046 Cottbus, Germany
[2]*Institut für Physik, Humboldt-Universität zu Berlin,*
Newtonstr. 15, 12489 Berlin, Germany

Keywords: synchrotron radiation, superconductor

*e-mail: dsch@b-tu.de

We report on a resonant photoemission (resPES) study of $Pb_{0,4}Bi_{1,6}Sr_{2,0}CaCu_2O_8$ ((Pb,Bi)-2212) (BISCO) single crystals to unravel the resonant decay mechanisms at the Cu2p absorption edge. The resPES studies on superconducting BISCO are performed at Bessy U49/2. We investigated BISCO single crystals whith different hole doping concentrations at temperatures between 300K and 17K. CuO films have been used as a reference.

Here we focus on the resPES data recorded at the Cu2p absorption edge. We find a strong polarization dependence for in-plane and out-of-plane geometries (with respect to the Cu-O plane) in our data which are caused by two independent Auger processes.

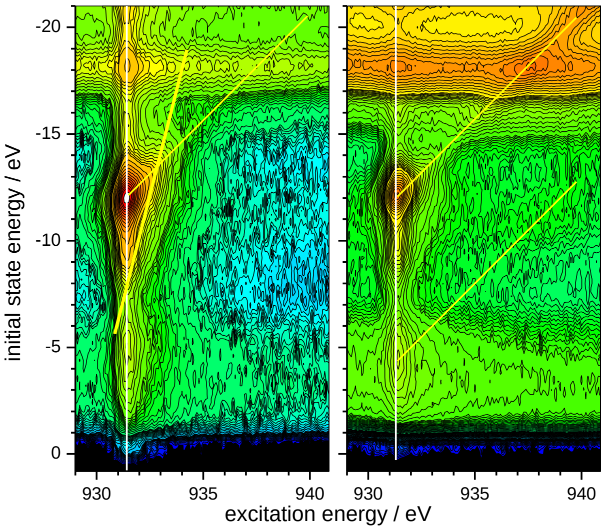

Figure 1: Cu- L_3 edge resonant photoemission profiles recorded in-plane (left) and out-of-plane (right). The thin white and the thick yellow lines mark the 3h-Auger and the Cu-LMM processes, respectively.

At the Cu2p absorption edge the most pronounced intensity is due to the Cu3d^8 satellite (initial state energy around -12eV in figs. 1). The intensity of the valence band states (around -4eV) with a 3d^9 configuration is much weaker. Very remarkable is the polarization dependence which in Fig.1 is shown for a polarization geometry parallel to the Cu-O plane (in-plane, left panel) and perpendicular to it (out-of-plane, right panel). In these data we identify two Auger processes. One is assigned to involve an in-plane ligand-to-metal CT state (yellow line, left panel). It originates right at the strong Cu3d^8 satellite and yields to a combined participator and spectator Auger decay with a three-hole (3h) final state [1]. The second Auger process is indicative of a Cu-LMM decay (white line, right panel). It appears only in out-of-plane geometry and involves Sr valence states as well. Fig.2 gives an example for the strong difference for the in plane and the out-of-plane polarization geometries. Here we use the integrated intensities (pIY) of the resPES profiles shown in Figs.1. In the lower panel we show the corresponding data for undoped and maximum doped BISCO samples. We discuss these resPES data in the context of previous assignments of the doping dependence where the shoulder in the main Cu2p absorption signal is used to determine the hole doping concentration [2].

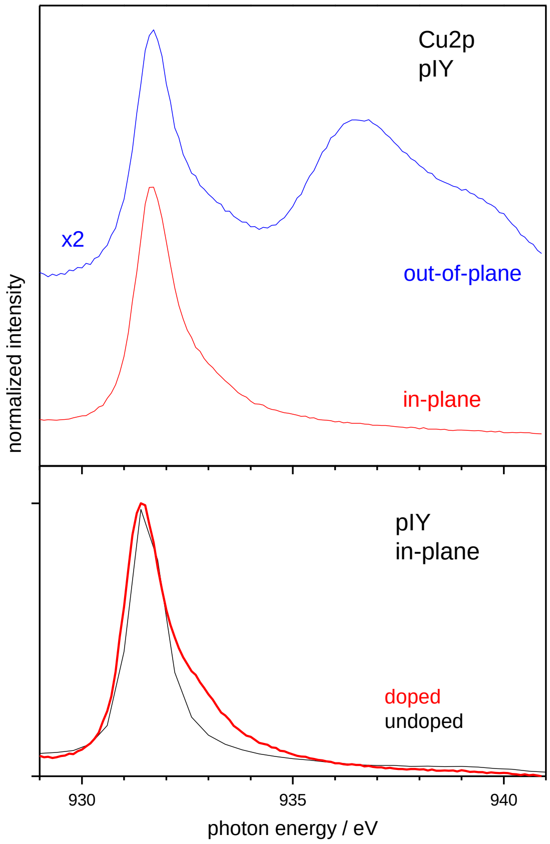

Figure 2: The Cu2p-pIY absorption signal: polarization dependence of the pIY curves of the two wallpapers in Fig.1 (top panel), doping dependence (bottom panel).

Our resPES data enable us to sort the individual resonant mechanisms at the Cu2p edge in more detail than recently anticipated [2]. We discuss our data in the context of the recent discussion about the applicability of the Zhang-Rice model [3].

Acknowledgments: This work was supported by DFG (SCHM 745/31-1). We thank A. Krapf (HU Berlin) for providing the BISCO samples.

---

[1] M.Richter, *et al.*, *Appl.Phys.Lett*. **102** (2013) 253904.
[2] N. B.Brookes, *et al.*, *Phys. Rev. Lett.* **115** (2015) 027002.
[3] C.-C.Chen, *et al.*, *Phys. Rev. B* **87** (2013) 165144.

O-05 **Session A, Tuesday, 14.06., 10^{40} - 11^{00}**

EXAFS and DAFS from particles of ω phase in β-Ti(Mo) single crystals

E. Piskorska-Hommel[1]*, D.Kriegner[2], J. Šmilauerová[2] and V. Holý[2]

[1]*Institute of Low Temperature and Structure Research, Polish Academy of Sciences, Wroclaw, Poland*
[2]*Faculty of Mathematics and Physics, Charles University in Prague, Czech Republic*

Keywords: Ti alloys, precipitates, martensitic transformation, x-ray absorption spectroscopy

*e-mail: e.piskorska@int.pan.wroc.pl

Metastable β titanium alloys are important materials for various construction purposes, as well as for biomedical applications. They contain enough β stabilizing elements to suppress martensitic transformation from body-centered cubic β phase to hexagonal close-packed α phase upon quenching to room temperature. However, due to the metastable nature of the β phase, various other phases can form during ageing at elevated temperatures. In a certain composition range, nm-sized particles of meta-stable hexagonal ω phase form upon quenching in the β matrix by a diffusionless displacive transformation [1]. When exposed to elevated temperatures, ω particles grow by a diffusion-assisted mechanism. The ω phase particles play a significant role in alloy hardening, as well as in subsequent phase transformations, i.e. ω-assisted nucleation of thermodynamically stable α phase [2].

The growth of the ω phase particles is accompanied by the diffusion of β-stabilizing elements from the volumes of the growing particles creating "clouds" of the impurity atoms around each particle. We have investigated the kinetics of the growth of the ω phase particles by high-energy small-angle x-ray scattering (SAXS) in situ during annealing of Ti(Mo) single crystals [3]. The results indicated indeed the presence of local areas with increased Mo content.

Recently we perform an ex situ anomalous X-ray diffraction and fluorescence measurements around the MoK absorption edge at ESRF Grenoble (beamline BM02) in samples after various annealing steps. As an example, we show in Fig. 1(a) the reciprocal-space distribution of the diffracted intensity around the ω-reciprocal lattice point $44\overline{82}$ of a Ti(Mo) sample after annealing at 370°C at 64h taken at 19.995 keV, just below the MoK absorption edge. Fig. 1(b) shows the energy dependence of the diffraction signal (XRD) integrated over the region denoted by a rectangle in Fig. 1(a), as well as the fluorescence signal collected far away from any reciprocal-lattice point. Both dependences clearly exhibit the EXAFS-like oscillations; however the fluorescence signal stems from the Mo atoms both in the ω particles and in the β matrix, whereas XRD originates exclusively from the ω particles.

The Athena program was used to subtract the pre-edge background, normalize to the experimental edge step and absorption data from the EXAFS data [4]. The DAFS spectrum χ(E) depends on the real (χ') and imaginary (χ") parts of the anomalous form-factor of the Mo atoms. The numerical Kramers-Kronig transformation was used to extract the imaginary part χ"(E) of the DAFS spectrum [5]. The Artemis program was used to analyse both EXAFS and DAFS data in order to obtain the structure parameters such as bond lengths (R), Debye-Waller factors (σ^2) and coordination numbers (N) [4]. The scattering amplitudes Mo-Ti were generated using the FEFF6 code implemented in Artemis program [6]. The magnitude of the Fourier transform (FT) of the EXAFS and DAFS oscillations is presented in Fig. 2. Although FTs for both cases look very similar some structural changes between EXAFS nad DAFS data are observed. In the presented paper the EXAFS and DAFS results for samples annealing in 300, 335 and 370°C in different time will be discussed in details.

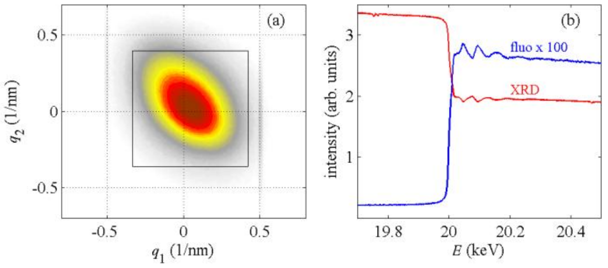

Figure 1. The reciprocal space intensity distribution around the maximum of the ω-phase (a) and the energy dependences of the diffraction and fluorescence signals (b).

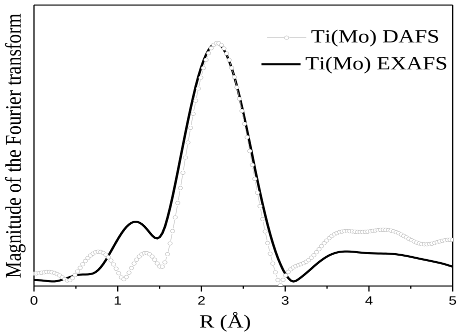

Figure 2. Magnitude of the Fourier transforms of the EXAFS and DAFS oscillation.

Acknowledgments: We acknowledge the assistance of H. Renevier (LMGP Grenoble) with the synchrotron measurement. The Czech co-authors acknowledge the support of the Czech Science Foundation (projects 14–08124S and 14–36566G).

---

[1] D. De Fontaine, *Acta Metall.* **18** (1970) 275.
[2] F. Prima et al., *Scripta Materialia* **54** (2006) 645.
[3] J. Šmilauerová et al., *Acta Mater.* **61** (2013) 6635; *Acta Mater.* **81**, (2014) 71; **100** (2015) 126.
[4] B. Ravel et al., *J. Synchrotron Rad.* **12**, 537 (2005).
[5] J. O. Cross, Ph.D. thesis, (University of Washington, Seattle, 1996).
[6] A. L. Ankudinov et al., *Phys. Rev. B* **58** (1998) 7565.

O-06 **Session A, Tuesday, 14.06., 12^{20} - 12^{40}**

Development and characterization of a compact laboratory laser-plasma soft X-ray source and its usage for contact microscopy

M. G. Ayele[1]*, P.W. Wachulak[1], J. Czwartos[1], D. Adjei[1], A. Bartnik[1], Ł. Wegrzynski[1], M. Szczurek[1], L. Pina[2] and H. Fiedorowicz[1]

[1]*Institute of Optoelectronics, Military University of Technology, Kaliskiego 2 Str., 00-908 Warsaw, Poland*
[2]*Faculty of Nuclear Sciences and Physical Engineering, Czech Technical University, Brehova 7, CZ-115 19 Prague 1, Czech Republic*

Keywords: laser-plasma, soft X-rays, gas-puff target, water window X-ray microscopy

*e-mail: mesfin.ayele@wat.edu.pl

Applications related to soft X-ray microscopy is quite attractive, because soft X-ray radiation can achieve good contrast images of unstained, wet, and several micrometers thick specimens in the ‘water window’ [1-2]. The ‘water window’ is a range of soft X-ray energy between K-absorption edges of oxygen (540 eV) and carbon (284 eV),. Within the ‘water window’ spectral range, water is relatively transparent, while carbon, nitrogen, and other elements found in the structure of biological specimens are still absorbing. For this reason, soft X-rays in the ‘water window’ spectral range can be utilized for living specimen study without chemical fixation or dehydration that is required in electron microscopy. Furthermore, the shorter wavelength of the X-ray radiation, relative to visible light, allows for better resolution imaging beyond the limits of optical microscopy.

Several sources including, synchrotrons and free electron lasers for generating ‘water window’ soft X-rays were developed. These devices are the state of art designed for cutting-edge experiments; however, limited access and high cost to such sources encourages the development of a laboratory based soft X-ray sources, which could provide a complementary platform to the large scale facilities. A number of laboratory laser-plasma soft X-ray source were developed for microscopy applications [3-5]. A solid target is conventionally used in such sources; however, debris production due to laser ablation is the main challenge. To eliminate this problem, the use of a gas-puff target instead of a solid target was proposed [6-7].

In this work, we present a laboratory laser-plasma source of soft X-rays, developed and characterized for contact microscopy application. The source is based on a double-stream gas puff target, irradiated with a commercially available Nd:YAG laser (from EKSPLA), delivering energy up to 740 Mj, with 4 ns pulse duration, and 10 Hz repetition rate. The target is formed by pulsed injection of working gas (argon) into a hollow stream of helium gas using a double nozzle electromagnetic valve [8]. The source is designed to produce nanosecond pulses of soft X-rays in the ‘water window’ spectral range, to enable the irradiation of samples both in vacuum and in helium atmosphere. The source delivers fluence of about 3.70 x 103 photon/μm2/pulse at a sample placed in air at a distance of 21 mm, downstream of the source. It also delivers a photon fluence of about 1.90 x 102 photon/μm2/pulse for a sample placed in helium atmosphere at the same position. The construction of the source, and results of the characterization measurements, as well as preliminary contact microscopy experiments are presented and discussed.

Acknowledgments: This Work is supported by the Education, Audiovisual and Culture Executive Agency (EACEA) Erasmus Mundus Joint Doctorate Programme Project No. 2012 – 0033. We also acknowledge the support from 7th Framework Programme Laserlab Europe project (No. 654148). This work is also supported by the National Centre for Science; award number DEC 2011/03/D/ST2/00296, the National Centre for Research and Development, Lider programme, award #LIDER/004/410/L4/12/NCBR/2013. We also acknowledge our collaborators, the Institute of Electronic Materials Technology (ITME, Poland) and the Institute of Nuclear Physics, Polish Academy of Sciences Kraków, Poland for the material support.

---

[1] J. Kirz, D. Sayre, *Synchrotron Radiat. Res* (1980) 277.
[2] T. W. Ford, A. D. Stead, R. A. Cotton, *Electron Microsc Res* **4** (1991) 269.
[3] P. Albertano, L. Reale, L. Palladino, A. Reale, R. Cotton, S. Bollanti, K. Vigli Papadaki, *J Microsc* **187** (1997) 96.
[4] T. Majima, *Trends Anal. Chem* **23** (2004) 520.
[5] M. Kado, H. Daido, Y. Yamamoto, K. Shinohara, M. C. Richardson. *Laser Phys Lett* **3** (2005) 205.
[6] H. Fiedorowicz, A. Bartnik, Z. Patron, P. Parys, *Appl. Phys. Lett.* **62** (1993) 2778.
[7] H. Fiedorowicz, A. Bartnik, J. Kostecki, M. Szczurek, SPIE **2723** (1996) 310.
[8] A. Bartnik, H. Fiedorowicz, R. Rakowski, M. Szczurek, F. Bijkerk, R. Bruijn, H. Fledderus, *Proc. SPIE* **4424** (2001) 406.

O-07 **Session A, Tuesday, 14.06., 12^{40} - 13^{00}**

Development of EUV and SXR nanoscale imaging systems based on double stream gas puff target sources

A. Torrisi[1]*, P.W. Wachulak[1], A. Bartnik[1],
Ł. Węgrzyński[1], T. Fok[1] and H. Fiedorowicz[1]

[1] *Institute of Optoelectronics, Military University of Technology, Kaliskiego 2 Str., 00-908 Warsaw, Poland*

Keywords: gas puff target, microscopy, compact sources

*e-mail: alfio.torrisi@wat.edu.pl

In the last 30 years much effort was made in order to develop compact laser-produced plasma sources emitting short wavelength radiations, especially in the so-called “water window” (λ=2.3-4.4 nm) and in the Extreme Ultraviolet (EUV, λ=1-120 nm) spectral ranges. Investigations in the micrometer scale, employing short wavelengths, open the possibility of developing table-top microscopes, to overpass the limitations imposed by large facilities, such as their high complexity, maintenance costs and the limited access.

The double stream gas puff target source, coupled with Fresnel zone plates (FZPs) represents a suitable platform for microscopy experiments in transmission mode, employing soft X-ray (SXR) and EUV radiations. It represents a valid complementary technique to synchrotrons and free-electron laser facilities. The source, which is very easy to be used by a single user, allows for efficient plasma generation with high EUV/SXR flux. Compact microscopes based on that source allow to capture EUV and SXR images of various samples, with 50-60 nm half-pitch spatial resolution and exposure time of the order of few seconds. Herein, we would like to present our recent developments and progress in compact desk-top SXR/EUV microscopy, including source and microscope optimization, examples of image acquisition and its possible applications.

Acknowledgments: This work is supported by the National Centre for Research and Development’s, LIDER programme, grant #LIDER/004/410/L-4/12/NCBR/2013 and the National Science Centre, Opus programme, grant agreement number UMO-2015/17/B/ST7/03718. The authors acknowledge also financial support from the EU FP7 Erasmus Mundus Joint Doctorate Program EXTATIC under framework partnership agreement FPA-2012-0033 and from the European Union’s Horizon 2020 research and innovation program under grant Laserlab-Europe IV, grant agreement No. 654148.

O-08 **Session B, Tuesday, 14.06., 12^{20} - 12^{40}**

Fe X-ray Absorption and X-ray Magnetic Circular Dichroism Studies on FeMo cofactor of Nitrogenase and Related Models

J. K. Kowalska[1]*, S. Lee[2], F. Meyer[3], T. Weyhermüller[1], R. Bjornsson[4], O. Einsle[5] and S. DeBeer[1,6]

[1]Max Planck Institute for Chemical Energy Conversion, Stiftstrasse 34-36, D-45470 Mülheim an der Ruhr, Germany
[2]Univeristy of Waterloo, 200 University Ave. W, N2L 3G1 Ontaria, Canada
[3]Georg-August-University, Tammannstr. 4, D-37077 Göttingen, Germany
[4]University of Iceland, Dunhagi 3, IS-107 Reykjavik, Iceland
[5]Albert-Ludwigs-Universität Freiburg, Albertstrasse 21, D-79104, Freiburg, Germany
[6]Cornell University, 144 East Ave, Ithaca,NY 14853 USA

Keywords: nitrogenase, FeMoco, nitrogen fixation, HERFD XAS, XMCD

*e-mail: joana.kowalska@cec.mpg.de

The process of reducing dinitrogen (N_2) to ammonia (NH_3) is essential for producing fertilizers that feed the world's growing population. Nowadays, the cleavage of the N-N bond is achieved industrially using heterogeneous catalysts in the Haber-Bosch process, while biological N_2 fixation is known to occur at the FeMo cofactor of nitrogenase enzyme found in diazotrophs. Although, both processes operate with relatively high efficiency, they require different thermodynamic limits: high temperature and pressure for the industrial process vs. ambient conditions for biological nitrogen reduction. These significant differences lead to a large interest in understanding the mechanism of biological nitrogen conversion in order to improve future industrial catalyst and processes.

The active site of nitrogenase is a $MoFe_7S_9C$ cofactor (FeMoco, Figure 1), which has brought out a fair amount efforts in understanding its' geometrical structure [1], however there's still a lack of information to complete the electronic structure of this complex system.

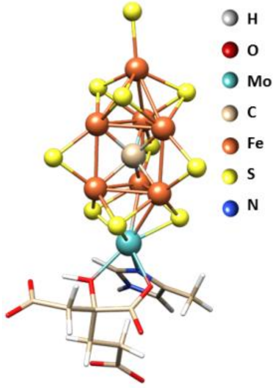

Figure 1. Structure of the FeMo cofactor of nitrogenase.

The current goal is to provide insights into the iron oxidation state distribution and magnetic coupling within this cofactor.

Recently applied X-ray spectroscopic studies revealed the presence of a central carbon in this cluster and also the Mo atom as Mo(III).[2,3] Based on these results, together with the EPR total spin of 3/2, three main oxidation state scenarios have been proposed, that need experimental verification. Therefore, we have utilized high energy resolution fluorescence detected (HERFD) X-ray absorption spectroscopy (XAS) on Fe K-edge to address this question. Although HERFD XAS allows one to obtain spectra with the energy resolution below the Fe 1s core hole lifetime, the presence of 7 iron atoms as well as lack of magnetic information limits the analysis of such spectra (Figure 2). A way to overcome these limitation is to apply L-edge XAS and also X-ray magnetic circular dichroism (XMCD) spectroscopy at the $L_{2,3}$-edge that enabling more quantitative assessment of the obtained data.

Fe K-edge HERFD XAS, L-edge XAS and XMCD data on model compounds and FeMoco will be presented. The observed trends upon oxidation state changes and ligand environment will be explained based on the changes in electronic structure of the studies systems. Moreover, the experimental data will be supported with theoretical calculations indicating possible scenarios of Fe oxidation state distribution in FeMoco.

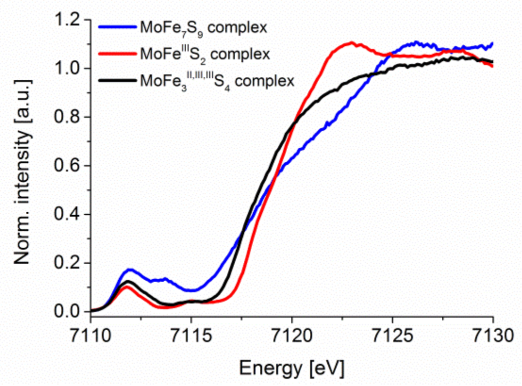

Figure 2. Fe HERFD XAS spectra of monomeric, tetrameric Mo-Fe-S model complexes and FeMoco.

Acknowledgments: This work was supported by the Max Planck Society and ERC Consolidator Grant. European Synchrotron Radiation Facility (ESRF) and French National Synchrotron Facility (SOLEIL) are acknowledged for provision of beamtime.

---

[1] J. Kowalska, S. DeBeer, *BBA Mol. Cell Res.* **1853** (2015) 1406.
[2] K. M. Lancaster, M. Roemelt, P. Ettenhuber, Y. Hu, M. W. Ribbe, F. Neese, U. Bergman, S. DeBeer, *Science* **334** (2011) 974.
[3] R. Bjornsson, F.A. Lima, T. Spatzal, T. Weyhermüller, P. Glatzel, E. Bill, O. Einsle, F. Neese, S. DeBeer, *Chem. Sci.* **5** (2014) 3096.

O-09 **Session B, Tuesday, 14.06., 12^{40} - 13^{00}**

Synchrotron radiation studies of ultrathin Pt/Co/Pt trilayers irradiated by nanosecond pulses from EUV plasma

I. Jacyna[1], D. Klinger[1], J. B. Pełka[1], R. Sobierajski[1], A. Bartnik[2], P Dłużewski[1], E. Dynowska[1], M. Jakubowski[1], M. Klepka[1], Z. Kurant[3], R. Minikayev[1], I. Sveklo[3], A. Wawro[1], A. Wolska[1], D. Eichert[4], F. Brigidi[4], I. Makhotkin[5], S. Yakunin[6] and A. Maziewski[3]

[1]*Institute of Physics, Polish Academy of Sciences, 02- 668 Al. Lotników 32/46, Warsaw.*
[2]*Institute of Optoelectronics, Military University of Technology, ul. gen. S. Kaliskiego 2, 00-908 Warsaw, Poland*
[3]*Laboratory of Magnetism, Faculty of Physics, University of Bialystok, K. Ciolkowskiego 1L, 15-245, Bialystok, Poland*
[4]*Elettra-Sincrotrone Trieste, S.S. 14 Km 163.5 in Area Science Park, 34149 Basovizza, Trieste, Italy*
[5]*MESA+ Institute for Nanotechnology, University of Twente, Netherlands*
[6]*NRC Kurchatov Institute, Moscow, Russia*

Keywords: nanosecond pulse, laser-plasma source, EUV light, ultrathin films, Pt/Co/Pt, structure modification

*e-mail:yatsyna@ifpan.edu.pl

We have studied structural mechanisms responsible for the magnetic reorientation between out-of-plane and in-plane magnetization in the Pt/Co/Pt trilayer systems modified with short light pulses. Ultrathin film systems containing magnetic component, like Co, sandwiched between nonmagnetic metals, with tunable magnetization direction (in-plane and out-of-plane) are of particular importance for spintronics as well as for technology of magneto-optical memory devices. In case of a Pt/Co/Pt trilayers irradiated with different light impulses [1-3], an out-of-plane to in-plane magnetization reorientation phase transition was evidenced, with an irradiation-driven intermixing and disordering at the Co–Pt interfaces. In comparison with conventional thermal annealing of the sample, the fast laser annealing provides possibility to create structural and magnetic changes at the interfaces while substrate temperature is almost unchanged which is important for technological applications.

In general sample irradiation may lead to such phenomena as blurring of originally sharp interfaces and – as a result of atomic interdiffusion – formation of a PtCo disorderd/ordered alloys and appearance of defects and strains. Such structural modifications change the basic parameters characterizing magnetic properties of multilayer structures – specifically magnetic anisotropy. In particular the interface blurring may reduce the surface anisotropy, while atomic interdiffusion leads to formation of alloys with specific magnetocrystalline anisotropy. In case of lattice deformation – magnetoelastic anisotropy contribution may become significant, as well.

We have investigated Pt(5 nm)/Co(3.5 nm)/Pt(5 nm) trilayers grown by the MBE method on the sapphire (0001) single crystal substrate. We have studied two series of samples – the Pt buffer layer was grown either at 750 °C, or at room temperature. Selected samples were irradiated with ns XUV pulses using laser produced plasma source. The whole sample surface was exposed quazi-uniformly. The irradiation fluences were in the range appropriate to switch the sytem into out-of-plane magnetization state. Magnetic stests were carried out after irradiations by means of magnetooptical Kerr effect (MOKE) based techniques. We have performed structural characterization of Pt/Co/Pt trilayers by means of complementary synchrotron radiation (SR) techniques. X-ray Reflectometry together with Grazing Incidence X-Ray Fluorescence providing information about the layer structure – interfacial roughness, layer thicknesses and about the depth profile of Co and Pt atoms. Polarized XAFS measurements give information about the atomic local structure around the Co atoms in the directions parallel and perpendicular to the layer surface. The structural properties obtained from the techniques based on the SR were correlated with the magnetic features and structural properties determined in other experimental methods (XRD, TEM, MOKE, neutron scattering and microscopic investigation).

Acknowledgments: This work has been supported by the Polish National Science Center (Grant No. DEC-2012/06/M/ST3/00475) and by the EU FP7 *EAgLE* project under the grant agreement *REGPOT*-CT-2013-316014. We acknowledge the Elettra facility for providing theaccess to the XRF beamline.

---

[1] J. Kisielewski, *et al., J. Appl.Phys.* **115** (2014) 053906.
[2] E. Dynowska, *et al. Nucl. Instrum. Methods Phys. Res. B* **364** (2016) 33.
[3] W. Szuszkiewicz, *et al., Phase Transitions* **89** (2016) 328.

O-10 **Session A, Wednesday, 15.06., 10^{20} - 10^{40}**

Photo-induced fragmentation of biomolecules in the gas-phase

T. J. Wasowicz[1]*

[1] *Department of Physics of Electronic Phenomena, Gdańsk University of Technology, ul. G. Narutowicza 11/12, 80-233 Gdańsk, Poland*

Keywords: synchrotron radiation, fragmentation, heterocyclic molecules, superexcitation, high-Rydberg fragments

*e-mail: twasowicz@mif.pg.gda.pl

Influence of radiations on biological tissues is of major concern in cancer therapy development. It is known that the primary ionizing photons and the secondary particles (electrons, ions, radicals, excited atoms and molecules) may induce important damages to DNA, with single- and double- strand breaks [1]. At the microscopic scale these lesions are related to the bond cleavages of the DNA building units. To determine the most sensitive part of the DNA molecular chains to the photon-induced bond rupture, it is important to explore the possible mechanisms leading to fragmentation of components of the DNA helix. In this perspective, investigations of the excitation, relaxation and fragmentation processes of the cyclic hydrocarbons containing oxygen and nitrogen heteroatoms (i.e. furan, tetrahydrofuran, isoxazole, pyridine and pyrimidine etc.) are of particular pertinence, because they are often considered to be simple prototypes of the structure units of the DNA. For instance, the molecules, tetrahydrofuran and furan, are built on furanose ring which may be discerned in the deoxyribose sugar of DNA. Pyrimidine molecule, on the other hand, is often considered to be an important precursor of the three nucleic bases of DNA and RNA, cytosine, thymine, and uracil, respectively. Thus, these molecules seem to be ideal candidates to characterize the mechanisms by which radiation produces their fragmentation, especially in the context of the DNA helix damage by the ionizing radiation.

In the present presentation I would like to discuss the results of recent projects performed at the Gas Phase beamline with collaboration with the Gas Phase research team at Elettra. In particular, I will show the results of the photon-induced fragmentation of the five and six-membered heterocyclic molecules (see Figure 1) in the inner-valence photon energy range of 13-70 eV [2-5]. These studies revealed molecular processes leading to formation of a number of the excited atomic H(n) and diatomic CH($A^2\Delta$), CN($B^2\Sigma^+$), $C_2(d^3\Pi_g)$ and NH($A^3\Pi$) fragments. In general, fragmentation mechanism involves initial excitation of these molecules into the superexcited states, which are inner-valence or high-Rydberg excited states, lying at higher energies above the first ionization threshold. These super-excited molecules, before they dissociate into the neutral atomic and molecular excited fragments, are further a subject of molecular isomerization and hydrogen atoms migration.

Moreover, the multifragmentation mechanisms of pyridine molecules by performing double or even triple coincidence measurements have been investigated (in these measurements the fluorescence of selected excited fragmentation products was detected in coincidence).

A new class of the mechanisms of the photon-induced fragmentation, namely recapture processes to Rydberg states by detection of the neutral high-Rydberg fragments field ionized and TOF mass analyzed after inner-shell C1s, N1s and O1s core excitations and ionization of the isoxazole and pyridine molecules will be also described. Up to now these processes have not been observed in the complex systems such as the heterocyclic molecules.

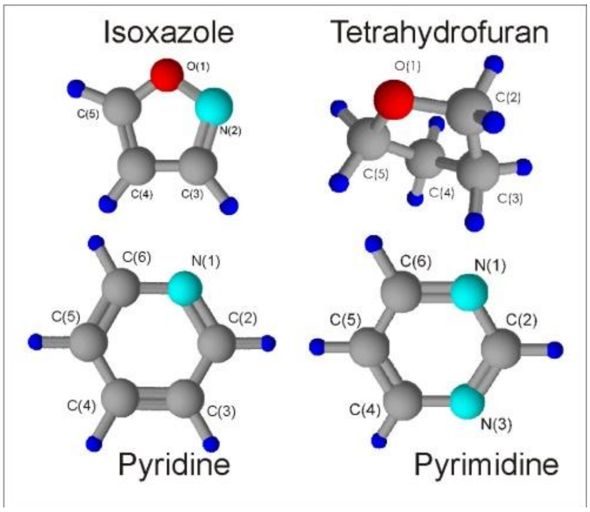

Figure 1. The five and six-membered heterocyclic molecules of interest.

Acknowledgments: This work was in part financially supported under the CALIPSO contract. Part of this work was performed during the Short Term Scientific Mission supported by the COST Action CM1204 (XLIC).

---

[1] M. A. Huels, B. Boudaïffa, P. Cloutier, D. Hunting, L. Sanche, *J. Am. Chem. Soc.*, **125** (2003) 4467.

[2] T.J. Wasowicz, A. Kivimäki, M. Coreno, M. Zubek, *J. Phys. B* **47** (2014) 055103.

[3] M. Zubek, T.J. Wasowicz, I. Dabkowska, A. Kivimäki, M. Coreno, *J. Chem. Phys.* **141** (2014) 064301.

[4] T.J. Wasowicz, A. Kivimäki, M. Coreno, M. Zubek, *J. Phys. B* **45** (2012) 205103.

[5] T.J. Wasowicz, A. Kivimäki, M. Dampc, M. Coreno, M. de Simone, M. Zubek, *Phys. Rev. A* **83** (2011) 033411.

O-11 **Session A, Wednesday, 15.06., 10^{40} - 11^{00}**

Polyamide 6 – the trouble with crystal polymorphism

M. Basiura-Cembala[1]*

[1]*Institute of Textile Engineering and Polymer Materials, University of Bielsko-Biala, Willowa 2, 43-309 Bielsko-Biala, Poland*

Keywords: Polyamide 6, polymorphism, synchrotron WAXD, thermal analysis

*e-mail: mbasiura@ath.bielsko.pl

Polyamide 6 (PA6) is one of the most popular semi-crystalline engineering thermoplastics polymer having excellent chemical stability and mechanical strength. One of the most remarkable features of PA6 is that, depending on thermo-mechanical or chemical treatment, it crystallizes in different crystal types.

Exploring the existing in literature "crystal form space" of PA6, one finds two well resolved and documented polymorphs, i.e. the α- and the γ-form [1.2]. Basically, both structures consist of hydrogen-bonded sheets with fully extended chains. Besides these crystal structures, depending on the thermal history, another molecular arrangement, known as a β–form, can co-exist with the α–form. The β–form is characteristic for poorly crystalline samples [3,4]. Furthermore, a plethora of other polymorphs of PA6 are described in literature, for example γ* [5,6], pleated α [7], paracrystalline monoclinc α, and nematic (pseudo)hexagonal γ [8]. It is widely accepted that these unstable forms can be transformed into the α-form using suitable thermal treatment [9,10]. In contrast, the γ- to α-form transition cannot take place, unless we employ reagents being able to interact with the hydrogen bonds, or unless we treat the sample at temperatures higher than its melting point [9].

The Differential Scanning Calorimetry (DSC) output of PA6 involves a multitude of thermal events. Specifically, the number of endotherms depends on the previous thermal history and heating rate. Understanding the crystallization behavior of PA6 (and other polymers) is often related to understanding of its melting mechanism. It is common to first introduce a defined thermal history to a sample and then, on the basis of the melting results, attempt is made to explain the crystallization process.

In this it work it is explained that such attempt should be made with care. The structural changes occurring to PA6 samples during heating after different thermo-chemical treatment are extracted from synchrotron Wide-Angle X-ray Diffraction experiments (WAXD) and are discussed in the context of parallel DSC data. The results reveals that:

- the β–form precedes the α–form upon cooling from quiescent melt;
- the X-ray diffraction patterns of the β–form are different from those of the γ–form;
- the thermal behavior of the β–form is different from those of the γ–form.

These results, being contradictory to the conventional wisdom, shows that due to crystalline polymorphism of PA6, interpretation of melting behavior revealed by DSC is not straightforward and should only be done when morphology sensitive techniques, like synchrotron X-ray diffraction, are used in conjunction with DSC. Besides the synchrotron experimental issues of this work are discussed as well.

Acknowledgments: This work was supported by:

- Polish Ministry of Science and Higher Education via research grant no N N508 469034;
- Foundation for Polish Science via grant received within the "HOMING Program" (financed by Iceland, Liechtenstein and Norway through the EEA Financial Mechanism).

Special thanks goes to prof. Bart Goderis from KULeuven, who made the experiments @ DUBBLE CRG beamline (ESRF) possible.

---

[1] D. R. Holmes, C. V. Bunn, D. J. Smith, *J. Polym. Sci*. **17** (1955) 159.

[2] H. Arimoto, M. Ishibashi, M. Hirai, Y. Chatani, *J. Polym. Sci.,Part A* **3** (1965) 317.

[3] I. Sandeman, A. Keller, *J. Polym. Sci*. **19** (1956) 401.

[4] A. Ziabicki, *Kolliod-Z.* **167** (1959) 132.

[5] K. H. Illers, *Makromol. Chem.* **179** (1978) 497.

[6] K. H. Illers, H. Haberkorn, P. Simák, *Makromol. Chem*. **158** (1972) 285.

[7] R. F. Stepaniak, A. Garton, D. J. Carlsson, D. M. Wiles, *J. Polym. Sci., Polym. Phys. Ed*. **17** (1979) 987.

[8] L. G. Roldan, H. S. Kaufman, *Polym. Lett*. **1** (1963) 603.

[9] J. P. Parker, D. H. Lindenmeyer, *J. Appl. Polym. Sci*. **21** (1977) 821.

[10] J. Gianchandani, J. E. Spruiell, E. S. Clark, *J. Appl. Polym. Sci*. **27** (1982)3527.

O-12 **Session A, Wednesday, 15.06., 12^{20} - 12^{40}**

DNA UV-damage investigated by X-ray spectroscopy

J. Czapla-Masztafiak[1,2*], J. Szlachetko[1,3], C. J. Milne[1],
E. Lipiec[2], J. Sá[4,5], T. J. Penfold[6], J. Schneider[1],
T. Huthwelker[1], C. Borca[1], R. Abela[1]
and W. M. Kwiatek[2]

[1]*Paul Scherrer Institut, CH-5232 Villigen, Switzerland*
[2]*Institute of Nuclear Physics Polish Academy of Sciences, PL-31342 Krakow, Poland*
[3]*Institute of Physics, Jan Kochanowski University in Kielce, 25-406 Kielce, Poland*
[4]*Department of Chemistry, Ångström Laboratory, Uppsala University, Sweden*
[5]*Institute of Physical Chemistry, Polish Academy of Sciences, Warsaw, Poland*
[6]*Department of Chemistry, Newcastle University, Newcastle upon Tyne, NE1 7RU, UK*

Keywords: X-ray spectroscopy, XAS, XES, DNA

*e-mail: joanna.czapla-masztafiak@psi.ch

X-ray spectroscopic methods are atom-specific techniques, using X-ray excitation to gather information about the electronic and geometric structure of the studied system. In biological research the advantages of X-ray absorption spectroscopy (XAS) are already exploited in wide range of studies, while the use of X-ray emission spectroscopy (XES) in this field is scarce although it is a rapidly developing spectroscopic tool. XAS reflects the unoccupied density of states while XES provides information about occupied states and, when combined, these two methods give detailed picture of electronic structure of studied element.

In the presented studies we demonstrate application of the X-ray spectroscopy to investigate the molecular structure of the damage caused by UV radiation in DNA. Understanding the interaction between radiation and molecules that make up the building blocks of the human organism is crucial for designing effective radiation therapy and protection. DNA, being one of the most important components of the human cell, is an influential target of radiation. Therefore, many fundamental studies have focused on the effects of radiation on DNA.

We used phosphorus K-edge X-ray absorption spectroscopy to study changes in chemical structure around the phosphorus atom of the phosphodiester DNA backbone caused by exposure to radiation. By combining the experimental results with theoretical calculations (see Fig. 1), it has been possible to establish the types and relative ratio of lesions produced by UVA around the phosphorus atoms in DNA. X-ray spectroscopy approach provides information not only about the damage types but also about changes in electronic structure around the phosphorus atoms associated with each damage type, which can help to establish the possible mechanisms involved [1]. The experimental procedure used does not require any sample chemical preparation or treatment, avoiding any additional sample preparation complications that may result in affecting the conclusions.

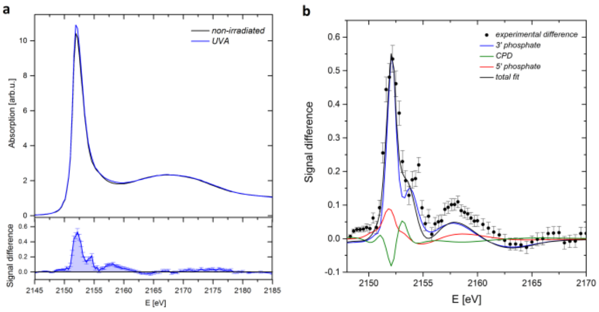

Figure 1. (a) Top: phosphorus K-edge x-ray absorption spectra of intact and UVA-irradiated aqueous DNA samples. Bottom: P K-edge XAS difference signal between the spectrum of damaged and reference DNA samples. (b) Experimental difference of P K-edge XAS obtained for a UVA-irradiated DNA sample fitted with theoretical spectra calculated in FEFF.

XAS studies are extended to XES spectroscopy allowing to acces occupied states of phosphorus site. Non-resonant Kβ X-ray emission spectra of the set of phosphorus compounds were measured with the use of dedicated compact chamber with von Hamos spectrometer setup that enabled us to perform experiment at high energy X-ray beamlines of Swiss Light Source (PSI, Villigen, Switzerland). Kβ lines, in contrast to Kα, provide with high sensitivity information on the chemical environment of the studied atom such as bonding, ligand type and symmetry The results obtained during the experiment showed changes in emission spectra, resulting from changes in chemical structure around phosphorus atom, particularly the number and type of the nearest neighbours of PO_4^{3-} group. Since changes in phosphodiester backbone of DNA caused by radiation are affecting mainly the phosphate groups, our results demonstrate the possibility of using X-ray emission spectroscopy in studies of DNA damage.

Acknowledgments: We acknowledge Swiss Light Source at Paul Scherrer Institute for granting the beamtime. The research leading to these results has received funding from the European Community's Seventh Framework Program (FP7/2007-2013) under grant agreement No. 290605 (COFUND: PSI-FELLOW).

[1] J. Czapla-Masztafiak, J. Szlachetko, C.J. Milne, E. Lipiec, J. Sá, T.J. Penfold, T. Huthwelker, C. Borca, R. Abela, W.M. Kwiatek, *Biophys J.* **110** (2016) 1304.

O-13 **Session A, Wednesday, 15.06., 12^{40} - 13^{00}**

XAFS study on the ultrathin Pt/Co/Pt trilayers modified with short light pulses

A. Wolska[1]*, M.T. Klepka[1], R. Sobierajski[1], I. Jacyna[1], D. Klinger[1], A. Wawro[1], J. Kisielewski[2], Z. Kurant[2], I. Sveklo[2], A. Bartnik[3] and A. Maziewski [2]

[1]*Institute of Physics, Polish Academy of Sciences, Warsaw, Poland*
[2]*University of Bialystok, Department of Physics, Poland*
[3]*Institute of Optoelectronics, Military Academy of Technology, Warsaw, Poland*

Keywords: synchrotron radiation, polarized XAFS, perpendicular magnetization, thin layers

*e-mail: wolska@ifpan.edu.pl

Ultrathin film systems containing magnetic component, like Co, sandwiched between nonmagnetic metals, with tunable magnetization anisotropy (in-plane and out-of-plane) are of particular importance for spintronics as well as for technology of magneto-optical memory devices. The perpendicular easy axis of magnetization is considered in these systems to be related to the structural features of magnetic film and interfaces. The Co/Pt systems are particularly interesting due to the strong magnetic anisotropy and high magneto-optical response in ultra violet range [1]. In case of a Pt/Co/Pt trilayers irradiated with different type of light pulses [2], an out-of-plane from in-plane spin reorientation transition (SRT) was evidenced. While earlier out-of-plane to in-plane SRT was observed and characterized as irradiation-driven intermixing and disordering at the Co–Pt interfaces. These processes lead to a reduction of the anisotropy, coercivity, magnetization and Curie temperature. This way a new possibility to induce the perpendicular magnetization becomes available. In particular, in comparison with conventional thermal annealing of the sample [3], the ultrafast laser annealing provides possibility to create structural and magnetic changes at the interfaces while substrate temperature is almost unchanged which is important for technological applications.

The investigations were performed for the series of the Pt (5 nm)/Co (3.5 nm)/Pt (5 nm) trilayers grown by the MBE method on the sapphire single crystal substrate. In part of the samples the lower Pt layer was grown at 750 °C, in others whole process was carried out at room temperature. Afterward selected samples were irradiated with light – either ns XUV pulses using laser produced plasma source or by fs optical laser pulses. The whole sample surfaces were exposed point by point in order to achieve quasi-uniform irradiated area. The light irradiation fluencies were adjusted to correspond to appearance of the out-of-plane magnetization state. Magnetic studies were carried out after irradiations by means of magnetooptical techniques exploiting Kerr effect. The X-ray absorption fine structure (XAFS) experiment was performed at the BM08 beamline in ESRF. Both regions X-ray Absorption Near Edge Structure (XANES) and Extended X-ray Absorption Fine Structure (EXAFS) were investigated. The signal was gathered in a fluorescence mode at 77 K in a normal (out-of-plane) and grazing (in-plane) incidence configurations. The measurements were carried out at the Co K-edge for the as-grown reference and modified samples.

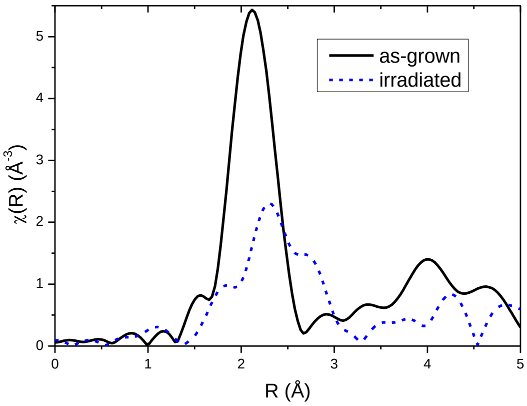

Figure 1. FT EXAFS: comparison between spectra of reference and irradiated sample, both in grazing incidence.

In case of the as-grown samples only the Co neighbors were found in the first shells. The bond lengths and local disorder are the same independently from the preparation method.

The irradiation causes significant changes in the local structure around Co atoms (Fig. 1). Mixing between Co and Pt atoms occurs. The bond lengths and local disorder increase. Moreover, detailed EXAFS analysis revealed that for all irradiated samples the bond lengths in the direction parallel to the layer surface are longer than in the perpendicular one. It suggests that after light irradiation tensile stress appeared in the Co layer.

Acknowledgments: This work has been supported by the Polish National Science Center (Grant No. DEC-2012/06/M/ST3/00475) and by the EU FP7 *EAgLE* project under the grant agreement *REGPOT*-CT-2013-316014. We acknowledge the European Synchrotron Radiation Facility for provision of synchrotron radiation facilities and we would like to thank Dr. Angela Trapananti for assistance in using beamline BM08.

---

[1] K. C. Kuiper, *et al.*, *Appl. Phys. Lett.* **105** (2014) 202402.
[2] J. Kisielewski, *et al.*, *J. Appl. Phys.* **115** (2014) 053906.
[3] J. Kim, *et al.*, *Phys. Rev. B* **65** (2002) 104428.

O-14 **Session B, Wednesday, 15.06., 10^{20} - 10^{40}**

Structural studies of *Pseudomonas syringae* effector protein HOPQ1 and its complex with plant 14-3-3 protein

M. Taube[1]*, F. Giska[2], J. Hennig[2] and M. Kozak[1,3]

[1]*Adam Mickiewicz University, Faculty of Physics, Joint Laboratory for SAXS studies, Umultowska 85, 61-614 Poznan, Poland*
[2]*Polish Academy of Science, Institute of Biochemistry and Biophysics, Laboratory of Plant Pathogenesis, Pawinskiego 5a, 02-106 Warsaw, Poland*
[3]*Adam Mickiewicz University, Faculty of Physics, Department of Macromolecular Physics, Umultowska 85, 61-614 Poznan, Poland*

Keywords: small angle X-ray scattering, HopQ1 protein, 14-3-3 protein, low resolution structure

*e-mail: mtaube@amu.edu.pl

Plant pathogenic bacteria *Pseudomona syringae* in order break the host innate immunity barriers introduce to the plant cell tens of different molecules called effectors [1]. Effectors modify plant proteins that are important in the early steps of pathogen recognition via pathogen-associated molecular pattern (PAMP)-triggered immunity (PTI) pathway [2]. PTI relays on recognition of evolutionarily conserved molecules, like flagellin protein a part of the bacterial motility apparatus, by the membrane receptors. Effectors could modify host factors by phosphorylation, degradation, ADP-ribosylation and changing the cellular localization. Effectors could also act as transcription factors. During evolution, plants also evolved the mechanism to recognize effectors and trigger, Effector Triggered Immunity (ETI), that leads to the programed cell death, called hypersensitive response (HR) at the site of the infection in order to stop spreading of the infection [2]. HopQ1 protein is one of the effector molecules that are transported via type III secretory system (T3SS) to the plant cells during infection [3]. HOPQ1 is a putative nucleoside hydrolase protein. This protein possess two domains: the N-terminal fragment predicted to be disordered and the globular nucleoside hydrolase like (NH) domain. NH domain is conserved structurally across in members of the family. This domain binds calcium ion in the active site of the enzyme. It is interesting that although HOPQ1 protein possess NH domain its enzymatic activity was not shown experimentally. In previous studies it was shown that HOPQ1 is phosphorylated at two sites and one of them, serine 51 is located in 14-3-3 protein binding motif [4].

14-3-3 proteins forms a large family of conserved regulatory factors that are mainly responsible for protein-protein interaction [5]. The regulatory mechanisms of 14-3-3 proteins are the change of cellular localization, conformation, stabilization and binding mode of target proteins.

In this work we proposed the structure of the *Pseudomona syringae* HOPQ1 protein and its complex with 14-3-3 from tobacco (*Nicotiana benthamiana)* protein in solution using small-angle X-Ray scattering technique. Using *ab-initio* and rigid body modeling, we discovered that N-terminal fragment of HOPQ1 in solution is disordered and has dynamic structure. We also tested the effect of calcium ions depletion on the structure of HOPQ1 protein and structure and behavior of HOPQ1 protein variant (Q2A) with mutated amino-acids within putative Ca^{2+} binding site. HOPQ1 protein in the presence of EGTA exist in solution as an elongated dimer. Dimerisation of HOPQ1 protein could be reversed by the addition of excess of Ca^{2+} ions. Q2A mutant also forms elongated dimers in solution regardless of the addition of EGTA. This confirms that calcium binding may regulate oligomerization of HOPQ1 protein.

HOPQ1 protein exists as a 1:1 complex with the dimer of 14-3-3 protein. In the obtained model of the complex between HOPQ1 and 14-3-3 proteins, 14-3-3 protein binds to the disordered tail of HOPQ1 protein possibly sterically blocking access to the putative nuclear translocation signal located downstream of 14-3-3 binding motif. Such interaction may explain the ability of 14-3-3 protein to change localization of HOPQ1 protein inside plant cell.

Acknowledgments: This work was supported by the grant (2012/05/N/ST3/03087) from National Science Center.

---

[1] M. Lindeberg, S. Cunnac, A. Collmer, *Trends Microbiol.* **20** (2012) 199.

[2] D. G. J. Jones, J. L. Dangl, *Nature* **444** (2006) 323.

[3] W. Li, Y. H. Chiang, G. Coaker, *PLoS One* **8** (2013) e59684.

[4] F. Giska, M. Lichocka, M. Piechocki, M. Dadlez, E. Schmelzer, J. Hennig, M. Krzymowska. *Plant Physiol.* **161** (2013) 2049.

[5] A. L. Paul, F. C. Denison, E. R. Schultz, A. K. Zupanska, R. J. Ferl, *Front Plant Sci.* **3** (2012) 190.

O-15 **Session B, Wednesday, 15.06., 10^{40} - 11^{00}**

Establishing nonlinearity thresholds with ultraintense X-ray pulses

J. Szlachetko[1,2]*

[1] *Institute of Physics, Jan Kochanowski University, Kielce, Poland*
[2] *Paul Scherrer Institut (PSI), Villigen, Switzerland*

Keywords: X-ray free-electron laser, nonlinear spectroscopy

*e-mail: jszlachetko@ujk.edu.pl, jakub.szlachetko@psi.ch

X-rays have long been used to explore the electronic and structural properties of all forms of matter, using sources as varied as X-ray tubes to accelerator-based storage rings. X-ray methods have evolved over decades to become specialized tools for a broad range of investigations, with techniques ranging from X-ray scattering through X-ray spectroscopy to X-ray tomography. In general these methods all rely on X-ray measurements that depend linearly on the number of incident X-ray photons. With the advent of X-ray free electron lasers (XFELs), the ability to reach extremely high photon numbers in ultrashort pulse durations has resulted in a paradigm shift in our ability to observe nonlinear X-ray signals. This enormous increase in peak power (pulse energy/pulse duration) has been a double-edged sword, with new and exciting techniques being developed but at the same time well-established techniques proving unreliable [1-3]. This requires a fundamental change in our approach to X-ray science at FELs, since this nonlinear regime is a largely unexplored area, making it hard to predict not only when to expect nonlinear contributions to a measurement, but also to understand the very nature of this response [4, 5].

We report an X-ray spectroscopic study that reveals important details on the thresholds for nonlinear X-ray interactions. By varying both the incident X-ray intensity and photon energy, we establish the regimes at which the simplest nonlinear process, two-photon X-ray absorption (TPA), can be observed. From these measurements we can extract the probability of this process as a function of photon energy as well as the sub-femtosecond lifetimes of the intermediate electronic states, allowing us to develop an analytical equation that predicts the efficiency of the TPA process on the basis of straightforward linear X-ray measurements. This result is the first step towards allowing scientists to perform XFEL measurements with some degree of certainty as to whether they are in the linear or nonlinear X-ray regime.

---

[1] K. Tamasaku, *et al., Nature Photon.* **8** (2014) 313.
[2] N. Rohringer, *et al., Nature* **481** (2012) 488.
[3] M. Beye, *et al., Nature* **501** (2013) 191.
[4] S. M. Vinko, *et al., Nature* **482** (2012) 59.
[5] T. E. Glover, *et al, Nature* **488** (2012) 603.

O-16 **Session B, Wednesday, 15.06., 12^{20} - 12^{40}**

Study of photoionized plasmas emission spectra of atomic and molecular gases excited by intense EUV pulses

I. Saber[1]*, A. Bartnik[1], P.Wachulak[1], H. Fiedorowicz[1] and W. Skrzeczanowski[1]

[1]*Institute of Optoelectronics, Military University of Technology, Warsaw, Poland*

Keywords: Extreme ultraviolet synchrotron radiation, free-electron laser, photoionization

*e-mail: ismaailsaberr@hotmail.com

Light-matter interaction is one of the most vital research topics in physics nowadays. In particularly, the advent of novel radiation sources, synchrotron radiation and free-electron laser (FEL), increased the experimental studies of matter at the atomic and molecular scales. The emitted radiation by electrons in particle accelerators is extremely intense and extends over a broad energy range from the infrared through the visible and ultraviolet, into the soft and hard x-ray regions of the electromagnetic spectrum. Using this energetic beam, photoionization with synchrotron radiation in the vacuum ultraviolet (VUV) or X-ray spectral range has been established for many years as a powerful tool to study many-electron dynamics on free atoms and molecules [1]. However, extremely short and powerful X-ray flashes from FEL make possible to study multiphoton ionization [2]. Furthermore, in a different way, photoionized plasmas are created with irradiation of atomic and molecular gases with high-intensity laser based on EUV sources [3].

In this context, we present the results of experimental and theoretical modeling of photoionized plasma emission spectra from atomic and molecular gases in the ultraviolet and visible light (UV/Vis) region by intense EUV pulses. In the experiment, the source was based on a debris-free gas-puff target [4,5] irradiated with 10 ns/10 J/10 Hz Nd:YAG laser systems. The EUV radiation pulses were collected and focused using a grazing incidence multifoil EUV collector. The laser pulses were focused on a gas stream, injected into a vacuum chamber, synchronously with the EUV pulses. Irradiation of gases resulted in the formation of low temperature photoionized plasmas, emitting radiation in the UV/Vis spectral range. Photoionized plasmas produced in this way consisted of atomic and molecular ions with various ionization states. However, the most observed spectral lines were originated from radiative transitions in singly and doubly charged ions. To get insight into plasma conditions, a collisional-radiative code PrismSPECT [6] and an atomic multiplet code based on Cowan's programs [7] have been used to obtain theoretical spectra. We compare the computed spectral lines with experimental data. Furthermore, the electron temperature was deduced using Boltzmann plots for some selected spectral lines. A detailed discussion of the results is presented.

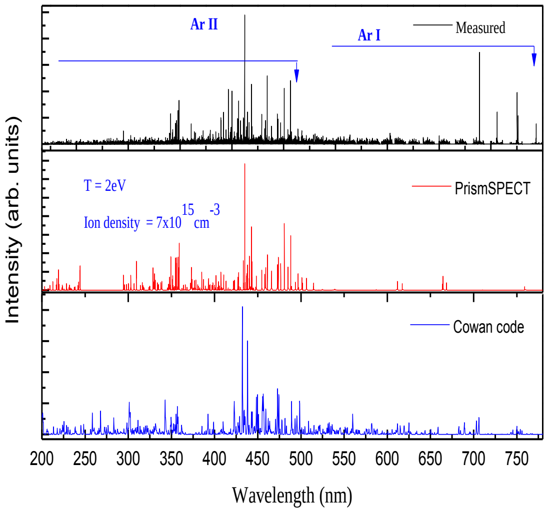

Figure 1. UV/Vis measured emission lines for Argon photoionized plasma induced using the laser-produced plasma EUV source pulses. Where most observed spectral lines were originated from radiative transitions in singly and up to doubly ionized charged ions. A comparison is presented with a theoretically computed spectra from PrismSPECT and Cowan code.

Acknowledgments: The authors acknowledge the financial support from the EU FP7 Erasmus Mundus Joint Doctorate Programme EXTATIC under framework partnership agreement FPA-2012-0033 with the support from 4th Framework Programmer's laserlab Europe project (No. 284464). This work is also supported by the National centre for Science, award number UMO-2013/09/B/ST2/01625. We also acknowledge our collaborators the Institute of Electronics Materials Technology (IMTE, Poland) and the institute of Nuclear Physics, Polish Academy of Sciences in Krakow, for the material supports.

---

[1] I. C. Lyon, J. B. West, K. Dolder, *J. Phys*. B **19** (1986) 4137.
[2] R. Moshammer *et al*, *Phys. Rev. Lett*. **98** (2007) 203001.
[3] A. Bartnik, *Phys. Plasmas* **21** (2014) 073303.
[4] A. Bartnik *et al. Nucl. Inst. Meth*. A **647** (2011) 125.
[5] A. Bartnik *et al. Laser* & *Particle Beams* **31** (2013) 195.
[6] Prism Computational Sciences, Inc., PRISMSPECT, Spectral Analysis Code, 455 Science Drive, Suite 140, Madison, WI, 53711(www.prism-cs.com/software/PrismSpect/PrismSPECT.htm).
[7] R. D. Cowan, *The Theory of Atomic Structure and Spectra*. (University of California Press, **1981**).

O-17 **Session B, Wednesday, 15.06., 12^{40} - 13^{00}**

CERIC-ERIC, the new multi-technique research infrastructure for materials research in Central-Eastern Europe

M. Girod[1]*

[1]*CERIC-ERIC, S.S. 14 – km163.5, 34149 Basovizza (TS), Italy*

Keywords: Research Infrastructure, multi-technique research, synchrotron radiation, material science, nano analytics

*e-mail: matthias.girod@ceric-eric.eu

Material science and nanotechnology are two of the main research fields to take up future challenges of Europe such as alternative energy sources and energy storage or biomedical and pharmaceutical materials. The scientific problems coming up in this fields have become more and more complex in the recent years and require an ever increasing number of instrumental and analytical techniques and disciplines. Such complexity requires the availability of expertise as well as open access to a wide range of probing techniques and many different complementary instruments.

The CERIC-ERIC research infrastructure was developed to face this challenge and to make a wide variety of instruments available through open access.

CERIC stands for Central European Research Infrastructure Consortium and is a distributed research infrastructure unifying several national institutions, under one roof.[1] This multinational facility was set up as a European Research Infrastructure Consortium (ERIC).[2] It brings together research facilities from Austria, Croatia,Czech Republic, Hungary, Italy, Poland, Romania and Slovenia. Statutory seat is in Trieste, Italy. All partners offer a set of complementary, cutting-edge instrumentation from national institutes for free and open access to excellent researchers all over the world (Fig 1).

CERIC-ERIC comprises synchrotron radiation, neutron radiation, microscopic techniques, ion-beam analysis methods and NMR.

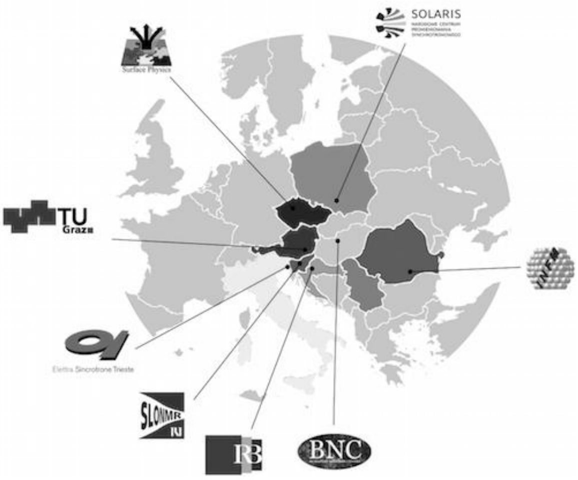

Figure 1. Locations and partners of CERIC-ERIC.

All instruments are available for open access through one single entry point. The selection of proposals and experiment time is done in a peer-review process and based on scientific excellence only. Following the nature of CERIC as a multi-probe facility, the open access operation allows to ask not only one instrument per proposal but to get experiment time granted for several complementary instruments with one proposal.

Being an ERIC means that CERIC is not only a consortium but a full legal entity. For this reason CERIC can act as partner in H2020 as well as ESIF proposals.

This talk will present CERIC, its structure and scientific focus. It will further highlight CERICs opportunities for researchers as well as the possibilities to act as a versatile and strong partner.

---

[1] Commission Implementing Decision, *Official Journal of the EU*, L184/49, **2014**

[2] Council Regulation (EC) No 723/2009 of June 25th **2009**.

O-18 **Wednesday, 15.06., 16^{20} - 16^{40}**

Latest developments in laboratory SAXS/WAXS instruments

S. Rodrigues[1]*, P. Panine[1], S. Desvergne[1], P. Høghøj[1], R. Mahé[1] and F. Bossan[1]

[1]Xenocs, 19 rue François Blumet, F-38360 Sassenage, France

Keywords: laboratory SAXS/WAXS, instrumentation, in-situ studies, macromolecules, block copolymers

*e-mail: sergio.rodrigues@xenocs.com

In parallel to the advent of dedicated synchrotron radiation sources and beamlines several breakthroughs have been accomplished for laboratory analytical X-ray instrumentation and in particular for Small Angle X-ray Scattering (SAXS) instrumentation. Breakthroughs include X-ray micro-focus sources with aspheric multilayer coated optics, scatterless collimation [1], sample environment, software and hybrid pixel photon counting detectors as well as instrument design with for example multiple source energy capability [2].

Today, these technologies combine to provide in-laboratory SAXS instruments, with a performance comparable to that previously achieved only at synchrotrons. Flexible instrument designs provide simultaneous measurement of Wide Angle X-ray Scattering (WAXS) signal in various sample forms (including thin film) and experimental conditions. The state-of-the-art performance opens the way for a wide range of applications, including scattering from soft matter. Performance and possibilities will be illustrated through a few application examples such as characterization of highly diluted macromolecules or in-situ dynamic studies of complex soft materials.

Study of 3D protein enveloppes with laboratory SAXS is now widely used as a complementary technique to electron microscopy and NMR. Different high brilliance sources technologies can be used to study highly diluted proteins including large macromolecular complexes. Data modelling of various proteins will be presented and compared including with synchrotron data.. Performance is now at a level where traditional sample holders such as capillaries, could be a limiting factor, overcome by innovative flow cells.

Physical behavior of soft materials is often complex and couples to environmental conditions such as stress and temperature. Studying the structure variations upon external fields over 2 or 3 decades in real space, i.e. from atomic scale up to the mesoscale is thus particularly useful in understanding complex materials. If fast transitions require intense flux of third generation synchrotrons, slow phenomena can be studied fruitfully in laboratory systems, offering in one hand less instantaneous flux but with unrivalled availability of beam time. Among others, this will be illustrated by the SAXS/WAXS kinetic study of washing powder exposed to moisture. Moreover fast transition studies are also possible with laboratory SAXS/WAXS systems with relative exposure times which match the standard measurement conditions used in Differential Scanning Calorimetry (DSC) of few degrees per minute for instance. Capability to measure simultaneously nanoscale structure and crystalline features during in-situ studies such as temperature controlled measurements on copolymer samples will be illustrated.

---

[1] Y.Li *et al., J. Appl. Cryst*. **41** (2008) 1134.
[2] S. Koppoju, *et al., J. Appl. Cryst.* **48** (2015) 2040.

O-19 **Wednesday, 15.06., 16^{40} - 17^{00}**

New developments in Near Ambient Pressure XPS – EnviroESCA, Small Spot and Imaging NAP-XPS Solutions

V. Simic-Milosevic[1]*, S. Bahr[1], M. Meyer[1], T. Kampen[1], O. Schaff[1] and A. Thissen[1]

[1]*SPECS Surface Nano Analysis GmbH, Voltastrasse 5, 13355 Berlin, Germany*

*e-mail: Violeta.Simic-Milosevic@specs.com

Over the last 15 years, Near Ambient Pressure (NAP-) XPS has demonstrated its promising potential in a wide variety of applications. Starting from the Catalysis and Ice paradigm, the focus has shifted towards solid-liquid interfaces, liquid jets and in-situ electrochemistry. Initially, the experiments had to be carried out using advanced synchrotron sources to reach reasonable count rates. This is still state-of-the-art for most sensitive analyses under NAP conditions. The windowless beam entrance stages, that have been developed by SPECS over the last years utilize all capabilities of modern synchrotron beamlines for NAP-XPS. Furthermore, SPECS PHOIBOS 150 NAP offers optimized transmission for electrons, even at pressures up to and above 100mbar, so researchers can now use it with conventional X-ray and UV sources in their own laboratories, as well. Because of the widened application fields, standard XPS is now also attainable when combined with easily adjustable monochromated X-ray sources that offer stable operation, small excitations spots, and high photon flux densities, even in Near Ambient Pressure conditions. The latest designs and results are presented showing small spot performance for spot sizes < 30 µm, while also showcasing the latest implementations of imaging NAP-XPS that uses a new concept allowing for lateral resolved measurements without a compromise in count rate and usability. Highlighting on how sample environments (in situ cells for gases and liquids, electrochemical cells, gas inlets) and integration are both absolutely essential to obtain relevant results from well-defined samples, the presentation will demonstrate the use of NAP-XPS systems for high throughput-XPS measurements, as well as a variety of applications. This all is integrated into a revolutionary system concept, the EnviroESCA.

O-20 **Friday, 17.06., 12^{20} - 12^{40}**

The status of the PEEM/XAS beamline at Solaris

M. Zając[1]*, A. Bianco[2], E. Busetto[2], P. Goryl[1], J. Korecki[3,4], M. Sikora[3,5], M.J. Stankiewicz[1], M. Ślęzak[3] and A.I. Wawrzyniak[1]

[1]*National Synchrotron Radiation Centre SOLARIS at Jagiellonian University, ul. Czerwone Maki 98, 30-392 Kraków, Poland*
[2]*Synchrotron ELETTRA, Strada Statale 14, 34149 Basovizza, Trieste, Italy*
[3]*Faculty of Physics and Applied Computer Science, AGH University of Science and Technology, Al. Mickiewicza 30, 30-059 Kraków, Poland*
[4]*Jerzy Haber Institute of Catalysis and Surface Chemistry, Polish Academy of Sciences, ul. Niezapominajek 8, 30-239 Kraków, Poland*
[5]*Academic Centre of Materials and Nanotechnology, AGH University of Science and Technology, Al. Mickiewicza 30, 30-059 Kraków, Poland*

Keywords: synchrotron radiation, beamline

*e-mail: mar.zajac@uj.edu.pl

The first bending magnet beamline built in the National Synchrotron Radiation Centre Solaris is optimized for the soft X-ray photon energy range 200-2000 eV. The calculated energy resolution (ΔE/E) is in the order of $2.5\text{x}10^{-4}$ or better. The chosen optical design based on the plane grating monochromator working in the collimated light has been studied by the Optical Group from Elettra. The dimensions of the focalized beam at the end station place, which will host a Photoemission Electron Microscope (PEEM), are 100µm (H) x 50µm (V). In the future additional refocusing device can be installed to increase the photon flux density on the sample for more demanding experiments. The first results of the front end components commissioning and actual time schedule will be presented.

Within the framework between Jagiellonian University and Jerzy Haber Institute of Catalysis and Surface Chemistry PAS, the Photoemission Electron Microscope will be main end station of the 04BM beamline. The PEEM was successfully tested at the Pollux beamline in the Swiss Light Source. Exchangeable with microscope we foresee to use separate chamber for X-ray absorption spectroscopy measurements. It will be dedicated to experiments in the field of biology, chemistry, catalysis, material science and physics. The current possibilities of both experimental stations will be presented. In the future, the spectroscopy chamber could be adapted to the other techniques like X-ray magnetic circular dichroism or scanning transmission X-ray microscope chamber.

Acknowledgments: Work supported by the European Regional Development Fund within the frame of the Innovative Economy Operational Program: POIG.02.01.00-12-213/09.

O-21 **Friday, 17.06., 12^{40} - 13^{00}**

Commissioning of ARPES beamline at the Polish National Synchrotron Solaris

K. Szamota-Leandersson[1]* and J. J. Kolodziej[2]

[1]*National Synchrotron Radiation Centre SOLARIS, Jagiellonian University, Kraków, Poland*
[2]*Jagiellonian University, Kraków, Poland*

Keywords: synchrotron radiation, Photoelectron spectroscopy

*e-mail: Karolina.szamota-leandersson@uj.edu.pl

Ultra high resolution Angle-Resolved Photoelectron Spectroscopy (UARPES) beamline has been constructed at the III generation synchrotron SOLARIS in Cracow, Poland.

The length of the UARPES beamline from source to the sample position is 28.5 m. The source of photon is 2.8–m-long, 120–mm period, quasi-periodic elliptically polarizing undulator (EPU) of Apple II type. The undulator with minimum gap of 20 mm, enables variable polarization (linear of any orientation, circular, and elliptical). The maximal radiative power of the undulator is 600 W. The UARPES EPU is the first undulator installed at 1.5 GeV SOLARIS storage ring of the Polish National Synchrotron Radiation Centre SOLARIS. The UARPES beamline is designed to cover the UV photon energy range from 8 eV to 100 eV. High resolving power of 20 000 over the whole energy range is achieved with the state-of-art monochromator combining NIM and PGM geometry in a single design. The beamline control system is integrated with SOLARIS machine using TANGO software. Each of the beamline devices is navigated with a dedicated device server. PLC system monitors all beamline's critical parameters and sends status information to the Graphical Users Interface (GUI). Beamline motors and encoders are controlled with state-of-art ICEPAP controllers. The ARPES beamline has been designed safe for users. The first beamline mirror is enclosed inside a safety hutch having 5 mm shielding lead wall. Much attention is paid to monitoring of the radiation level during operations.

The Endstation includes two separated chambers: the sample preparation chamber equipped with devices for surfaces cleaning and surface diagnostic as well as the analysis chamber including state-of-the-art energy spectrometer DA-30 L from VG-Scienta, Sweden. The spectrometer facilitates measurements within the solid angle of 30° without sample rotation. The system is equipped with a cryogenic 5- axis manipulator including LHe flow type cryostat, stabilizing the sample temperature within the range 10 K to 500 K.

The SOLARIS synchrotron is a newcomer to the synchrotron world, and the ARPES beamline is the first beamline to be commissioned at SOLARIS. This situation is obviously a challenge for the SOLARIS team. Fortunately there are experts from other, well established synchrotron centers assisting with their advices. At the beginning the beamline is configured for the linearly (horizontally) polarized light and monochromator working in the PGM mode. The photon beam geometry along the beamline is monitored using currents intercepted by collimating baffles and photodiodes, as well as using beam images on the YAG screens.

Figure 1. An image from YAG screen - first photons at the ARPES beamline. The acquisition was performed for electron beam values: energy 1.5 GeV and current 10 mA. The undulator gap equals to 100 mm.

The success of guiding the light from the source up to the Endstation to a large extent depends on fiducialisation and carefull metrology of the beamline component. The used metrology procedures (a so-called blue lining) has allowed to transmit the photon beam along the beamline using only minimal corrections. The carefully performed checking of numerical models by SOLARIS alignment group has been crucial for correct placement of the beamline elements.

Acknowledgments: This work was supported by European Regional Development Funds.

O-22 **Friday, 17.06., 18^{10} - 18^{30}**

Self-absorption free HEROS method applied to a time-resolved study following oxidation of single site Ta catalysts

W. Błachucki[1]*, J. Szlachetko[2,3], J. Hoszowska[1], J.-Cl. Dousse[1], F. Zeeshan[1],Y. Kayser[2], M. Nachtegaal[2], and J. Sá[4,5]

[1]*Department of Physics, University of Fribourg, Chemin du Musée 3, CH-1700 Fribourg, Switzerland*
[2]*Swiss Light Source, Paul Scherrer Institut, CH-5232 Villigen-PSI, Switzerland*
[3]*Institute of Physics, Jan Kochanowski University, 25-406 Kielce, Poland*
[4]*Department of Chemistry, Uppsala University, 752 37 Uppsala, Sweden*
[5]*Institute of Physical Chemistry, Polish Academy of Sciences, 01-224 Warsaw, Poland*

Keywords: synchrotron radiation, time-resolved high energy resolution off-resonant X-ray spectroscopy, catalysts

*e-mail: wojciech.blachucki@unifr.ch

In this work we employed the high energy resolution off-resonant spectroscopy (HEROS) technique [1] for a time-resolved study of the density of unoccupied states of Ta atoms in a chemical system under reaction conditions [2]. In the HEROS approach, off-resonant X-ray emission spectra, which carry information on the density of unoccupied states [3,4], are recorded at a single incident beam energy fixed below the absorption edge of interest. As a result, the impact of the self-absorption effect on the density of unoccupied states data obtained from the measured HEROS spectra is reduced to only the probability of reabsorption of the emitted fluorescence radiation in the target which is usually nearly constant in the measured emission energy range [5]. We show that the self-absorption freeness and swiftness of the HEROS approach make it a powerful tool to study the chemical surrounding of the given atoms in chemical systems under reaction conditions [2].

The measurements were carried out at the SuperXAS beam line, Swiss Light Source, PSI, Switzerland. The investigated silica supported Ta complexes, Ta(V) carbene bisalkyl and Ta hydride, were loaded into a quartz-capillary reactor at a 20 ppm O_2 atmosphere. The Ta(V) carbene bisalkyl complex was prepared at the University of Lyon and the Ta hydride was obtained by subjecting Ta(V) carbene bisalkyl to reaction with 10% H_2/He gas mixture at the temperature increased slowly in the range 20 °C – 140 °C. The samples were exposed to the synchrotron radiation beam (~10^{11} photons/s) of energy 9.863 keV and 9.867 keV for Ta(V) carbene bisalkyl and Ta hydride, respectively (i.e. 18 eV and 14 eV below the Ta L_3-edge binding energy, respectively). The induced fluorescence was detected in the energy range around the Ta $L\alpha_1$ emission line (8.146 keV) by means of a wavelength-dispersive von Hamos-type spectrometer consisting of two cylindrically curved segmented-type Si(444) crystals [6] and a two-dimensional PILATUS 100K detector. The HEROS spectra were collected one by one with an acquisition time of 40 s each. From the full width at half maximum (FWHM) of a Gaussian fit to the elastic scattering peak an experimental resolution of 1.6 eV was found.

For both studied complexes the fingerprint Ta $L\alpha_1$ HEROS spectra were recorded before and after oxidation to determine temporal changes in the species' concentration. Analysis of the fingerprint spectra revealed formation of dimeric Ta species caused by the reaction with oxygen. As can be seen in Figure 1(a), during reaction of Ta(V) carbene bisalkyl with oxygen only about 20% of the sample first turned into its oxidized form and the remaining 80% transformed afterwards. The demonstrated step-wise transition is an effect of different reaction rates for oxidation and dimerization. Such a behavior was not observed in the case of Ta hydride which was found to oxidize suddenly after about 6800 s, as shown in Figure 1(b).

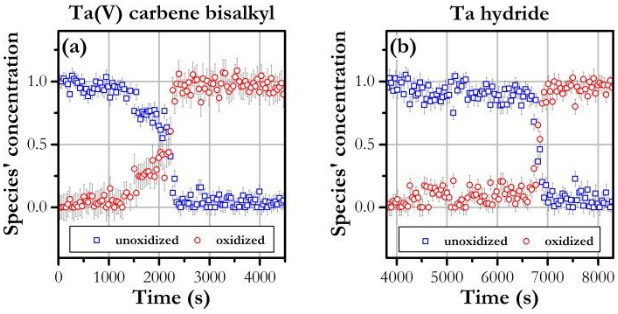

Figure 1. Relative concentration of Ta(V) carbene bisalkyl [2] (a) and Ta hydride (b) during oxidation as a function of time.

The present study demonstrates that HEROS allows probing the density of unoccupied states with high temporal resolution. In particular, since the HEROS spectra are not affected by the self-absorption effect, HEROS is a powerful tool to perform time-resolved studies on systems under reaction conditions.

Acknowledgments: This work was performed at the Swiss Light Source, Paul Scherrer Institute, Villigen, Switzerland. Some of us (W. B., J. H., J.-Cl. D., F. Z. and Y. K.) also acknowledge the financial support of the Swiss National Science Foundation.

---

[1] J. Szlachetko *et al.*, *Chem. Commun.* **48** (2012) 10898.
[2] W. Błachucki, J. Szlachetko, Y. Kayser, J.-Cl. Dousse, J. Hoszowska, D. L. A. Fernandes, J. Sá, *Phys. Chem. Chem. Phys.* **17** (2015) 18262.
[3] H. A. Kramers, W. Heisenberg, *Z. Phys.* **31** (1925) 681.
[4] J. Tulkki, T. Åberg, *J. Phys. B: At. Mol. Phys.* **15** (1982) L435.
[5] W. Błachucki, J. Szlachetko, J. Hoszowska, J.-Cl. Dousse, Y. Kayser, M. Nachtegaal, J. Sá, *Phys. Rev. Lett.* **112** (2014) 173003.
[6] J. Szlachetko et al., *Rev Sci Instrum* **83** (2012) 103105.

O-23 **Friday, 17.06., 18^{30} - 18^{50}**

Determination of electronic structure of iron compounds using resonant X-ray emission spectroscopy

M. Nowakowski[1]*, J. Czapla-Masztafiak[1,2],
J. Szlachetko[2,3] and W. M. Kwiatek[1]

[1]*Institute of Nuclear Physics Polish Academy of Sciences, PL-31342 Krakow, Poland*
[2]*Paul Scherrer Institut, 5232 Villigen, Switzerland*
[3]*Institute of Physics, Jan Kochanowski University in Kielce, 25-406 Kielce, Poland*

Keywords: synchrotron radiation, RXES, XAS, iron

*e-mail: michal.nowakowski@ifj.edu.pl

X-ray spectroscopy is dynamically developing and powerful tool to examine electronic structure of materials. Coupling this method with unique properties of synchrotron radiation allows to study more subtle effects and gather information with high precision

Resonant X-Ray Emission Spectroscopy (RXES) is a scattering experiment that is extremely useful in electronic properties studies. In proper experimental geometry with dispersive spectrometer it allows simultaneously record X-ray emission (XES) and absorption (XAS) spectra. This way both occupied and unoccupied electronic levels in material can be examined. Additionally, resonantly excited absorption and emission offers a possibility to study electronic states in very high resolution, much higher than in conventional Total Fluorescence Yield XAS or XES experiment [1].

Using RXES method iron foil, α-Fe_2O_3 (hematite) and $Fe(NO_3)_3$ were examined. Experiment was performed at SuperXAS beamline (Swiss Light Source,Paul Scherrer Institut, Villigen, Switzerland). RXES measurements were carried out around the Fe K-edge and X-ray detection was performed using a wavelength-dispersive spectrometer in the von Hamos geometry [2].

Data was obtained in a form of 2D RXES planes for each compound. From each plane non- and high resolution XAS and XES spectra were extracted and compared with calculated Density of States (lDOS) functions to identify electronic structure of studied materials. XAS, XES spectra and corresponding lDOS functions were calculated in FeFF9.6 software [3] using Full Multiple Scattering approach. Results for α-Fe_2O_3 (hematite) are shown in Fig. 1. Analysis was focused on valence to core and pre-edge regions of XES and XAS spectra, respectively. The contribution of molecular orbitals of iron and neighbouring atoms to the absorption and emission spectra was established, giving the insight into occupied and unoccupied states of studied compounds.

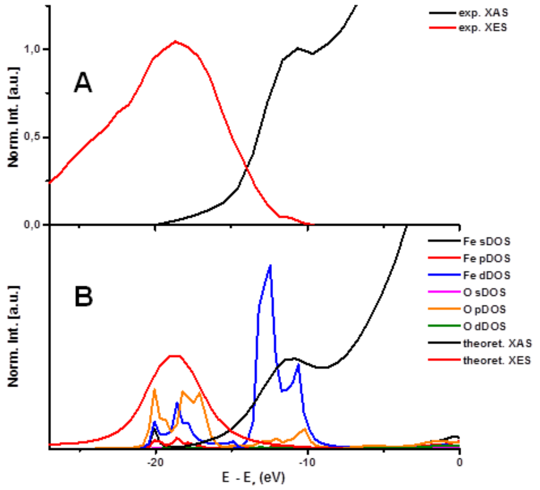

Figure 1. Example results for α-Fe_2O_3 (hematite) extracted from 2D RXES plane **A** - Experimental XES spectrum and XAS spectrum in valence to core and pre-edge region respectively. **B** – Theoretically calculated spectra and corresponding lDOS functions.

The results showing that the combination of RXES method with theoretical calculations that allow fast and accurate examination of electronic structure of materials will be presented.

Acknowledgments: We acknowledge Swiss Light Source at Paul Scherrer Institute for granting the beamtime.

---

[1] L. J. P. Ament, M. van Veenendaal, T. P. Devereaux, J. P. Hill, J. van den Brink *Rev. Mod. Phys.* **83** (2011) 705.
[2] J. Szlachetko, M. Nachtegaal *et al.*, *Rev. Sci. Instrum.* **83** (2012) 103105.
[3] J. J. Rehr, J. J. Kas, F. D. Vila, M. P. Prange, K. Jorissen, *Phys. Chem. Chem. Phys,* **12** (2010) 5503.

O-24 **Saturday, 18.06., 10^{20} - 10^{40}**

Local atomic structure evolution around dopant ions in YSZ+Mn solid solution

J. Stępień[1]*, M. Sikora[2], D. Pomykalska[3], M.M. Bućko[3] and Cz. Kapusta[1]

[1]AGH University of Science & Technology, Faculty of Physics & Applied Computer Science, Department of Solid State Physics, 30-059 Krakow, Poland
[2]AGH University of Science and Technology, Academic Centre for Materials and Nanotechnology, Mickiewicza 30, 30-059, Kraków, Poland
[3]AGH University of Science & Technology, Faculty of Materials Science & Ceramics, Department of Ceramics and Refractory Materials, Mickiewicza 30, 30-059 Krakow, Poland

Keywords: yttria stabilized zirconia YSZ, EXAFS, XANES

*e-mail: jstepien@agh.edu.pl

Yttria stabilized zirconia (YSZ) is a popular material for electrolyte in Solid Oxide Fuel Cells (SOFCs). Aliovalent doping of ZrO_2 with cations that have oxidation state lower than IV generates oxygen vacancies in the material and significantly increases ionic conductivity (naturally occurring in this material at high temperature) so that its magnitude is reasonable for real life applications. Oxygen vacancies are necessary for stabilizing cubic fluorite structure of ZrO_2 and to prevent material from destruction during SOFC operation. Globally, up to solubility limit, the right amount of dopants introduced to ZrO_2 forms solid solution, however locally increased density of oxygen vacancies creates disorder in the atomic structure [1].

The influence of manganese dopant on YSZ structure and properties is interesting because during cell operation Mn ions can diffuse to electrolyte from cathode, which is often built of $LaMnO_3$ based material. Also, intentional mixing of electrodes and electrolyte material to create Mixed Ionic-Electronic Conductors (MIECs) is explored in order to reduce electrical loses during cell functioning [2-4].

The series of $Mn_x(Y_{0,148}Zr_{0,852})_{1-x}O_{2-\delta}$ ceramics [4] was systematically studied by means of X-ray absorption spectroscopy. EXAFS and XANES results show that the most significant changes in the measured spectra concern Mn ions and their environment, while the local structure evolution around Y and Zr is less pronounced. X-Ray diffraction and EXAFS measurements also indicate the presence of Mn_3O_4 precipitates for the samples with higher manganese content.

We show that gradual evolution of the local atomic environment around Mn ions in the YSZ phase takes place upon increasing manganese content. This is due to changes in the average Mn oxidation state and structural relaxation caused by growing amount of oxygen vacancies.

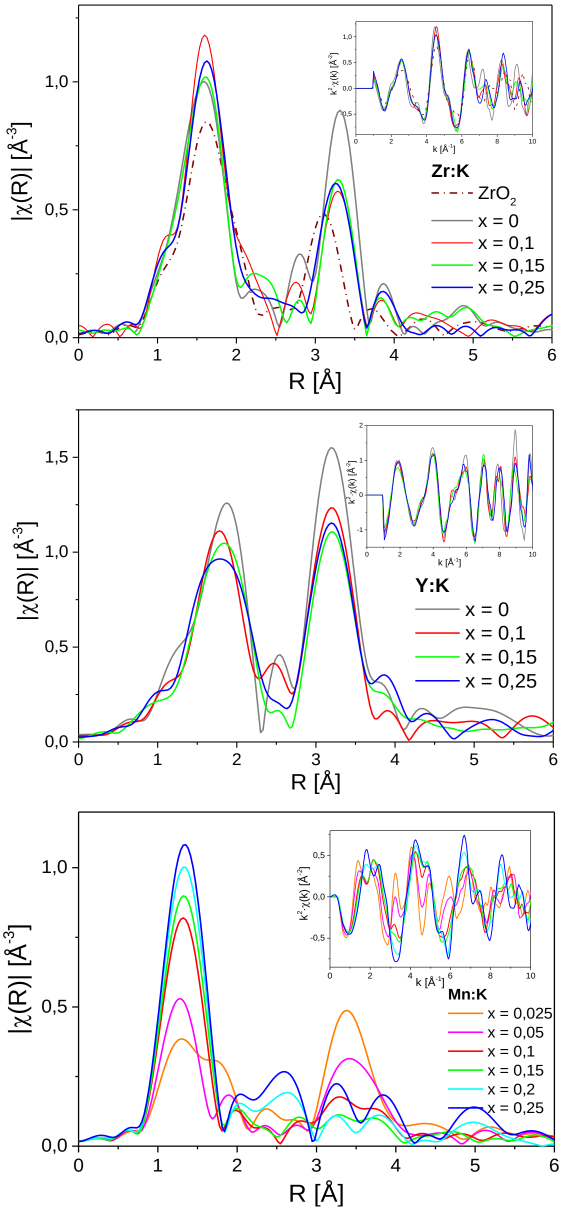

Figure 1. K edge EXAFS spectra in the R and k (inset) space of (top to bottom) Zr, Y and Mn.

---

[1] E.H. Kisi and C.J. Howard, *Key Engineering Materials* **153-154** (1998) 1.
[2] H. Chen, K. Cheng, F. Ye, W. Weng, *Ceramics International* **37** (2011) 1209.
[3] J. H. Kim, G. M. Choi, *Solid State Ionics* **130** (2000) 157.
[4] D. Pomykalska, M. M. Bućko, M. Rękas, *Solid State Ionics* **181** (2010) 48-52.

P-01

Extended Abstract

Data mining in synchrotron radiation

W. Dwiecki[1]*

[1]*Faculty of Chemistry, Adam Mickiewicz University in Poznan, Poznan, Poland*

Keywords: synchrotron, data mining, Google Scholar

*e-mail: wojciechdwiecki@wp.pl

INTRODUCTION

Growing popularity and availability of synchrotron radiation-based techniques in recent years results in increase in the number of publications and articles which can be easily found in scientific databases or popular web browsers [1]. Due to the amount and variety of publications it is a serious problem to predict how issues related to synchrotron will develop in future. However, analysing the data from past 30 years collected with commonly available tools for example Google Scholar and appropriate combination of queries can provide some information about trends and research areas where synchrotron radiation will develop and be the most frequently applied [2].

DATA SOURCE SELECTION

The most important issue in data exploration is a selection of the right data source. In this presentation there was compared with one another: Google Scholar and two databases: Scopus and Academic Search Complete (ASC) [3].

Searched results presented in *Figure 1.* and in *Table 1.* confirm that Google Scholar is definitely the largest "mine" of knowledge about the synchrotron as was predicted. Such large differences in results are because: (a) Google Scholar searches queries in entire document, Scopus and ASC searches only in title, abstract and keywords of publication; (b) Google Scholar is in fact a collection of results from all existing databases.

Despite the fact that Scopus and ASC allows for searching with more advanced options than Google Scholar, number of publications current in databases are much smaller and require from user very precise typing of queries which can be time-consuming.

MEASUREMENT TECHNIQUES USING SYNCHROTRON RADIATION

Using Boolean operators (such as OR and AND) number of results in Google Scholar could be limited to the most accurate. During data exploration *synchrotron* was combined with abbreviations of most common measurement techniques which were inserted between quotation marks (equivalent to searching WITH EXPRESSION). In this way number of publications related to the following techniques was investigated: Extended X-ray absorption fine structure (EXAFS), X-ray absorption fine structure (XAFS), X-ray absorption near edge structure (XANES), Energy-dispersive X-ray diffraction (EDXRD), Small-angle X-ray scattering (SAXS) and Wide-angle X-ray scattering (WAXS). Results given in *Figure 2.* show that most popular measurement technique is EXAFS. This kind of queries combined with another words could be a useful tool in evaluation the best method for the measurement of specific material.

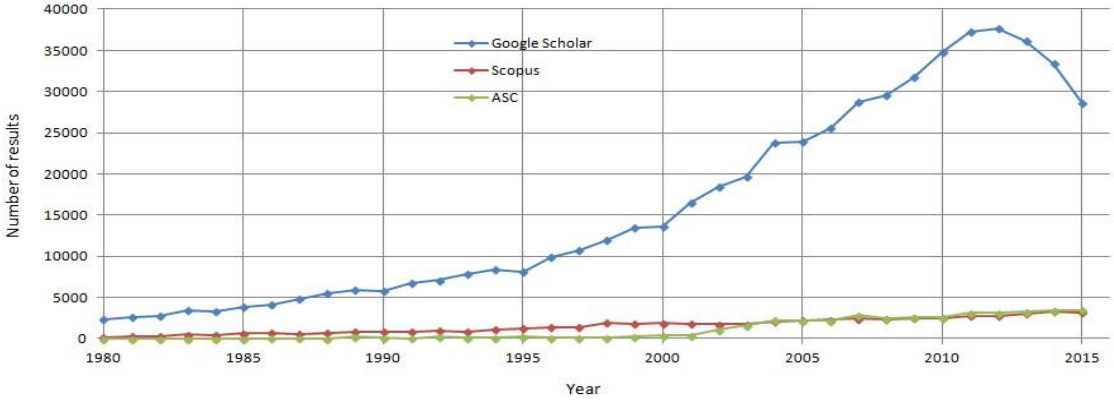

Figure 1. Comparison of number of results *synchrotron* collected in different sources in the period 1980 – 2015.

	Google Scholar	Scopus	ASC
Number of results	567530	56058	39191
Fraction of all results (%)	85,63%	8,46%	5,91%

Table 1. Number of results *synchrotron* in different sources in the period 1980 – 2015.

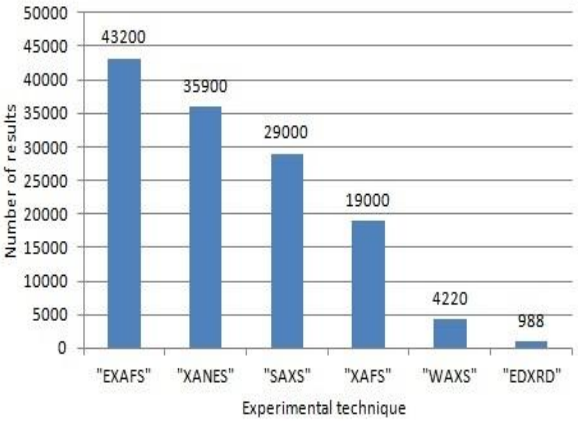

Figure 2. Number of results containing names of measurement techniques received in Google Scholar.

SYNCHROTRON RADIATION IN CRYSTALLOGRAPHY

Investigations focused on crystallographic structure of material can be divided into two groups: diffraction of single crystals and powder diffraction. Google Scholar gives the answer which of these two techniques are used more commonly in the synchrotron radiation (*Figure 3.).*

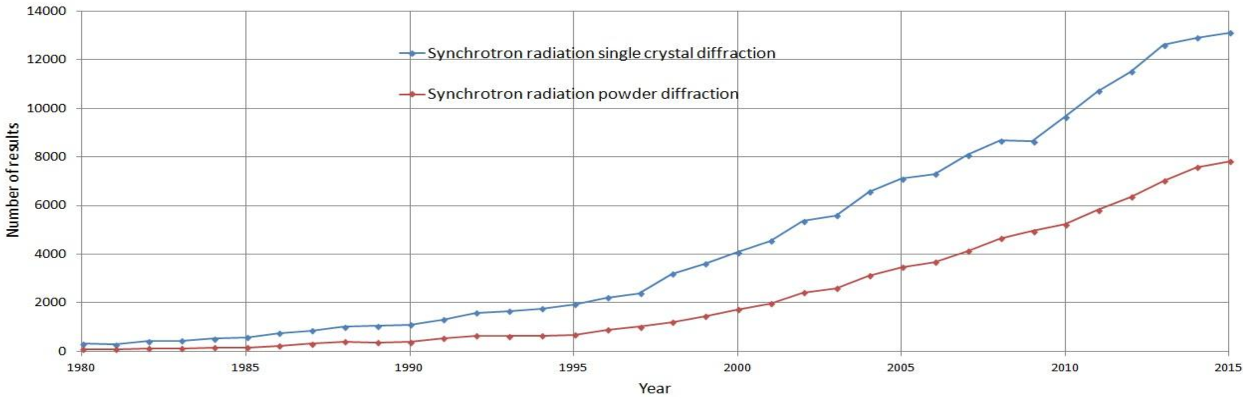

Figure 3. Numbers of results SRSCD/SRPD in the period 1980 – 2015 received in Google Scholar.

This trend can indicate that amount of materials which can be measured using *synchrotron radiation powder diffraction* (SRPD) is more limited than those which are measured using *synchrotron radiation single crystal diffraction* (SRSCD) or, what is also possible, SRSCD gives better rusults than SRPD. More advanced data searching will help in choosing the most suitable technique for specific material.

SYNCHROTRON POPULARITY IN JOURNALS

Advanced search in Google Scholar allows determining the frequency with which the word *synchrotron* appears in the most prestigious scientific journals. One of Google Scholar built-in function is a list of journals which are divided into different areas of science. In data analysis was used journals titles from bookmark "Chemistry and material science" with the highest h5 index [4].

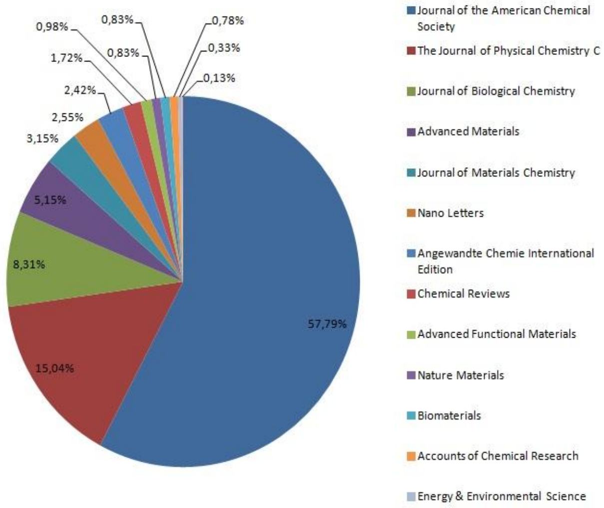

Figure 4. Number of results *synchrotron* in journals [%] received in Google Scholar.

Results in *Figure 4.* show interests of this journals in topics related to synchrotron and can help in the selection of the journal to which the future publication will be sent.

---

[1] A-W. Harzing, S. Alakangas, *Scientometrics* (2013) 1-18.
[2] Jankowski W., Hoffmann M., *J Med Internet Res* **18** (2) (2016) e38.
[3] H. R. Jamali, M. Nabavi, *Scientometrics* **105** (2015) 1635.
[4] A. Martín-Martín, J. M. Ayllón, E. Orduña-Malea, E. Delgado López-Cózar, EC3 Working Papers, 17 (2014).

P-02

Extended Abstract

LEEM and XPEEM studies of electroforming process in Fe-doped $SrTiO_3$ epitaxial films

J. Kubacki[1,2]*, D. Kajewski[1], A. Koehl[3], R. Dittmann[3], M. Pilch[1], A. Zakharov[4] and J. Szade[1, 2]

[1]*A. Chełkowski Institute of Physics,University of Silesia, Uniwersytecka 4, Katowice, Poland*
[2]*Silesian Center for Education and Interdisciplinary Research, 75 Pułku Piechoty 1A, 41-500 Chorzów*
[3]*Peter Grünberg Institut, JARA-FIT, Forschungszentrum Jülich, 52425 Jülich, Germany*
[4]*Max IV labolatory, Lund, Sweden*

Keywords: $SrTiO_3$, Fe doping, thin film, LEEM, XPEEM, valence band

*e-mail: jerzy.kubacki@us.edu.pl

In the last decade the resistive switching effect occurring mainly in oxide materials was intensively study [1]. The strontium titanate (STO) is a potential candidate for future applications in random access memories due to the interesting properties related to resistive switching [2].

The electrical properties of STO can be tuned by doping. It was found that doping with iron or niobium influences the STO resistive switching properties [3].

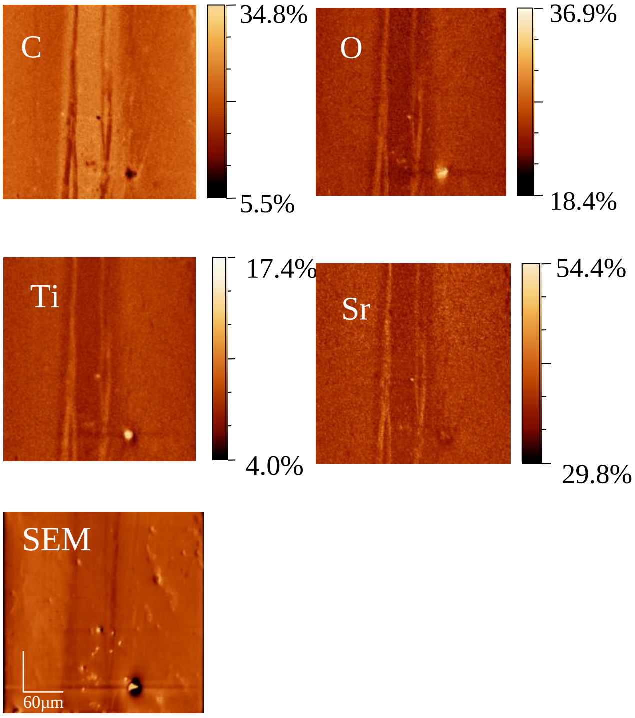

Figure 1. The AES chemical distribution maps for carbon, oxygen, titanium and strontium of the contact area with the electrode for the Fe doped STO film. The SEM image of the analysed area was added.

In our earlier work the ultra thin epitaxial films of strontium titanate doped with 1%, 2% and 5% (STO:Fe) iron were studied with the use of synchrotron radiation. X-ray absorption spectroscopy (XAS) results indicate existence of two Fe oxidation states 2+ and 3+ in the films independent of Fe concentration. Moreover, Fe 2+ appeared to be situated mostly on the surface of films [4]. The Fe 2+ and 3+ ions in STO:Fe films were found to give different contributions (the partial density of states - PDOS) to the structure of valence band through the resonant photoemission (RESPE) study [5]. An increased density of states in the energy-gap region for iron doped films was found in all performed PES studies [5].

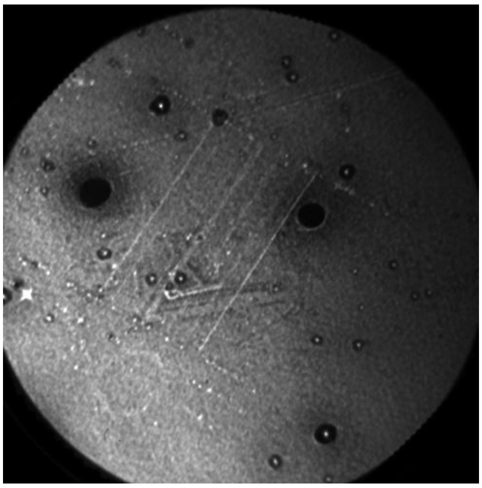

Figure 2. The LEEM image of 2% Fe doped STO film recorded from the area with the diameter of 20 micrometers. The white parallel lines are the effect of earlier contact with the biased AFM tip.

The electroforming process is usually necessary prior to attain stable switching. However, the origin of this behaviour is not clear. In order to get insight to this phenomenon we tested modification of the Fe:STO thin films surface properties after treatment with the biased electrode. Two kinds of experiment were performed – both took place in the UHV chambers.

First was realised by application of aluminium foil electrode with a positive bias of +10 V to Fe:STO film. The electro-modified surface was examined in-situ by RESPE and XAS methods. The results showed a slight decrease of the density of states in the band-gap region originating from the +2 Fe ions [6]. A similar effect was observed from the XAS studies during heating of films at elevated temperature [4]. It was found that the electroforming process does not influence the shape of the Fe PDOS for 3+ state but changes the Fe PDOS +2 contribution. The influence of the atmosphere on the electroformed sites was studied by the AES method. The maps, presented in Figure 1 show the chemical distribution of carbon, oxygen, titanium and strontium in the region which was treated by the biased aluminum foil electrode. The maps show strong chemical modification of the film surface as the effect of contact with the positively biased electrode. The effect was stable despite the stay of the sample in air for a few days. It shows that electroformation is not only related with the forced depletion of oxygen but leads to chemical modification of the surface region.

To verify the results obtained in our previous studies, the LEEM (Low-energy Electron Microscopy) [7] and XPEEM (X-ray Photoemission Electron Microscopy) [7] investigations of the 2% Fe doped STO film were performed. The sample was electroformed in UHV by the conducting AFM tip biased with the voltage up to 10 V. Then it was transferred in air to the LEEM chamber. The scanned modified area was 8x8 micrometers.

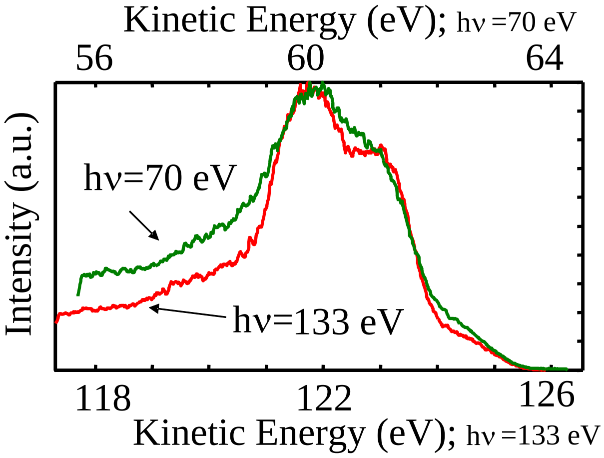

Figure 3. The photoemission spectra obtained with two various photon energy from electro-modified by AFM tip area.

The LEEM study presented in Figure 2 showed clear changes in contrast within the modified area. The lighter parallel lines originate from the contact with the biased AFM tip. The lines consisted of many small dots, which probably can be assigned to the edges of dislocations. It was found that density of dislocations in the STO films deposited by the PLD method is much higher than in the single crystals of STO, for which equals about 10^9 per cm^2 [2]. On the other hand, the electron diffraction (LEED) images showed no structural difference between the virgin and electroformed area. The origin of the contrast visible in LEEM is probably related with the local changes of the work function, and consequently various adsorption of contaminations from air mainly those containing carbon.

The XPEEM spectra from the electroformed area obtained at photon energy of 133 eV and 70 eV and showing the valence band region are presented in Figure 3. The general shape of the valence band is in agreement with the spectra obtained for the macroscopic area including the in-gap region [8].

The various shape of the spectra obtained for two photon energies can be explained by different photoionization cross-section coefficients.

After heating the sample in situ to about 120 ^{0}C the LEEM contrast disappeared but no changes in the XPEEM images were detected.

In Figure 4 the valence band spectra recorded from the electroformed and virgin area are shown. Additionally, the spectrum obtained after annealing was added. A slightly lower intensity of photoemission was found at binding energy of about 2 eV for the not modified area. A small increase of photoemission was found at about 3 eV after heating.

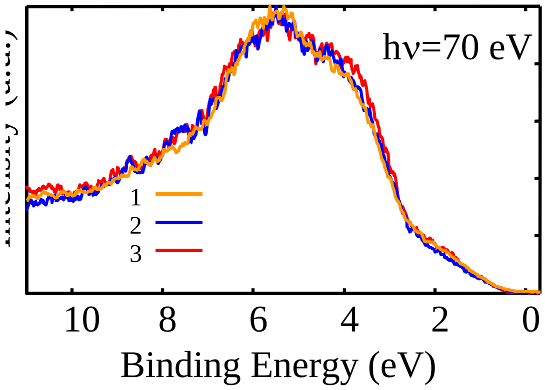

Figure 4. The valence band spectra recorded for: 1 – area electroformed by the biased AFM tip, 2 – outside electroformed area, 3 – after annealing at 120 °C.

Our studies showed that electroforming leads to a significant modification of the surface region of the STO films doped with Fe. The positive bias applied to the surface causes the movement of oxygen ions along dislocations towards to the surface. The chemical change is stable even after reoxidation of the films in air.

Acknowledgments: This work was supported by the NCBiR within the project NCBiR/ERA-NET-MATERA/3/2009.

---

[1] R. Waser, R. Dittmann, G. Staikov, K. Szot, *Adv. Mater.* **21** (2009) 2632.

[2] K. Szot, W. Speier, G. Bihlmayer and R. Waser, *Nature Materials* **5** (2006) 312.

[3] T. Menke, R. Dittmann, P. Meuffels, K. Szot, and R. Waser, *J. Appl. Phys.* **106** (2009) 114507;
R. Muenstermann, R. Dittmann, K. Szot, Sh. Mi, Ch. L. Jia, P. Meuffels and R.Waser *Appl. Phys. Let.* **93** (2008) 023110.

[4] A. Köhl, D. Kajewski, J. Kubacki, C. Lenser, R. Dittmann, P. Meuffels, K. Szot, R. Waser, and J. Szade *Phys. Chem. Chem. Phys.* **15** (2013) 8311.

[5] J. Szade, K. Szot, M. Kulpa, J. Kubacki, Ch. Lenser, R. Dittman, R. Waser, *PhaseTransitions* **84** (2011) 489;
J. Szade, D. Kajewski, J. Kubacki submitted to *Phys. Chem. Chem. Phys.*

[6] J. Kubacki, D. Kajewski, A. Koehl, Ch. Lenser, R. Dittmann and J. Szade, *X- Ray Spectr.* **44** (2015) 339.

[7] L. H. Veneklasen *Rev. Sci. Instrum.* **63** (1992) 5513.

[8] J. Kubacki, D. Kajewski, A. Koehl, Ch. Lenser, R. Ditmann and J. Szade, *Syn. Rad. Nat. Sci.* **14** (2015) 23.

P-03

Inelastic X-ray scattering as a tool to study the phonon dispersion in PbTe and (Pb,Cd)Te solid solution

R. Minikayev[1]*, R. Kuna[1], M. Trzyna[2],
A. Szczerbakow[1], K. Gas[1,3], J. Łażewski[4], A. Bosak[5]
and W. Szuszkiewicz[2,1]

[1] *Institute of Physics, Polish Academy of Sciences, Al. Lotników 32/46, 02-668 Warszawa, Poland*
[2] *Faculty of Mathematics and Natural Sciences, University of Rzeszów, ul. S. Pigonia 1, 35-310 Rzeszów, Poland*
[3] *Institute of Experimental Physics, University of Wrocław, pl. M. Borna 9, 50-204 Wrocław, Poland*
[4] *Institute of Nuclear Physics PAS, ul. Radzikowskiego 152, 31-342 Kraków, Poland*
[5] *ESRF - The European Synchrotron, 71 avenue des Martyrs, 38000 Grenoble, France*

Keywords: synchrotron radiation, thermoelectric materials inelastic X-ray scattering

*e-mail: minik@ifpan.edu.pl

Thermoelectric materials are of great interest for the energy applications because they can transform heat into electricity [1]. An efficient thermoelectric material should exhibit the same time a low heat conductivity and a high electric conductivity. A good knowledge of the lattice dynamics is essential in order to understand both heat and electron transport in such material.

Lead telluride (PbTe) is well known thermoelectric semiconductor (SC) crystallizing in the rock-salt (RS) structure, cadmium telluride (CdTe) is the SC exhibiting the sphalerite structure [2]. The difference in PbTe and CdTe crystal symmetry was in the past the principal reason of many problems in a growth of the (Pb,Cd)Te solid solution. Recent successful growth of big (with a volume exceeding 1 cm^3), metastable (Pb,Cd)Te single crystals with the RS structure obtained by Self-Selecting Vapour Growth (SSVG) method at the Institute of Physics PAS [3] changed this situation. In the present work the bulk, single PbTe crystal and the (Pb,Cd)Te solid solution with 2% of CdTe grown by the SSVG were used to investigate the phonon dispersion.

Primary parameters describing collective atom motion in the crystal lattice are momentum transfer (Q) and energies (E), that could be obtained via experimental method, such as the inelastic neutron scattering (INS). In the middle of 70's an idea has appeared to investigate the lattice dynamics using an inelastic X-ray scattering (IXS) [4] and it was the experimental technique applied in the present work. The ID28 beamline in ESRF equipped with the IXS spectrometer enabling one to study phonon dispersion in condensed matter was used for this purpose. The high energy of incident photons (E = 17.8 keV) leads to a possibility to investigate phonons for every momentum in Brillouin zone (BZ). The phonon dispersion in the PbTe and (Pb,Cd)Te solid solution was investigated along Γ-X [100] and Γ-K [110] high-symmetry directions in the BZ. We determined the phonon dispersion for all modes along the [100] direction and for two phonon branches only (TO, TA) along the [110] direction both in PbTe and (Pb,Cd)Te. Due to the extremely high energy resolution of scattered photons ($\Delta E/E = 10^{-7}$) the accuracy of relevant phonon dispersion was comparable to that corresponding to the INS measurements in spite of low energy of phonons in the PbTe-based crystals. The IXS results confirmed the INS data obtained previously for PbTe and show an increase of the full-width at half-maximum (FWHM) value for TO phonon mode close to the BZ center along Γ-X and Γ-K directions.

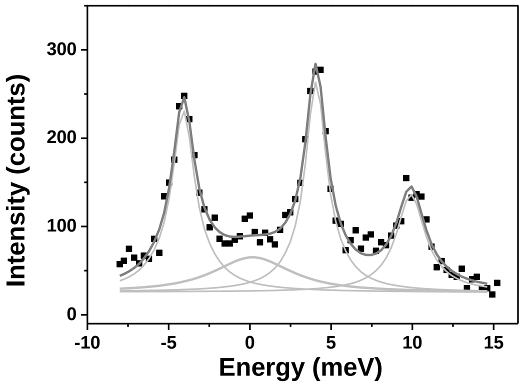

Figure 1. Part of the IXS spectrum taken for PbTe for Q = (0,0,0.7). Points – experimental data, solid lines – result of the fit. Two high-intensity structures correspond to the absorption and the excitation of LA phonon, third structure is due to the excitation of the LO phonon.

Acknowledgments: This work was partially supported by the research grant (UMO-2014/13/B/ST3/04393) from National Science Center (Poland), by the European Synchrotron Radiation Facility (ESRF), Grenoble (France) and by the EAgLE project (Project Number: 316014) from EU.

---

[1] O. Delaire, et al. *Nat. Mater.* **10** (2011) 614.
[2] M. Szot, et al. *Acta. Phys. Pol. A*. **116** (2009) 959.
[3] M. Szot, et al. *Cryst. Growth. Des.* **11** (2011) 4794.
[4] W. Cochran, *Phonons* (ed. by R.W.H. Stevenson, Oliver and Boyd, London 1966).

P-04

The MD simulations for the interpretation of thermally activated decomposition of (Ga,Mn)As thin layers at medium temperature post growth annealing

Y. Melikhov[1]*, J. Domagala[1], J. Sadowski[1,3], S. Kret[1],
P. Konstantynov[1], M. Chernyshova[2], R. Minikayev[1]
and I.N. Demchenko[1]

[1]*Institute of Physics PAS, Warsaw, Poland*
[2]*Institute of Plasma Physics and Laser Microfusion, Warsaw, Poland*
[3]*MAX IV Laboratoriet, Lund, Sweden*

Keywords: synchrotron radiation, XAFS, molecular dynamic, DFT, FEFF

*e-mail: melikhov@ifpan.edu.pl

A potential simultaneous use of the ferromagnetic and semiconductors properties in spintronics has attracted a great interest to diluted magnetic semiconductors (DMS) with the most studied material being (Ga,Mn)As. With the optimized MBE growth and post growth annealing procedures nowadays (Ga,Mn)As layers have achieved the Curie temperature, T_C, as high as about 200 K. This is remarkably high as for DMS, but still too low in view of potential application in spintronics devices. From physics point of view, an indirect coupling between localized spins mediated by charge carriers is of paramount importance for the possibility of magnetic ordering in DMS [1]. However, the Ruderman-Kittel-Kasuya-Yosida (RKKY) interaction mechanism, which is used to describe the properties of DMS systems, has limitations predicting an increase of T_C with increasing concentration of Mn impurities, the situation which is not always experimentally observed. Further studies not only on the influence of microstructure and its inhomogeneities upon material's properties but also on transformation processes (including formation and migration of point defects) which occur in (Ga,Mn)As during growth and post growth annealing should lead to an improved understanding of the microstructure evolution and could potentially lead to a further progress in reaching larger T_C in (Ga,Mn)As.

The goal of this project is to check the effectiveness of classical molecular dynamics (MD) simulations for the interpretation of x-ray absorption fine structure (XAFS) of thermally activated decomposition of DMS, namely, (Ga,Mn)As after medium temperature post growth annealing. The (Ga,Mn)As layer was grown in a SVTA MBE system [2] on GaAs (100) substrate. After growth it was cleaved into four pieces: one was left intact (as-grown) and three were annealed at 250, 350, and 450°C, respectively. Finally, the separation of the (Ga,Mn)As layer from the GaAs substrate was performed by chemical etching, a so-called "lift-off" procedure [3].

In order to determine the local atomic structure around Mn atoms the XAFS spectra at the K-edges of Mn were gathered at the BL22 CLÆSS beamline at ALBA light source [4] at LN temperature. Figure 1 presents normalized XANES spectra around Mn K edge, whereas, an inset shows modulus of Fourier transforms, FT(R), of the EXAFS function for each of the samples. The analysis of XANES spectrum of the "as-grown" sample indicates that Mn atoms most likely substitute Ga in the GaAs matrix, which is also supported by our own *ab initio* simulation results. The annealed samples show: (i) reorganization of the near edge electronic structure; together with (ii) a dramatic decrease of FT(R) amplitude with increase of the annealing temperature. Such behavior of XAFS signal is a likely indicator of a redistribution/diffusion of Mn atoms in the host matrix, which allowes us to propose the following working hypothesis: starting from the randomly distributed substitutional manganese, Mn_{Ga} (referred as monomers), and point defects like Mn_i (interstitial manganese), V_{As} or V_{Ga} (corresponding vacancies) formation of non-regular distributed areas of "*N-mers*" (dimer, trimer and so on combined through As) could occur, which eventually could lead to formation of Mn-rich (Ga,Mn)As clusters. Theoretical support of this working hypothesis comes from our *ab initio* calculations performed by WIEN2k code, as well as theoretical studies by Raebiger *et al.* [5].

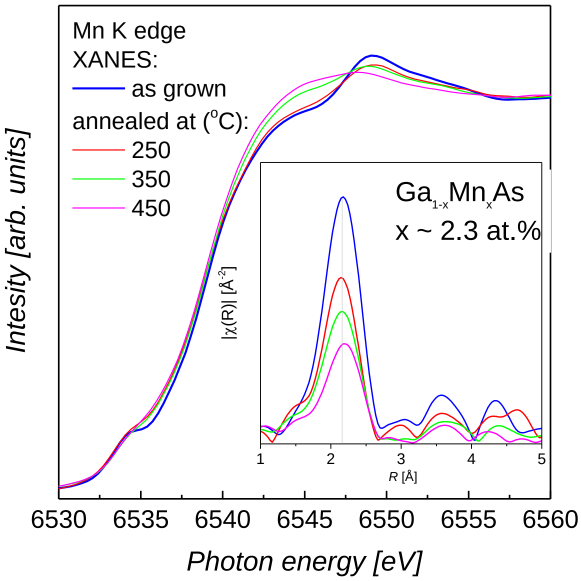

Figure 1 Normalized Mn K-edge XANES spectra of the (Ga,Mn)As layers (i.e. after the "lift-off" procedure) (The inset shows Fourier transforms of the k-weighted Mn K-edge EXAFS χ function).

Based on our working hypothesis we constructed the model structures (4x4x4 supercell) which are expected to correspond to different stages of annealing process. The NVT-type classical MD simulations using GULP code were performed where each structure was equilibrated at 90 K (the temperature of the EXAFS experiment), and a set of instantaneous atomic configurations was accumulated during the production run and averaged. XAFS spectra for each averaged atomic configuration (constructed by the FEFF code) were used to perform qualitative/quantitative analysis of the EXAFS/XANES spectra of the annealed samples, respectively. This analysis showed that the signal is a combination of signals coming from both Mn monomers and "*N-mers*".

Acknowledgments: We acknowledge the support from the EAgLE project (Project Number: 316014) and from ICM infrastructure.

---

[1] H. Ohno et al. *Appl. Phys. Lett.* **69** (1996) 363.

[2] J. Sadowski, J. Z. Domagala, chapter 2 in *Advanced Functional materials: A perspective from theory to experiment* (Eds. B. Sanyal and O. Eriksson) Elsevier, 2012.

[3] S. Decoster et al., *Synchrotron Rad.* **20** (2013) 426.

[4] *BL22 CLÆSS beamline: Technical description*, ALBA light source, Spain, http://www.cells.es/en/beamlines/bl22-claess.

[5] H. Raebiger et al., *Appl. Phys. Lett.* **89** (2006) 012505.

P-05

High-resolution Powder Diffraction Study of $Ca_9R(VO_4)_7$ (R = La, Gd) Crystals

W. Paszkowicz[1]*, A. Shekhovtsov[2] and A. Fitch[3]

[1]*Institute of Physics, Polish Academy of Sciences, al. Lotnikow 32/46, PL-02668 Warsaw, Poland,*
[2]*Institute for Single Crystals, NAS of Ukraine, Lenin Ave. 60, 61001, Kharkov, Ukraine*
[3]*European Synchrotron, ESRF, Grenoble, France*

Keywords: powder diffraction, vanadate

*e-mail: paszk@ifpan.edu.pl

Whitlockite is a mineral of the formula $Ca_9(MgFe)(PO_4)_6PO_3OH$ (*R*3*c* space group). Whitlockite-related materials form an extended family of compounds. Those of the $Ca_9R(VO_4)_7$ formula (R = a rare earth) are considered for applications in optoelectronics, *e.g.*, in white-light emitting diodes and lasers. In the $Ca_9R(VO_4)_7$ structure the R atoms partially occupy the Ca sites with occupation depending on the choice of the R atom. In this work, $Ca_9R(VO_4)_7$ (R – La, Gd) single crystals are studied. They were grown by the Czochralski method. The structure was refined using the powder diffraction data collected at a high-resolution synchrotron beamline. The structural details of the samples will be discussed.

P-06

Evaluation of zirconia dioxide tetragonal phase degradation introduced by grinding with dental burr

A. Piosik[1]*, K. Żurowski[2], W. Hędzelek[1] and M. Kozak[3]

[1]*Department of Prosthodontics, Poznań University of Medical Sciences, Bukowska 70, 60-812 Poznań, Poland*
[2]*Industrial Institute of Agricultural Engineering, Starołęcka 31, 60-963 Poznań, Poland*
[3]*Department of Macromolecular Physics, Faculty of Physics, Adam Mickiewicz University Umultowska 85,61-614 Poznań, Poland*

Keywords: zirconium dioxide, dental processing, X-ray diffraction

*e-mail: adampiosik@gmail.com

Thanks to the evolution of CAD/CAM systems, zirconia is increasingly popular as ceramic material for dental restorations. Most often zirconia is used as modified yttria (Y_2O_3) tetragonal zirconia polycrystal (Y-TZP). Between the different ceramics utilized in dental prosthodontics, zirconia shows optimum properties: superior toughness, strength, and fatigue resistance, excellent wear properties and biocompatibility. Pure zirconia presents the phenomenon of allotropy, that is, same chemical composition but different in atomic arrangement, namely: orthorhombic, monoclinic, tetragonal, cubic, liquid. Y-TZP is a metastable material, however incorrect dental processing may induce unfavorable phase transitions, gaining more monoclinic amount and in turn, corrupting mechanical properties of the material [1,2].

The aim of the analysis was verification of the influence of dental processing protocols, on phase transition of yttrium stabilized zirconium dioxide. Evaluation of Y-TZP structure was performed with scanning electron microscopy (SEM) and X-ray diffraction (XRD). Zirconia samples were grinded with different dental burs (varies in diamond grit size) to simulate the procedures that usually the material undergoes. At the same time recorded with infrared camera for evaluation of generated temperature.

XRD study revealed impact of mechanical processing methods on the range of transition from tetragonal to monoclinic phase of the tetragonal zirconia polycrystals. The results were correlated with process accompanying generated temperature.

---

[1] A. Della Bona, O. E. Pecho, R. Alessandretti, *Materials* **8** (2015) 4978.

[2] L. Vanni, S. Valter, *Dental Materials* **26** (2010) 807.

P-07

Structural and magnetic changes of ultrathin Pt/Co/Pt trilayers under the influence of irradiation by an excimer laser

E. Dynowska[1*], W. Szuszkiewicz[2,1], R. Minikayev[1],
J. Z. Domagala[1], F. Ott[3], M. Jakubowski[1], A.Wawro[1],
R. Sobierajski[1], M.O. Liedke[4], Y. Yuan[4], S, Zhou[4],
I. Sveklo[5], Z. Kurant[5] and A. Maziewski[5]

[1]Institute of Physics, Polish Academy of Sciences,
al. Lotników 32/46, 02-668 Warsaw, Poland
[2]Facultyof Mathematics and Natural Sciences,
University of Rzeszów, ul Pigonia 1, 35-310 Rzeszów, Poland
[3]Laboratoire Léon Brillouin, CEA-CNRS, CEA Saclay,
91191 Gif sur Yvette Cedex, France
[4]Helmholtz-Zentrum Dresden-Rossendorf,
Bautzner Landstraße 400, 01328 Dresden, Germany
[5]Department of Physics of Magnetism, University of Białystok,
ul. Ciołkowskiego 11, 15-245 Białystok, Poland

Keywords: X-ray diffraction, X-ray reflectivity, polarized neutron reflectivity, magnetic anisotropy

*e-mail: dynow@ifpan.edu.pl

The Co/Pt-based ultrathin films are nowadays intensively studied due to their interesting physics and potential applications in a magnetic devices (high-density information storage devices, sensor or actuators). The initial magnetic properties of ultrathin Co-Pt system can be modified by an external factor like ion or laser irradiations. It was shown that the irradiation of Pt/Co/Pt trilayers by extreme ultraviolet (EUV) light pulses causes reorientation of the magnetic anisotropy through the creation of $Pt_{1-x}Co_x$ disordered alloy [1].

In this paper we present the results of structural studies of several Pt/Co/Pt trilayer samples irradiated by an excimer laser (homogeneous beam, profile 308 nm wavelength, 25 ns pulse duration, at two fluences: 400 and 600 mJ/cm^2). The trilayers deposited by the molecular beam epitaxy (MBE) onto (0001)-oriented Al_2O_3 substrate consisted of 5 nm thick Pt buffer, 3.5 nm thick Co layer and 5 nm thick Pt cover. As-deposited samples as well as those modified by excimer laser were studied by means of X-ray diffraction, X-ray reflectivity, polarized neutron reflectivity and magnetooptical magnetometry methods.

The diffraction studies confirmed the [111] growth direction of the Pt/Co/Pt/ Al_2O_3 structure. Due to small thickness of the layers the thickness fringes originated from Pt buffer prevent the direct observation of the diffraction peaks from the Pt and Co layers, but the position of Pt 111 peak can be found in the center between two strongest fringes as shown in the Fig.1a. The value of the 111 lattice spacing calculated from the position of the Pt peak indicates a compressive strain with strain parameter γ equal 2.50 for the Pt buffer layer (without strain: $\gamma = 2.45$ – see Ref. [1]). Irradiation at the fluence D = 400 mJ/cm^2 results only in a reduction of the strain state of Pt layer to the value of $\gamma = 2.46$ without changing the value for the relaxed lattice parameter of Pt. The further irradiation with the fluence D = 600 mJ/cm^2 results in creation of the $Pt_{0.72}Co_{0.28}$ alloy distributed in the whole structure. This layer is under tensile strain ($\gamma = 2.39$) with the relaxed lattice parameter value equal to $a_{\mathrm{rel}} = 3.851(4)$ Å what confirms creation of ordered Pt_3Co alloy with primitive cubic structure and lattice parameter $a = 3.8541$ Å [2].

Moreover, irradiation with higher fluence caused the smoothing of the surface layer as evidenced by the thickness oscillations visible in the Fig.1b.

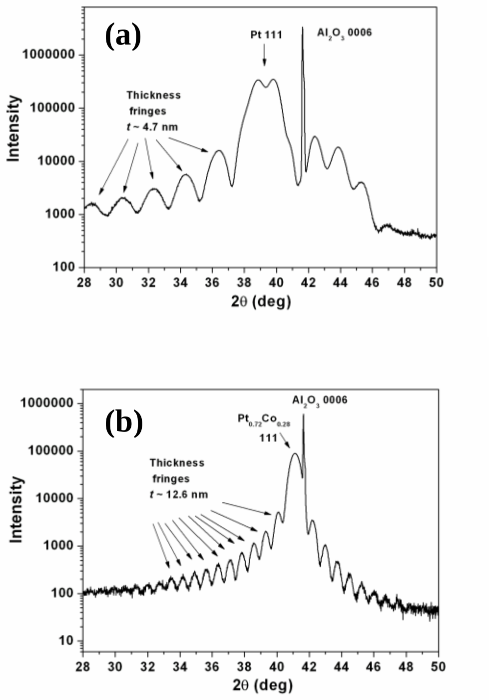

Figure 1. X-ray diffraction patterns in the vicinity of 111 Pt reflection performed for: (a) – as-deposited sample, (b) – irradiated by excimer laser with fluence D = 600 mJ/cm^2.

The X-ray reflectivity and polarized neutron reflectivity measurements confirmed the results obtained by X-ray diffraction studies.

In-plane magnetization state was observed for as-deposited samples. After the irradiation with lower fluence of 400 mJ/cm^2, the increase of magnetic anisotropy has been observed. The further increase of fluence up to 600 mJ/cm^2 results in an appearance of the out-of-plane magnetization state.

Concluding, for lower applied fluence the strain modification in trilayer is the only observed irradiation effect. Despite the lack of Pt and Co intermixing in trilayer system, the observed strain modification is sufficient for increase of magnetic anisotropy.

Acknowledgments:
The work was partially supported by the National Science Centre (Poland) [grant DEC-2012/06/M/ST3/00475].

---

[1] Dynowska E, Pelka JB, Klinger D, et al. *Nucl Instrum Methods Phys Res B.* **364** (2015) 33.
[2] JCPDS, Reference code 29-0499.

P-08

Catalytic centre of double metal cyanide catalysts as resulted from XAS studies

K. Lawniczak-Jablonska*[1] and A. Chrusciel[2]

[1]*Institute of Physics, Polish Academy of Sciences, Al. Lotnikow 32/46, 02-668 Warsaw, Poland*
[2]*MEXEO, Energetykow Str 9, 47-225 Kędzierzyn-Koźle, Poland*

Keywords: DMC catalyst, catalytic centre, XAS

*e-mail: jablo@ifpan.edu.pl

Double metal cyanide (DMC) catalysts are commonly applied at industrial ring opening polymerization of the epoxides. Nevertheless, the knowledge on the molecular nature of their high activity and selectivity is limited. XAS studies were performed to look for possible catalytic centre in this family of catalysts.

The DMC catalysts and the reference material were synthesized at *MEXEO Kędzierzyn-Koźle* according to the method described in [1]. The reference material was hydrated trizinc *bis*-[hexacyanocobaltate(III)] compound ($Zn_3[Co(CN)_6]_2 \cdot nH_2O$) of negligibly low catalytic activity, not suitable for practical application. The investigated DMC materials were synthesized from $ZnCl_2$ and potassium hexacyanocobaltate(III) solution, in presence of two organic ligands: *tert*-butanol ^{t}BuOH) and glyme ($CH_3OCH_2CH_2OCH_3$). These ligands are frequently used in commercial application of this family of DMC catalysts. These catalysts were denote here as DMC BuOH and DMC glyme, respectively.

The local atomic structure around Zn and Co atoms was determined by EXAFS. Experiments were performed at beamline SAMBA of the Soleil synchrotron at room temperature in atmospheric pressure and in transmission mode. Appropriate amounts of the samples were mixed with cellulose and pressed into a pellet. The analysis was performed using IFEEFIT package [2].

The catalysts are heterogeneous materials. Moreover, they did not form the mix of several phases. As was discussed in ref. [3] the diffraction pattern of the part of catalysts with crystalline phase till now was not resolved and probably is not responsible for good catalytic properties of these materials. Catalysts have a considerable fraction of amorphous material. Therefore we have applied in analysis the least squares linear combination (LC) method, the most popular for analyzing the content of different chemical compounds of given element in heterogeneous material. Several models of atomic order around Zn were considered. The models proposed in the literature discussing the role of O and Cl atoms in DMC catalysts were taken into account [4, 5, and 6].

Similar as in paper [3] the best fit to the EXAFS data was obtained for the model assuming two different local atomic order around Zn atoms. Local atomic order of the considerable fraction of Zn atoms was as should be in the reference anhydrous material with rhombohedral structure. Zn was bonded directly to four cyanide groups. The rest of Zn had Cl in the first coordination sphere (Fig. 1). According to synthesis procedure, there is an access of Zn atoms in catalyst. And indeed we found that only 84(3) % and 79(5) % of Zn atoms have 4 NC near neighbour groups for DMC BuOH and DMC glyme, respectively. For the rest of Zn atoms Cl was identified in the first coordination sphere in the distance 2.24 Å. This Zn-Cl bond length is close to that in $ZnCl_2$ (2.30Å), therefore can be considered as characteristic for Zn-Cl bond. Nevertheless, the existence of $ZnCl_2$ compound was not confirmed, because the model with the atomic order characteristic for $ZnCl_2$ (in first coordination shell 2 Cl in distance 2.3 Å and 2 Cl in distance 3.2 Å and next 4 Zn atoms at distance 3.75 Å and 2 Cl in distance 3.8 Å) could not be fitted. Substituting some of Cl atoms with oxygen leads to an increase of the errors of estimated parameters and to an increase of the R_f parameter which estimate the quality of the fit. Nevertheless, one cannot exclude that oxygen atoms can be bonded to Zn but in very limited amount. In many reports it is emphasized that the type (coming from water or ligands) and amount of oxygen atoms coordinated to Zn should play an important role in the ring opening polymerization of propylene oxide since oxygen atoms coordinated to a zinc ion are believed to be a real active center of DMC catalyst [6]. From the performed EXAFS studies we cannot confirm this role. Instead we do confirm the location of Cl close to Zn atoms. The role of Cl is also discussed in the literature on the base of experiment [4] and molecular calculation [5]. In the paper by Zhang et al., [4] based on overall chemical premises the role of Cl atoms in the catalytic properties of DMC was postulated and reported that the ligand influences on catalytic activity only by helping to form the amorphous structure.

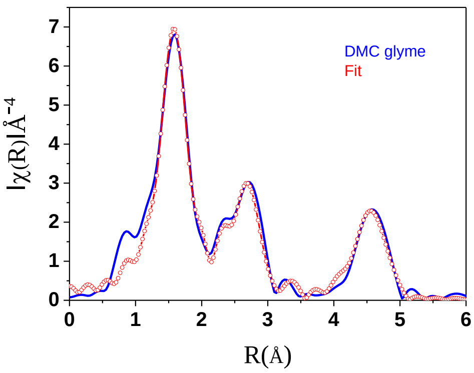

Figure 1. Fit to the EXAFS data of the model for DMC glyme.

The local atomic order around Co atom was practically not changing for all investigated materials (Fig. 2). In fits to given catalyst the differences in number of oxygen atoms in distance 3.10 Å and 4.62 Å were only noticed.

These oxygen atoms can originate from water molecule or ligand. The error indicated by IFEFFIT code for the number of these atoms is quite large demonstrating that oxygen can be distributed no homogeneously. This confirms that Co metallic center is not active during the catalyst preparation. Interestingly, the atomic order around Co remains like in hydrated form of $Zn_3[Co(CN)_6]_2{\cdot}nH_2O$ with cubic (*Fm*-3*m*) structure. Therefore, in catalyst both metals have different atomic order. Zn atoms like in anhydrous structure (rhombohedral (*R*-3*c*)) bonded with four NC groups and Co atoms like in hydrated structure bonded with six CN groups.

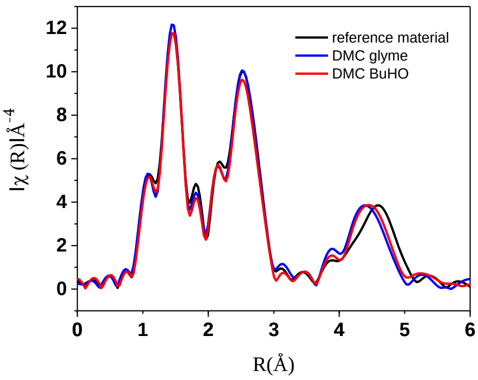

Figure 2. K-edges of Co. The comparison of FT module of the experimental spectra of the investigated catalysts and hydrous reference material.

Summarizing the performed studies, one can stated that results of the EXAFS analysis support the model proposed by Zhang et al., [4] and the model resulting from molecular calculation performed by Wojdeł et al., in [5]. These models postulate the important role of Zn-Cl bonds in the activity of examined catalysts. The role of Zn-O bond postulated in other papers [e.g. [6] and references therein] is not confirmed. We do not detected Zn atoms in the distance 4.38 Å as resulted from calculation performed in the ref. [6]. Therefore, our earlier postulate that catalysts with BuOH ligand form cluster-like complexes [3] was confirmed now also for catalysts with glyme ligands. The Zn atoms inside the clusters have changed atomic order which becomes like in anhydrous structure (tetrahedral coordination). Whereas, the Co atomic structure remains not affected, as compared to reference cubic hydrated material. Remaining Zn atoms can be bonded partially with groups of cyanide and with chlorine atoms. These atoms can be located at the surface of the clusters and be catalyst active centres. EXAFS analysis does not confirm the existence around Zn atoms the atomic order like in $ZnCl_2$ compounds. Therefore, the performed XAS studies give direct evidence that formula $Zn_3[Co(CN)_6]_2{\cdot}x\,ZnCl_2{\cdot}y\,L$ used to describe DMC catalyst is not valid. Instead the nanoclusters are formed in catalyst with different atomic order around Co and Zn with new structure, which incorporates Cl atoms.

---

[1] A. Chruściel, W. Hreczuch, J. Janik, K. Czaja, K. Dziubek, Z. Flisak, A. Swinarew, *Ind. Eng. Chem. Res.* **53** (2014) 6636.

[2] B. Ravel, M. Newville, J. *Synchrotron Rad.* **12** (2005) 537.

[3] K. Lawniczak-Jablonska, E. Dynowska, W. Lisowski, *et al., X-Ray Spectrometry* **44** (2015) 330.

[4] X-H. Zhang, Z-J. Hua, Sh. Chen, F. Liu, X-K. Sun, G-R. Qi, *Applied Catalysis* **325** (2007) 9.

[5] JC. Wojdeł, ST. Bromley, F. Illas, JC. Jansen, *J. Mol. Model.* **13** (2007)751.

[6] N. Almorea-Barrios, S. Pogodin, L. Bellarosa, *et al., ChemCatChem* **7** (2015) 928.

P-09

Structural and magnetization changes induced in Pt/Co/Pt trilayers irradiated by femtosecond XUV FEL pulses

R. Sobierajski[1]*, D. Klinger[1], I. Jacyna[1], P. Dłużewski[1],
M. M. Klepka[1], Z. Kurant[2], J. B. Pełka[1], I. Sveklo[2],
A. Wawro[1], J.Chalupsky[3], V.Hajkova[3]
and A. Maziewski[2]

[1]Institute of Physics, Polish Academy of Sciences, 02- 668 Al. Lotników 32/46, Warsaw.
[2]Laboratory of Magnetism, Faculty of Physics, University of Bialystok, K. Ciolkowskiego 1L, 15-245, Bialystok, Poland
[3]Institute of Physics, ASCR, Na Slovance 2, Prague 8, 182 21, Czech Republic

Keywords: FLASH, FEL ultrathin films, Pt/Co/Pt, structure modification, magnetic reorientation

*e-mail:ryszard.sobierajski@ifpan.edu.pl

We have studied threshold energy density for structural and magnetic modifications (spin reorientation between out-of-plane and in-plane magnetization) in the Pt/Co/Pt trilayer systems modified with femtosecond XUV light pulses. Ultrathin film systems containing magnetic component, like Co, sandwiched between noble metals, with tunable magnetization direction (in-plane and out-of-plane) are of particular importance for spintronics as well as for technology of magneto-optical memory devices. In case of a Pt/Co/Pt trilayers irradiated with different light impulses [1-3], an out-of-plane to in-plane magnetization reorientation phase transition was evidenced, with an irradiation-driven intermixing and disordering at the Co–Pt interfaces. In comparison with conventional thermal annealing of the sample, the fast laser annealing provides possibility to create structural and magnetic changes at the interfaces without substrate overheating which is important for technological applications.

In general sample irradiation may lead to such phenomena as blurring of originally sharp interfaces and - as a result of atomic interdiffusion - formation of a PtCo disordered/ordered alloys and appearance of defects and strains. Such structural modifications change the basic parameters characterizing magnetic properties of multilayer structures – specifically magnetic anisotropy. In particular the interface blurring may reduce the surface anisotropy, while atomic interdiffusion leads to formation of alloys with specific magnetocrystalline anisotropy. In case of lattice deformation – magnetoelastic anisotropy contribution may become significant, as well.

We have investigated Pt(5 nm)/Co(3.5 nm)/Pt(5 nm) trilayers grown by the MBE method on the sapphire (0001) single crystal substrate. We have studied two series of samples – the Pt buffer layer was grown either at 750 ^{0}C, or at room temperature. Selected samples were irradiated with fs XUV pulses using Free Electron LASer in Hamburg (FLASH). Samples were exposed to single pulses, each at a pristine position, at two incidence angles (normal and grazing angle of 20 degree). The irradiation fluences were in the range appropriate to switch the system between in-plane and out-of-plane magnetization states. Magnetic tests were carried out after irradiations by means of magnetooptical Kerr effect (MOKE) based techniques. We have performed morphological and structural characterization of Pt/Co/Pt trilayers by means of optical microscopy, AFM, SEM and TEM. The structural properties were correlated with the magnetic features and radiation fluence (see Figure 1). Thus it was possible to associate the magnetic modifications with the required radiation dose and their structural context.

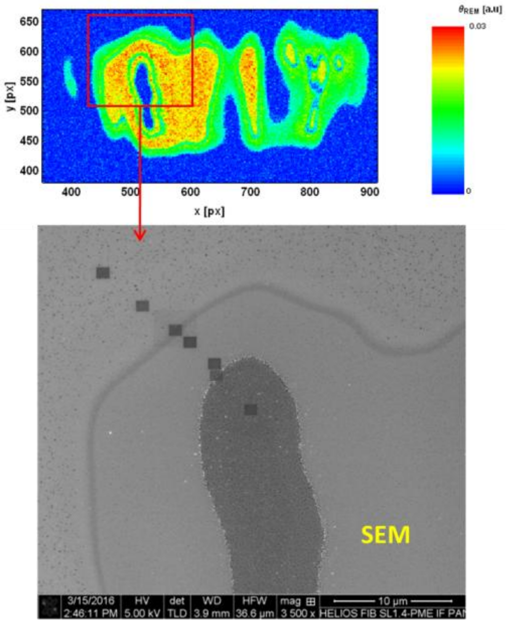

Figure 1. Magnetization (top) and surface morphology (bottom) images of an irradiated spot measured by means of MOKE and SEM techniques, respectively. Black squares at the SEM images correspond to positions of previous SEM detailed studies (carbon contamination of the surface).

Acknowledgments: This work has been supported by the Polish National Science Center (Grant No. DEC-2012/06/M/ST3/00475).

---

[1] J. Kisielewski, *et al., J. Appl. Phys* **115** (2014) 053906.
[2] E. Dynowska, *et al., Nucl. Instrum. Methods Phys. Res., Sect. B* **364** (2016) 33.
[3] W. Szuszkiewicz, *et al., Phase Transitions* **89** (2016) 328.

P-10

The role of surfactants with different length of alkyl chains in the dispersion of carbon nanomaterials

A. Moliński[1]*, M. Skupin[1], J. Iżykowska[1], J. Zaręba[1], W. Andrzejewska[1], S. Jurga[1] and M. Kozak[1,2]

[1]*Department of Macromolecular Physics, Faculty o Physics, Adam Mickiewicz University, Umultowska 85, 61-614 Poznań, Poland*
[2]*Joint SAXS Laboratory, Adam Mickiewicz University, Umultowska 85, 61-614 Poznań, Poland*

Keywords: carbon nanomaterials, nanotubes, FTIR, NMR

*e-mail: augustyn222@gmail.com

Carbon nanofluids (suspensions of carbon nanomaterials) have been proven to have wide variety of distinct applications, starting from thermal conductivity [1] to creation of microcapsules [2]. Improving the stability of such suspensions would have a great impact on development of new materials. Furthermore, the possibility to manipulate surface properties of carbon nanofluids (CN) would be of great use to numerous industrial applications. The discovery new synthesis methods of carbon nanotubes, fullerene or graphene offers exciting opportunities for the development novel high property materials. It is very important to learn how to manipulate the surface properties in order to achieve products with the desired properties.

Carbon nanomaterials (CN) show very strong surface hydrophobic interactions [3]. In our work we focused on the noncovalent modification of carbon surface using dicationic surfactants in aqueous solution. The surfactant molecules can create for example steric barrier between CN surfaces [4]. Surfactants can interact with CN through various interaction modes: hydrophobic interaction between aliphatic chains of surfactants and side walls of CN [5] or π-π interaction of imidazolium rings from surfactant molecules with CN surface [6]. So far in several works have been reported the dispersion of multi-wall carbon nanotubes by conventional single chain surfactants, like SDS, CTAB or DTAP.

In this work we focused on amphiphilic dicationic surfactants, known as gemini surfactants. This type of surfactants have a number of unique aggregation properties in comparison to conventional single-chain surfactants, such as: low CMC, ability to form of different morphology of aggregates and others [7].

For this study we selected a series of gemini surfactants (with imidazolium head groups) with different length of alkyl chains, with potential applications as efficient systems for dispersing nanostructures in aqueous solutions.

The stability of the CN suspensions in water solutions was investigated using UV/VIS spectroscopy. The CN concentration was fixed and only selected concentrations of surfactants were tested to evaluate their stabilization efficiency. The microstructure of the stable, concentrated suspensions of CN was investigated using high-resolution Transmission Electron Microscopy. In addition NMRD (nuclear magnetic resonance dispersion) profiles were also examined in order to check quantative parameters of stability of selected suspensions.

Acknowledgments: This work was supported by Ministry of Science and Higher Education. Project *„Najlepsi z najlepszych!"* (dec. - POWR.03.03.00-00-P001/15), European Funds Knowledge Education Development.

European Funds
Knowledge Education Development

European Union
European Social Fund

---

[1] D. Wen, Y. Ding, *J. Thermophys Heat Transfer* **18** (2004) 481.

[2] M. M. Caruso, S. R. Schelkopf, A. C Jackson, A. M. Landry, P. V. Braun, J.S Moore *J. Mater. Chem.* **19** (2009) 6093.

[3] R. H. Baughman, A. A. Zakhidov, W. A. de Heer *Science* **297** (2002) 787.

[4] H. D. Napper, *Polymeric Stabilization of Colloidal Dispersions (*Academic Press: Orlando Florida 1993).

[5] L. Vaisman, H. D. Wagner, G. Marom, *Adv. Colloid Interface Sci.* **128** (2006) 37.

[6] A. Crescenzo, S. Cambre, R. Germani, P. Profo, A. Fontana, *Langmuir* **30** (2014) 3979.

[7] C. Lamprecht, J. T. Huzil, M. V. Ivanova, M. Foldvari, *Drug Deliv. Lett.* **1** (2011) 45.

P-11

Valence of RE ions on surface and in volume of semiconductor compounds

B. A. Orlowski[1]*, E. Guziewicz[1], A. Reszka[1]
and B. J. Kowalski[1]

[1]*Institute of Physics, Polish Academy of Science,*
Al. Lotnikow 32/46, 02-668. Warsaw, Poland

Keywords: resonant photoemission, Fano resonance, rare earth 4f electrons

*e-mail: obro@ifpan.edu.pl

The rare earth RE (4f) atoms impurities introduced to the valence band of semiconductor compounds can contribute as an ions with 2+ or 3+ valence. The open shell 4f electrons introduce magnetic properties to the valence band of volume crystal as well as to the crystals of reduced dimension like surface 2D, wires (1D) or dots (0D). As an impurity in semiconductor compounds $A_{II}B_{VI}$ or $A_{III}B_V$ RE ions prefer to take a sit of cation with its valence as well in the volume of a crystal as like a deposited atoms on clean surface of the crystal. Thermal annealing of the samples leads to the transition of ions to the valence of semiconductor crystal cation. The application of Fano type Resonant Photoemission Spectroscopy (RPS) for study valence of RE(4f) ions needs to apply continuous spectrum synchrotron radiation in the range of energy between 100 and 200eV.

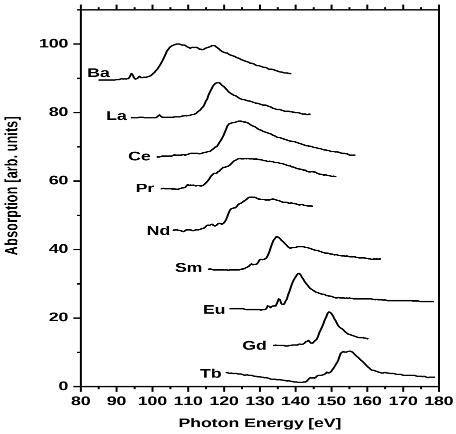

Figure 1. Set of selected rare earth atoms 4f electrons absorption spectra.

The Fig. 1 presents regions of energy corresponding to the optical transitions 4f - 4d absorption spectra for set of metal atoms, starting from Barium up to Terbium [1].

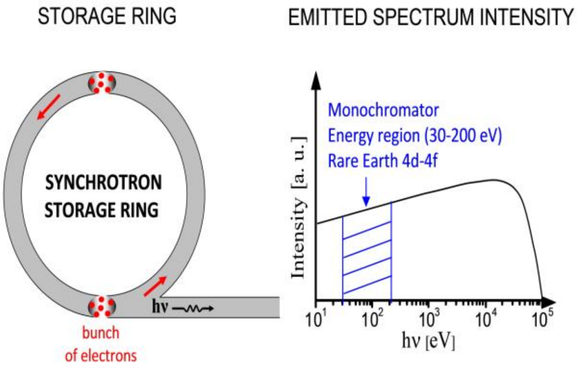

Figure 2. Storage ring and emitted spectrum with marked region of energy used in the experiment.

The Fig. 2 illustrates the synchrotron source (Hamburg, DESY) of strong continuous radiation spectrum in the wide photon energy range used to measure the Fano type resonant photoemission spectra in indicated radiation energy range [1,2]. The results are presented as a set of Energy Distribution Curves spectra measured for the valence band region of following semiconductors crystals GaN, CdTe and PbGdTe, doped by following Re atoms: Eu and Sm. For GaN and CdTe crystals surface the set of spectra were measured for Sm atoms sequentially deposited. on the crystals surface. The obtained spectra were divided on two groups of peaks corresponding to two resonant energy of radiation hν equal 136eV or 141eV. This groups correspond to the Sm 4f-4d transitions of Sm ion with valence 2+,corresponding to hν energy 136eV and 3+ corresponding to hν energy 141eV. The spectra obtained for $Pb_{1-x}Eu_xTe$ crystal presents the effect of Eu^{3+} ion transition to the Eu^{2+} ion, under the crystal annealing. The results allow to determine contribution of RE(4f) electrons structure to the valence band of the semiconductor crystals.

Acknowledgments: This work was supported by Polish National Centre for Research and Development (NCBiR) through the project DZP/PBSII/1699/2013 and to the Polish National Science Centre (NCN) Grant No. DEC-2012/07/B/ST5/02484.

---

[1] B. A. Orlowski *Spektroskopia fotoemisyjna rezonansowa typu Fano* in *Promieniowanie synchrotronowe w spektroskopii i badaniach strukturalnych,* editors B. J. Kowalski, W. Paszkowicz, E. A. Gorlich, (Polish Synchrotron Radiation Society, 2011) (in Polish).

[2] E. Guziewicz, B. A. Orlowski, B. J. Kowalski, I. A. Kowalik, A. Reszka, L. Wachnicki, S. Gieraltowska, M. Godlewski, R.L. Johnson, *Appl. Surf. Science* **82** (2013) 326.

P-12

Classification and clustering multivariate statistical methods for hyperspectral datasets in R Environment

K. Banas[1]*, A. Banas[1], E. Jasek-Gajda[2], M. Gajda[2], W. M. Kwiatek[3], B. Pawlicki[4] and M. Breese[1]

[1] *Singapore Synchrotron Light Source, National University of Singapore, 5 Research Link, Singapore 117603, Singapore*
[2] *Department of Histology, Jagiellonian University Medical College, Kopernika 7, 31-034 Krakow, Poland*
[3] *Institute of Nuclear Physics PAN, Radzikowskiego 152, 31-342 Krakow, Poland*
[4] *Gabriel Narutowicz Hospital, Pradnicka 37, 31-202 Krakow, Poland*

Keywords: synchrotron radiation, x-ray fluorescence, multivariate statistical analysis, classification techniques

*e-mail: slskb@nus.edu.sg

The experiments performed at synchrotron light sources very often provide as the result big datasets. This is especially true with 2D spectroscopy. Hyperspectral datasets (spectra with additional information for example about the position of the place where spectrum was recorded) should be treated in a special way. They are highly correlated in two-fold way: each spectrum is a superposition of the number of peaks with additional baseline function, but also spectra from adjecent regions are usually very similar due to local homogenity of the sample. Additionaly, very often these datasets represent so-called wide data case where the number of variables is bigger than the number of observations.

While there is a number of software solution for evalution of the experimental results in the image format (for example for imaging and tomography experimental results) hyperspectral data evaluation standardised approach is still missing.

In this contribution discussion and comparison of two methods for X-ray fluorescence (XRF) spectral datasets evaluation is presented.

Traditionally each spectrum is deconvoluted by fitting the model in order to obtain elemental concentration values, subsequently these concentrations are used as the variables in building classification models by using linear discriminant analysis (LDA) or partial least-square discriminant analysis (PLSDA).

Proposed alternative approach is using directly complete spectral datasets. By using multivariate statistical techniques reduction of the dimension is performed, then new variables (principal or latent components) are included for constructing classification functions.

Comparison of the performance of models constructed with both methods and LDA or PLSDA will be shown.

Cross-validation of the models is done by leave-one-out (LOOCV) method. Alternative approach for unsupervised classification based on hierarchical cluster analysis allows for additional independent validation.

XRF spectral data were recorded at beamline L of Hasylab synchrotron source. Samples were 15 microns thin sections of biological material stretched on Mylar foil. Policapillary was used to focus X-rays into small spot size allowing spatially resolved study of heterogenous material.

Complete data preprocession, evaluation and visualization (except deconvolution of XRF spectra model fitting) was performed with R environment [1] for statistical analysis and RStudio Graphic User Interface [2].

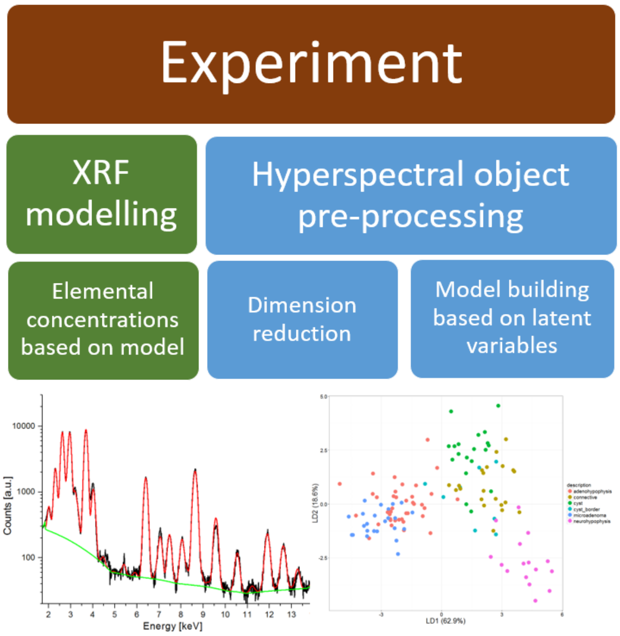

Figure 1. Diagram showing two possible approaches for hyper-spectral data analysis.

Acknowledgments: This work was partially supported by NUS Core Support C-380-003-003-00 and the European Community under the Contract RII3-CT-2004-506008 (IA-SFS) (HASYLAB project No II-20052050 EC)

---

[1] R Core Team, R: A Language and Environment for Statistical Computing. R Foundation for Statistical Computing: Vienna, Austria, 2016.

[2] RStudio: Integrated development environment for R. 2016; http://www. rstudio.com

P-13

Trace elements concentration in normal and pathological tissues of pituitary gland

A. Banas[1]*, K. Banas[1], A. Furgal-Borzych[2], E. Jasek-Gajda[2], M. Gajda[2], W. M. Kwiatek[3], B. Pawlicki[4] and M. B. H. Breese[1]

[1]Singapore Synchrotron Light Source, National University of Singapore, 5 Research Link, Singapore 117603, Singapore
[2]Department of Histology, Jagiellonian University Medical College, Kopernika 7, 31-034 Krakow, Poland
[3]Institute of Nuclear Physics PAN, Radzikowskiego 152, 31-342 Krakow, Poland
[4]Gabriel Narutowicz Hospital, Pradnicka 37, 31-202 Krakow, Poland

Keywords: pituitary gland, SRIXE, trace elements

*e-mail: slsba@nus.edu.sg

Pituitary gland is a small pea-shaped organ located at the base of the brain. It is under control of the central nervous system via its morphological and functional link to the hypothalamus. The pituitary is often referred as “master organ” since it releases hormones regulating activities of other endocrine glands.

Pituitary disorders most commonly result from the growth of benign tumors and they can produce a wide spectrum of clinical symptoms [1]. These symptoms are effects of over- / underproduction of particular hormones or they result from compression of the tumor on optic nerve or on other cranial nerves. Diagnosis of pituitary disease may be extremely difficult since it is often confused with other disorders [2].

The characterization of trace element species in solid biomatrix like pituitary gland is necessary to understand their complex functions and interactions. µ-SRIXE with simultaneous multielemental detection is capable to address these challenges and hence plays a fundamental role as a nuclear reference analytical technique. For the study we used 10 µm-thick histological sections of human pituitary glands. Experiments were performed at beamline L of DORIS III light source at DESY, Hasylab. Energy was set to 15 keV and use of polycapillary enabled detection of broad range of elements (P, S, Cl, K, Ca, Cr, Mn, Fe, Cu, Zn, As) in a very good spatial resolution (15 µm).

Various structures of normal gland and pituitary microadenomas were analyzed showing accumulation or depletion of certain trace and essential elements. Examples of Fe and Cr concentration distributions are presented in Figure 1.

Our results indicate that intracellular metabolism is most likely to be different in healthy and affected tissues. Furthermore, they can shed light on molecular pattern of the pathogenesis of the diseases.

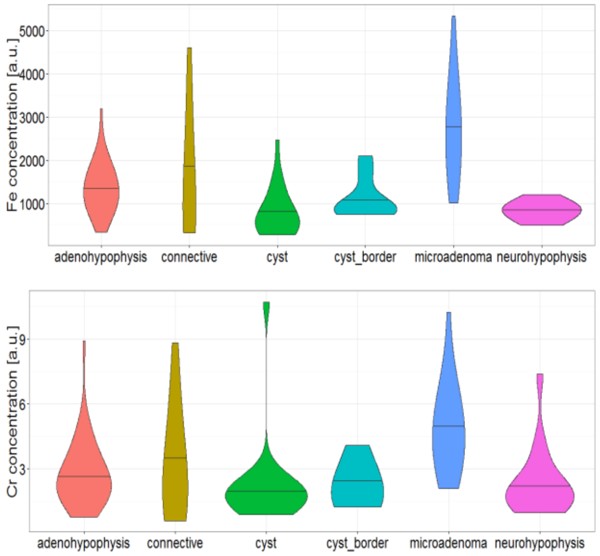

Figure 1. Violin plots for Fe (top) and Cr (bottom) concentration distribution in pituitary tissue specimens.

Acknowledgments: This work was partially supported by NUS Core Support C-380-003-003-00 and the European Community under the Contract RII3-CT-2004-506008 (IA-SFS) (HASYLAB project No II-20052050 EC)

---

[1] G. Kontogeorgos. *Pituitary tumours*. (In: J. M. Polak, editor. *Diagnostic Histopathology of Endocrine Tumours*. London: Churchill Livingstone, 1993:227–69).

[2] O. Cooper, S. Melmed, *Best Pract Res Clin Endocrinol Metab*. **26** (2012) 447.

P-14

Structural and optical properties of Cu-doped zinc oxide nanostructures

H. Drozdowski[1,2]*, E. Robak[1,2]
and M. Śliwińska-Bartkowiak[1,2]

[1]*Adam Mickiewicz University,Umultowska 85, 61-614 Poznań, Poland*
[2]*NanoBioMedical Centre, Adam Mickiewicz University,Umultowska 85, 61-614 Poznań, Poland*

Keywords: semiconductor nanostructures, absorption of light, X-ray diffraction (XRD)

*e-mail: riemann@amu.edu.pl

1. Research problem

- Determination of the influence of metal nanoparticles on the optical and electronic properties of semiconductor nanostructures – plasmonic effects
- The study of optical and electronic properties of semiconductor nanostructures doped with metal
- Investigation of transport and recombination of the electron at the interface and in doped structures

2. Materials and methods

- **Numerical simulations** - performed by employing a Finite Integration Technique (CST Microwave Studio) – the study of plasmonic light's absorption enhancement and coupling in the system consisted of **silicon nanowire-gold bow-tie nanostructure** [1] and **zinc oxide nanowire-gold nanoparticles** of different shapes
- **Materials Synthesis**– Zinc oxide nanowires undoped and doped with copper [2,3], gold nanoparticles with different shapes (spheres, rods, triangles) [4,5].
- **Characterization Techniques**-Scanning and Transmission Electron Microscope (SEM,TEM), X-ray diffraction (XRD), absorption (ABS) and photoluminescence (PL) measurements, nanoindentation, Raman spectroscopy, Atomic Force Microscopy (conductive mode), X-ray photoelectron spectroscopy (XPS) Electrochemical Impedance Spectroscopy (EIS), Small-Perturbation Techniques (intensity-modulated photocurrent and photovoltage spectroscopy – IMPS, IMVS).

Acknowledgments: This work was supported by Grant NCN Opus Nr. Dec – 2013/09/B/ST4/03711

---

[1] E. Robak, M. Kotkowiak, H. Drozdowski, *J. Phys. D: Applied. Phys.* **49** (4) (2016) 045104.

[2] E. Robak, E. Coy, M. Kotkowiak, S. Jurga, K. Zaleski, H. Drozdowski, *Nanotechnology*, **27** (17) (2016) 175706.

P-15

The application of X-Ray diffraction and computer experiments in the studies of structure of liquids and amorphous solids

M. Śliwińska-Bartkowiak[1,2]*, H. Drozdowski[1,2]
and E. Robak[1,2]

[1]*Adam Mickiewicz University,Umultowska 85,*
61-614 Poznań, Poland
[2]*NanoBioMedical Centre, Adam Mickiewicz*
University,Umultowska 85, 61-614 Poznań, Poland

Keywords: X-ray diffraction, computer experiments, coordination numbers for liquids

e-mail: msb@amu.edu.pl

The application of the X-ray diffraction method for study the structure of liquids and amorphous solids is described. The main sources of errors are discussed. A numerical analysis is performed of the influence of X-ray data termination on the normalization constants, radial distribution functions (RDF), and on interatomic distances and coordination numbers determined from these functions. Computations are carried out for liquid dichloroalkanes [1,2], carbon tetrachloride [3,5] and naphthalene [4]. The strong dependence of coordination number on the termination angle, observed by other authors, is confirmed. An approximately linear dependence of coordination numbers on wave vector *S* is found.

Use of RDF, to compute a coordination number, N_1, for liquids is discussed for four methods: 1/ symmetrizing the first peak in RDF; 2/ symmetrizing the first peak in r^2 *RDF(r)*; 3/ decomposition of r^2 *RDF(r)* into shells; 4/ computation of area to the first minimum in r^2 *RDF(r)*.

Figure 1 shows the calculated RDF of 1,12-dichloroalkanes decomposed into the various atomic peaks. These composite peaks are resolved into atomic peaks on the assumptions that the shape of an atomic peak can be represented by an equation of the form: $e^{-x^2/c}$ where *c* is a constant, i. e. that the curve is Gaussian, and also that the area under an atomic peak formed by two atoms multiplied by the distance between the two atoms is proportional to the product of the scattering powers of the two atoms.

The coordination numbers and interatomic and intermolecular distances in a liquid are mean values and undergo fluctuations. Therefore, it seems that the best method to estimate the total experimental uncertainty of RDF determination is a comparison of results obtained independently by X-ray diffraction [4].

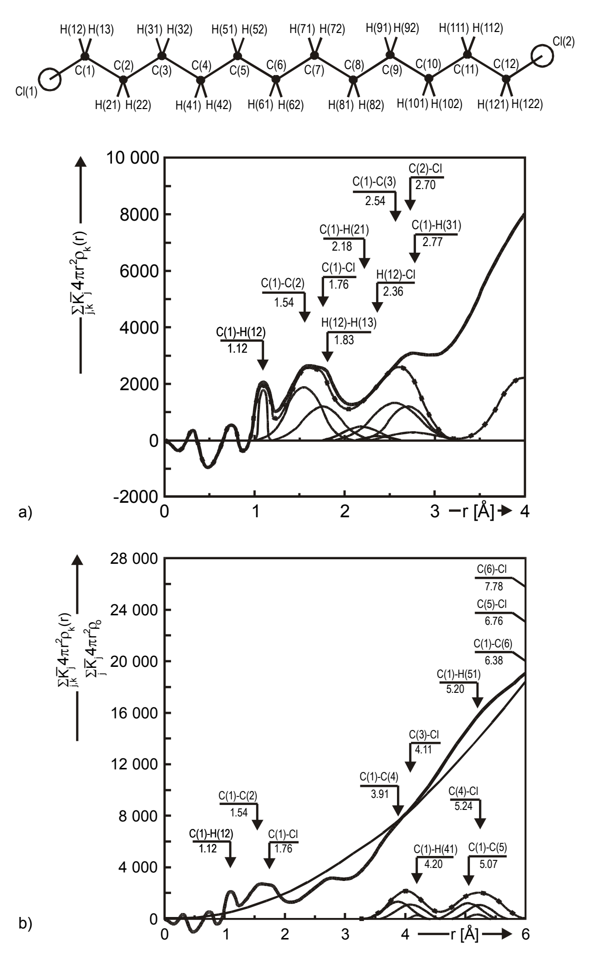

Figure 1. The experimental RDF of 1,12-dichlorododecane decomposed into its atomic peaks.

Acknowledgments: This work was supported by Grant NCN Opus Nr. Dec – 2013/09/B/ST4/03711

---

[1] H. Drozdowski, *J. Mol. Liquids* **122** (1–3) (2005) 32.
[2] H. Drozdowski, *Phys. Chem. Liquids* **42** (6) (2004) 577.
[3] M. Śliwińska-Bartkowiak, H. Drozdowski, M. Kempiński, M. Jażdżewska, Y. Long, J. C. Palmer, K. E. Gubbins, *Phys. Chem. Chem. Physics* **14** (19) (2012) 7145.
[4] H. Drozdowski, *Acta Phys. Slovaca* **54** (5) (2004) 447.
[5] Y. Long, M. Śliwińska-Bartkowiak, H. Drozdowski, M. Kempiński, K.A. Phillips, J.C. Palmer, K. Gubbins, *Coll. Surf. A: Physicochem. Engineer. Aspects* **437** (2013) 33.

P-16

X – ray examination of the serum coming from patients with selected types of cancer

H. Drozdowski[1,2]*, K. Domin,[1,2],
M. Śliwińska-Bartkowiak[1,2] and Z. Błaszczak[1]

[1]*Adam Mickiewicz University,Umultowska 85,*
61-614 Poznań, Poland
[2]*NanoBioMedical Centre, Adam Mickiewicz University,Umultowska 85, 61-614 Poznań, Poland*

Keywords: X-ray diffraction method; X-ray marker Ω_{rtg}

*e-mail: riemann@amu.edu.pl

We report the results of the investigations of the blood serum samples which were collected from the patients who suffered from neoplasmic diseases by the X-ray diffraction method. Blood serum consists in majority of water and also of a low concentration of proteins and ions which are dissolved in water.

Diffraction images obtained for different preparations were compared with the image of diffraction for distilled water. Diffraction images for the distilled water differ from the ones obtained for the test preparations. The difference is the in disappearance of a collateral maximum which indicate the disturbance in the water tetrahedral structure forming part of the serum. The numerical method of Newton's allowed tangents to determined Ω_{rtg} coefficients for the examined preparations. Compared values of the coefficients Ω_{rtg} of the test serum with the Ω_{rtg} of the distilled water show that the smaller the coefficient Ω_{rtg} the greater the severity of cancer.

The experimental part presents functions of angular distributions of X-ray intensities scattered in the examined preparations, which was distilled water, multielektrolyte fluid and blood serum of patients suffering from ovarian tumors and pelvic tumors.

Numerical method tangens Newton helped to determine the coefficients for the test formulations (Fig. 1).

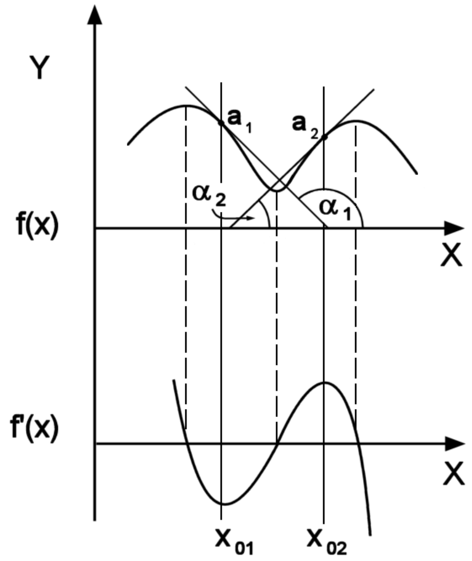

Figure 1. The function and the derivative of the intensity distribution corresponding to distilled water.

Compared coefficients test serum with distilled water shows that the smaller the value of the higher the degree of advancement of cancer [1,2].

---

[1] H. Drozdowski, Z. Błaszczak, *X-ray diffraction studies of blood serum*, (Innovative Technologies in Biomedicine, Conference Materials p. 44, 2013 Kraków).

[2] Z. Błaszczak, H. Drozdowski, *X-Ray study of blood plasma from patients with neoplasmic disease*, (International Soft Mater Conference, Conference Materials p. 235, 2010, Granada, Spain).

P-17

XAFS studies of copper complexes with coumarin acid derivatives

M. T. Klepka [1], A. Drzewiecka-Antonik [1], A. Wolska [1*], P. Rejmak[1] and M. Struga[2]

[1]Institute of Physics, Polish Academy of Sciences,
Al. Lotnikow 32/46, 02-668 Warsaw, Poland,
[2]Medical University of Warsaw, Żwirki i Wigury 61, 02-091 Warsaw, Poland

Keywords: coumarin, coumarin acid derivatives, copper, XAFS

*e-mail: wolska@ifpan.edu.pl

Coumarins represent an important type of *O*-donor heterocycles with typical benzopyrone framework. The natural as well as synthetic coumarins, have a large spectrum of biological activity. Such derivatives proved its usefulness as anti-coagulants [1], antibacterial agents [2], antifungal agents/medicines [3], biological inhibitors [4], chemotherapeutics [5] and as bio-analytical reagents [6]. It has been found out that coordination of metal ions to therapeutic agents (such as simple coumarins) can improve their efficacy and accelerate bioactivity [7]. In many cases such metal complexes are more potent and less toxic comparing to the parent drug. Therefore, among others, also biologically active metal complexes of coumarin based ligands are being widely investigated. There are some reports about biological activity of coumarin acids complexes, however, among reports about biological activity there is very little information concerning metal organic ligand binding mechanism.

Such situation is caused mainly due to lack of experimental techniques which allows to study compounds which do not have long range order in its structure. X-ray absorption fine structure (XAFS) technique already proved its usefulness in similar studies [7] and was applied in this case. The great advantage of XAS is that it can be used for crystal as well as amorphous materials.

The XAFS measurements were performed at Cu K-edge at XAFS beamline at Elettra (Trieste, Italy). Complexes were investigated in both powder and liquid form. For the complexes in the form of microcrystalline powder the transmission detection mode was used, whereas for liquid samples (which concentration was in the mmol range) the fluorescence detection mode was required and applied.

In order to find out whether chemical method used for obtaining complexes introduces some structural changes, powder samples were synthesized using two methods: direct and electrochemical. In order to obtain liquid samples, the dimethyl sulfoxide (DMSO) and dimethylformamide (DMF) were used as solvents. Both of them are popular organic solvents used during the synthesis of such compounds and are commonly used for crystallization of Cu complexes. Moreover, DMSO is most often used (as it was in our case) during microbiological activity tests procedures. It is possible that the molecules of solvents can modify the coordination sphere of metal cation and therefore modify the properties of studied complexes.

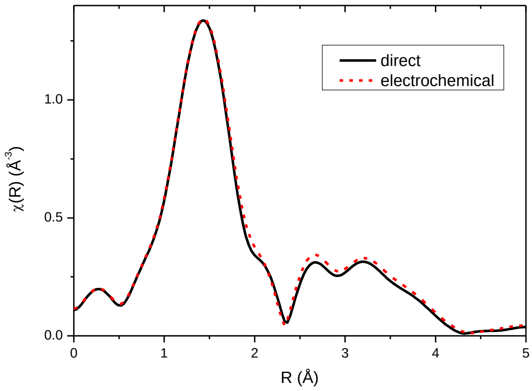

Figure 1. Comparison of the FT EXAFS oscillations for one of the powder compounds obtained using direct (black solid line) and electrochemical (red dotted line) method.

We plan to show and discuss the structural results obtained for powder and liquid form of Cu complexes with coumarin acid derivatives.

Acknowledgments: Experimental research was funded from the Polish National Science Centre (Grant No. UMO-2012/07/D/ST5/02251). This research was supported in part by PL-Grid Infrastructure. Financial support from the EU FP7 EAgLE project under the grant agreement REGPOT-CT-2013-316014 is gratefully acknowledged.

---

[1] J.W. Suttie, *Clin. Cardiol.* **13** (VI) (1990) 16.
[2] A.H. Bedair, N.A. El-Hady, M.S. Abd El-Latif, A.H. Fakery, A.M. El-Agrody, *Il Farmaco* **55** (2000) 708.
[3] T. Patonay, G. Litkei, R. Bognar, J. Eredi, C. Miszti, *Pharmazie* **39** (1984) 86.
[4] C. Gnerre, M. Catto, F. Leonetti, P. Weber, P.A. Carrupt, C. Altomare, A. Carotti, B.J. Testa, *Med. Chem.* **43** (2000) 4747.
[5] D.A. Egan, P. James, D. Cooke, R. O_Kennedy, *Cancer Lett.* **118** (1997) 201.
[6] M. Jime´nez, J.J. Mateo, R. Mateo, *J. Chrom. A* **870** (2000) 473.
[7] M.T. Klepka, A. Drzewiecka-Antonik, A. Wolska et al. *J. Inorg. Biochem.* **145** (2015) 94.

P-18

Evidence of the β-nucleating activity of montmorillonite during the formation of PP/MMT composite fibers

Cz. Ślusarczyk[1]*, J. Fabia[1]

[1]*Institute of Textile Engineering and Polymer Materials, University of Bielsko-Biala, Willowa 2, 43-309 Bielsko-Biala, Poland*

Keywords: WAXS, montmorillonite, polypropylene fibers

*e-mail: cslusarczyk@ath.bielsko.pl

Isotactic polypropylene (PP) is of polymorphic composition, having at least four modifications: α, β, γ, and smectic. The chain conformation of each modifications is the classical 3_1 helix. The difference in the crystallography is the manner in which the chains are packed in the unit cell. Among all the crystal forms of iPP, the β one has many performance characteristics, such as improved elongation at break and impact strength, so much attention has been paid to investigate the β phase of iPP during the past few decades. The β form is thermodynamically metastable and difficult to obtain under normal processing conditions. It can only be obtained through special crystallization procedures, such as in temperature gradient, shear-induced crystallization, or adding nucleating agents.

The structure of fibers formed during spinning is the result of the processes of orientation and crystallization occurring by solidifying the polymer stream. During the formation of a fiber, the process of crystallization occurs under non-isothermal conditions and different types of flow fields (shear, extension, mixed). It is known that these flow conditions strongly influence the process of crystallization and the resulting crystalline morphology. The addition of nanoclay particles into sheared polymer melts complicate the crystallization process and the morphology that subsequently forms.

In this study, we have observed for the first time, in our opinion, the appearance of the metastable β phase during the formation of nanocomposite fibers of isotactic polypropylene (PP) and an organically modified montmorillonite (MMT), Cloisite 15A (Fig. 1). Fibers were formed from the melt and spun at different take-up velocities.

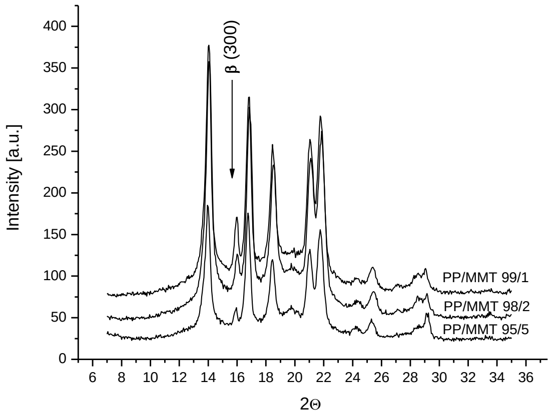

Figure 1. WAXS patterns of composite fibers prepared with different amounts of Cloisite 15A.

We have observed the β-form of iPP only in nanocomposite fibers spun at the lowest take up velocity. The β-form crystals are sensitive to the level of shear, so for fibers spun at higher take-up velocity this polymorphic form disappears.

The purpose of this paper is to present some detailed experimental results about the effect of the nucleating activity of MMT on the crystallization behavior of PP.

P-19

Surface investigation of medieval silver coins using ultra-fast infrared spectroscopic imaging

C. Paluszkiewicz[1]*, E. Pięta[1], M. Nowakowski[1],
J.M. del Hoyo-Meléndez[2] and W.M. Kwiatek[1]

[1]*Institute of Nuclear Physics, Polish Academy of Sciences, 31-342 Krakow, Poland*
[2]*Laboratory of Analysis and Non-Destructive Investigation of Heritage Objects, The National Museum in Krakow, 31-109 Krakow, Poland*

Keywords: infrared spectroscopy, silver coins, numismatic collections

*e-mail: czeslawa.paluszkiewicz@ifj.edu.pl

This study presents preliminary research concerning the distribution of chemical components on the surface of medieval silver coins.

The studied coins, namely the denarii of Boleslaus the Brave minted between 995 and 1020 AD (Figure 1), belong to the numismatic collection of the National Museum in Krakow. They were examined without performing any cleaning or pretreatment step. This spectroscopic analysis may be useful in discussing many historical aspects such as coinage production, provenance of raw materials, forgeries, and conservation treatments [1-5].

Figure 1. Photographic image of the studied Boleslaus denar.

Ultra-fast infrared imaging and mapping have been used for recording a visual image of component distribution and collecting vibrational spectra, respectively. This analysis is a necessary step prior to carrying out synchrotron studies. The aforementioned method is non-destructive and non-invasive making it adequate due to the uniqueness of the investigated objects, the first Polish coins.

The obtained data revealed that there are significant differences in the chemical compound distribution identified on the coins' surfaces (Figure 2). A detailed discussion about the relationship between the compounds distribution and the historical and political contexts has been conducted.

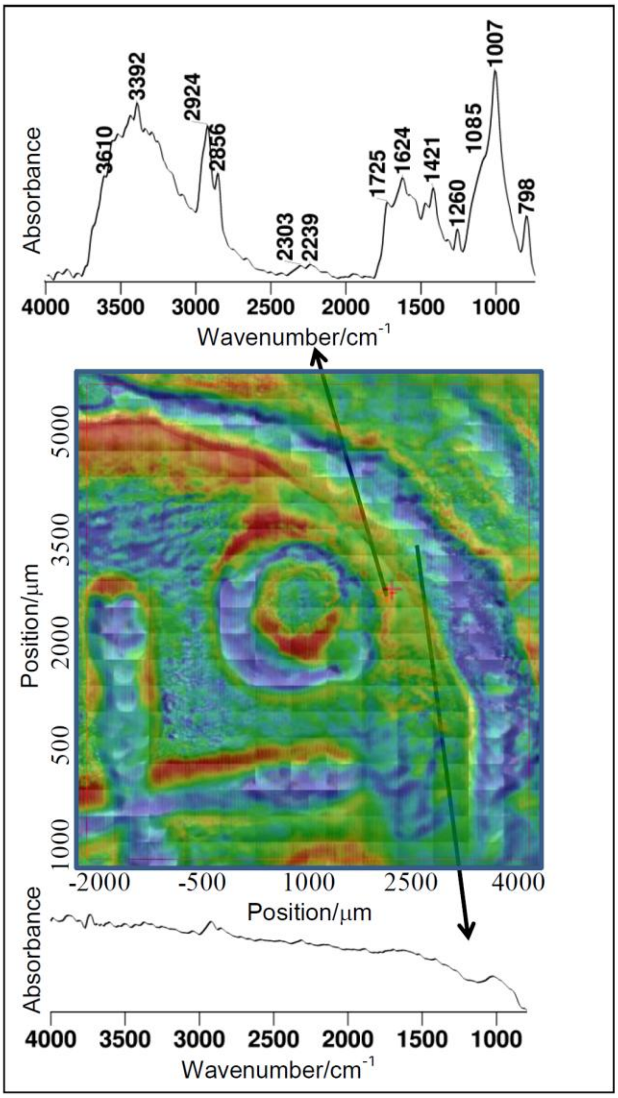

Figure 2. FT-IR image mosaic and exemplary collected spectra of the evaluated coin.

Acknowledgments: This research was performed using equipment purchased as a part of the project co-funded by the Małopolska Regional Operational Program Measure 5.1 Krakow Metropolitan Area as an important hub of the European Research Area for 2007-2013, project No. MRPO.05.01.00-12-013/15.

---

[1] J. M. del Hoyo-Melendez, P. Świt, M. Matosz, M. Woźniak, A. Klisińska-Kopacz, Ł. Bratasz, *Nucl. Instrum. Meth. B* **349** (2015) 6.
[2] D. Attanasio, G. Bultrini, G.M. Ingo, *Archaeometry* **43** (2001) 529.
[3] A. Kirfel, W. Kockelmann, P. Yule, *Archaeometry* **53** (2011) 930.
[4] R. Linke, M. Schreiner, G. Demortier, M. Alram, *X-Ray Spectrom.* **32** (2003) 373.
[5] A. Pitarch, I. Queralt, *Nucl. Instr. Meth. Phys. Res. B* **268** (2010) 1682.

P-20

Structural study of the Cu complexes with benzofuran derivatives

D. Kalinowska[1]*, A. Wolska [1], M. T. Klepka [1],
A. Drzewiecka-Antonik [1], K. Ostrowska[2] and M. Struga[2]

[1]*Institute of Physics, Polish Academy of Sciences,*
Al. Lotnikow 32/46, 02-668 Warsaw, Poland,
[2]*Medical University of Warsaw, Żwirki i Wigury 61, 02-091 Warsaw, Poland*

Keywords: benzofuran derivatives, copper, XAFS, FTIR spectroscopy

*e-mail: diana.kalinowska@ifpan.edu.pl

The derivatives of benzofuran (heterocyclic compounds consisting of fused benzene and furan ring) are important group among biologically active compounds. A broad spectrum of biological activities, such as antimicrobial (antifungal and antibacterial), antiviral, anti-inflammatory, antitumor, antihyperglycemic, analgesic or antipyretic make the complexes of benzofuran derivatives with metal ions perfect as potential pharmacological agents [1–5].

Copper is an essential element of a living organism. As a critical component of enzymes and proteins it plays an important role in biological processes [1]. Copper complexes are very effective anti-inflammatory agents. They also demonstrate considerable potential in the treatment of chronic diseases, including gastric ulcers and bowel disease, epilepsy, cancer and diabetes [5]. Knowledge of their structure is extremely important in the planning of chemical reaction, intended to obtain the compounds of the assumed physical and chemical properties. However, quite often it is impossible to obtain a complex in a crystalline form. Therefore, the X-ray absorption fine structure (XAFS) technique was implemented. The great advantage of XAFS is that it can be used for amorphous materials as well as for crystals. XAFS analysis provides information about atom's local environment (the coordination number, the distance from metal to neighboring atoms) and information about relative structural disorder.

As ligands for the complexation reaction the derivatives of benzo[b]furan were used. FTIR spectroscopy was used for monitoring the complexation reactions and for identifications of possible coordinating group to the metallic center. Due to fact that XAFS analysis requires initial model Cambridge Structural Database (CSD) was searched for it.

XAS measurements at Cu K-edge were performed at CEMO beamline at DESY (Hamburg). The samples in a form of powder were pressed into a carbon tape. Spectra were collected at liquid nitrogen temperature using transmission detection mode. EXAFS analysis was performed using the Athena and Artemis programs based on the IFEFFIT library of numerical XAFS algorithms [6].

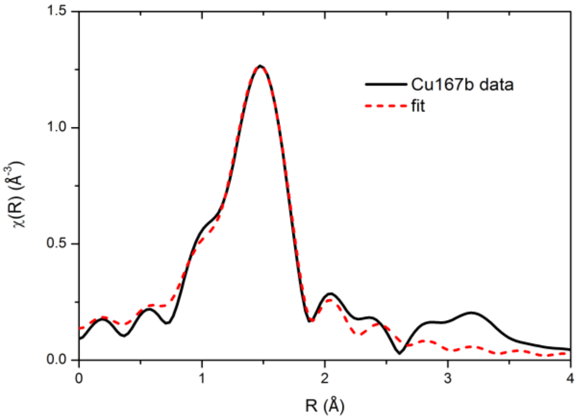

Figure 1. FT EXAFS oscillations for one of the investigated complexes (black solid line) and fitting result (red dotted line).

The EXAFS analysis revealed that the first coordination sphere is composed only from oxygen atoms and depending on the complex their quantity differs. Structural details obtained from the analysis will be discussed on the presentation.

[1] A. Drzewiecka, A. E. Kozioł, M. T. Klepka, A. Wolska, H. Przybylińska, S. B. Jimenez-Pulido, K. Ostrowska, M. Struga, J. Kossakowski, T. Lis, *Polyhedron* **43** (2012) 71.

[2] A. Drzewiecka, *Struktura potencjalnych ligandów O-donorowych i ich kompleksów organicznych z jonami metali* (Lublin, 2010).

[3] H. Khanam, Shamsuzzaman, *Eur. J. Med. Chem*, **97** (2015) 483.

[4] A. Radadiya, A. Shah, *Eur. J. Med. Chem*, **97** (2015) 356.

[5] G. Cerchiavo, A. M. da Costa Ferreira, *J. Braz. Chem. Soc*, **17** (2006).

[6] B. Ravel, M. Newville, *J. Synch. Rad.* **12** (2005) 537.

P-21

Thermal and elastic microstrain in lithium-manganese oxide

J. Darul[1], C. Popescu[2], F. Fauth[2] and P. Piszora[1]*

[1]*Department of Materials Chemistry, Faculty of Chemistry, Adam Mickiewicz University, Umultowska 89b, 61-614 Poznań*
[2]*CELLS-ALBA Synchrotron Light Facility, 08290 Cerdanyola, Barcelona, Spain*

Keywords: high pressure, $LiMn_2O_4$, strain

*e-mail: pawel@amu.edu.pl

Ternary oxides of the form $Li_xMn_{3-x}O_4$ have been extensively studied for their interesting physical properties, in particular, as cathode materials for rechargeable lithium secondary batteries [1]. When pressure is applied to some lithium-manganese spinels, a phase transition to the so-called “post-spinel” phase is induced [2]. During the last decade, high-pressure (HP) studies of $Li_xMn_{3-x}O_4$ under the nonhydrostatic stress condition have generated a large amount of attention, with stress being an efficient tool in transforming crystal structure of this materials [3,4]. Strain measurement is possible i.a. with the electrochemical strain microscopy and it allows probing a wide range of functional properties of lithium-manganese spinels at the nanoscale [5].

The $Li_{0.95}Mn_{2.05}O_4$ spinel sample was obtained from the appropriate amounts of thoroughly mixed powders of α-Mn_2O_3 and Li_2CO_3 (99.0% Merck) by thermal treatment in air at 1048 K. After heating, the specimen was quenched rapidly in solid CO_2. Structural analyses showed the expected stoichiometry of the obtained powder and confirmed that no spurious phases were present.

The microstructural properties of $Li_{0.95}Mn_{2.05}O_4$ under pressure and at elevated temperature were studied up to 13 GPa by X-ray powder diffraction at the MSPD-BL04 beamline of the ALBA synchrotron [6]. Diffraction patterns were recorded on image plates and then integrated to yield intensity vs 2θ diagrams. Synchrotron X-ray diffraction experiments were conducted using a polydimethyl-siloxane oil as the pressure-transmitting medium. The lithium manganese oxide in a powder form was studied at room temperature and at elevated temperature in pressure loading cycles using DAC. Gold has been chosen as a pressure standard because of its moderate compressibility, chemical inertness, and large X-ray scattering power. A small lump of gold with a purity of 999.9 and an average particle size of about 30 μm was put in the hole of a rhenium gasket. Rietveld refinements were performed using the program GSAS.

Anisotropic peak broadening mainly caused by lattice strain was observed with broadening of the diffraction peaks. The phenomenological microstrain model of Stephens with 4 and 2 refinable parameters for tetragonal and cubic symmetry respectively was used to model the anisotropy in FWHM of the individual peak profiles. This microscopic picture is completed by analyzing the isosurface of the anisotropic microstrain which reflects the strong shear strain of neighboring coordination polyhedra in the lithium manganese structure.

We apply a comparative approach for microstrain analysis between the sample at HP/HT and at HP condition to illustrate the differences between microcrystalline properties of the high-pressure crystalline phase with and without thermal treatment.

It is important to note that, although the overall deformation during the experiments should be quasi-hydrostatic, individual powder particles experience a very heterogeneous deformation because of possible point contacts between the particles. We conjectured that grain-tograin interactions and nonhydrostatic stress component induced a phase transition because of high stress concentration during powder compaction. It is quite possible that a limited hydrostaticity of the pressure transmitting medium and the grain boundaries in the polycrystalline aggregates play a decisive role in defining the sample microstructural properties at high pressure.

Acknowledgments: These experiments were performed at MSPD-BL04 beamline at ALBA Synchrotron with the collaboration of ALBA staff.

---

[1] Y. Wu, (Ed.). *Lithium-Ion Batteries: Fundamentals and Applications* (Vol. 4) (CRC Press, 2015).

[2] K. Yamaura, Q. Huang, L. Zhang, K. Takada, Y. Baba, T. Nagai, M. Yoshio K. Kosuke, E. Takayama-Muromachi, *J. Am. Chem. Soc.* **128**(29) (2006) 9448–9456.

[3] J. Darul, C. Lathe, P. Piszora, *RSC Adv.* **4**(110) (2014) 65205-65212.

[4] J. Darul, W. Nowicki, C. Lathe, P. Piszora, *Rad. Phys. Chem.* **80**(10), (2011) 1014-1018.

[5] D. O. Alikin, A. V. Ievlev, S. Y. Luchkin, A. P. Turygin, V. Y. Shur, S. V. Kalinin, A. L. Kholkin, *Appl. Phys. Lett.* **108**(11) (2016) 113106.

[6] F. Fauth, , I. Peral, C. Popescu, M. Knapp, *Powder Diffr.* **28** (2013) S360 −S370.

P-22

Structural studies of multiwall carbon nanotubes suspensions in presence of selected monomeric and dimeric surfactants and comparison to suspensions stabilized by pluronics

J. Zaręba[1]*, J. Iżykowska[1], M. Skupin[1], A. Moliński[1], W. Andrzejewska[1], S.Jurga[1] and M. Kozak[1,2]

[1] *Department of Macromolecular Physics, Faculty of Physics, Adam Mickiewicz University, Umultowska 85, 61-614 Poznań, Poland*
[2] *Joint SAXS Laboratory, Adam Mickiewicz University, Umultowska 85, 61-614 Poznań, Poland*

Keywords: carbon nanomaterials, nanotubes, FTIR, NMRD

*e-mail: zarebajakub@wp.pl

Carbon nanotubes (CNT) are tubular nanostructures, characterized by unique physical and chemical properties. However, because of the hydrophobic nature of CNTs surface and very strong interactions between these nanoparticles, it is a question how to prepare the homogenous suspension of CNTs in water and then effectively separate CNTs aggregates into individual tubes while maintaining their properties. Recently, there are two approaches to solve this problem: the chemical functionalization of the nanotubes surface (which can strongly affect the electronic structure of the tube) and the non-covalent modification by using dispersive agents. It has been shown that the non-covalent modification using amphiphilic molecules of the CNTs surface effectively leads to the formation of stable suspensions of carbon nanotubes in water[1].

Nowadays, one of the most frequently used dispersing agents are block copolymers named Pluronics (poly(ethylene oxide)-poly(propylene oxide)-poly-(ethylene oxide) [PEO-PPO-PEO]) [2], that are biocompatible, nontoxic and commercially available. However researches are looking for alternative, more efficient systems for dispersing nanotubes in aqueous solutions. In present studies monomeric and dimeric surfactants with imidazolium group are used. Preliminary study indicate that suspension of MWCNT with dimeric imidazolium surfactants are stable for more than 3 months (Figure 1).

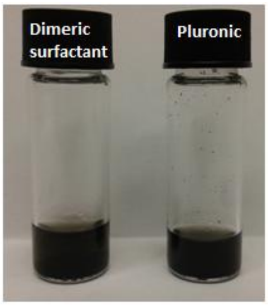

Figure 1. Suspensions of MWCNT with dimeric imidazolium surfactant as a dispersing agent (left) and with pluronic P123 (right).

The influence of PEO-PPO-PEO and bis-imidazolium surfactants on the MWCNTs structure in aqueous suspensions and the water dynamics had been studied. The morphology was investigated by means of Transmission Electron Microscopy (TEM) and the water dynamics in MWCNTs suspensions was analyzed using Nuclear Magnetic Relaxation Dispersion (NMRD) method. The NMRD profiles provide information about slow molecular motions that affect the spin-lattice relaxation and allow to understand more the nature of processes taking place at the water-MWCNTs interface [3]. In addition spectroscopic (FTIR/Raman) methods were used. The results from all these studies can be used to assess the dispersion of MWCNTs in water, thus the quality of the aqueous MWCNTs suspensions.

Acknowledgments: This work was supported by Ministry of Science and Higher Education. Project *„Najlepsi z najlepszych!”* (dec. - POWR.03.03.00-00-P001/15), European Funds Knowledge Education Development.

European Funds Knowledge Education Development
European Union European Social Fund

---

[1] R. H. Baughman, A. A. Zakhidov, W. A. de Heer, *Science* **297** (2002) 787.
[2] I. Szleifer, R. Yerushalmi-Rozen, *Polymer* **46** (2005) 7803
[3] S. Godefroy, J. P. Korb, M. Fleury, *C.R.Acad.Sci.Paris Chimie/Chemistry* **4** (2001) 857.

P-23

Radiation effects induced in solids and biological materials by intense XUV and X-ray beams

J. B. Pełka[1]* and I. Jacyna[1]

[1]*Institute of Physics, Polish Academy of Sciences, 02- 668 Al. Lotników 32/46, Warsaw*

Keywords: Radiation Damage, Structure Modification, Near-Surface Properties, Synchrotron, Free Electron Laser

*e-mail:pelkay@ifpan.edu.pl

It is often said that the x-ray investigation techniques are non-invasive in terms of conservation of specimen structure, as well as its physical and, where applicable, biological properties. However, it is well known, that structural destructions and functional modifications are inherently associated with irradiation of all types of samples. Radiation damage is an important issue not only in case of biological matter but also should be taken into consideration when studying the inorganic solids.

With the advent of increasingly sophisticated and powerful X-ray sources: first synchrotrons and more recently short-wavelength free electron lasers, the importance of damage–related considerations is rapidly growing. The achievable dose rates using 3rd generation synchrotron beams are, typically, on the order of a few to a dozen or more kGy/s. The X-ray free electron lasers can deliver a MGy doses of monochromatic unfocused radiation in a single pulse only, that lasts typically few tens of femtoseconds.

In our concise communication we compare the doses and fluences delivered by X-ray beams from different sources. We focus on basic radiation damage mechanisms occurring both in inorganic solids and in biological matter. Discussed are also the secondary effects of strong ambient ionization around the sample, capable to significantly modify the properties in near-surface regions of even inorganic solids, as well as post-radiative effects in live tissues, like bystander effect or, waking numerous controversies, impact of very low doses on carcinogenic transformation.

P-24

Evaluation of characteristics of physical and chemical in vitro study of modified titanium surfaces

M. Łukaszewska-Kuska[1]*, B. Leda[1], P. Gajdus[1]
and W Hędzelek[1]

[1]*Department of Prosthodontic, Poznan University of Medical Sciences, Bukowska 70, 60-812 Poznan, Poland*

Keywords: titanium, surface modification, SEM, EDS, profilometry

*e-mail: m.lukaszewska.kuska@gmail.com

Introduction

Development of dental implantology is focused, among other things, on devising active surface of the implant, conditioning acceleration of the implant’s integration with the bone. Increased roughness, characteristic for group of implants with developed surface, altered topography and chemically modified implant's surface determines increased implants stability.

Objective

Evaluation of characteristics of titanium modified to develop its surface in in vitro studies.

Materials and methods

Titanium discs with four different surfaces were used: turned (TS); aluminium oxide-blasted (Al_2O_3); resorbable material blasted (RBM); sandblast and then etched with a mixture of acids (SAE). Titanium discs were tested using scanning electron microscopy for analysis of the surface’s topography, spectroscopic analysis for surface’s chemical composition, 2D and 3D profilometric analysis for the surface’s roughness.

Results

SEM image of the turned surface shows parallel folds on discs surface, Al_2O_3-blasted and RBM surfaces presents numerous cavities, and clearly sharp-edged rims, SAE surface is similar to sand-blast surfaces but has less sharp contours. Spectroscopic analysis revealed titanium and carbon as a main ingredients of all samples. Al_2O_3 surface also contains aluminum and sodium and RBM surface calcium and phosphorus. In SAE surface, the etching resulted in increased the amount of carbon. 2D and 3D roughness parameters revealed diversity of roughness profiles and existence of statistically significant homogenous group among examined titanium surfaces.

Conclusions

Topographic structure of the surfaces in SEM images corresponds to the results obtained in profilometric measurements. TS control surface is isotropic while the remaining surfaces – Al_2O_3-blasted, RBM, SAE – are anisotropic. Physical and chemical modifications of titanium surface change its microstructure (typical for SAE) and increase its roughness (highest for Al_2O_3-blasted and RBM surfaces). The introduced modifications develop titanium surface – 10 times for SAE surfaces, 16 times for Al_2O_3-blasted surfaces, and 20 times for RBM surfaces.

P-25

Managing beamlines at Solaris from an IT point of view

Ł. Dudek[1]*, P. Goryl[1], G. Kowalski[1], K. Szamota-Leandersson[1], J. Szota-Pachowicz[1], T. Szymocha[1], M. Zając[1], Ł. Żytniak[1,2]

[1] *National Synchrotron Radiation Centre Solaris, Jagiellonian University, Czerwone Maki 98, 30-392 Kraków, Poland*
[2] *MAX IV Laboratory, Ole Römers väg 1, 223 63 Lund, Sweden*

Keywords: synchrotron, Solaris, Tango, control system, DUO

*e-mail: lukasz.j.dudek@uj.edu.pl

The synchrotron light source that is the heart of National Synchrotron Radiation Centre Solaris would be useless without research that will be conducted at its beamlines. The initial setup of the facility includes two of those: one getting radiation from a bending magnet with two endstations (PEEM and XAS) and one utilising an insertion device – undulator – with a single ARPES endstation. The latter is finished and undergoing commissioning while the former has several pieces of hardware still in installation [1].

Since the main purpose of constructing and maintaining beamlines is inviting scientists to conduct their research there, the facility should have reliable systems to guide them through the process of registration, obtaining beam time, using equipment on a beamline to run measurements and processing results. The heterogeneous nature of the aforementioned systems is quite clear: on the one hand, there is a control system that enables the users to control beamline's hardware and on the other there are all other services that they might require outside of the experimental hall. Both aspects are equally important and necessary in order to provide a painless experience for the researchers.

The control system's task it to administer hardware and software, provide a link between them, supervise them and supply operators with control over both segments. The former consist mostly of vacuum equipment, diagnostics in form of cameras, YAG screens, etc., PLC, motion controllers and endstations. The latter is based on Tango which is an open-source framework used in managing distributed control systems in large physics facilities. It was created at ESRF, Grenoble, France and is now maintained by a consortium of synchrotrons from the whole Europe (Solaris is also a part of it) [2]. There is a separate instance of the Tango control system for each beamline.

The system for providing services to the users is called Digital Users Office. It's still in development phase – there is a collaboration between Solaris and Cyfronet, a part of University of Science and Technology in Kraków.

Acknowledgements: This work was supported by the whole Solaris team as well as colleagues from Elettra and Cosylab who delivered the UARPES beamline (the hardware and the software, respectively).

---

[1] A.I. Wawrzyniak et al., "*Solaris storage ring commissioning*", IPAC'16, Busan, Korea, WEPOW029
[2] Tango Controls website: http://www.tango-controls.org/

P-26

Origin of ferromagnetism in nanocomposite iron oxide films

K. Pitala[1]*, K.Kollbek[2], M. Piskorz[1], M.Sikora[2] and
A. Szkudlarek[2]

[1]*AGH, University of Science and Technology, Faculty of Physics and Applied Computer Science, Al. Mickiewicza 30, 30-059 Cracow, Poland*
[2]*AGH, University of Science and Technology, Academic Centre for Materials and Nanotechnology, Al. Mickiewicza 30, 30-059 Cracow, Poland*

Keywords: XAFS, nanocomposites, iron oxides, magnetic properties

*e-mail: krzysztof.t.pitala@gmail.com

Hematite, α-Fe_2O_3, is the most stable iron oxide under ambient conditions and is commonly found in nature. Its magnetic properties have been studied extensively both in bulk form and in the form of ultrafine particles. Below the Néel temperature, T_N ~950 K, bulk hematite is a weak ferromagnet, which undergoes a reorientation magnetic phase transition at the Morin temperature, T_M ~265 K, to a purely antiferromagnetic phase. Magnetic properties of hematite depend strongly on the grain size and display most interesting effects when the single crystal particles approach the size range of nanometers. As the particle size decreases, the Morin temperature is reduced and tends to vanish for particles smaller than ~20 nm.[1] If the particles become small enough, the direction of the magnetic moment in a single domain fluctuates due to thermal agitation, leading to superparamagnetic behavior and to spatial freezing of the effective magnetic moment of particles below the - blocking temperature T_B, [2] which is strongly dependent on particle size and shape.

We have studied thin films (10-20 nm thick) of hematite deposited on cold Si substrate by means of reactive magnetron sputtering using different sputtering conditions (controlled sample bias, partial pressure of nitrogen in deposition atmosphere and sample rotation). Microscopic images obtained with SEM and TEM revealed chemical inhomogeneity and presence of elongated precipitates. Their morphology is dependent on deposition conditions. VSM measurements have shown that magnetic properties of the films are significantly influenced by that morphology (Fig.1). The most intriguing is observation of opening of hysteresis loop for selected samples and directions, which indicates significant magnetic anisotropy.

We suspect that ferromagnetism can be attributed to different structure and chemical state of precipitates, e.g. maghemite or magnetite, with respect to hematite matrix. This hypothesis has been tested using XAFS experiment performed at SuperXAS beamline of SLS at PSI. (Fig. 2). Indeed, the iron K absorption spectra do shift edge towards lower incident photon energy for the samples revealing strongest magnetic effect.

The relation between morphology, magnetic and chemical properties of the samples of the nanocomposite iron oxides will be discussed in details.

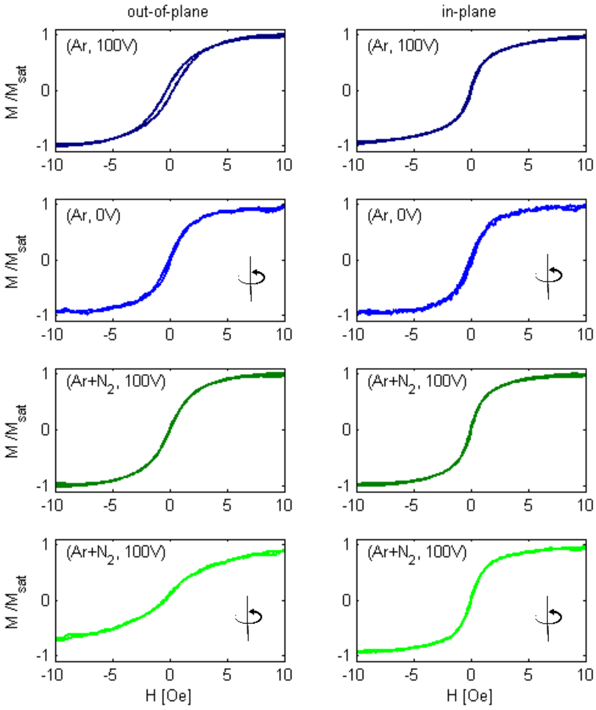

Figure 1. Hysteresis loops obtained via VSM. Deposition conditions (atmosphere, sample bias) indicated in brackets. Arrow determine presence of rotation during the process.

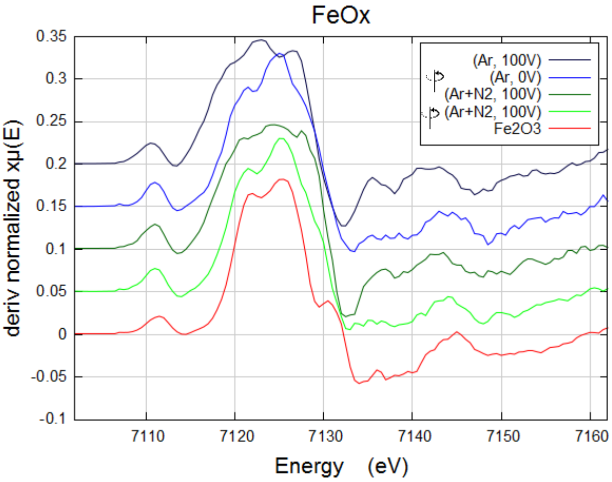

Figure 2. First derivative of Fe K-edge XAFS spectra of films studied and reference hematite powder (SA corrected).

Acknowledgments: This work was supported by National Science Center of Poland. We acknowledge SLS for granting beam time. We thank Dr. Olga Safonova, Dr. Jakub Szlachetko and Dr. Maarten Nachtegaal for kind help during synchrotron measurements.

[1] F. Bødker, et al., *Phys. Rev. B* **61** (2000) 6826.
[2] F. Jiao, et al., *J. Am. Chem. Soc.* **128** (2006) 5468.

P-27

XAS study of Ti-Al-C and Ti-Al-N based MAX phases

K. Goc[1]*, T. Strączek[1], W. Prendota[1], W.Tokarz[1],
M. Kapusta[2], L. Chlubny[2], J. Lis[2] and Cz. Kapusta[1]

[1]AGH University of Science and Technology, Faculty of Physics and Applied Computer Science, Department of Solid State Physics, al. A. Mickiewicza 30, 30-059 Kraków, Poland
[2] AGH University of Science and Technology, Faculty of Material Science and Ceramics, al. A. Mickiewicza 30, 30-059 Kraków, Poland

Keywords: MAX phases, structure, electronic properties, XANES, EXAFS

*e-mail: Kamil.Goc@fis.agh.edu.pl

The compounds called MAX phases comprise metals and non-metals crystallising in layered structures. Their exciting physical properties originate from the interplay of covalent and metallic bonds. They exhibit excellent mechanical properties including machineability and self-healing, which have already been broadly investigated and relatively well described. However, the other physical features, such as the thermal and electrical conductivities, thermoelectric properties and their relation to the crystallographic order, local atomic structure and electronic properties are still far from a complete description.

Structural differences between the respective members of the family of MAX phases concern the number of M layers separating the A-layers, e.g. in the 211's there are two, whereas in the 312's - three M-layers. This specific structure of MAX phases results in features typical for structural ceramics (high bending strength and fracture toughness) combined with new set of properties, such as ductility and low hardness. It also brings about unusual properties concerning their electrical, magnetic or thermal characteristics, which makes them attractive functional materials.

The aim of this work is to study the local structure and electronic properties of the Ti_2AlN and Ti_3AlC_2 MAX phase compounds with X-ray Absorption Spectroscopy (XAS) in the XANES (X-ray Absorption Near Edge Structure) and EXAFS (Extended X-ray Absorption Fine Structure) ranges. To synthesize the precursor powders of polycrystalline nanolaminate materials the Self-Propagating High-temperature Synthesis (SHS) was used. Subsequently, uniaxial hot pressing (HP) technique was used for the consolidation of powders. The samples obtained were found to be of 95% purity MAX phases.

XAS measurements have been carried out at the SuperXAS beamline of the Swiss Light Source, PSI, Switzerland (partial fluorescence yield mode, room temperature). The spectra in the XANES range of the Ti:K-edge are shown in Fig.1.

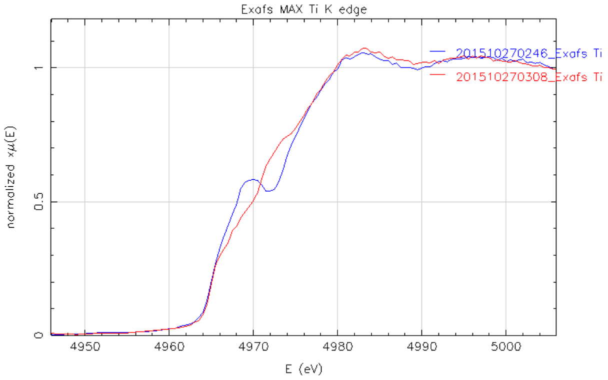

Figure 1. The XANES spectra of titanium K-edge in Ti_3AlC_2 (blue) and Ti_2AlN (red).

The EXAFS functions $\chi(R)$ obtained by Fourier transformation of the oscillations above the Ti:K-edge are shown in Fig.2.

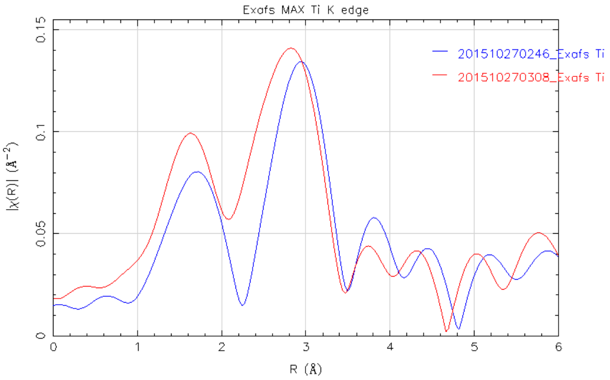

Figure 2. The EXAFS functions at titanium K-edge in Ti_3AlC_2 (blue) and Ti_2AlN (red).

The XANES spectra reveal a pronounced bump in the middle of the absorption edge of Ti_3AlC_2 (blue), whereas two smooth steps are observed there for Ti_2AlN. The EXAFS function $\chi(R)$ shows the intensity of the 1st neighbor peak (N or C)) higher for Ti_2AlN than for Ti_3AlC_2 due to a higher scattering factor for nitrogen than for carbon. Also the 1st and 2nd neighbor peaks are at slightly smaller distance for Ti_2AlN. The results are compared with the simulated XAS data and discussed in terms of their relation to the electronic and thermal transport properties of the materials.

Acknowledgments: Financial support from National Science Centre, Poland, Project No. 2013/11/B/ST5/02275 is acknowledged. Work partly supported by the Ministry of Science and Higher Education (MNiSW), Poland.

P-28

Small-angle X-ray scattering (SAXS) studies of the structure of mesoporous silicas

M. Zienkiewicz-Strzałka[1*], M. Skibińska[2] and S. Pikus[2]

[1]*Department of Physicochemistry of Solid Surface, Maria Curie-Skłodowska University, sq. Maria Curie-Skłodowska 3, 20-031 Lublin, Poland*
[2]*Department of Crystallography, Faculty of Chemistry, Maria Curie-Skłodowska University, sq. Maria Curie Skłodowska 3, 20-031 Lublin, Poland*

Keywords: mesoporous silica, small angle scattering

*e-mail: gosiazienkiewicz@wp.pl

Mesoporous silica materials are mesostructured objects with structural units on the nanometer dimension. A hallmark is significantly developed pore structure and excellent textural properties like high surface area and high pore volume. The unique properties remain function of nature of the material, their porosity, structure and geometry of pores. Due to the exceptional properties they are object of interest and a real challenge in catalysis, adsorption methods, and many other areas of modern chemistry. Porous silica materials are willingly used as adsorbents, catalyst support and drug delivery system due to its high thermal stability, tunable properties, possibility of modification and inactive behavior in relation to active phases and solvents [1-5]. Depending on type of precursors and synthesis conditions silicate structured mesoporous materials may have ordered or disordered pore structures. In a large family of mesopores silica materials, the most valuable and useful are SBA-15 (Santa Barbara Amorphous) [6], MCM-41 (Mobile Crystalline Material) [7,8] and MCF (Mesostructured Cellular Foam) [9]. MCM-41 has a hexagonal arrangement of one-dimensional mesopores with diameters ranging from 2 to 10 nm. SBA-15 exhibit 2D hexagonal network with high degree of structural ordering and presence of two type of porosity (micropores (below 2 nm) and mesopores in the range from 5 to 10 nm). Mesostructured Cellular Foams are three-dimensional (3D) structures with ultra large mesopores with size up to 50 nm. It is composed of uniform sphere-shaped sections interconnected by window pores with anarow size distribution.

Small-angle X-ray scattering (SAXS) measurements of mesoporous silica materials provides information on the distribution of electron density in the mesoporous material. In particular, structure and size of the unit cell as well as type of ordered structure. SAXS can be used to characterize the nanoscale structure both of ordered materials (analisys of position of diffraction peaks) as well as disorded materials for example MCFs. In the case of materials from mesostructured cellular foam family, SAXS measurements, the pore size distribution function and many other derivatives parameters can be obtained.

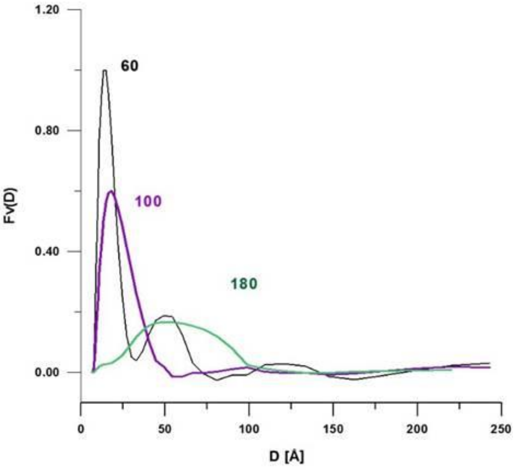

Figure 1. Pore volume distribution function of micropores in SBA-15 materials after hydrothermal treatment in 60°C, 100°C and 180°C respectively.

In this work, the SAXS measurements as well as analysis of SAXS spectra were performed for SBA-15, MCM-41 and MCF structures. Presented materials contained various proportional content of micropores and mesopores. It was found that SAXS technique allows to define parameters for describing micro and mesoporosity regardless of the the ordering degree.

---

[1] N. K. K. Raj, S. S. Deshpandale, R. H. Ingle, T. Raja, P. Manikandan, *Catal. Lett.* **98** (2004) 217.
[2] X. Zhang, Y. Yue, Z. Gao, *Catal. Lett.* **83** (2002) 19.
[3] S. Wang, *Microporous Mesoporous Mater.* **117** (2009) 1.
[4] M. Vallet-Regí, F. Balas, D. Arcos, *Angew. Chem. Int. Ed.* **46** (2007) 7548.
[5] W. K Cheah, Y. L. Sim, F. Y. Yeoh, *Mater. Chem. Phys.* **175** (2016) 151.
[6] D. Zhao, Q. Huo, J. Feng, B. F. Chmelka, G.D. Stucky, *J. Am. Chem. Soc.* **120** (1998) 6024.
[7] D. Zhao, J. Feng, Q. Huo, N. Melosh, G. H. Fredrickson, B. F. Chmelka, G. D. Stucky, *Science* **279** (1998) 548.
[8] D. Zhao, Q. Huo, J. Feng, F. Chmelka, G. D. Stucky, *J. Am. Chem. Soc*. **120** (1998) 6024.
[9] P. Schmidt-Winkel, *J. Am. Chem. Soc*. **21** (1999) 254.

P-29

Nanocrystalline peak profile analysis revisited

M. Zieliński[1]*, Z. Kaszkur[1]

[1]*Institute of Physical Chemistry, Polish Academy of Science,*
Kasprzaka 44/52, 01-224 Warszawa, Poland

Keywords: peak profile analysis, nanocrystals

*e-mail: MZielinski@ichf.edu.pl

In our paper [1] we have shown that Warren-Averbach peak profile analysis in the case of metal nanocrystals meets substantial problems and results in not reliable crystallite size estimation. The principal problem lays in peak asymmetry caused by the lattice parameter being dependent on the crystallite size. The effects of surface relaxation (or reconstruction) are becoming increasingly important with lowering the crystal size.

As a solution, we propose now a different approach to the analysis enabling estimation of both: lattice parameter size dependence and the crystal size distribution. The method consists in fitting the peak profile to a number of Gaussian profiles of different widths. A stable fit has been obtained for 4 Gaussian components. Accurate data then reveal peak position-width (corresponding to lattice parameter- crystal size) dependency (Fig.1) for a sample of nanocrystalline Au supported on amorphous carbon measured in situ while exposed to three gaseous environments: H_2, He, O_2. These values are compared to the lattice parameter-crystal size dependency obtained from atomistic simulations results for a range of sizes of Au cubooctahedra. The model clusters were energy relaxed using Sutton-Chen type potentials and their diffraction patterns calculated via Debye formula determining the diffraction measured lattice parameter.

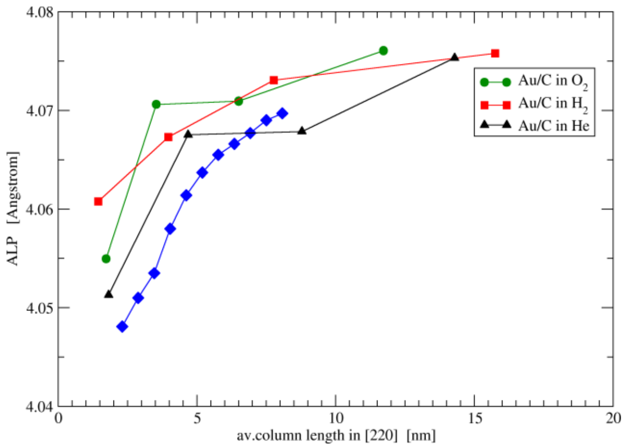

Figure 1. Experimental lattice parameter-crystal size dependency from 220 Au peak profile compared to values simulated theoretically (blue diamonds).

We present results of this peak profile analysis for 220 reflection of gold. The difference between peak profiles in different atmosphere is detectable and analyzed in terms of variation of the average crystal shape leading to a noticeable reshaping of the column length distribution.

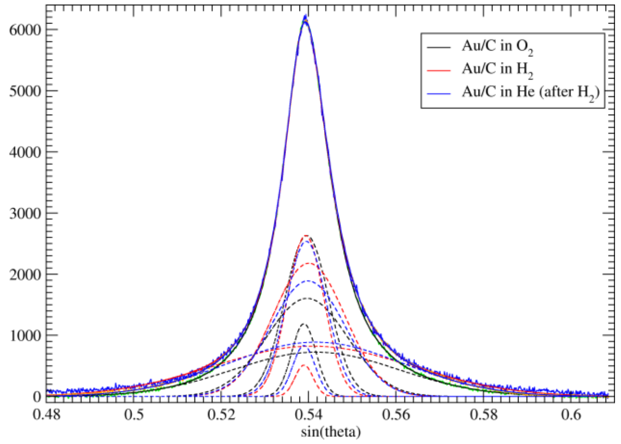

Figure 2. 220 peak profiles of nanocrystalline gold exposed to three gaseous atmospheres H_2, He, O_2. The component Gaussian profiles are given as dashed lines.

The resulting column length distribution calculated assuming no strain, is compared to the distributions from FW1/5M and FW4/5M method [2] differing from the latter.

Gold, similarly like other 5d metals, is susceptible to surface reconstruction occurring on free surfaces as well as on the chemisorbed or physisorbed crystal faces. Our in situ diffraction results provide evidence of bonding states of various gases on nanocrystalline gold corresponding e.g. to bonding energy of approx. 0.2 eV per atom for oxygen adsorption. The diffraction peak shifts on exposition to reactive gases are detectable for crystallites up to 20 nm size.

Acknowledgments: This work was supported by National Science Centre, Poland, research grant no. 2014/13/B/ST4/04619 .

---

[1] Z. Kaszkur, B. Mierzwa B., J. Pielaszek, *J.Appl.Crystallogr.* **38** (2005) 266.
[2] R. Pielaszek, *J.Alloy Compd.* **382** (2004) 128.

P-30

Magnetic Anisotropy of Ferrite Nanostructures: towards RIXS-MCD measurements

M. Piskorz[1]*, K. Pitala[1], A. Żywczak[2], A. Szkudlarek[2] and M. Sikora[2]

[1]AGH University of Science and Technology, Faculty of Physics and Applied Computer Science, University of Science and Technology, al. Mickiewicza 30, 30-059, Cracow, Poland
[2]AGH University of Science and Technology, Academic Centre for Materials and Nanotechnology, al. Mickiewicza 30, 30-059, Cracow, Poland

Keywords: RIXS-MCD, nanostructures, iron oxides, magnetism

*e-mail: piskorz.magda@gmail.com

Ferrites are of particular interest due to their wide variety of applications in electronics, spintronics and magnetic storage technology. Probing in operando magnetic behavior of nanodevices require quick and responsive experimental methods. RIXS-MCD technique was successfully used for measurements of micro magnetic properties of iron oxides [1-3] and we propose the same approach for complex nanostructures.

At first we studied heterostuctures of 15-40 nm thick magnetite films with different metallic layers deposited on MgO substrate in order to investigate magnetic anisotropy of oxide layer. We present comparison of angular dependence of hysteresis loops probed with bulk sensitive VSM, element specific RIXS-MCD magnetometry (Fig.1), and layer sensitive theoretical modelling using OOMMF software.

In the next stage we aim to probe if magnetic anisotropy can be controlled by shape of nanostructures. We have prepared ladder type nanostructures (1 µm, 500nm and 100nm thick and 100 µm long stripes) from selected magnetite heterostructures using electron beam lithography and argon ion-beam etching. Micromagnetic simulations reveal that in plane magnetic properties are anisotropic and depends strongly on shape of nanostructures (Fig.2).

Probing magnetic properties of such small structures is challenging using conventional methods (e.g. VSM, SQUID) due to negligible amount of magnetic material. Other methods such us MOKE, SXMCD, and MFM provide information only about surface properties. Therefore, they are insensitive to buried and thick layers, that could be probed with 1s2p RIXS-MCD.

Based on results of preliminary 1s2p RIXS measurements of nanostructures we discuss the feasibility of application of RIXS-MCD method as a selective probe of magnetization lurking inside oxide spintronic nanodevices.

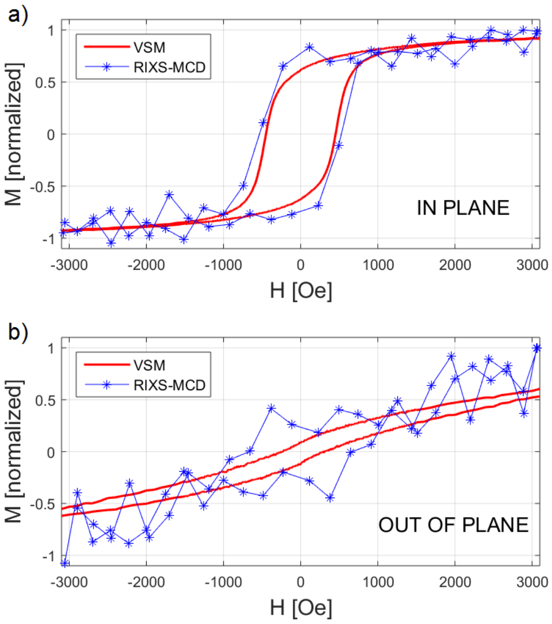

Figure 1. Comparison between hysteresis loops measured using VSM and RIXS-MCD technique for magnetic field applied a) in plane and b) perpendicular to 15nm thick Fe_3O_4 film covered with 2nm of Co and 10 nm of Pt.

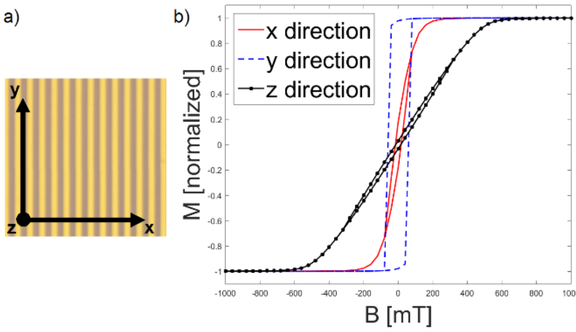

Figure 2. a) Optical microscope image of magnetite ladder type nanostructure with 1 µm tick stripes b) simulations of hysteresis loop for ladder type nanostructure.

Acknowledgments: This work was supported by National Science Center of Poland. We acknowledge ESRF and SLS for granting beam time on ID26 and SuperXAS beamlines, respectively. We thank Dr. Olga Safonova, Dr. Jakub Szlachetko, Dr. Mauro Rovezzi, Dr. Pieter Glatzel, and Dr. Amelie Juhin for kind help during synchrotron measurements and many fruitful discussions.

[1] M. Sikora, A. Juhin, T. C. Weng, P. Sainctavit, C. Detlefs, F. de Groot, P. Glatzel, *Phys. Rev. Lett.* **105** (2010) 037202.

[2] M. Sikora, A. Juhin, K. Biernacka G. Simon, M. Zając, K. Biernacka, Cz. Kapusta L. Morellon, M. R. Ibarra, P. Glatzel. *J. Appl. Phys.* **111** (2012) 07E301.

[3] A. Juhin ,A. López-Ortega, M. Sikora, C. Carvallo, M. Estrader, S. Estradé, F. Peiró, M. D. Baró, P. Sainctavit, P. Glatzel and J. Nogués, *Nanoscale* **6** (2014) 11911.

P-31

Characterization of submicron sized fluorescent silica particles

M. Jarzębski[1,2,*], T. Śliwa[3], B. Peplińska[2],
J. Jakubowicz[4], R. Kuzioła[5], J. Kościński[6],
T. Białopiotrowicz[1] and J. Gapiński[2,7]

[1] *Department of Physical Chemistry and Physochemical Basis of Environmental Engineering, John Paul II Catholic University of Lublin, Institute of Environmental Engineering in Stalowa Wola, Kwiatkowskiego 3A, 37-450 Stalowa Wola, Poland*
[2] *NanoBioMedical Centre, Adam Mickiewicz University, Umultowska 85, 61-614 Poznań, Poland*
[3] *Faculty of Technology of Chemistry, Poznan Univeristy of Technology, Berdychowo 4, 60-965 Poznan, Poland*
[4] *Institute of Materials Science and Engineering Poznan Univeristy of Technology, Jana Pawła II 24, 60-965 Poznan, Poland*
[5] *Department of Environmental Analytical Chemistry, John Paul II Catholic University of Lublin, Institute of Environmental Engineering in Stalowa Wola, Kwiatkowskiego 3A, 37-450 Stalowa Wola, Poland*
[6] *Poznań University of Medical Sciences Chair and Department of Neurosurgery and Neurotraumatology 49 Przybyszewskiego Str. 60-355 Poznań, Poland*
[7] *Molecular Biophysics Division, Faculty of Physics, Adam Mickiewicz University, Umultowska 85, 61-614 Poznan, Poland*

Keywords: fluorescet submicron particles, size determination, fluorescence correlation spectroscopy, material characterization

*e-mail: maciej.jarzebski@o2.pl

Silica nanoparticles and submicron particles are one of the most frequently modified and common uses materials. Various enhanced methods of the fluorescent particles preparations give the opportunities for applications of fluorescent SiO_2 as a model system for biomedical interactions between the particles and biostructures in colloidal systems such as cells. Fluorescent particles are usually made as a core-shell structures, where the fluorescent agent is included in core and then surrounded by protective shell. Nevertheless, for microscopic investigations are crucial to precise where exactly the fluorescent part is. Additional processes might occurred in core-shell fluorescent particles type i.e. fluorescent agent diffusion. In some applications the dye distribution within fluorescently labeled nanoparticles and its stability over long periods of time are important issues.

In present paper, fluorescent submicron silica particles were prepared by modified Stober technique [1,2]. As a fluorescent agent Rhodamine-B isothiocyanate was used. The core-shell tunneling size structure was formed by addition of TEOS (tetraethyl orthosilicate) to the base mixture. The size of the particles were investigated by dynamic light scattering (DLS), nanoparticle tracking analysis (NTA), fluorescence correalation spectroscopy (FCS). Shape and morphology were studied by the transmission and scanning electron microscopy (TEM and SEM). The fluorescence behavior of the particles was confirmed using NTA in the fluorescent mode and LSM (laser scanning microscope). We focused at the examinations of the particles with the hydrodynamic diameter in the range between 300 – 1000 nm using the FCS technique. As we presented in the previous papers [3,4], in the case of submicron sized fluorescent particles investigations with FCS need a correction of the confocal volume. XRD spectra of fluorescent SiO_2 were also obtained.

In this study main differences between the fluorescent submicron particles characterization methods are pointed out according to the tips presented by Bell et al. [5].

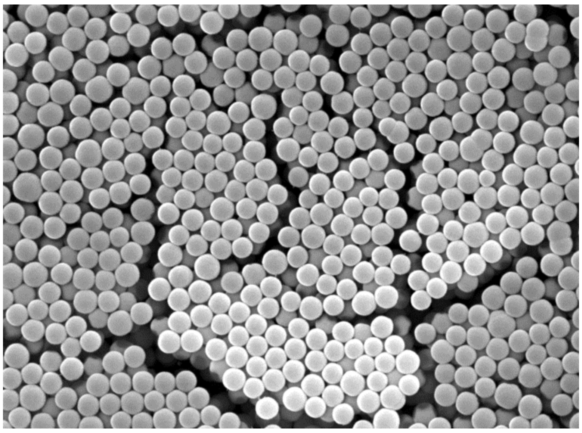

Figure 1. SEM image of fluorescent submicron silica particles.

[1] A. van Blaaderen, A. Vrij, *Langmuir* **8** (1992) 2921.
[2] M. Jarzębski, T. Śliwa, M. Jarzębska, K. Szutkowski, *Curr.Top.Biophys.* **37** (2014) 35.
[3] T. Deptuła, J. Buitenhuis, M. Jarzębski, A. Patkowski, J. Gapinski, *Langmuir* **31** (2015) 6681.
[4] J. Gapinski, M. Jarzębski, J. Buitenhuis, T. Deptula, J. Mazuryk, A. Patkowski, *Langmuir* **32** (2016) 2482.
[5] N. C. Bell, C. Minelli, J. Tompkins, M. M. Stevens A. G. Shard, *Langumir* **28** (2012) 10860.

P-32

Electron momentum density of hexagonal zinc studied by high-resolution Compton scattering

M. Brancewicz[1]*, E. Żukowski[1], A. Andrejczuk[1],
M. Pylak[2], Y. Sakurai[3] and M. Itou[3]

[1]*University of Bialystok, Faculty of Physics, Ciolkowskiego 1L, 15-245 Bialystok, Poland*
[2]*National Centre for Nuclear Research, Hoza 69, 00-681 Warsaw, Poland*
[3]*Japan Synchrotron Radiation Research Institute (JASRI), SPring-8, Sayo, Hyogo 679-5198, Japan*

Keywords: Zn, synchrotron radiation, Compton profile, theoretical band calculations

*e-mail: m.brancewicz@uwb.edu.pl

Compton scattering is a powerful method for investigating the electronic structure of condensed matter. The spectrum of inelastically scattered monoenergetic photon beam in a target is related through the Doppler effect to the momentum density distribution $\rho(\mathbf{p})$, which is directly connected with the electron wave function in reciprocal space $\chi(\mathbf{p})$ and hence with the Fourier transform of the wave function in real space $\psi(\mathbf{r})$:

$$\rho(\mathbf{p}) = |\chi(\mathbf{p})|^2 = \left|\int \psi(\mathbf{r}) e^{i\mathbf{p}\cdot\mathbf{r}} d^3r\right|^2$$

Thus the Compton scattering technique is the most direct test of solid state theories, where electron wave functions are calculated from the first principles.

The final result of single Compton scattering experiment is the Compton profile (CP, $J(p_z)$), which is the one-dimensional projection (double integral) of the electron momentum density $\rho(\mathbf{p})$ onto the scattering vector direction (usually chosen as Z axis):

$$J(p_z) = \int_{-\infty}^{+\infty}\int_{-\infty}^{+\infty} \rho(\mathbf{p})\, dp_x dp_y$$

Contribution to CP from core electrons is isotropic, but valence electrons contribution is modified by the crystal potential in solid. Therefore CPs differ when measured in different crystallographic directions set along the scattering vector. Subtraction of the profiles measured at two different directions removes all isotropic contributions to the profiles and forms the so-called difference profile. Difference profiles show the anisotropy of the electron momentum density. Small effects are then emphasized and sharp features near Fermi momentum begin to appear after subtraction.

Theoretical KKR calculations of Zn directional CPs were calculated by S. Kaprzyk and already presented in [1] and [2]. In this theory the electron wave functions outside the muffin-tin spheres are approximated by the combination of spherical harmonics. The Lam-Platzman correction for the correlated electron gas was also included. Medium resolution (0.42 a.u.) experimental CP anisotropies measured with the use of 662 keV radiation from ^{137}Cs isotope source at University of Bialystok [1] shows reasonably good agreement with theoretical KKR calculations except the low momentum region (up to 1 a.u.). High resolution (0.16 a.u.) anisotropies measured later with the use of 57 keV synchrotron radiation in ESRF [2] showed even worse agreement with KKR theory. This motivated us to measure the high resolution directional Compton profiles once more. The new high resolution (0.12 a.u.) experiment was performed in SPring-8 BL08W beamline with the use of high energy (115.6 keV) synchrotron radiation.

We also present the new theoretical CP calculations based on the DTF theory, where calculations were carried out within the full potential (linearized) augmented plane wave method with local orbitals (FP-LAPW+lo).

We observed a significant improvement of the agreement between experimental and theoretical CP anisotropies compared to the previous results (Fig. 1). Despite the differences observed between both, KKR and DFT calculations it is difficult to say unequivocally which theory describes the data more adequately.

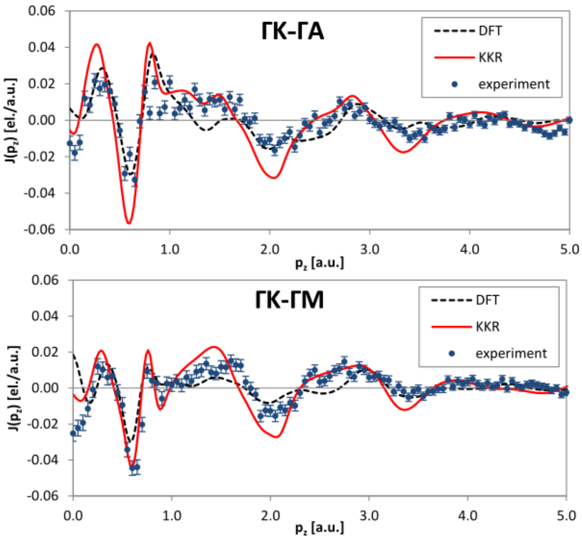

Figure 1. Two examples of directional Compton profile anisotropy measured along the three high-symmetry directions ΓA, ΓK and ΓM. Dashed and solid lines represent theoretical DFT and KKR calculations respectively, convoluted to 0.12 a.u. resolution of the experiment plotted by solid circles.

Acknowledgments: Authors want to thank Prof. Stanisław Kaprzyk for KKR theoretical calculations of Compton profiles and Prof. Heinrich Sormann for lending the program code for DFT theoretical calculations of Compton profiles. This experiment was performed with the approval of JASRI (proposal no. 2015A1129).

---

[1] H. Reniewicz, A. Andrejczuk, L. Dobrzyński, E. Żukowski, S. Kaprzyk, *J. Phys.: Condens. Matter* **13** (2001) 11597.

[2] Ch. Bellin, V. Honkimäki, H. Reniewicz, P. Zaleski, A. Andrejczuk, L. Dobrzyński, E. Żukowski, S. Kaprzyk, *J. Alloys Compd.* **362** (2004) 314.

P-33

Chemical analysis of the growth rings in the bamboo corals

M. Trzciński[1*], P. Mack[2], D. Nowak[1] and J. Nowak[1]

[1]*Institute of Environmental Engineering, the John Paul II Catholic University of Lublin, Poland*
[2]*Thermo Fisher Scientific Inc. Thermo Fisher Scientific, East Grinstead, West Sussex, UK*

Keywords: photoelectron spectroscopies XPS, SEM EDS, Raman spectroscopy, Keratoisis corals

*e-mail: mariuszt86@gmail.com

Bamboo corals are common in the Indo-Pacific and Atlantic Ocean. These corals (family Isididae) are among the most easily recognized deep-water octocorals due to their articulated skeleton comprised of non-sclerite calcareous internodes alternating with proteinaceous nodes. Colonies live in seas below 800 m [1] and are shaped in different way, as a rule they are branched, bushy or fan-like and can range in size from tens of centimeters to even a few meters. Bamboo corals form large underwater, very fertile meadows and forests populated by individuals up to 10 m high and with bases as wide as 3 m. The sequence of consecutive light inorganic and dark organic parts along the length of the branch gives the organisms a bamboo-like appearance. The ring structure similar to growth rings in trees is clearly visible on a transverse cross section of internodes. Chemical composition and state of Keratoisis coral skeletons (bamboo corals) have been analyzed by the Scanning Electron Microscopy coupled with Energy Dispersive X-ray (SEM/EDX) and photoelectron spectroscopy (XPS). Raman microspectroscopy has been shown to be very powerful technique for the identification and distribution an organic groups and compounds.

Mappings of the chemical composition of inorganic and organic parts of the coral rings show diversity in the location and concetration of elements and a specific microzones inside growth rings (see Fig 1) correlated with aminoacids distribution.

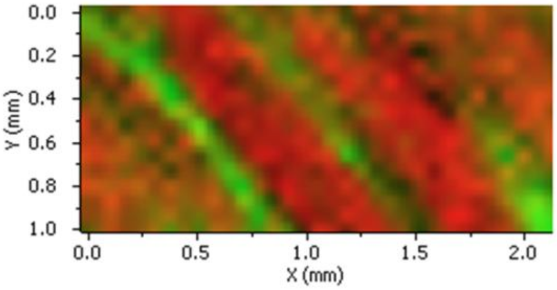

Figure 1. XPS mapping of Ca and Br in the coral growth rings. Signal Ca 2p is green whilst Br 3d5 is red.

Acknowledgments: This work was supported by the European Union as part of the Operational Programme Development of Eastern Poland for 2007–2013 EU-PL project No. POPW. 01.03.00-18-016/12-00.

---

[1] P. Etnoyer, L. Morgan, *Habitat-forming deep-sea corals in the Northeast Pacific Ocean*. In Freiwald A, Roberts JM (eds.), Cold-water corals and ecosystems. Springer-Verlag Berlin Heidelberg (2005), pp.331-343.

P-34

The study of the conformational flexibility and oligomerization state of the N-terminal fragment of the HYL1 protein by the small-angle X-ray scattering and the circular dichroism spectroscopy

P. Wieczorek[1]*, M. Taube[2], A. Jarmołowski[1] and M. Kozak[2,3]

[1]*Adam Mickiewicz University, Faculty of Biology, Department of Gene Expression, Umultowska 89, 61-614 Poznań, Poland*
[2]*Adam Mickiewicz University, Faculty of Physics, Joint Laboratory for SAXS studies, Umultowska 85, 61-614 Poznań, Poland*
[3]*Adam Mickiewicz University, Faculty of Physics, Department of Macromolecular Physics, Umultowska 85, 61-614 Poznań, Poland*

Keywords: synchrotron radiation, small angle X-Ray scattering, miRNA biogenesis

*e-mail: przemwiecz@amu.edu.pl

The HYPONASTIC LEAVES 1 (HYL1) protein from *Arabidopsis thaliana* is one of the core components of microRNA biogenesis machinery alongside the SERRATE (SE) and the DICER-LIKE 1 (DCL1) proteins [1]. It was shown to interact with both SE and DCL1 *in vitro* and *in vivo* and to be required for accurate excision of mature miRNAs from the precursors (pri-miRNA). The N-terminal fragment of HYL1, possessing two double-stranded RNA-binding domains (dsRBD1 and dsRBD2) was shown to be sufficient for rescue of the HYL1-deficient phenotype of *Arabidopsis thaliana* plants, restoring the level of miRNA accumulation. The crystal structures of dsRBD1 and dsRBD2 revealed the double-stranded RNA binding surface and dimerization interface, respectively [2]. The dimerization was further confirmed by the *in vivo* and *in vitro* experiments and found crucial for proper selection of the DLC1 cleavage sites within the miRNA precursor. The dsRBD2 is also responsible for interaction with SE and DCL1 proteins.

The in-solution structure of N-terminal fragment containing both dsRBDs connected by the linker of 15 amino acids (residues 15-172, $\mathrm{HYL}_{15\text{-}172}$) was examined by the circular dichroism (CD) spectroscopy and the small-angle X-ray scattering (SAXS). Since the Kratky plot suggested clear conformational flexibility of the protein, we applied Ensemble Optimization Method (EOM) [3] for the SAXS data analysis. EOM generates pool of models consisting of the rigid bodies connected by linkers of random conformation. In the next step, the software uses the genetic algorithm to select the ensemble of models that fits best to the experimental data. In the modeling we used two pools of models - one generated for monomeric and second one generated for dimeric assembly of $\mathrm{HYL}_{15\text{-}172}$ - to check the oligomerization state of the protein. We performed EOM analysis using both pools individually and after mixing them both. The best fit ($\chi^2 = 0.951$) was obtained for the ensemble consisting of seven models of the $\mathrm{HYL}_{15\text{-}172}$, one of which being model for the dimeric $\mathrm{HYL}_{15\text{-}172}$ with an abundance of ~ 7% and radius of gyration (R_g) of ~ 42 Å and the rest being models for the monomeric protein with R_g ranging from 21 to 30 Å, which indicates flexibility. The best χ^2 value obtained from EOM analysis for the ensemble consisting of the monomers only was 0.958 with slight discrepancy of the fit at low scattering angles, prompting the conclusion that a small fraction of the dimer was indeed present in the studied sample. This stays in agreement with previously published data, indicating that the purified full-length HYL1 is monomeric but can be shiftted towards the dimeric state by addition of the dsRNA [2].

The results of EOM analysis were complemented by the CD spectroscopy measurements. Fitting the experimental CD spectrum with the Contin-LL algorithm revealed that almost 40% of the $\mathrm{HYL}_{15\text{-}172}$ protein is disordered, pointing the low level of the ordered secondary structures and suggesting possible conformational disorder.

These results together indicate that the dsRNA-binding domain of the HYL1 protein is connected with the second domain responsible for the dimerization and protein-protein interactions *via* flexible linker and that $\mathrm{HYL1}_{15\text{-}172}$ protein has dynamic structure in solution. They also demonstrate the usefulness of the EOM tool in determination of the oligomerization state of protein in the studied sample, as was also shown in the previous works [4]. Hopefully, presented data together with future studies will provide a step towards understanding the miRNA biogenesis in plants on the structural level.

Acknowledgments: This work was supported by KNOW RNA Research Centre in Poznań (01/KNOW 2/2014)

---

[1] Z. Szweykowska-Kulińska, A. Jarmołowski, F. Vazquez, *Plant Signal Behav.* **8** (2014) e26955.

[2] S. W. Yang,H. Y. Chen ,J. Yang, S. Machida, N. H. Chua, Y. A. Yuan., *Structure* **18** (2010) 594.

[3] G. Tria, H. D. Mertens, M. Kachala, D. I. Svergun, *IUCrJ* **2** (Pt 2) (2015) 207.

[4] M. Møller, S. S. Nielsen, S. Ramachandran, Y. Li, G. Tria, W. Streicher, M. V. Petoukhov, R. A. Cerione, R. E. Gillilan, B. Vestergaard, *PLoS One* **8** (2013) e74783.

P-35

Preliminary results of human PrP^C protein examination by spectroscopic techniques

M. Nowakowski[1]*, J. Czapla-Masztafiak[1,2], M. Kozak[3], I.Zhukov[4] and W. M. Kwiatek[1]

[1]*Institute of Nuclear Physics Polish Academy of Sciences, PL-31-342 Krakow, Poland*
[2]*Paul Scherrer Institut, 5232 Villigen, Switzerland*
[3]*Adam Mickiewicz University in Poznań, Faculty of Physics, PL-61-614, Poznań, Poland*
[4]*Institute of Biochemistry and Biophysics Polish Academy of Sciences, PL-02-106 Warszawa, Poland*

Keywords: prion protein, XAS, AFM

*e-mail: michal.nowakowski@ifj.edu.pl

There are almost 90 proteins that are considered to be potential amyloidegenic factors [1]. One of them, prion protein (PrP) is natural glycoprotein which occurs on surface of cell membranes. It has been shown that PrP protein is able to transform itself in post-translation conversion from native cellular (PrP^C) state to pathological, proteinase resisted amyloid (PrP^{Sc}) form. Such conformation alteration of PrP is directly linked to non-curable transmissible spongiform encephalopathies (TSE) diseases.

Little is known about role of native PrP^C protein in cell activity, however it was proven that it is able to bind Cu^{2+} ions [2] as well as other metal ions on 2+ oxidation state. 3D structure of PrP^C protein contains two domains, N-terminal part, composed of 102 amino acid residues (residues: 23-124), is presented as unstructured domain which has ability to coordinate Cu^{2+} ions mostly through a conservative fragment consisting four tandem repeats of the PHGGGWGQ sequence [3]. Amount of bonded ions varies with ion concentration in solution. Second C-terminal domain (residues 128 - 231) has globular fold built with three α–helices and two antiparallel β-sheets [4]. PrP^C protein has already been examined using various methods including SR-SAXS spectroscopy on purified amyloid plaques [4] and biochemical approaches. Structure of Cu-binding sites remains unknown due to high mobility of unstructured domain which provide to unambiguous results. However, application of X-ray absorption spectroscopy supported by other spectroscopic methods have to deliver data about coordination of Ci(II) binding site.

Main research objective is to obtain structural information about coordination of Cu(II) in PrP^C protein. Our project request detail analyze of coordination environment and structures of both native and mutated PrP^C forms and with Cu^{2+} ion substituted by Zn^{2+}.

In the initial stage, the PrP^C purifying protocol of obtained lyophilized PrP proteins with and without bounded Cu(II) ions has been established. First preliminary XAS measurements have already been carried out on SuperXAS beamline (SLS, PSI Villigen) on both PrP^C-Cu(II) and PrP^C-Zn(II) complexes and results were compared with theoretical predictions using FeFF9.6 [6] software (Figure 1).

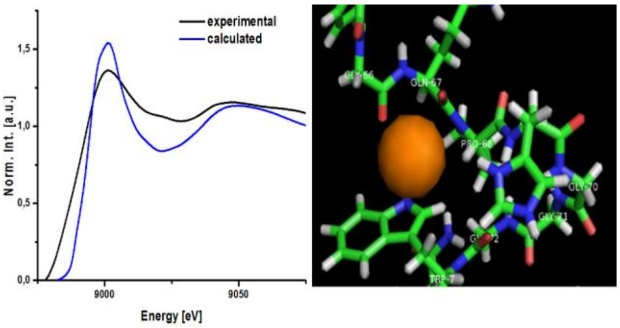

Figure 1. Results for XAS mesurment on PrP^C-Cu complex compared with theoretical predictions based on modified crystallographical structure. (left) smoothed XANES spectrum compared to calculated theoretical one; (right) 3D structure of hypothetical binding site of Cu^{2+} ion (orange sphere). Structure was taken from PDB database, PDB ID: 2kkg and modified manually.

Complementary to XAS data, AFM measurements have been performed to obtain general structural information about sample and to establish a protocol of fixing protein molecules on solid substrate in order to perform next step of experiments. It has been found out that C-terminal domain of PrP^C molecule has around 5 nm in diameter.

Presented results reveals that both XAS and AFM methods are promising tools in further examination of human PrP^C protein and its mutants. However more spectroscopic techniques have to be applied in order to have complex view of studied system.

Acknowledgments: The research was performed using equipment purchased as part of a the project co-funded by the Małopolska Regional Operational Programme Measure 5.1 Krakow Metropolitan Area as an important hub of the European Research Area for 2007-2013, project No. MRPO.05.01.00-12-013/15.This work was supported by the OPUS NCN grant No. 2014/15/B/ST4/04839.

---

[1] V. N. Uversky A. Fink (2007) *Protein Misfolding, Aggregation and Conformational Diseases: Part B: Molecular Mechanisms of Conformational Diseases (Protein Reviews)*, Springer.
[2] C. Migliorini, E. Porciatti, M. Łuczkowski, D. Valensin, *Coord. Chem. Rev*. **256** (2012) 352.
[3] J T. Pedersen, K. Teilum, N. H. H. Heegaard, J. Ostergaard, H. W. Adolph, L. Hemmingsen, *Angew. Chem. Int. Ed*. **50** (2011) 2532.
[4] N. J. Cobb, W. K. Surewicz, *Biochemistry* **48** (2009) 2574.
[5] H. Amenitsch, F. Benetti, A. Ramos, et al. *Prion* **7** (2013) 496.
[6] J. J. Rehr, J. J. Kas, F. D. Vila, M. P. Prange, K. Jorissen, *Phys. Chem. Chem. Phys*. **12** (2010) 5503.

P-36

Impact of different type of surfactants on molecular mechanisms of amyloid β-peptide aggregation

M. Skupin[1]* and M. Kozak[1,2]

[1]*Department of Macromolecular Physics, Faculty o Physics, Adam Mickiewicz University, Umultowska 85, 61-614 Poznań, Poland*
[2]*Joint SAXS Laboratory, Adam Mickiewicz University, Umultowska 85, 61-614 Poznań, Poland*

Keywords: amyloid beta peptide, surfactants, FTIR, CD, SAXS

*e-mail: mskupin@amu.edu.pl

One of the most common neurodegenerative disorder is Alzheimer's disease. It is estimated that in 2050 at least 1.25 % of population might have Alzheimer's disease [1]. It is supposed that the most critical changes relevant for the progress of this disease are related to development and deposition of amyloid plaque whose main components are amyloid β-peptides (Aβ) [2]. An innovative research approach is an attempt to create a prototype of medical nanosystem, which supports breaking process of formed fibrils into soluble forms.

The aim of our study was characterization of the structure and conformational changes of β-amyloid peptides in the presence of a several different surfactants. In our work we selected two groups of surfactants (dicationic and zwitterionic) and different types of β-amyloid peptides. The effect of surfactant concentration was tested on 1-42 Aβ peptide and its several shorter variants (N-terminal with hydrophilic properties and hydrophobic C-terminal fragment).

Analysis of the secondary structure of Aβ peptide in different concentrations of surfactants was carried out using FTIR spectroscopy (Bruker, Tensor 27 spectrometer) and circular dichroism (Jasco, J-815 spectropolarimeter) methods. The kinetic study of the aggregation behavior of different peptides in solution was also undertaken. The kinetics of aggregation processes of the peptides and formation of plaques was studied using fluorescence spectroscopy (Jasco, FP-6300 spectrofluorimeter) and Thioflavin T assay. The size distribution of aggregates of Aβ peptide was evaluated on the basis of gel electrophoresis.

Results of our study showed different impact of surfactants studied on the conformations of beta-amyloid peptides. A series of the small angle scattering of X-ray measurements using the synchrotron radiation (SR-SAXS) were performed for selected solutions of tested surfactants. The SAXS data for these surfactants were collected on P12 beam line of EMBL Hamburg Outstation on PETRA III storage ring at DESY. Preliminary examination of the cytotoxicity of selected surfactants on HeLa and fibroblasts cells was conducted in order to verify their suitability for therapeutic purposes.

Acknowledgments: This work was supported by research grant from Ministry of Science and Higher Education (Poland) – programme „Diamentowy Grant” decision number 0011/DIA2015/44

---

[1] C. P. Ferri, et al., *The Lancet* **366** (2006) 2112.
[2] J. Hardy, D. J. Selkoe, *Science* **297** (2002) 353.

P-37

Current status of the DBA blocks alignment in the 1.5 GeV storage ring at Solaris

J. Wiechecki[1]*, A. I. Wawrzyniak[1], P. Król[1],
M. Boruchowski[1], K. Karaś[1], R. Nietubyć[2]
and C. J. Bocchetta[3]

[1]*National Synchrotron Radiation Centre SOLARIS, Jagiellonian University, Czerwone Maki 98, 30-387 Kraków, Poland*
[2]*National Center for Nuclear Research, ul. A. Sołtana 7, 05-400 Otwock, Poland*
[3]*European Splalation Source ERIC, Tunavägen 24, 223 63 Lund, Sweden*

Keywords: synchrotron radiation, synchrotron, double bend achromat magnet, integrated magnets, alignment, mechanics, storage ring

*e-mail: jaroslaw.wiechecki@uj.edu.pl

National Radiation Center Solaris is the first synchrotron in Poland, located in Cracow. The facility is basing on the Swedish concept, designed by the MAX IV Laboratory [1,2], whereas Solaris storage ring is a replica of MAX IV 1.5GeV storage ring. The "heart" of the synchrotron comprises twelve integrated Double Bend Achromat magnets. A single achromat magnet is a novel design that merges sets of several smaller magnets, which constitute a magnetic lattice unit cell, closed in one block (see Fig.1). On one hand, this solution eases the installation of the storage ring, but on the other hand causes new problems unknown so far in the synchrotron technologies. This publication presents and focuses on one of the most important case – the survey of the storage ring components, focusing mostly on the DBA magnets. Their proper position [4] is extremely important, in order to get the most appropriate parameters of the electron beam and throughout this, the best parameters for the photon beam.

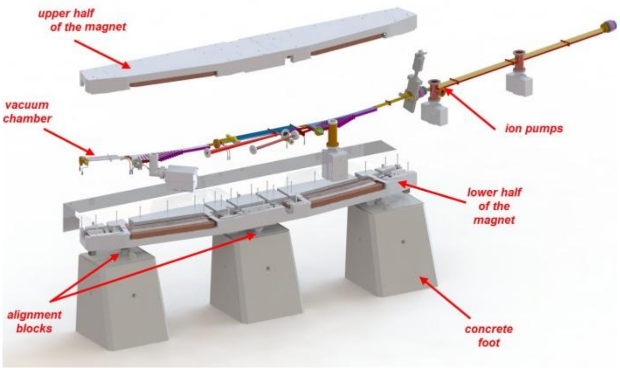

Figure 1. Double Bend Achromat Magnet (DBA) layout.

The Solaris storage ring alignment was a complexed procedure that has been divided into 3 steps: the survey of the building, rough and smooth alignment of the components. During the survey of the building, a detailed information about the behavior of the building has been provided. This data was used as a starting point to combine the theoretical 3D model of the building and the machine, with the real shape of the building and configuration of the machine. The reference network of the building was used to align both accelerating unit as also storage ring. A special attention has been put to, so called smooth alignment – a part of the survey that considers changes in the surrounding environment (e.g. air fluxes, temperature changes, ground stability, functionality of the devices etc.). Each iteration of the network adopts to the new conditions and can be easily measured also in accordance to the accumulated electron beam position inside the storage ring. The measurements shows that the storage ring is currently aligned within the range of ±120 μm RMS from the ideal orbit in horizontal plane, and ±60 μm RMS from the average high of orbit in vertical plane, i.e. Fig.2.

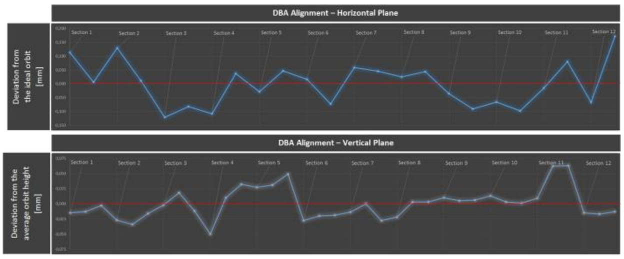

Figure 2. DBA alignment tolerances in horizontal (upper diagram) and vertical (lower diagram) planes.

The alignment is a complicated and arduous task that requires constant verification. In 2015 Solaris has stepped into commissioning phase [3,5], which revealed [6] that further survey of the machine is required, in order to get the photon beam with the most appropriate parameters. Small changes applied to the magnets position, can significantly influence the beam dynamics. In spite of a good coupling and fitting the theoretical 3D model into the real object, further measurements are planned in order to improve the parameters of the electron and photon beam.

---

[1] M. Johansson *Design of the MAXIV/Solaris 1.5 GeV storage ring magnets*, IPAC'11 San Sebastian WEPO016, 2430-2432 (2011). http://www.JACoW.org
[2] *MAXIV Detailed Design Report*, https://www.maxlab.lu.se/node/1136 (25 August 2010)
[3] A.I. Wawrzyniak, C.J. Bocchetta, et al, *First results of Solaris synchrotron commissioning*, Proceedings of IBIC2015, Melbourne, Australia - Pre-Release Snapshot 17-Sep-2015 10:30 WEDLA01
[4] J. Wiechecki, et al., *Mechanical aspects of installation of integrated magnets at Solaris synchrotron storage ring*, *Proc. SPIE* 9662, Photonics Applications in Astronomy, Communications, Industry, and High-Energy Physics Experiments 2015, 966234 (September 11, 2015)
[5] A.I. Wawrzyniak, et al., *Solaris Storage Ring Commissioning*, WEPOW029, IPAC'16, Busan, Korea, within these proceedings; WEPOW029
[6] J. Wiechecki, et al., *Impact of the DBA blocks alignment on the beam dynamics of the storage ring in Solaris*, WEPOW032, IPAC'16, Busan, Korea, within these proceedings; WEPOW032

P-38

Conformational changes of peptides based on human Cystatin C steric zipper region in the presence of gemini surfactants

W. Andrzejewska[1]*, J. Ludwiczak[1], E. Iłowska[2],
A. Szymańska[2] and M. Kozak[1,3]

[1]*Department of Macromolecular Physics, Faculty of Physics, Adam Mickiewicz University, Umultowska 85, Poznan, Poland*
[2]*Faculty of Chemistry, Gdańsk University, Wita Stwosza 63 80-308 Gdańsk, Poland,*
[3]*Joint SAXS Laboratory, Adam Mickiewicz University, Umultowska 85, 61-614 Poznan, Poland*

Keywords: human Cystatin C, peptides, steric zipper, circular dichroism

*e-mail: weronika.andrzejewska@amu.edu.pl

Human cystatin C (hCC) is a monomeric protein which exhibits amyloidogenic properties. This protein refolds to produce very tight, two-fold symmetric dimers. The dimerization process occurs *via* three-dimensional domain swapping. The crystal structure of native protein provided some clues about the tendency of hCC to dimerization and suggested a mechanism for its aggregation [1]. One of possible driving forces of this process may be provided by the presence of amyloidogenic steric zipper motif in the hCC sequence that undergoes significant exposure as a result of the domain swapping.

The aim of this project was an investigation of the influence of dicationic (gemini) surfactants on conformations of amyloidogenic peptides using variety of spectroscopic methods (CD, FTIR or spectrofluorimetry). In this work we used a synthetic peptides corresponding to the steric zipper motif derived from the cystatin C sequence, which has the ability to form cross-beta structure. The gemini surfactants used in the work are bis-imidazolium dichlorides with general formula C12JCn (n=2-12), where n stands for the number of methylene groups in the spacer group [2].

Acknowledgments: This research project has been financed by the funds from the National Science Centre (Poland) granted on the basis of decision No. DEC-2012/06/M/ST4/00036

---

[1] R. Janowski R., M. Kozak, E. Jankowska, S. Grzonka , A. Grubb, *Nat. Struct. Biol*. **1** (2008) 316.
[2] W. Andrzejewska, Z. Pietralik, M. Taube, A. Skrzypczak, M. Kozak, *Polimery* **59** (2014) 39.

P-39

Nanocarriers of siRNA based on selected gemini surfactants

W. Andrzejewska[1]*and M. Kozak[1]

[1]*Department of Macromolecular Physics, Faculty of Physics, Adam Mickiewicz University, Umultowska 85, Poznan, Poland*

Keywords: synchrotron radiation, small angle X-ray scattering, siRNA, gemini surfactants, gene carriers

*e-mail: weronika.andrzejewska@amu.edu.pl

Gemini surfactants belong to one of the most intensively studied group of chemical compounds, because of their specific properties like ability to formation of complex spatial structures and to the stable binding of the nucleic acids [1]. The process of complex formation between cationic gemini surfactants and nucleic acids is very interesting and important from the point of view of gene therapy. The most essential thing is to find the best vector for gene delivery into infected or genetically damaged cells [2-5].

In particular, the aim of this study was to analyzed nanocomplexes of cationic gemini surfactants (1,n-alkanebis[(oksymethyl)dimethyldodecylammonium] dichlorides)) with siRNA oligomers using agarose gel electrophoresis, small angle scattering of synchrotron radiation, circular dichroism spectroscopy and polarization microscopy.

Prepared by us nanocomplexes were found to be stable and the process of their formation was reproducible, efficient and immediate. Their morphology, spatial nanostructure and conformation of nucleic acid inside them was characterized. Based on this knowledge we categorized our systems as potential gene carriers.

Acknowledgments: This work was supported by the funds from the National Science Centre (Poland) granted on the basis of decision no. DEC-2011/01/B/ST5/00846.

---

[1] R. Zieliński, *WUP*, 2009, Poznan.
[2] P. C. Bell, M. Bergsma, I. P. Dolbnya, W. Bras, M. C. A. Stuart, A. E. Rowan, M. C. Feiters, J. B. N. Engberts, *J. Am. Chem. Soc.* **125** (2003) 1551.
[3] W. C. Brunner, M. F. Maestre, *Biolpolym*. **13** (1974) 345.
[4] D. Simberg, D. Danino, Y. Talmon, A. Minsky, M. E. Ferrari, C. J. Wheller, Y. Barenholtz, *J. Biol. Chem.* **276** (2001) 47453.
[5] S.D. Wetting, I. Badea, M. Donkuru, R.E. Verrall, M. Foldvari, *J. Gene Med.* **9 (**2007) 649.

P-40

Crystallographic structure study of $Fe_{64}Mn_{30}Si_6$ shape memory alloys

W. Prendota[1]*, S. Miyazawa[2], T. Strączek [1], K. Goc[1],
Cz. Kapusta[1] and A. Takasaki[2]

[1]*AGH University of Science and Technology, Cracow, Poland*
[2]*Shibaura Institute of Technology, Tokyo, Japan*

Keywords: Memory Shape Alloy, Memory Shape Effect

*e-mail: Witold.Prendota@fis.agh.edu.pl

Memory Shape Alloys (MSA) are the family of materials exhibiting the Shape Memory Effect (SME), which basically allows a deformed material to obtain its previous shape after subsequent heating. It is related to a martensite-to-austenite transformation (deformation) and a reverse process during heating: ε↔γ phases change. There are many systems which exhibit the SME. The most common are Ni-Ti alloys, because they are e.g. biocompatible and long term corrosion resistant [1]. The MSA play important role in industrial and medical applications. In order to reduce costs, the Fe-Mn-Si system has been studied.

In the Fe-Mn-Si material preparation process the iron (64 at.%; purity: 99,9%), manganese (30 at.%, purity: 99,9%) and silicon (6 at.%, purity: 99,9%) powders were mixed, mechanically alloyed (30 hours, 600 rpm, 1:8 ball to weight ratio, argon atmosphere), sintered (10 minutes, 900 °C temperature, 20 MPa uniaxial pressure, vacuum), and annealed (1 hour, 600 °C, vacuum). After deformation compression performed in uniaxial geometry parallel to the external stress of the sintering (room temperature, 1 mm/min, 4 % deformation). Last step was subsequent heating the samples in furnance to 200, 300, 400, 500 and 600°C, respectively.

In this study, X-Ray Diffraction (XRD) and X-ray Absorption Spectroscopy (XAS) in the XANES (X-ray Absorption Near Edge Structure) and EXAFS (Extended X-ray Absorption Fine Structure) ranges were used. XRD measurements were done on Rigaku Ultima IV (Cu-Kα radiation, 0.154 nm wavelength). Synchrotron measurements were carried out at the SuperXAS beamline of the Swiss Light Source, Paul Sherrer Institute, Switzerland (partial fluorescence yield mode, room temperature).

X-Ray measurements were performed in the temperature range, starting from room temperature, up to 600°C (five temperature points) in vacuum. The results obtained are presented in Figure 1. They reveal a crystallographic structure change during heating due to the ε⟶γ transformation.

Figure 2 presents results of the XAS study for the unannealed sample (Room Temperature) and after 600°C heating. Fourier transforms obtained from the EXAFS part of the Fe K-edge data, reveal one main peak at 1.96 and 2.06Å for the unannealed and 600°C annealed sample, respectively.

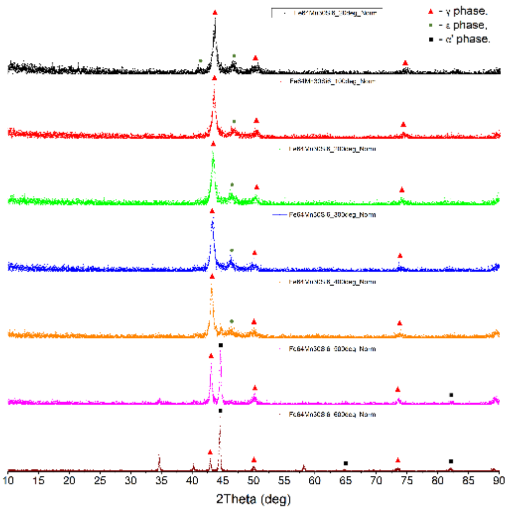

Figure 1. Results of XRD temperature measurements.

For the Mn K-edge EXAFS the obtained peaks are at 2.09 and 1.99Å for the unannealed and 600°C annealed sample, respectively. Small differences observed in the XANES region can be attributed to slight changes in the electronic state of the elements.

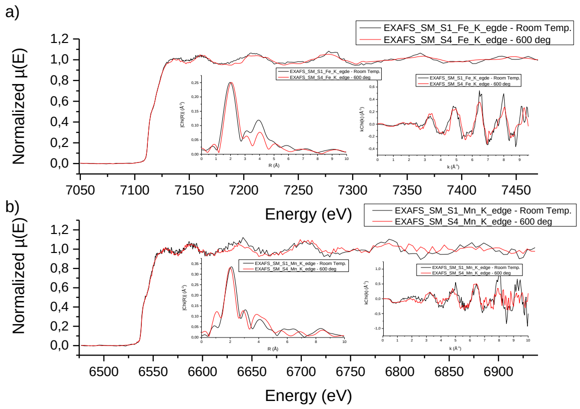

Figure 2. XANES/EXAFS results obtained for room temperature and 600°C for a) Fe and b) Mn K-α.

The results obtained show that in the case of 600°C sample the dominant phase (based on XRD) is α-BCC which is consistent with the Fe and Mn K-edge XAS (1st neighbour shell at 1.96Å and 1.99 Å, respectively). In the unannealed sample the γ-phase dominates (1st neigbour shell at 2.06Å and 2.09 Å, respectively).

Acknowledgments: This work was supported partially by the Ministry of Science and Higher Education (MNiSW), Poland and Shibaura Institute of Technology, Japan.

[1] V. P. Panoskaltsis (2013). *Mechanics of Shape Memory Alloys - Constitutive Modeling and Numerical Implications, Shape Memory Alloys - Processing, Characterization and Applications*, Dr. Francisco Manuel Braz Fernandes (Ed.), InTech, DOI: 10.5772/52228.

P-41

Control System at SOLARIS Synchrotron

W. T. Kitka[1]*, Ł. J. Dudek[1], P. Gałuszka[1], P. P. Goryl[1], A. Kisiel[1], M. Kopeć[1], P. Kurdziel[1], M. Ostoja-Gajewski[1], M. J. Stankiewicz[1], A. I. Wawrzyniak[1], K. Wawrzyniak[1], Ł. Żytniak[1,2], V. Hardion[2], J. Jamróz[2], D. Spruce[2], I. Dolinsek[3] and U. Legat[3]

[1]*National Synchrotron Radiation Centre Solaris, Kraków, Poland*
[2]*MAX IV Laboratory, Lund, Sweden*
[3]*Cosylab, Ljubljana, Slovenia*

Keywords: control system

*e-mail: wojciech.kitka@uj.edu.pl

A National Synchrotron Radiation Centre Solaris is a synchrotron light source in Krakow, Poland. The control system is fully operational and is used in the commissioning process of the accelerator.

Software platform for the control system is Tango Controls [1]. It is popular framework used in other European synchrotron facilities. The control system based on Tango Controls has a lot of elements: Tango Host server with database, archiving system, high level and low level software. At Solaris are three instances of Tango: one for a linac and a storage ring and one per each of two beamlines. They are responsible for acquisition of more than 5000 signals. An archiving system is using TDB and HDB tools from Soleil [2]. At Solaris low level applications developed in the Python programming language using an API to the Tango core – the PyTango package. Device servers are used for connection of hardware to the control system. There are 61 device servers at Solaris. The Taurus and the Sardana packages from ALBA (Barcelona, Spain) are used for writing a high level software, like GUIs. For browsing Tango database and checking each device operators use an open source application ControlProgram. It was developed and delivered by commercial company Cosylab (Ljubljana, Slovenia). The ControlProgram is also used for running Tango tools and another GUIs. The Matlab Midlayer is used for accelerator physics control.

There are two different PLC systems at Solaris. The first is MPS (Machine Protection System). It is used for protection of the machine against work in unwanted conditions. It is based on Rockwell Automations solutions. The second one is PSS (Personal Safety System). It provides radiation safety. It is based on Siemes S7-300 fail-safe controller.

The timing system at Solaris is based on Micro Research Finland (MRF) hardware. It consists of event generators (EVG) and event receivers (EVR). The EVGs generate a stream of events and send them to the EVRs. After receiving an event EVR performs action.

IcePAP drivers are used for high-precision movement control. They are configured with IcePAP Control Management System from ALBA.

Acknowledgments: This work was supported by:

- Solaris Team,
- MAX-IV Team,
- Tango Community,
- ELETTRA,
- ALBA,
- ESRF,
- SOLEIL,
- Others.

---

[1] Tango Controls website: http://www.tango-controls.org/
[2] G. Abeille et al., "Tango Archiving Service Status", ICALEPCS'11, Grenoble, 2011.

P-42

XAS study of oxide-fluoride glass-ceramics

A. Czajka[1], A. Jurczyk[1], T. Strączek[1], D.A. Zając[1],
M. Kasprzyk[2], M. Środa[2], and Cz. Kapusta[1]

[1]*AGH University of Science and Technology, Faculty of Physics and Applied Computer Science, Department of Solid State Physics, al. A. Mickiewicza 30, 30-059 Kraków, Poland*
[2]*AGH University of Science and Technology, Faculty of Material Science and Ceramics, al. A. Mickiewicza 30, 30-059 Kraków, Poland*

Keywords: XAS, oxide-fluoride glass-ceramics

*e-mail: anna.jurczyk@emiloo.pl

The materials studied represent a novel class of rare earth containing oxide-fluoride glass-ceramics exhibiting luminescent properties. Such materials are candidates for applications in optical devices such as converters or solid state lasers.. They combine excellent optical properties of fluorides with good chemical and thermal parameters of the oxide phase. Rare earth ions act as optically active centers there. To reduce the impact of phonon relaxation processes on the luminescent decay, optically active rare earth centers should be located in the low-energy phonons environment, such as e.g. in heavy metal fluorides. This allows getting a higher luminescence efficiency and longer lifetimes of excited states.

In order to achieve particular properties e.g. for applications in optoelectronics, partial crystallization is induced. The material obtained consists of a glass matrix containing crystallites of various sizes dispersed in it. Choosing the appropriate route of thermal treatment it is possible to obtain glass-ceramics with the crystallite size less than 100 nm, i.e. much less than the optical wavelength, when they are transparent.

For the study two types of oxide-fluoride glasses have been used: glass G1 doped with erbium and G2 glass doped with europium. X-ray Absorption Spectroscopy (XAS) measurements have been performed in the Helmholtz-Zentrum Berlin at a bending magnet beamline of the synchrotron radiation storage ring BESSY II. The spectra were recorded in the total electron yield (TEY) and partial fluorescence yield (PFY) modes at room temperature. The energy range covering the areas of O:K, F:K, Na:K, Eu:M, Gd:M, ErM, and Al:K have been scanned.

The O:K edge TEY spectra of the G1+Er samples in the XANES range are presented in Fig.1.

Except for the main edge at about 540 eV additional peaks appear at the energies of 60 eV and 80 eV higher, which are assigned to two-electron excitations involving metal atom neighbours. They are not observed for the unnanealed glass.

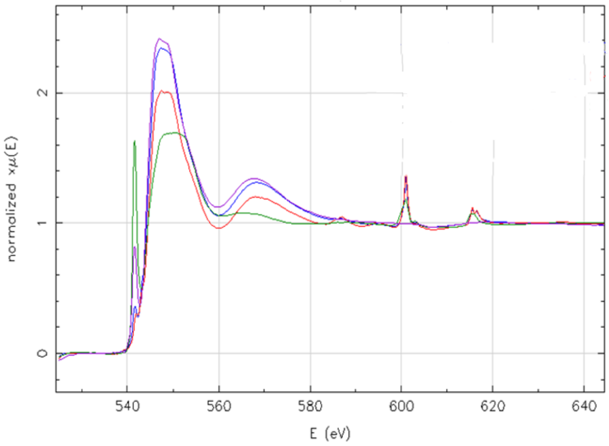

Figure 1. XAS spectra for the O:K edge of the of the G1+Er samples.

A similar behaviour is observed for the F:K edge. The effect is attributed to a modification of the local atomic environments at the surfaces and fluorine escape upon annealing.

Figure 2 illustrates the TEY spectrum at the M5 and M4 edges of erbium in the G1+Er powder glass before and after annealing,.

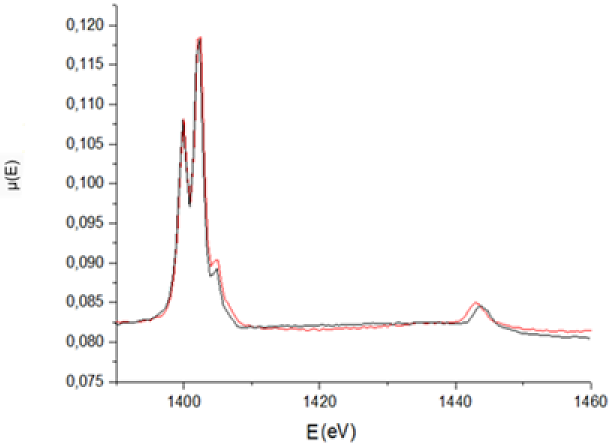

Figure 2. XAS spectra for Er edges M4, M5 for the G1+Er powder sample before (red) and after (black) annealing.

For powdered samples a significant shift of the M4 edge white line corresponding to the final states 4f5/2 to higher energies is observed, which mean they stronger bonding energy in the annealed sample.

The effects are analysed and discussed in terms of modifications of local atomic neighborhoods on annealing (ceramization) and differences in electronic interactions between fluoride and oxide environments.

P-43

Photon-photon delayed-coincidence spectroscopy as a tool probing the cascade transitions produced after the Ar 2*p* excitation

T. J. Wasowicz[1]*, A. Kivimaki[2,3], M. Coreno[3,4]
and M. Zubek[1]

[1]*Department of Physics of Electronic Phenomena, Gdańsk University of Technology, ul. G. Narutowicza 11/12, 80-233 Gdańsk, Poland*
[2]*CNR-IOM, Laboratorio TASC, 34149 Trieste, Italy*
[3]*Gas Phase beamline@Elettra, Basovizza Area Science Park, 34149, Trieste, Italy*
[4]*CNR-IMIP, Monterotondo, 00016 Roma, Italy*

Keywords: synchrotron radiation, photon-photon delayed-coincidence technique, argon

*e-mail: twasowicz@mif.pg.gda.pl

Many investigations have been devoted to obtain information on the electronic excitation and relaxation of the atoms and molecules. In particular the 2*p* excitation and relaxation of atomic Ar in the energy region between 240 and 255 eV have been studied by several different techniques, including photoabsorption [1], photoionization [2], electron-energy-loss spectroscopy [3], threshold electron–Auger electron coincidence technique [4], and UV-VIS fluorescence spectroscopy [5]. Photoabsorption and electron-energy loss spectra of Ar show pronounced structures below the Ar 2*p*-ionization thresholds that are attributed to resonant excitations of a *2p* electrons into low-lying *ns* and *nd* Rydberg states [1,3]. These core-excited states decay predominantly via resonant Auger transitions that serve as a start for relaxation processes occurring through the emission of fluorescence light [5]. But, the emission attributed to ionic states may not be directly formed by primary excitation processes. Therefore, the occurrence of cascade transitions has been proposed to play an important role in electronic relaxation [5]. This, however, complicates the interpretation of the fluorescence spectra. Fortunately, the coincidence measurements allow to avoid these problems and to provide more insight into the dynamics of the corresponding processes.

In the present study, observation of coincidences between fluorescence photons from the decay of the 2*p* inner shell excited argon in the 240-255 eV energy range was performed. The experiments were carried out at the low-energy branch of the Gas Phase Photoemission beamline at the Elettra synchrotron radiation facility utilizing the photon-induced fluorescence spectroscopy (PIFS) [6]. The branch line operated in the photon energy range 14-280 eV. For purposes of these studies a dedicated fluorescence detection system was constructed at Gdańsk University of Technology and transferred to Elettra Gas-phase beamline. It consisted of a beamsplitter and two optical channels, each incorporating interference filter followed by a photomultiplier tube (Figure 1). Outside the vacuum chamber, this system allowed to divide fluorescence signal into two parts with the aid of a beam splitter, which was selected according to the wavelength range of the studied emission. The reflected part of the split beam went through a color filter before being detected by a photomultiplier tube (PMT). A filter with the band pass was most often used in this arm of the experiment. The transmitted part of the light beam was filtered with a narrow-band interference filter before it was detected by a PMT tube. The signals from the two PMTs were fed into a time-to-digital converter system and coincidences between the two photon signals were searched after the completion of the measurement by using the data analysis program Igor.

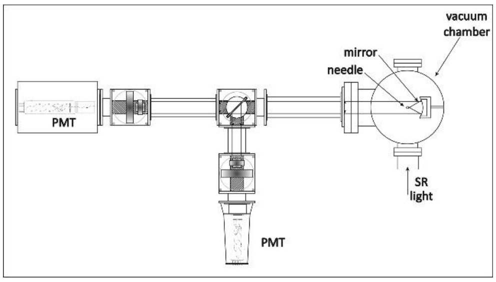

Figure 1. Scheme of detection system.

Here, we have measured fluorescence yields of the 4d′ ^{2}F→4p′ ^{2}F (335 nm) and 5s′ ^{2}D→4p′ ^{2}F (393 nm) decay (see Figure 2) lines and of wideband 380-540 nm emission arising at the 2*p* inner shell excitation of argon. To identify the spectral features we compared these yields with the total ion yield. In consequence, a state-selective behavior was found for those fluorescence excitation spectra. Thus, the coincidence measurements have been performed for the 335 and 459 nm and 393 and 459 nm photons combinations (Figure 2) at various photon energies corresponding to different resonances in argon. For those cascade transitions the coincidence charts and life times of the upper states have been obtained.

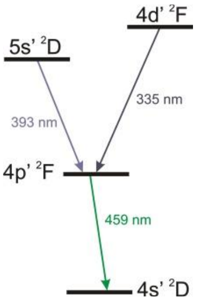

Figure 2. Schematic diagram of cascade transitions measured after the Ar 2*p* excitation.

Acknowledgments: This work was in part financially supported under the CALIPSO contract.

---

[1] M. Nakamura, et al, *Phys. Rev. Lett.* **21** (1968) 1303.
[2] J. A. Samson, et al, *Physical Review A* **54** (1996) 2099.
[3] G. C. King, et al, *J. Phys. B* **10** (1977) 2479.
[4] P. Lablanquie, et al, *J. Phys. B* **38** (2005) L9.
[5] R. Flesch, et al, *Phys. Rev. A* **61** (2000) 062504.
[6] T. J. Wasowicz, et al, *Phys. Rev. A* **83** (2011) 033411.

P-44

Production of neutral high-Rydberg fragments via inner-shell excitation and field ionization detection in the CO_2 molecule

A. Kivimäki[1], T. J. Wasowicz[2]*, C. Stråhlman[3],
J. A. Kettunen[4] and R. Richter[5]

[1]*CNR – Istituto Officina dei Materiali (IOM), Laboratorio TASC, 34149 Trieste, Italy*
[2]*Department of Physics of Electronic Phenomena, Gdansk University of Technology, ul. G. Narutowicza 11/12, 80-233 Gdansk, Poland*
[3]*MAX IV Laboratory, Lund University, P.O. Box 118, 22100 Lund, Sweden*
[4]*Department of Physics, University of Oulu, P.O. Box 3000, 90014 Oulu, Finland*
[5]*Elettra – Sincrotrone Trieste, Area Science Park Basovizza, 34149 Trieste, Italy*

Keywords: synchrotron radiation, high-Rydberg states, K edges, CO_2 molecule

*e-mail: twasowicz@mif.pg.gda.pl

Atoms and molecules have long-living metastable states with lifetimes which are considerably longer than those of ordinary excited states. In particular, the excited states having an electron in a high-Rydberg (HR) orbital and energy below the first ionization potential (IP) belong to those long-living states. Their lifetimes are expected to rise proportionally to n^3 [1], where n is the principal quantum number. Recently Kivimäki *et al.* [2, 3] have discovered a new class of the mechanisms of the photon-induced fragmentation, namely recapture processes to Rydberg states by detection of the field ionized TOF mass spectra of neutral high-Rydberg fragments after inner-shell C1s and S2p core excitations and ionization of the CH_4 and SF_6 molecules, exploiting a combined soft x-ray excitation with pulsed field ionization and ion time-of-flight (TOF) spectrometry. These measurements showed that core ionization of small molecules with a photon energy just above the 1s or 2p ionization potentials leads to ultrafast photoelectron recapture processes where the photoelectron is pushed back to high-Rydberg orbital of the molecular ion. Then, neutral high-Rydberg fragments can be created together with ions after subsequent dissociation processes. Those fragments may also be produced following resonant Auger decay after core–excitation.

In the present study we have studied the production of neutral high-Rydberg fragments and their intensities in the CO_2 molecule after inner-shell C1s and O1s core excitations and ionization, using soft x-ray excitation with pulsed field ionization and ion TOF spectroscopy. The experiments were carried out at the Gas Phase Photoemission beamline at the Elettra synchrotron radiation facility exploiting the TOF mass spectrometer that was modified for pulsed field ionization measurements [2]. The experimental set-up also allows the measurements of the yields of neutral HR fragments, ions, and of the photoelectron-photoion coincidence spectra.

First of all, we have measured the NEXAFS spectra by recording total ion yields (TIY) at both the C1s and O1s inner-shell edges without field ionization. In the second step, we have switched on field ionization and measured the sum (or total yield) of HR fragments and energetic photons (THRY). Figure 1 shows the example patterns of total ion yield and HR fragments+VUV photons yield recorded in CO_2 at the O1s edge in the photon energy range of 538-543.8 eV. Both yields are normalized to the photon flux and scaled to have the same intensity at the lowest energy resonance. In Figure 1, the THRY resembles the TIY only over the 3pσ/4sσ and 4pσ/5sσ resonances. But around the ionization energy (IP~541.3 eV) very strong peak occurs that can be attributed to the production of neutral fragments in the HR states by recapture processes where the photoelectron is pushed back to HR orbital of the molecular ion [2]. Recapture processes lead to the population of $\text{val}^{-2}\ \text{HR}^1$ states, whose dissociation can then yield neutral fragments in HR states. In order to identify particular HR fragments, the TOF spectra have been measured at the selected energies using field ionization. The HR fragments with the energy sufficiently close to the IP entered the first stage of the TOF spectrometer. Then, they were ionized by a pulsed electric field and pulled into the spectrometer. Ions produced in that way were detected using the MCP detector mounted at the end of the drift tube; their flight times allowed the identification of the initial neutral HR fragments. The mass spectra of neutral HR fragments revealed high intensity peaks due to atomic fragments C(HR) and O(HR).

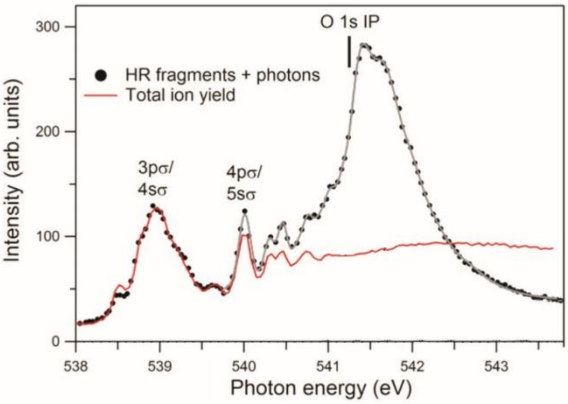

Figure 1. The HR fragment and ion yields measured at the O 1s edge of the CO_2 molecule.

Acknowledgments: Part of this work was performed during the Short Term Scientific Mission supported by the COST Action CM1204 (XLIC).

---

[1] W. A. Chupka, *J. Chem. Phys.* **98** (1993) 4520.
[2] A. Kivimäki, *et al., J. Chem. Phys.* **143** (2015) 114305.
[3] A. Kivimäki, *et al., J. Electron Spectrosc. Relat. Phenom.* **209 (**2016) 26.

P-45

Ru 4p → 4d Fano resonance in the $SrRuO_3$ valence band

S. Mickevičius[1]*, S. Grebinskij[1], M. Senulis[1] and A. Maneikis[1]

[1] *Semiconductor Physics Institute of Center for Physical Science and Technology, Saulėtekio av. 3, LT-10222 Vilnius, Lithuania*

Keywords: synchrotron radiation, photoelectron spectroscopy, valence band, Fano resonance

*e-mail: sigism@pfi.lt

The photoemission spectroscopy (PES) is a powerful tool for studying electron correlation effects in solids since the valence band (VB) spectra can directly reveal many body effects. However, experimentally measured VB spectra represent a superposition of both Ru *4d* and O *2p* states, making it difficult to interpret the results. Furthermore, the published PES on $SrRuO_3$ VB also was not totally consistent with each other and interpretations of spectroscopic data are often controversial [1,2]. The electronic structure of thin epitaxial $SrRuO_3$ films has been investigated using resonant photoemission spectroscopy (RPES).

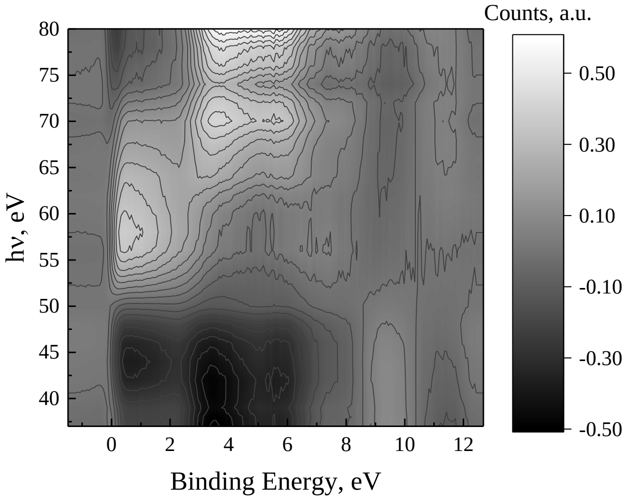

Figure 1. Countur plot of RPES spectra for $SrRuO_3$ thin film. For illustration purposes the difference between measured and the averaged over all *hν* spectra were shown.

Valence band data were collected at photon energies corresponding to *Ru 4p → 4d* threshold and analyzed using Fano expression:

$$F(h\nu) \approx (qw + h\nu - E_{\mathrm{Res}})^2 / [w^2 + (h\nu - E_{\mathrm{Res}})^2] \qquad (1)$$

The values of resonance energy E_R, width w, and asymmetry factor q were obtained by PES spectra fitting assuming the Fano behavior of *Ru 4p → 4d* resonance with a linear background corresponding to the monotonic decrease of the Ru 4d and O 2p photoionization cross-sections.

The evident resonant features were observed in the constant-initial-state mode of photoemission in the entire VB binding energy (BE) range ~ 0÷8 eV(see Fig. 1). And may be divided into two regions: Region A (BE ≤ 2.5 eV) – with resonance energy ~ 43÷45 eV and Region B (BE ≥ 5 eV) with resonance energy > 80 eV. Such separation of the valence band is clearly manifested in the distribution of the Fano parameters (see Fig. 2).

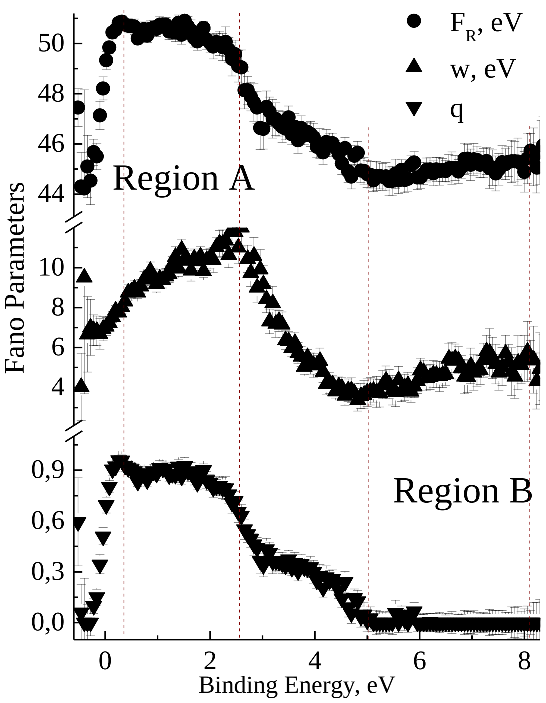

Figure 2. Parameters describing Ru 4d states Fano resonance in $SrRuO_3$ thin epitaxial film. Error bars corresponds to the standard deviation of fitting.

In accordance with theoretical models [3,4] *Ru 4d* states in Reg. A may be attributed to coherent and incoherent states of ruthenium, while states dominating at higher energies to bonding (around 5–7 eV) and nonbonding (around 3 eV) hybridized *Ru 4d – O 2p* states.

Another important result is that in the case of Fano-parameters varying along the valence band, the difference spectrum is no longer directly reflects the density of states and CIS spectra fitting procedure becomes necessary.

Acknowledgments: This work was partially supported by DESY and the European Commission under Grant Agreement ELISA 226716, IA-SFS Project No. DESY-D-I-20100305 EC.

---

[1] S. Grebinskij, M. Senulis, H. Tvardauskas, V. Bondarenka, V. Lisauskas, B. Vengalis, B.A. Orlowski, R. L. Johnson, S. Mickevicius, *Rad. Phys. Chem.* **80** (2011) 1140.

[2] E.B. Guedes *at al.*, *Phys. Rev.* **86** (2012) 235127.

[3] J. Park, S.-J. Oh, J.-H. Park, D. M. Kim, C.-B. Eom, *Phys. Rev. B* **69** (2004) 085108.

[4] S. Grebinskij, S. Masys, S. Mickevicius, V. Lisauskas, V. Jonauskas, *Phys. Rev. B* **87**, (2013) 035106.

P-46

Structural durability of Fe local neighbourhood in nitrogen-modified Fe/C composite used as fuel cell electrocatalyst: XAFS and XPS study

A. Witkowska[1]*, G. Giuli[2], M. Renzi[3], S. Marzorati[4], M. Longhi[4] and F. Nobili[3]

[1]*Gdansk University of Technology, Department of Solid State Physics, Narutowicza 11/12, 80-233 Gdansk, Poland*
[2]*University of Camerino, Geology Division, Camerino, Italy*
[3]*University of Camerino, Chemistry Division, Camerino, Italy*
[4]*University of Milano, Chemistry Department, Milano, Italy*

Keywords: Pt-free electrocatalysts, XAFS, XPS

*e-mail: agnieszka@mif.pg.gda.pl

Nowadays, Direct Hydrogen Fuel Cells (DHFCs) represent one of the most promising alternatives for the development of low temperature power devices. However, one of the most severe limitations to a large-scale application of this technology is the high cost of both polymeric membranes and of catalytic electrode materials, commonly requiring noble metals as Pt. In this context, non-precious metal catalysts are actively searched for. Among various materials, nitrogen-modified carbons containing non-precious transition metals (such as e.g. Fe, Co, Cu) are considered interesting because of their optimized morphology (in terms of porosity and specific surface area), activity closely approaching those of commercial Pt catalysts and reliability [1, 2].

Present contribution is dedicated to nitrogen-modified Fe/C composite used as Pt-free electrocatalyst for oxygen reduction reaction in DHFCs. Innovation of considered catalyst involves the use of organic compound, glucose, as a precursor of carbon (hereafter catalyst is shortly called Fe-GAG). Catalyst was prepared by high-temperature pyrolysis in N_2 atmosphere [2]. Catalytic ink and electrodes for FC tests were prepared in a standard way. Resulting Fe loading in the catalytic layer was about 0.1-0.2 mg/cm^2. For the structural study pristine powder, conditioned and degraded in real FC electrodes were used. Three types of aging procedure were applied to test the catalyst durability. Cathode electrocatalyst was subjected to operation under: i) steady state condition at 0.8 V (SS08), ii) steady state condition at 0.4 V (SS04) and iii) accelerate stress condition by load cycling from 0.4 V to 0.6 V (square wave potential cycling, SW04-06). All durability procedures were performed by 50 hours. Every 15 minutes of operation fast polarization curve collection was performed to check the pathway of the degradation process, data necessary to determine whether and to what extent changes in the iron local environment affect the catalyst electrochemical stability and fuel cell performance. Then, the electrodes were recovered for ex situ X-ray Absorption Fine Structure (XAFS) and X-ray Photoelectron Spectroscopy (XPS) experiments. XAFS and XPS measurements and analysis were performed to define the location and local structure of metal centres and their chemical states. Fe K-edge XAFS spectra in both near-edge (XANES) and extended (EXAFS) range were recorded at ELETTRA 11.1XAFS station. XANES data were analyzed on the base of the theoretical calculation realized by means of the MXAN code [3], whereas EXAFS data-analysis were performed using the GNXAS method [4]. The XPS spectra were collected using a laboratory non-monochro-matic source (Mg Kα). Then, standard peak-fitting analysis was carried out using a non-linear Shirley background and taking into account various chemical components.

In all studied samples Fe-Fe configurations (up to 4th coordination shell) precisely reconstruct metallic Fe-bcc structure. However, reduction of coordination numbers and higher value of disorder parameters, in respect to bulk metallic iron, indicate the presence of nanostructured Fe. Only in the case of Fe-GAG pristine powder the Fe-C/O/N distribution is well defined, giving in EXAFS signal comparable contribution with the Fe metallic phase. This observation confirms XANES estimated Fe metallic phase contents which equals only of about 20% in Fe-GAG pristine powder and over 60% in all studied electrodes. Additionally, it should be underlined that the main working conditions induced changes are correlated with Fe metallic phase and precisely follow the changes in relative current density loss: metallic phase is more degraded (smaller coordination number, higher disorder) larger loss in relative current density is observed. Thus, differences noted between electrodes subjected to various degradation protocols clearly indicate that the highest electrochemical and simultaneously structural stability Fe-GAG catalyst exhibits at SS08 working condition. On the other hand, it is least suitable for operation under SW04-06 condition.

Acknowledgments: We acknowledge the support of the SLL ELETTRA in Italy in providing SR facilities (XASF11.1) for 2035398 experiment. This research has been carried out within the PRIN Project: "Advanced nanocomposite membranes and innovative electrocatalysts for durable PEM FCs".

---

[1] M. Lefevre, E. Proietti, F. Jaouen, J-P. Dodelet, *Science* **324** (2009) 71.
[2] I. Galbiati, C. L. Bianchi, M. Longhi, A. Carra, L. Formaro, *Fuel Cells* **10** (2010) 251.
[3] M. Benfatto, A. Congiu-Castellano, A. Daniele, S. DellaLonga, *J. Synchr. Rad.* **8** (2001) 267.
[4] A. Filipponi, A. Di Cicco, C. R. Natoli, *Phys. Rev. B* **52** (1995) 15122.

P-47

EUSpec Modern Tools for Spectroscopy on Advanced Materials: a European Modelling Platform

A. Witkowska[1]*, A. Wolska[2], H. Ebert[3] and D. Sébilleau[4]

[1]Gdansk University of Technology, Department of Solid State Physics, Narutowicza 11/12, 80-233 Gdansk, Poland
[2]Institute of Physics, Polish Academy of Sciences, Poland
[3]Ludwig-Maximilians University, Germany
[4]University of Rennes-1-CNRS, France

Keywords: theoretical spectroscopy; experimental spectroscopy; scientific network

*e-mail: agnieszka@mif.pg.gda.pl

A deep knowledge of the properties of the materials on the atomic scale is necessary in order to understand the origin of their macroscopic behavior. The information provided by spectroscopy is a indispensable tool for academic and industrial research. Examples are found in physics (structural, electronic, magnetic, optical and elastic properties), chemistry (organic and inorganic chemistry, structural chemistry, catalysis), biology (structural study of proteins, cell biology, photosynthesis), environmental science (speciation in heterogeneous soils, sediments and plants).

EUSpec [1,2] is a COST Action MP1306 which brings together the expertise of experts from 26 European countries (and from two cooperating countries: Japan and Russia), from different fields of science such as physics, chemistry and biology who are working on advanced materials in order to build a coherent theory and computing platform with a new common data format to model sophisticated spectroscopy experiments performed at advanced radiation sources (ARS) as well as at academic and industrial research laboratories. In this Action theoretical and experimental scientists work hand in hand to improve the theoretical description of spectroscopy experiments, interpret experimental results, and develop new experiments (Figure 1). Main activities of EUSpec are focused on (Figure 2):

– coordination of Short Term Scientific Missions (STSMs) to promote early stage researchers (ESRs) activity,
– creation of a think-tank of ESRs in charge of making emerge new scientific ideas,
– promotion of interdisciplinary researches,
– organization of summer schools, training courses, scientific workshops and conferences,
– creation of a network of contact points at ARSs,
– providing a common platform for theory:
  - ○ definition of common format for data exchange,
  - ○ providing I/O-tools for common data format,

– enhancing interaction between theory and experiment;
– creation and development of the EUSpec website site.

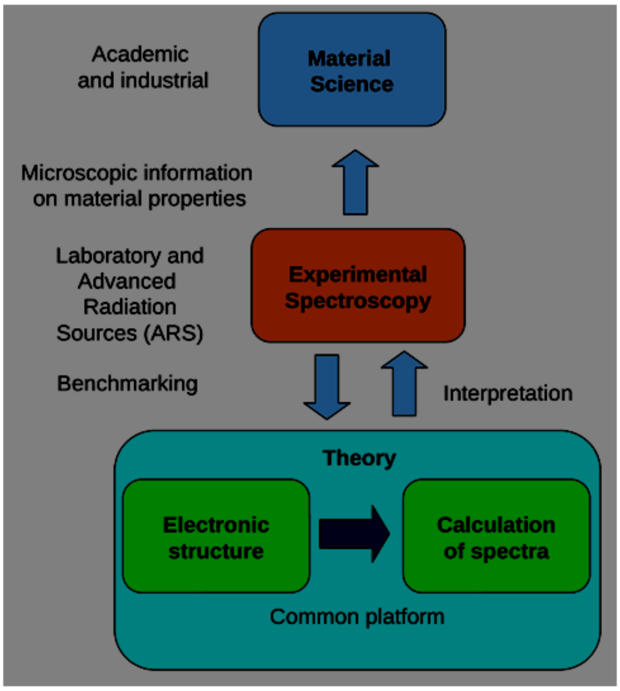

Figure 1. A schematic representation of the main objective of the EUSpec Action.

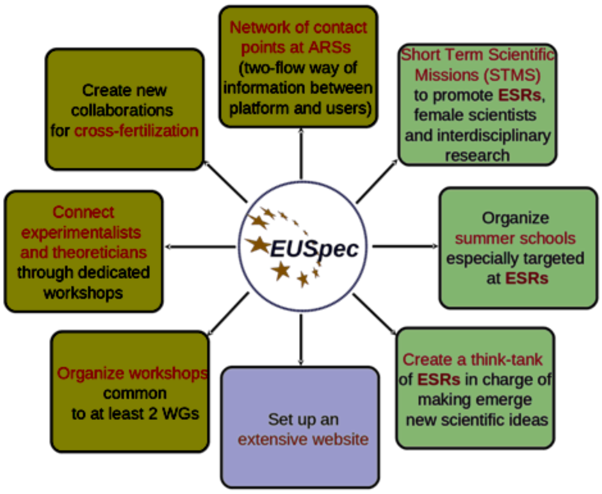

Figure 2. EUSpec activities.

Acknowledgments: COST is supported by the EU RTD Framework Programme.

---

[1] http://www.euspec.eu/
[2] http://www.cost.eu/COST_Actions/mpns/MP1306

P-48

Structural transformations in Mn_3O_4 at high pressure and high temperature

J. Darul[1]*, C. Lathe[2] and P. Piszora[1]

[1]*Department of Materials Chemistry, Faculty of Chemistry, Adam Mickiewicz University, Umultowska 89b, 61-614 Poznań, Poland*
[2]*Helmholtz-Zentrum Potsdam, Deutsches GeoForschungsZentrum GFZ, Telegrafenberg 14473 Potsdam, Germany*

Keywords: hausmannite (Mn_3O_4), postspinel oxide, high-pressure high-temperature phase transition

*e-mail: jola@amu.edu.pl

Structural transformations are a very fertile research area where physicochemical ceramics and earth sciences overlap to investigate basic aspects of the materials and possible applications. At high pressures, spinel compounds can transform to $CaMn_2O_4$-, $CaFe_2O_4$-, or $CaTi_2O_4$-type structures, often regarded as post-spinel phases [1]. In this work the results of *in-situ* synchrotron X-ray diffraction studies of hausmannite up to 7.2 GPa and 1273 K are reported. The Mn_3O_4 tetragonal spinel is found to transform to a 9.6 % denser polymorph of the $CaMn_2O_4$-type structure at 7.2 GPa and 673 K, under milder conditions than those of any transformations to postspinel phase described so far. Upon heating at high pressure, the Mn_3O_4 phase undergoes decomposition and finally disappears in favor of MnO at temperatures above 1073 K [2]. Finally, a reconstructive hausmannite-to-postspinel transformation is connected with a full octahedral movement. Manganese cations go from one octahedral site to the next by edge-crossing, which requires energy input. This is the likely reason why together with high pressure the high temperature is also needed to facilitate a transformation of the highly stable hausmannite to marokite-like structure. One interesting property of the post spinel compounds is the potentially high mobility of cations through the lattice, what makes post spinel phases promising candidates for cathode research.

Acknowledgments: A part of this research was carried out at the beamline F2.1 of the light source DORIS III, at DESY/Hamburg. The research leading to these results has received funding from the European Community's Seventh Framework Programme (FP7/2007-2013) under grant agreement n° 312284.

---

[1] A. Yamanaka, A. Uchida, Y. Nakamoto, *Am. Mineral.* **93** (2008) 1874.
[2] J. Darul, C. Lathe, P. Piszora, *J. Phys. Chem. C* **117** (2013) 23487.

P-49

Spin-crossover transition in iron(II) coordination polymers induced by high pressure

D. Paliwoda[1]*, M. Książek[2], M. Weselski[3], R. Bronisz[3], J. Kusz[2] and M. Hanfland[1]

[1]*European Synchrotron Radiation Facility, B.P.220, F-38043 Grenoble Cedex, France*
[2]*Institute of Physics, University of Silesia, Uniwersytecka 4, 40-007, Katowice, Poland*
[3]*Faculty of Chemistry, University of Wrocław, F. Joliot-Curie 14, 50-383 Wrocław, Poland*

Keywords: spin-crossover,

*e-mail: damian.paliwoda@gmail.com

Spin-crossover (SCO) transition can occur in some metal complexes wherein the spin state of the complex changes due to external stimuli like temperature, pressure or light irradiation.[1]

Till now, a vast amount of iron(II) complexes showing temperature- and light-induced spin-crossover transition have been reported, but only several systems have been investigated under high pressure.[2]

We have focused our attention on low-temperature light-induced excited spin-state trapping (LIESST) and high-pressure X-ray diffraction studies of the SCO transitions of one-dimensional iron(II) coordination polymers. For these purposes we have chosen two isostructural complexes $[Fe(3L)_3]X_2$ (where L=1,3-di(tetrazol-1-yl)propane, X = BF_4^- or ClO_4^-). Both complexes form hexagonal crystals of space group $P\bar{3}c1$.

A series of high-pressure single-crystal diffraction experiments on $[Fe(3L)_3](BF_4)_2$, $[Fe(3L)_3](ClO_4)_2$ and $[Zn(3L)_3](ClO_4)_2$ (reference sample) have been performed at High Pressure ID09A Beamline at ESRF using parallel monochromatic X-ray beam (E = 30 keV, λ = 0.413 Å) focused to 30 × 30 μm^2 on the sample loaded into membrane Diamond Anvil Cell and topped by silicon oil. A significant transformation of Fe-N bonds compressed up to 1.4 GPa have been observed, which allow us to postulate an occurrence of spin-crossover transition.

---

[1] P. Gutlich, Y. Garcia, H. A. Goodwin, *Top. Curr.Chem.* **233** (2004) 1;
M. A. Halcrow, Spin-crossover materials: properties and applications, John Wiley & Sons, Ltd., 2013.
[2] P. Gutlich, V. Ksenofontov, A. B. Gaspar, Coord, Chem. Rev, **249** (2005) 1811;
D. Pinkowicz, M. Rams, M. Misek, K. V. Kamenev, H. Tomkowiak, A. Katrusiak, B. Sieklucka *J. Am. Chem. Soc.* **137** (2015) 8795.

P-50

Preliminary spectroscopic and thermodynamic studies of binding Zn^{2+} ions to human PrP^C

M. Gielnik[1], I. Zhukov[2] and M. Kozak[1,3]

[1]Department of Macromolecular Physics, Faculty of Physics, Adam Mickiewicz University, Umultowska 85, 61-614 Poznań, Poland
[2]Institute of Biochemistry and Biophysics Polish Academy of Sciences, PL-02-106 Warszawa, Poland
[3]Joint Laboratory for SAXS Studies, Faculty of Physics Adam Mickiewicz University, Umultowska 85, 61–614 Poznan, Poland

Keywords: conformational stability of proteins, circular dichroism

*e-mail: maciejgielnik@amu.edu.pl

T Human prion protein (PrP) is a neuronal membrane protein exposed into synaptic cleft [1]. Mature form of PrP is 208 amino acids long and can exist in two different structural conformations: normal (PrP^C), and pathogenic (PrP^{Sc}). PrP^C consists of two domains: unstructured and flexible N-terminal domain containing four tandem octarepeats and structured C-terminal domain with three α-helices and twoanti-parallel β-sheets. Pathogenic PrP^{SC} contains predominantly β-sheets [2] and is involved in development of nine human [3] and seven animal neurodegenerative diseases [4] called transmissible spongiform encephalopathies (TSE).

Zinc is the second most common metal in living organisms. The highest concentration of zinc is observed in the nervous system [5]. During synapse excitation, concentration of zinc in synaptic cleft can reach even mM concentration. PrP can bind zinc with binding constant $3{\times}10^{-4}$ M^{-1} and is considered to be responsible for the zinc uptake [6]. What is also important from TSE point of view conversion of PrP^C to PrP^{Sc} decreases concentration of zinc in neural system up to 70%. PrP binds zinc ions by an octarepeat region [7].

Main goal of our studies was to measure conformational stability of PrP^C, with and without zinc ions. In order to measure conformational stability of human PrP^C far UV circular dichroism spectroscopy (CD) was used to detect changes in secondary structure. Spectrum of PrP had double minima at 219 nm and 209 nm and a single maximum at 191 nm (Fig. 1). The biggest changes between specta were 219 nm therefore this wavelength was used to perform thermal melting using CD spectroscopy.

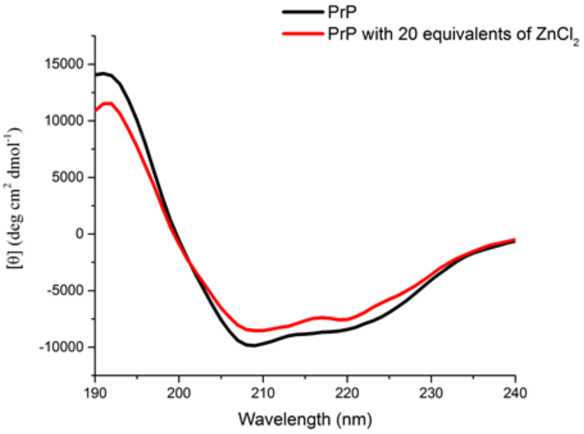

Figure 1. Far UV CD spectra of 20μM wild-type human PrP with and without 400μM of $ZnCl_2$.

Acknowledgments: This work was supported by the funds from the National Science Centre (Poland) granted on the basis of decision no. No. 2014/15/B/ST4/04839.

[1] J. Herms, T. Tings, S. Gall, A. Madlung, A. Giese, H. Siebert, P. Schürmann, O. Windl, N. Brose, H. Kretzschmar, *J. Neurosci* **19** (1999) 8866.
[2] J. Singh, J. B. Udgaonkar, *Biochemistry* **54** (2015) 4431.
[3] M. Imran, S. Mahmood, *Virology Journal* **8** (2011) 493.
[4] M. Irman, S. Mahmood, *Virology Journal* **8** (2011) 559.
[5] A. Parakash, K. Bharti, A. B. A. Majeed, *Fundam Clin Pharmacol* **29** (2015) 131.
[6] K. Pan, C-W Yi, J. Chen, Y. Liang, *Biochem Biophys Acta* **1854** (2015) 907.
[7] S. Sharma, M. Ebadi, *Neurochem Int* **65** (2014) 40.
[8] A. Parakash, K. Bharti, A. B. A. Majeed, M. Svandrlik, F. Parmigiani, *Fundam Clin Pharmacol* **29** (2015) 131.

P-51

EAXFS study of Mn and Ni doped maghemite nanoparticles

T. Strączek[1*], S. Fiejdasz[1], W. Prendota[1],K. Goc[1],
J. Jurczyk[1], J. Przewoźnik[1], Sz. Zapotoczny[2],
M. Nowakowska[2], J. Szmyd[3] and Cz. Kapusta[1]

[1]*AGH University of Science and Technology, Faculty of Physics and Applied Computer Science, Krakow, Poland*
[2]*Jagiellonian University, Faculty of Chemistry, Krakow, Poland*
[3]*AGH University of Science and Technology, Faculty of Energy and Fuels, Krakow, Poland*

Keywords: EXAFS, maghemite, nanoparticles

*e-mail: straczek@fis.agh.edu.pl

Superparamagneticnanoparticles are a group of materials whichhave attracted much attention of researchers in recent years. The reason of that is a wide range of applications, e.g. in medicineas MRI contrast agents or in magnetic hyperthermia, which is very promising for development of modern cancer therapy. They can be used in combination of a targeted delivery of nanoparticle agents, e.g. using monoclonal antibodies, and the Magnetic Resonance Imaging (MRI) detection of localization of these agents. Thus, nanoparticle materials that could play such a dual role are sought.Among them SPIONs (Superparamagnetic Iron Oxide Nanoparticles) are very promising candidates.

For the improvement of theirdetectability e.g. with X-Ray Fluorescence (XRF) and/or XANES (X-ray Absorption Near Edge Structure) spectromicroscopy, the material has been modified by replacement of iron in 10% by manganese and in 10% by nickel. The nanoparticles coated with cationic derivative of chitosan (CCh) were obtained using coprecipitation method. The proper amounts of Fe, Mn and Ni salts were dissolved in aqueous solution of CCh. Nanoparticles were formed upon the addition of ammonia. Finally, the precipitated nanoparticles, were purified by magnetic filtration.

The crystallographic structure of the material obtained has been determined with X-ray diffraction (XRD) and the diffractogram is presented in the Fig. 1.

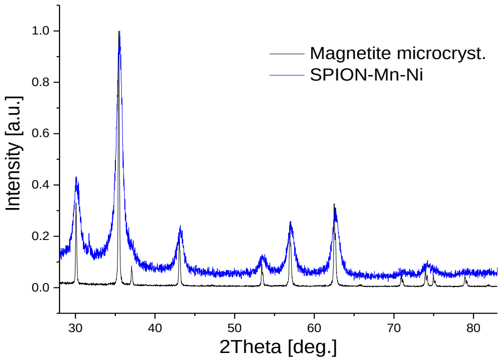

Figure 3. X-Ray diffraction pattern of Mn and Ni doped SPION nanoparticles together with that of microcrystalline magnetite.

It shows, that the material has the same crystallographic structure as magnetite, i.e. of inversed spinel. A large broadening of the diffraction peaks, comparing with magnetite, indicates a nanometric size of the crystallites of the material. The Williamson-Hall analysis of the widths of the peaks provided the information on the density of defects and the average crystallite size, which was estimated at 9 nm.

The Moessbauer measurements carried out at room temperature resulted in a magnetically split, relaxational spectrum, indicating a superparamagnetic character of the nanoparticles. This was also proven by the measurements of a DC magnetic susceptibility and magnetization curves.

The X-ray Absorption measurements were taken at the Swiss Light Source, PSI, Switzerland,at the SuperXAS beamline in the fluorescence mode at room temperature. The EXAFS functions $\chi(R)$ obtained by Fourier transformation of the oscillations above the Fe, Mn and Ni K-edges are shown in the Fig.2.

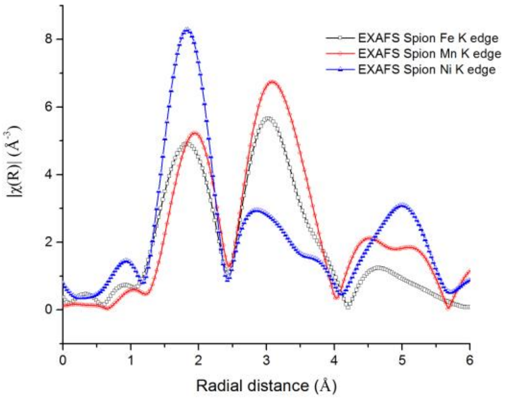

Figure 4. EXAFS functions $\chi(R)$ for the Fe, Mn and Ni K-edges.

The EXAFS functions $\chi(R)$ show a much higher intensity ratio of the 1st neighbor peak (oxygen) to the second neighbor peak (metal) for Ni. This possibly indicates location of Ni at the tetrahedral sites having cation vacancies, appearing at the octahedral sites, in the second neighbor shell. The results are compared with the simulated XAS data and discussed in terms of their relation to the local structure and magnetic properties of the materials.

Acknowledgments: Financial support from National Science Centre, Poland, Project No. 2012/07/B/ST8/ 03109 is acknowledged. Work partly supported by the Ministry of Science and Higher Education (MNiSW), Poland.

---

[1] S. Laurent, D. Forge, M. Port, A. Roch, C. Robic, et al. *Chem Rev* **108** (2008) 2064.
[2] A. Szpak, S. Fiejdasz, W. Prendota, T. Strączek, C. Kapusta, J. Szmyd, M. Nowakowska, S. Zapotoczny, *J.Nanopart. Res.* **16** (11) (2014) 1.

P-52

Oligomerization and structural characterization of native human cystatin C and its single-point mutants

Z. Pietralik[1]*, A. Szymanska[2], J. R. Kumita [3],
C. M. Dobson[3] and M. Kozak[1,4]

[1]Department of Macromolecular Physics, Faculty of Physics, Adam Mickiewicz University, Umultowska 85, 61-614 Poznań, Poland
[2]Faculty of Chemistry, University of Gdansk, Sobieskiego 18, 80-952 Gdansk, Poland
[3]Department of Chemistry, University of Cambridge, Lensfield Road, Cambridge, United Kingdom, CB2 1EW
[4]Joint Laboratory for SAXS Studies, Faculty of Physics Adam Mickiewicz University, Umultowska 85, 61–614 Poznan, Poland

Keywords: HCC, oligomerization, FTIR, CD

*e-mail: zuzannap@amu.edu.pl

The foundation of properly operating human body are the processes of protein production and degradation and also the balance between them. One of the enzymes responsible for regulating these processes in human is a small monomeric protein Cystatin C (HCC). It belongs to the type 2 cystatin family, which function is the inhibition of papain- and legumain-like proteases [1]. This protein consists of 120 amino acids forming 5 anti-parallel beta sheets surrounding a long helical fragment [2]. This protein can form aggregates throughout the domain swapping mechanism [3].

The study of the oligomerization is extremely important because during this process the protein undergoes from soluble non-toxic monomeric form to insoluble, amyloid deposits, which are associated with neurodegenerative diseases [4]. Therefore, the intermediate forms are of great interest in order to find a way to counteract the development of these diseases. However, they are highly unstable and difficult to study. In case of HCC, it was shown that insertion of a disulfide bridge prevents transition into amyloid fibrils [5] and also the disulfide-stabilized cystatin C was used to produce stable intermediary oligomers of cystatin C [6].

Hereby we present a study conducted to obtain high weight oligomers from not stabilized HCC. In order to do that, we tested various conditions, using the protocol applied for stab-HCC as a starting point. Also, we tested proteins with single-point mutations, particularly concerning the residues 68 and 57. The first, because it is the location of naturally occurring mutation in cystatin C gene, changing L68 into Q68, leading to hereditary cystatin C amyloid angiopathy (Icelandic type, HCCAA-I) and the second, as the source of instability leading the dimer formations [7]. The formation of aggregates was detected by native gel electrophoresis and fluorescent studies using Thioflavin T assay. Both, oligomers and fibers, were then visualized by atomic force microscopy and transmission electron microscopy. Additionally, we assessed the secondary structure content in the wide range of temperatures for all studied proteins using infrared spectroscopy and circular dichroism spectroscopy.

We were able to produce aggregates form all studied proteins and examine the dependence of oligomerization process on factors like protein concentration, type of movement or type of confinement. The obtained results showed that mutants at the same conditions differ significantly in the time needed to form fibrils. They also vary in the content of secondary structure forms. For example, protein with a point mutation in the residue 68 (L68V) has the highest content of beta sheets and also undergoes the processes of oligomerization almost instantly whereas wild type cystatin C requires more than 24 h to form aggregates.

Acknowledgments: This work was supported by HARMONIA3 grant (Project No. 2012/06/M/ST4/00036) from National Science Centre (Poland).

---

[1] A.O. Grubb, *Adv. Clin. Chem*. **2001** (2000) 63.
[2] A. Szymańska, A. Radulska, P. Czaplewska, A. Grubb, Z. Grzonka, S. Rodziewicz-Motowidlo, *Acta Biochim Pol.* **56** (2009) 455.
[3] R. Janowski, M. Abrahamson, A. Grubb, M. Jaskolski, *J. Mol. Biol.* **341** (2004) 151.
[4] F. Chiti, C.M. Dobson, *Annu. Rev. Biochem.* **75** (2006) 333.
[5] M. Nilsson, X. Wang, S. Rodziewicz-Motowidlo, R. Janowski, V. Lindstrom, P. Onnerfjord, G. Westermark, Z. Grzonka, M. Jaskolski, A. Grubb, *J. Biol. Chem*. **279** (2004) 24236.
[6] G. Ostner, V. Lindstrom, P. Hjort Christensen, M. Kozak, M. Abrahamson, A. Grubb, *J. Biol. Chem.* **288** (2013) 16438.
[7] M. Orlikowska, E. Jankowska, R. Kołodziejczyk, M. Jaskólski, A. Szymańska, *J. Struct. Biol.* **173** (2011) 406.

P-53

Dicationic surfactants with glycine counterions for oligonucleotides transportation

Z. Pietralik[1]*, A. Skrzypczak[2] and M. Kozak[1,3]

[1] *Department of Macromolecular Physics, Faculty of Physics, Adam Mickiewicz University, Umultowska 85, 61-614 Poznan, Poland*
[2] *Institute of Chemical Technology and Engineering, Poznan University of Technology Berdychowo 4, 60-965 Poznan, Poland*
[3] *Joint Laboratory for SAXS Studies, Faculty of Physics, Adam Mickiewicz University, Umultowska 85, 61–614 Poznan, Poland*

Keywords: SAXS, Amino acid counterion, Gene Therapy, Gemini Surfactant, Lipoplex

*e-mail: zuzannap@amu.edu.pl

Dicationic gemini surfactants (consisting of two hydrophobic tails and two cationic head groups linked by a spacer group and two counteranions) are potentially good candidates to bind, protect and deliver nucleic acids [1–3]. Hereby, the aspect of amino acid, namely glycine as counterions of gemini surfactants was explored for application in gene therapy. This study was conducted on small, double-stranded DNA and RNA oligomers and two quaternary bisimidazolium salts, having 2,5-dioxahexane and 2,8-dioxanonane spacer groups.

Surfactants toxicity level has been assessed by conducting MTT assay and their ability to bind nucleic acid has been tested by electrophoretic tests. Nucleic acid conformation and its changes upon the addition of surfactants were established by circular dichroism and Fourier transform infrared spectroscopies. The structures of formed complexes were characterised by small angle scattering of X–ray synchrotron radiation.

A series of SAXS data sets were collected at EMBL, at BioSAXS beamline P12 of the Petra III synchrotron (Hamburg, Germany) [4]. All SAXS measurements were conducted on an automated system consisting of a BioSAXS sampler robot, thermostated capillary (diameter 1 mm) and a Pilatus 2M detector. In a typical measurement, the data were collected over a period of 60 s as twenty independent images (3 seconds each), which were subsequently combined and averaged.

Both tested surfactants appear to be extremely promising components for delivery systems for small nucleic acids [5]. These surfactants are able to form stable complexes with both DNA and RNA oligonucleotides at low, not harmful concentrations, causing condensation of the nucleic acids but also ensuring the maintenance of their native conformation. Furthermore, a variety of structures is formed in the studied systems which is a feature connected to a high transfection efficiency.

The surfactant with the 2,5-dioxahexane spacer was proven to be less effective at binding DNA and RNA oligonucleotides and has a higher CMC value compared with the 2,8-dioxanonane surfactant, nevertheless it is characterized by lower toxicity. The DNA duplex maintains the B-form and the RNA oligomer maintains the A-form upon addition of the surfactants. The studied surfactants form a micellar phase in solution and micelles were present in all studied lipoplexes; however in the system whit short spacer surfactant and DNA a hexagonal phase is also formed; and the 2,8-dioxanonane surfactant-based systems have a tendency to form a cubic phase both with RNA and DNA.

Acknowledgments: This work was supported by the funds from the National Science Centre (Poland) granted on the basis of decision no. DEC-2011/01/B/ST5/00846. We would like to thank the EMBL (Hamburg, Germany) for beamtime allocation and the P12 beamline personnel for assistance.

---

[1] A. L. Barrán-Berdón, S. K. Misra, S. Datta, M. Muñoz-Úbeda, P. Kondaiah, E. Junquera, et al., *J. Mater. Chem. B.* **2** (2014) 4640.
[2] V. D. Sharma, M. A. Ilies, *Med. Res. Rev.* **34** (2014) 1.
[3] A. Bajaj, P. Kondaiah, S. Bhattacharya, *Biomacromolecules.* **9** (2008) 991.
[4] C. E. Blanchet, A. Spilotros, F. Schwemmer, M. A. Graewert, A. Kikhney, C.M. Jeffries, et al., *J. Appl. Crystallogr*. **48** (2015) 431.
[5] Z. Pietralik, A. Skrzypczak, M. Kozak, *ChemPhysChem*. (2016) doi:10.1002/cphc.201600175.

P-54

Complexes based on trigemini surfactants and natural lipids as new effective carriers for gene therapy

Ż. Kołodziejska*[1], Z. Pietralik[1], M. Weiss[2] and M. Kozak[1]

[1]*Department of Macromolecular Physics, Faculty of Physics, Adam Mickiewicz University, Umultowska 85, 61-614 Poznań, Poland*
[2]*Institute of Physics, Poznan University of Technology, Piotrowo 3, 60-965 Poznań, Poland*

Keywords: gene therapy, trigemini surfactants, lipoplex

*e-mail: zan.ka@amu.edu.pl

Gene therapy is a method which permits the repair of organism throughout the adjustment of genetic information. The underlying mechanism of gene therapy is transfection - the process of delivery of genetic material into cells. Carriers used in gene therapy should be effective, non-toxic, non-viral and as similar as possible to the cell membrane (biocompatible) [1].

One of the potential carriers for gene therapy are complexes based on surfactants and lipids [1, 2]. Natural lipids are biocompatible with body cells and non-toxic, as opposed to polycationic surfactants which are also biocompatible but often are toxic. In such complexes the presence of surfactant molecules is necessary due to their ability to bind nucleic acids [3, 4].

Our studies focus on trimeric surfactants. They are characterized by improved properties in comparison to dimeric or monomeric counterparts. This study was performed on mixed systems composed of two types of trigemini surfactant and mixtures of lipids (DMPC, DOPE, DPPC). Additionally, DNA varying in size were tested.

To obtain structural information about formed systems, small angle X-ray scattering measurements using synchrotron radiation were performed in DESY, at beam line P12 (EMBL Outstation Hamburg, Germany). The morphology of the complexes was also characterized by the use of Atomic Force Microscopy. To determine the thermodynamic parameters of the phase transitions in lipid containing systems, the infrared spectroscopy and differential scanning calorimetry were used. Additionally, to identify the conformational changes of DNA molecules upon the addition of surfactant, circular dichroism spectroscopy was used. The surfactants ability to bind nucleic acids was assessed by electrophoretic experiments.

Trigemini surfactants formed stable complexes with DNA at concentrations lower than working concentrations of gemini surfactants (they are more efficient). The addition of lipids also improved the efficiency of the complexation and thus led to the reduction of cytotoxicity.

Acknowledgments: This work was supported by the funds from the National Science Centre (Poland) UMO-2014/15/N/ST5/02003

---

[1] D. W. Emery, *Clin. Appl. Immunol. Rev.* **4** (2004) 411.
[2] D. Ibraheem, A. Elaissari, H. Fessi, *Int. J. Pharm.* **459** (2014) 70.
[3] R. Zana, *Adv. Colloid Interface Sci.* **97** (2002) 205.
[4] L. Karlsson, M. C. P. van Eijk, O. Söderman, *J. Colloid Interface Sci.* **252** (2002) 290.

P-55

Low resolution structure of the plant HSP90-SGT1 complex with ADP

M. Taube[1]*, A. Jarmołowski[2] and M. Kozak[1,3]

[1] *Adam Mickiewicz University, Faculty of Physics, Joint Laboratory for SAXS studies, Umultowska 85, 61-614 Poznan, Poland*
[2] *Adam Mickiewicz University, Faculty of Biology, Institute of Molecular Biology and Biotechnology, Department of Gene Expression, Umultowska 89, 61-614 Poznan, Poland*
[3] *Adam Mickiewicz University, Faculty of Physics, Department of Macromolecular Physics, Umultowska 85, 61-614 Poznan, Poland*

Keywords: small angle X-ray scattering, HSP90 protein, chaperones, low resolution structure

*e-mail: mtaube@amu.edu.pl

HSP90 is a protein (MW=90kDa), which belongs to the family of heat shock proteins, molecular chaperons involved in protein folding and maturation [1,2]. This protein is involved in heat shock response and against other stresses but is also engaged in maintaining protein homeostasis during normal growth of the cell. HSP90 protein binds to the partially folded client proteins and interacts with many co-chaperones that modulate HSP90 client folding cycle through inhibition/activation of HSP90 ATPase activity.

Three structural domains (N-terminal - responsible for nucleotide binding and its hydrolysis, middle domain which is mainly involved in the substrate binding and C-terminal domain - responsible for dimerisation) form the HSP90 molecule. In solution HSP90 protein exists in equilibrium between open conformation and closed conformations in the absence and in complex with various nucleotides [3]. Equilibrium is also species dependent. In bacteria HSP90 homolog exists as a mixture of open and closed states as opposed to the human homolog which exists mainly in open conformation and closed state could be observed in electron microscopy after cross-linking.

Co-chaperone of HSP90 is SGT1 protein (suppressor of G2 allele of SKP1). This protein plays important role in innate immunity in both plants and animals. It is required for proper function and stability of nucleotide binding leucine-rich repeats (NB-LRR) class of cytosolic receptors that recognizes pathogenic molecules inside the cell and triggers immune response [4,5]. SGT1 molecule is composed of three domains: TPR (N-terminal domain) - required for dimerisation, middle CS domain that interacts with HSP90 and RAR1 protein, SGS domain (C-terminal) required for association with R proteins.

The aim of our study was characterization of low resolution structure of the complex between deletion mutants of HSP90 protein or full length HSP90 protein (HSP90-FL with SGT1ΔSGS protein (SGT1 protein with deleted SGS domain) in the presence of ADP. The pure SAXS curves of the complexes were obtained from experimental SAXS data using MCR-ALS algorithm. The modelling of the low resolution structures (bead models) was performed using *ab-initio* modeling approach. HSP90 in complex with SGT1 exists in open conformation so there is no interaction between HSP90 monomers that could disrupt SGT1 binding. We also proved that N-terminal domain is sufficient for the protection of monomeric state of the SGT1ΔSGS protein. The analysis of molecular mass of the HSP90-FL: SGT1ΔSGS complex obtained from SAXS revealed 2:1 stoichiometry. Our results are unexpected because each HSP90 monomer possesses one binding site for CS domain of SGT1 and also SGT1ΔSGS exists as a dimer in solution.

Acknowledgments: This work was supported by the grant (2012/05/N/ST3/03087) from National Science Center.

---

[1] M. Taipale, D.F. Jarosz, S.Lindquist S. *Nat Rev Mol Cell Biol.* **11** (2010) 515.
[2] A. Röhl, J. Rohrberg, J. Buchner. *Trends Biochem Sci.* **38** (2013) 253.
[3] K. A. Krukenberg, T. O. Street, L. A. Lavery, D. A. Agard, *Q Rev Biophys.* **44** (2011) 229.
[4] Y. Kadota, K. Shirasu. *Biochim Biophys Acta.* **1823** (2012) 689.
[5] Y. Kadota, K. Shirasu, R. Guerois. *Trends Biochem Sci.* **35** (2010) 199.

P-56

Photoemission studies of $Mn_{1.1}Fe_{0.9}P_{0.5}As_{0.5-x}Si_x$ bulk compounds exhibiting giant magnetocaloric effect

K. Balin[1,2]*, J. Kubacki[1,2], Ł. Hawełek[3], P. Włodarczyk[3], P. Zackiewicz[3], M. Kowalczyk[4] and J. Szade[1, 2]

[1] *A.Chełkowski Institute of Physics, University of Silesia, Uniwersytecka 4, 40-007 Katowice, Poland*
[2] *Silesian Center for Education and Interdisciplinary Research, 75 Pułku Piechoty 1A, 41-500 Chorzów, Poland*
[3] *Institute of Non-Ferrous Metals, ul. Sowinskiego 5, 44-100 Gliwice, Poland*
[4] *Faculty of Materials Science and Engineering, Techincal University of Warsaw, Wołoska 141, 02-507 Warsaw, Poland*

Keywords: photoemission, magnetocaloric materials

*e-mail: katarzyna.balin@us.edu.pl

Magnetocaloric materials exhibiting large magnetocaloric effect (MCE), due to their possible application in magnetic cooling devices, have been recently widely studied. [1] Prominent advantages of magnetocaloric materials over the currently used vapor compression-expansion technique results from its high efficiency and environmental compatibility.

An interesting group of compounds exhibiting giant MCE are compounds belonging to the large MM'X family of materials (M and M'-3d/4d/5d transition metal and X - p-block element). The MM'X group of compounds shows large entropy changes in a wide temperature range near room temperature [2, 3]. Our studies are focused on compounds from the MnFe(As,P,Si) system exhibiting giant MCE.

The electronic structure of obtained with the use of Spark Plasma Sintering (SPS) technique bulk compounds $Mn_{1.1}Fe_{0.9}P_{0.5}As_{0.5}$, $Mn_{1.1}Fe_{0.9}P_{0.5}As_{0.4}Si_{0.1}$ and $Mn_{1.1}Fe_{0.9}P_{0.5}As_{0.45}Si_{0.05}$ was studied with the use of X-ray photoelectron spectroscopy. Obtained results have been confronted with the magnetic and structural properties of the compounds.

The X-ray diffraction studies showed single phase structure of the Fe_2P type.

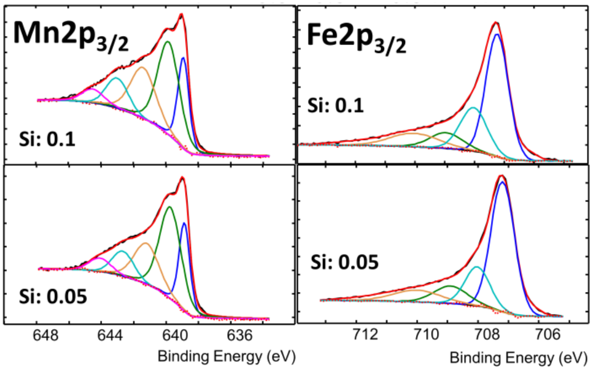

Figure 1. Mn2p and Fe2p high resolution photoemission spectra.

The atomic concentrations of both samples indicate that the iron content in the samples is undervalued in relation to nominal composition. High resolution photoelectron spectra of Fe2p, O1s, Mn2p, Si2p, As3d, P2p and valence band have been collected from fractured in UVH sample surfaces. The analysis was focused on determination of chemical states of sample components; it indicates that iron and manganese are in metallic state, however in case of manganese some traces of oxides have been observed (see Fig. 1).

Further structural characterization was realized with the use of Time of Flight Secondary Ion Mass Spectrometry (TOF-SIMS, ION OTF TOF.SIMS5 spectrometer). In this part of our studies we focused on microstructure of the compounds investigating the distribution of the [Mn, Fe, P, Si, As]$^{+,-}$ ions. Analysis of the microstructure (TOF-SIMS) revealed inhomogeneity within the distribution of Mn, Fe, Si, P ions (see. Fig 2). On both samples Si exhibit tendency to segregation in the form of ~1-2micron precipitates.

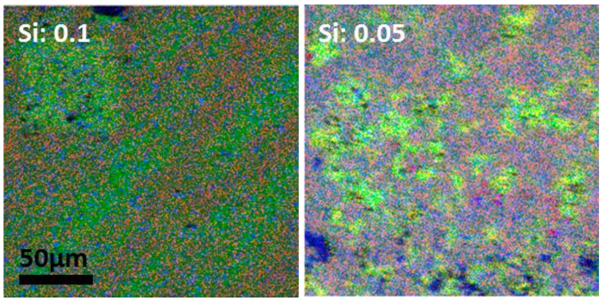

Figure 2. Overlay of distribution maps Fe2+ (red), Mn+ (green), Si+ (blue). Particular distribution maps were normalized.

The highest MCE exhibit undoped $Mn_{1.1}Fe_{0.9}P_{0.5}As_{0.5}$ sample, it shows adiabatic temperature change of about 4 K at field of 1.7 T. Hower Si-doped samples prepared by the SPS method also exhibit high MCE for the Si=0.1 adiabatic temperature change of about 3.8K and for the Si=0.05 of about 3K. Partial oxiadation of manganese and nonuniformity in the distribution of particular elements affects MCE properties of Si doped samples; however the MCE effect still remains giant.

Acknowledgments: This work was supported by European Fund for Regional Development: POIG.01.03.01-00-058/08.

---

[1] B. G. Shen, J. R. Sun, F. X. Hu, H. W. Zhang, Z. H. Cheng, *Adv. Mater.* **21** (45) (2009) 4545.
[2] R. Zach, M. Guillot, R. Fruchart, *J. Magn. Magn. Mater.* **89** (1990) 221.
[3] M. Bacmann, J. L. Soubeyroux, R. Barett, D. Fruchart, R. Zach, S. Niziol, R. Fruchart, *Magn. Magn. Mater.* **134** (1994) 59.

P-57

XMCD studies of Pt/Co/Pt nanostructures modified by Ga$^+$ ion irradiations

P. Mazalski[1,2], I. Sveklo[1], Z. Kurant[1], K. Olefs[3], A. Rogalev[3], F. Wilhelm[3], J. Fassbender[4], A. Wawro[5] and A. Maziewski[1]

[1] *Faculty of Physics, University of Białystok, Ciolkowskiego 1 L, 15-245 Białystok, Poland*
[2] *Jerzy Haber Institute of Catalysis and Surface Chemistry, Polish Academy of Sciences, Niezapominajek 8, 30-239 Kraków, Poland*
[3] *European Synchrotron Radiation Facility, B.P.220, F-38043 Grenoble Cedex, France*
[4] *Helmholtz Zentrum Dresden-Rossendorf, PO Box 510119, Dresden 01314, Germany*
[5] *Institute of Physics, Polish Academy of Sciences, Al. Lotnikow 32/46, Warszawa 02-668, Poland*

Keywords: synchrotron radiation, magnetic anisotropy, ion irradiation

*e-mail: piotrmaz@uwb.edu.pl

Magnetic anisotropy of ultrathin films are usually tuned by varying the film thickness, chemical composition or structure. Increasing Co film thickness d above d_{RPT}(~2nm) transition from out-of-plane into in-plane magnetization state is observed. It was discovered [1,2] that He ions irradiation also induces transition to in-plane state for $d>d_{RPT}$. However it was recently reported [3,4] a new effect - Ga$^+$ ion irradiation drives multiple both vanishing and creation of perpendicular magnetic anisotropy (PMA). Two branches of PMA were reported on the 2D maps (d, F) Co thickness and Ga ions fluence F. Possibilities of ion driven modification of magnetic nanostructures are important for patterning [5] especially by focus ion beam technique, where Ga ions are used.

The Co films with different buffer (Au or Pt) and overlayer (Au or Pt) were deposited by molecular beam epitaxy technique and magnetooptically studied for different d and F. Magnetooptical studies show strong influence of the Au and Pt on magnetic anisotropy changes ploted as a (d, F) maps. For the following sapphire/Pt(20nm)/Co(d=3nm)/(Pt or Au (5nm)) trilayers were selected for XAS/XMCD measurements: non-irradiated and two uniformly irradiated with fluences F_1 and F_2 corresponding to the first and second PMA branches, respectively. Synchrotron studies were performed in ID12 ESRF beamline using XAS and XMCD techniques on Co K-edge and Pt $L_{2,3}$ edges. XAS studies for both irradiated samples showed: (i) changes of the spectra shapes and (ii) big changes of the spectra amplitude for the fluence F_2 connected with etching process. Changes of shape spectra are probably related to the mixing of the layers at the interfaces which forces a modification of the 3d and 4p shells of the Co atoms. The electronic structure of transition metals is very sensitive to changes of their local environment. Higher number of Pt atoms in the nearest vicinity of Co atoms modifies their d and p shells due to hybridization with the d-states of Pt atoms. Above mentioned process create very good conditions for the Co-Pt alloy formation in irradiated samples – shape of obtained spectra on Co and Pt absorption edges are similar to those for Co-Pt alloy [6].

XMCD spectra for both Pt and Au cap layer in non-irradiated samples obtained at the Co K-edge are similar to the XMCD spectra obtained for a pure hcp Co layer. For the samples irradiated with fluences F_1 and F_2 it is possible to distinguish two additional peaks located energetically in the same position like for $Co_{0.5}Pt_{0.5}$ alloy with well developed $L1_0$ structure. This results is an indication that the Co–Pt alloy is formed and probably responsible for the enhanced magnetic anisotropy in branches 1 and 2. However in samples with Au cap layer effect is weaker because of presence only one Co/Pt interface - mixing of Co and Au does not have influence on magnetic changes.

XMCD Pt $L_{2,3}$-edge studies revealed increase of the spectra amplitude for samples irradiated with fluences F_1 and F_2 in relation to the non-irradiated sample. This fact reflects the appearance of magnetic moments at the Pt atoms which are induced by the magnetic moments of adjacent Co atoms because of Co-Pt alloy formation. However amplitude of the spectra for sample with Au cap layer is smaller than for Pt cap layer because of smaller number of Pt atoms close to Co in the Au/Co/Pt - only at the one interface Co–Pt alloying take place. Such behaviour is also visible in magnetic moments of Pt atoms obtained from the sum rules calculations. The moments at the Pt atoms in Pt/Co/Au are slightly smaller than in Pt/Co/Pt. This might be related with different number of Pt atoms in the Co surrounding. However for both irradiated systems the magnetic moment is larger than in the non-irradiated sample.

Acknowledgments: This work was supported by FUGA project financed by the Polish National Science Centre, DEC-2015/16/S/ST3/00450

---

[1] C. Chappert et al., *Science* **280** (1998) 1919.
[2] T. Devolder and H. Bernas, *Material Science with Ion Beams,edited by H. Bernas, Topics in Applied Physics*, 116 (Springer-Verlag, Berlin, 2010).
[3] A. Maziewski et al. *Phys. Rev. B* **85** (2012) 054427.
[4] P. Mazalski et al., *J. Appl. Phys.* **113** (2013) 17C109.
[5] J. Ferré and J.-P. Jamet, *Handbook on Magnetism and Advanced Magnetic Materials* (H. Kronmüller & S.-J. Parkin, Wiley,Chichester, UK, 2007), Vol. 315.
[6] Y.S. Lee, J.Y. Rhee, C.N. Whang, Y.P. Lee, *Phys. Rev. B* **68** (2003) 235111.

P-58

Crystal lattice deformation in (001)-oriented CdTe/SnTe/CdTe trilayers MBE-grown on 2° offcut GaAs

A. Sulich[1]*, J.Z. Domagala[1], E. Łusakowska[1]
and P. Dziawa

Institute of Physics PAS, Al. Lotników 32/46, PL-02-668 Warsaw, Poland

Keywords: high resolution X-ray diffraction, SnTe, CdTe, crystal lattice deformation

*e-mail: sulich@ifpan.edu.pl

SnTe is known as a topological crystalline insulator [1, 2]. Topological crystalline insulators constitute a new class of materials with many interesting properties, important especially for electronics and spintronics [3], thus they are currently investigated [4-6].

The aim of our research was to perform a crystallographic study on the lattice deformation in (001)-oriented CdTe/SnTe/CdTe trilayers. Samples were MBE grown on GaAs substrate. Each of them had a 4 µm CdTe buffer layer, ca. 1 µm SnTe layer and a 50 nm CdTe cap. The substrate was (001) oriented with 2° offcut toward [100] direction allowing for growth of good quality CdTe film comparable with literature data [7].

As an experimental technique the high-resolution X-ray diffraction (Philips X'Pert MRD diffractometer with CuK$_{\alpha1}$ radiation) was used. To evaluate lattice parameters and structural quality of samples, we measured rocking curves, $2\theta/\omega$ scans and reciprocal space maps for both, symmetrical and asymmetrical Bragg reflections. Atomic force microscopy (AFM) was used as a complementary technique applied for sample surface assessment.

The main part of work consisted in checking, how the conditions of MBE growth determine the lattice parameters of CdTe and SnTe layers. We investigated the samples which had been grown mainly at 310°C and at a variable Te/SnTe molecular streams ratio.

The experimental results indicate that for all studied samples the CdTe cubic crystal structure undergoes a tetragonal distortion. According to the data from literature, it is attributed to the lattice mismatch and the difference of the thermal expansion coefficients between CdTe and GaAs [8]. Next, the strains are relaxed by formation of misfit dislocations at the interface [9] and another mechanism, which cause significant (001) plane inclination together with twist of adequate in-plane directions. It is observed that the SnTe layer lattice also is tetragonally distorted and next relaxed.

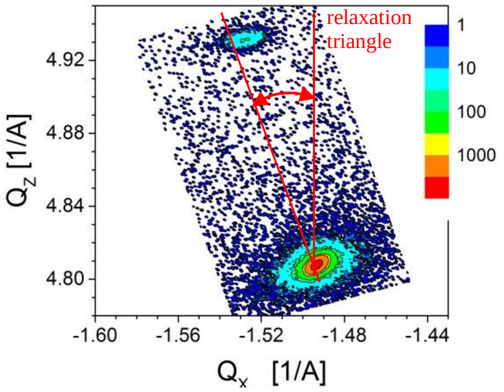

Figure 1. Reciprocal space map of CdTe (lower node) and SnTe (upper node) lattices for -1-15 Bragg reflection. The shift of nodes towards the horizontal Q$_x$ axis shows almost full relaxation of SnTe layer.

Acknowledgments: This work has been supported by the research project No 2014/13/B/ST3/04489 financed through the National Science Centre (Poland).

---

[1] L. Fu, *PRL* **106** (2011) 106802.
[2] T.H. Hsieh et al., *Nature Communications* 3 (2012) 1.
[3] J.E. Moore, *Nature* **464** (2010) 194.
[4] P. Dziawa et al. *Nature Mat.* **11** (2012) 1023.
[5] K. Sun, *Nature Mat.* **14** (2015) 262.
[6] Y. Ando, L. Fu, *ANNU REV CONDEN MA P* **6** (2015) 361.
[7] H. Nishino et al., *Jpn. J. Appl. Phys.* **38** (1999) 5775.
[8] H. Tatsuoka et al., *J. Appl. Phys.***65** (1989) 2073.
[9] K. Wichrowska et al., *Acta Phys Pol A*, **126** (2014) 1083.

Synchrotron SOLARIS – getting ready for the first users

Agata Chrześcijanek[1], Adriana Wawrzyniak[1]

[1]*Solaris National Synchrotron Radiation Centre, Jagiellonian University, Czerwone Maki 98, 30-392 Kraków, Poland*

Last September the Opening Ceremony of National Synchrotron Radiation Centre SOLARIS took place.

SOLARIS has been constructed as the result of the *National Electromagnetic Radiation Centre for Research Purposes (Stage I)* project which was granted by the Polish Ministry of Science and Higher Education in April 2010. It was financed from the European Union Regional Development Fund within the Innovative Economy Operational Program. The project was completed in December 2015.

In few months the facility will be opened to the first users. This signals new chapter for Polish researchers.

During the final year of the completion of the project the installation and integration of the storage ring was achieved (April 2015) and SOLARIS team commenced the machine startup and commissioning (May 2015). This resulted in the systematically increased amount of the stored ring current. Eventually first photons were detected at the beamlines input detectors. Following this success, in summer 2015 the 5th straight section vacuum chamber was replaced and an APPLE II type undulator was installed. By the autumn, after tedious optimizations and commissioning procedures, nominal optics parameters were achieved in the storage ring. 100mA stored current was reached at the target 1.5 GeV energy with the lifetime of few hours. After that, at the beginning of 2016, the next action was undertaken and Landau cavities were installed in order to improve the electron bunches quality leading to the extension of the lifetime and intensification of the stored current. The accelerator systems of SOLARIS reached their assumed configuration in February 2016. However the further development is foreseen in the future – mostly for linac – to avoid ramping and providing the top-up operation.

Since February, the final commissioning process has begun. The stored current is systematically being increased and the vacuum systems outgassed. After 30Ah of accumulated beam dose, 511 mA of stored current was reached at 525 MeV energy and 200 mA at 1.5 GeV (see Picture 1).

SOLARIS control systems, including software have been also continuously tested, debugged and if necessary modified and improved.

Concurrently to the efforts to improve the machine performance and reach the stable final mode of operation, there has been very steep progress towards the commissioning of the two experimental beamlines.

The Project budget has allowed for construction of two beamlines. The first one operates from the bending magnet providing photons in 200 eV- 2000 eV energy range and is equipped with two experimental stations: Photo Emission Electron Microscope (PEEM) and X-ray Absorption Spectroscopy (XAS) chamber. Since July 2016 the components of the beamline front-end have been commissioned and tested. The beamline subsystems are being tested and integrated. First test experiments with synchrotron radiation in the end-stations are foreseen at the beginning of 2017.

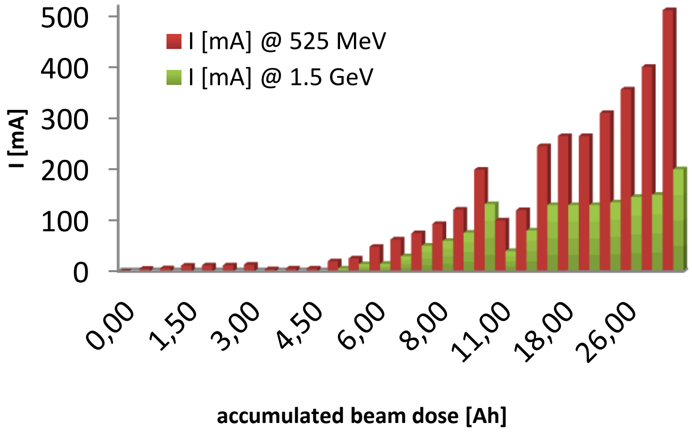

Picture 1. Maximum value of stored electro current versus the accumulated beam dose.

The second beamline operates from an APPLE II type undulator in the photon energy range 8 -100 eV and allows for Ultra high resolution Angular Resolved Photo Electron Spectroscopy (UARPES) measurements. All subsystems of this beamlines have been integrated and UHV environment has been achieved. At the end of April the first light was fed to the beamline and after some alignment corrections and undulator adjustment the first photons reached the experimental chamber (see Pictures 2 and 3). The UARPES commissioning process has already begun and the first test measurements are planned at the end of 2016.

At the end of February 2016, due to the mutual initiative of Swedish and Polish research groups almost complete set of components of yet another beamline arrived to SOLARIS. Until then the beamline (I1011) was part of MAX-lab SR facility in Lund, installed at the closed in December 2015 MAX II 1.5 GeV ring. The beamline was decommissioned and transported to Kraków by the Polish group of technicians and researchers from different institutions led by SOLARIS team. After necessary adaptations, modifications and re-equipping enabling its installation at SOLARIS, it will provide research options in the soft X-ray energy range exploring X-ray Magnetic Circular Dichroism and X-ray Magnetic Linear Dichroism phenomena.

In parallel to the above described activities there has been ongoing undertakings targeted at assuring the future position of SOLARIS as the key national and international research facility. Eventually, in March 2016, by the governmental decision, Poland joined CERIC-ERIC consortium delegating SOLARIS as the Partner Facility. The mission of CERIC-ERIC consortium is to share between its Central European members an integrated multidisciplinary and multiprobe Research Infrastructure open for external basic and applied users in the fields of Materials, Biomaterials and Nanotechnology. Each of the 7 participating countries provide for the others free access to its outstanding research infrastructure (Representing Facility). Joining CERIC-ERIC is very important for SOLARIS. Apart of the other aspects, it enables new options regarding the financial support on the national and international level, e.g. joined (with other CERIC-ERIC members) applications for funds for new beamlines granted directly by European Union.

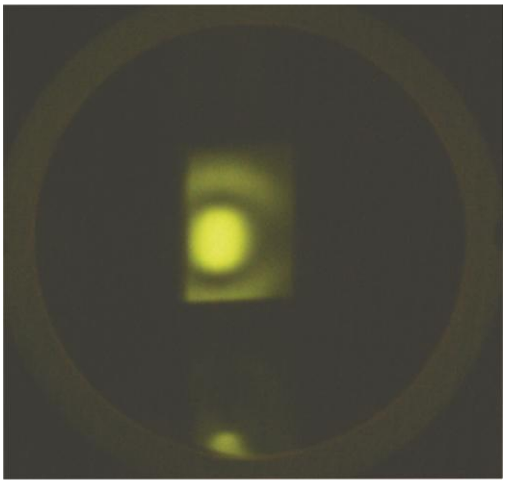

Picture 2. First harmonics radiation (140 eV) from the UARPES beamline undulator registered on the YAG screen placed 16m from the source. There is a clear diffraction pattern: central spot of 5mm diameter surrounded by the first order ring. *(Photo by J. Kołodziej)*

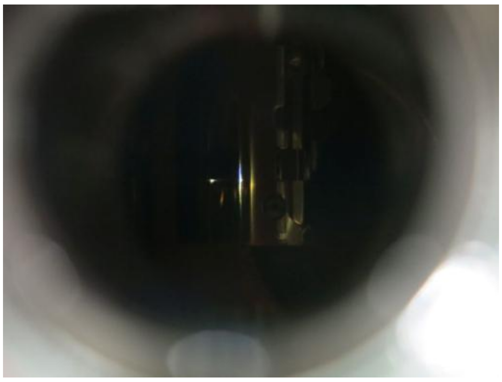

Picture 3. White synchrotron radiation (monochromator at zero order) registered at the UARPES experimental chamber manipulator *(Photo by M. Stankiewicz)*

A-02 **News from the European Synchrotron Radiation Facility**

State-of-the-art: status of the European Synchrotron

G.D. Admans[1]* and A.J. Joly[1]

[1]*European Synchrotron Radiation Facility, CS40220, 38043 Grenoble Cedex 9, France*

Keywords: synchrotron radiation, X-ray source, upgrade, high-energy, structural biology

*e-mail: admans@esrf.fr

The European Synchrotron (ESRF) is a user facility producing intense X-ray beams in the hard X-ray range. The ESRF is funded by 21 countries, most European, with the latest affiliates being South Africa in 2013 and the Russian Federation in 2014. Over a period of 21 years, the ESRF has established itself as the world's most intense source of synchrotron-generated light and has been at the forefront of scientific research, providing unrivalled opportunities for an international community of scientists in the exploration of materials and living matter in a very wide variety of fields: material physics, chemistry, archaeology and cultural heritage, structural biology and medical applications, environmental sciences, information science and nanotechnologies. Each year, the 43 highly-specialised beamlines accommodate around 6500 academic and industrial researchers who either travel to Grenoble to carry out their research or send in their samples for remote access experiments or data collection services. In 2015, a total of 1,653 public experiment sessions took place, resulting in 6,409 user visits, and 14,160 shifts of 8 hours were delivered.

For academic research, access to the beamlines is gained through a peer reviewed proposal system with two proposal rounds per year, in March and September. In 2015, 1937 proposals were received of which 46.5% were accepted. The publication of results from academic research is necessary. For proprietary research, applications are assisted by a dedicated office and beam time or data collection services are charged for. In this case, the research is confidential and there is no obligation to publish.

The facility has just completed its 168 m€ Phase I Upgrade Programme (2009-2015), with the creation of 19 new experimental stations, a new 8,000 sq m experimental hall and the upgrade and renewal of the majority of equipment. Compared to pre-Upgrade Programme operation, in 2015, there have been increased numbers for experiments and user visits although less beamtime was delivered as two beamlines remained closed and two beamlines are still being upgraded. Of these beamlines, the new materials chemistry and materials engineering beamline, ID15A, is being eagerly awaited by it future users as it received 87 proposals, the highest number of all the beamlines, in the March 2016 round.

While Phase I focussed on the beamlines, the next evolution of the facility will focus on the X-ray source. New concepts for accelerators have emerged in recent years [1], leading to the possibility of building a new generation of storage rings with an increase in brilliance of two orders of magnitude. Key areas of research would benefit from such a project, including coherent diffraction imaging and microscopy in the mesoscopic scale, spectroscopy with nanometre spatial resolution, and time-resolved studies in the millisecond to sub-nanosecond scale. The ESRF has been one of the leaders in the development of these new concepts and, in 2015, launched the second development phase of the Upgrade Programme: the ESRF Extremely Brilliant Source Programme, or ESRF-EBS. This new programme is centred on the construction of a new storage ring that will adopt an all-new hybrid multi-bend achromat lattice design with an equilibrium emittance of about 135 pm·rad [2], which, after taking into account radiation damping by the insertion devices, should deliver a final horizontal emittance of about 100 pm rad – at least a factor of 10 better than any other synchrotron source of similar energy constructed or presently under construction and a factor 40 better than the present ESRF double-bend achromat lattice.

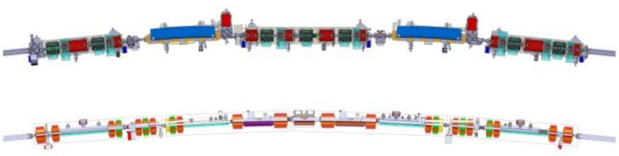

Picture 1. Layout of the existing (above) and the new hybrid multi-bend achromat lattice (below). The new lattice is expected to deliver X-ray beams to the ESRF beamlines with approximately 100 times increase in brilliance and coherence.

Advances in accelerator control technology and better magnet materials have made such a design feasible. An associated benefit through the use of permanent magnets in place of many electromagnets will be a reduction in the electricity consumption of the new storage ring.

The ESRF-EBS project is now well underway and already 90% of the design work for the components has been completed and prototypes for key components have already been tested.

An exceptional shutdown period in 2019 is planned for the construction of the new storage ring. To exploit this major enhancement of the X-ray source, the project is accompanied by an ambitious scientific instrumentation programme, construction of new beamlines and enhanced computing facilities.

The ESRF-EBS represents an investment of 150 M€ over the period 2015-2022. It has been recognised as one of the "landmarks" by the European Strategy Forum on Research Infrastructures (ESFRI), highlighting its scientific excellence, pan-European relevance, socio-economic impact and innovation.

Major steps have already been made in preparation for the new storage ring. Very recently, top-up operation has been tested over a period of four weeks. Top-up provides users with better beam stability, low vertical emittance in all filling modes (with correspondingly higher brilliance and resolution) and a nearly constant beam current.

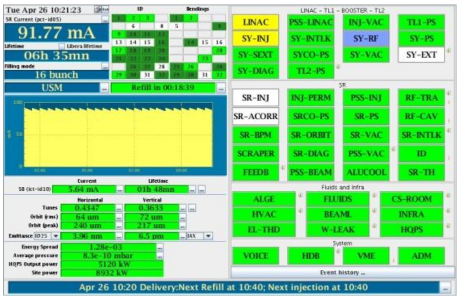
Tue Apr 26 10:21:23
SR Current (pct-id05) 91.77 mA
Lifetime 06h 35mn
Filling mode 16 bunch
USM
Refill in 00:18:39
SB (ict-id10) Current 5.64 mA Lifetime 01h 48mn
Tunes: Horizontal 0.4347, Vertical 0.3633
Orbit (rms): Horizontal 64 um, Vertical 72 um
Orbit (peak): Horizontal 240 um, Vertical 217 um
Emittance ID25: Horizontal 3.96 nm, Vertical 6.5 pm
Energy Spread 1.28e-03
Average pressure 8.3e-10 mbar
HQPS Output power 5120 kW
Site power 8932 kW
Apr 26 10:20 Delivery:Next Refill at 10:40; Next injection at 10:40

Figure 2. Top-up operation in 16-bunch mode. This snapshot of the control room synopsis screen shows the 20-minute injection periods and a low vertical emittance of 6.5 pm rad.

As a hard X-ray source, the majority of the ESRF's beamlines are currently optimised for X-rays between 5 and 30 keV. An extended range is provided by one soft X-ray beamline reaching down to 0.3 keV and eight high-energy beamlines with upper limits between 60 and 750 keV. One of these high-energy beamlines is ID31, a beamline for interfaces and materials processing, that opened to users in November 2015. Users appreciate the high photon flux (a gain by a factor of 10 over beamline ID15A that it replaces) in the high-energy range and the new detector, a Pilatus 2M, with frame-rates up to 250 Hz. The beamline is currently focusable to the micrometre level and its exceptional flux makes following processes inside reaction vessels or energy storage devices feasible.

Figure 3. ID31 experimental hutch during construction of the beamline. Credit ESRF/P. Jayet.

Users at this beamline recently set a record for the highest quantity of data collected in one experiment: 100 Tb in just over 1 week, despite using the detector at only 60 Hz. The ESRF-EBS project will futher enhance this a beamline by a futher increase in brilliance and a reduction in size of the beam which will provide far greater precision when probing buried interfaces.

The legendary structural biology cluster of four beamlines, ID14, has been replaced by MASSIF (Massively Automated Sample Selection Integrated Facility) comprising 3 end stations and ID30B [3]. MASSIF-1, beamline ID30A-1, was the first of the new beamlines to enter user operation, starting in July 2014. This beamline is the world's first fully-automated facility. It comprises robotic sample handling and positioning and an expert system to control data collection. The performance of this beamline has recently been reviewed [4]: 9872 crystals were analysed automatically during 2015. These crystals typically came from projects involving a large amount of screening to find the one crystal out of many that diffracts sufficiently or where large numbers of repetitive data collections are required, such as fragment screening campaigns. The benefits of a fully automated beamline are:

- Optimal use of beamtime by collecting data both day and night.
- Eliminates human error: automatic centring of crystals using X-rays is more accurate than a human operator relying on visible light.
- Optimised data collection strategies taking into account the crystal size and diffraction quality produce higher-quality data than equivalent human operated beamlines through a reduction in radiation damage.

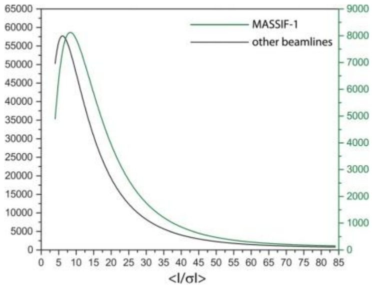

Figure 4. Data quality comparison for data sets automatically processed on MASSIF-1 and the ESRF human-operated beamlines in 2015: Plot of signal to noise ratios <I/σ(I)> vs number of crystals. Credit [4].

The software workflows developed for MASSIF-1 have been deployed to the other ESRF structural biology beamlines and can be run by users. Currently, the X-ray centring routine is the most frequently used.

Beamline ID30B is a variable-focus, tuneable-energy beamline. It features FlexHCD, a new generation of high-throughput sample changer robot developed at the EMBL (European Molecular Biology Laboratory). FlexHCD accepts samples in either EMBL/ESRF pucks or Unipucks and it can even manipulate crystallisation trays for *in situ* screening and data collection. FlexHCD will become the standard sample changer, soon to be installed at other ESRF structural biology beamlines.

Serial millisecond crystallography (SMX) has recently been tested at the microfocus beamline, ID13 [5]. Using lipid cubic phases as the delivery medium, this experiment aimed to reproduce an experiment typically carried out at XFEL (X-ray free-electron laser) sources but with millisecond timing, and so bridging the gap between the traditional protein crystallography experiments at synchrotron sources and the serial femtosecond crystallography experiments of XFELs. At room temperature, a stream of many thousands of bacteriorhodopsin microcrystals (less than a mg) were delivered using a microfluidics system such that exposure time to each crystal was between 10 and 50 µs. Merging the data from 5700 frames for structure solution culminated in a 2.4 Å resolution structure that was comparable to one obtained through a conventional cryocooled crystallography experiment on a single crystal. Some minor radiation damage was evident, which could be avoided in future.

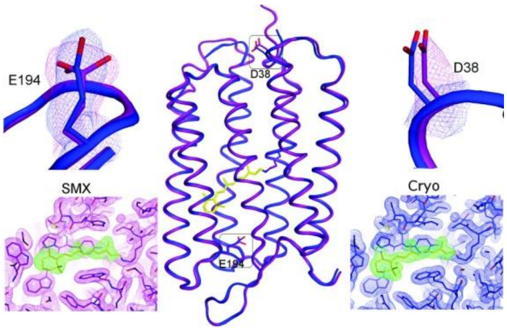

Figure 5. Comparison of bacteriorhodopsin structures solved by serial millisecond crystallography (SMX) and conventional cryocrystallography (Cryo). Credit [5].

MeshAndCollect [6] is another approach to synchrotron serial crystallography. It involves automatic identification of many cryocooled crystals mounted on the same sample holder. The crystals are ranked, partial datasets collected, and hierarchical cluster analysis is used to provide the best combination. This method holds promise for difficult to crystallise proteins such as membrane proteins grown in lipidic mesophase and is available for users.

The ESRF-EBS will provide a smaller and more intense X-ray beam which will enhance SMX, permitting faster timescales and creating opportunities for room-temperature kinetics studies, e.g. via laser excitation.

At the microtomography beamline, ID19, experiments have explored time-resolved diffraction imaging exploiting the temporal structure of the X-ray beam [7]. In single-bunch beam mode with 10 mA in the single bunch, a 140 ps X-ray flash is produced at a frequency of 355 kHz, corresponding to 2.81 µs, which is long enough to allow separation of individual flashes by a commercial CMOS-based camera. Making use of the coherence properties of the beamline, crack propagation was tracked in a piece of glass breaking from the impact of an accelerated bolt. In a more recent experiment, direct transmission and diffraction X-ray imaging were combined to follow crack propagation and strain in real time [8]. The resulting movie of crack propagation in a silicon wafer with a 1.28 µs frame rate revealed that the crack propagates in fits and starts.

For X-ray diffraction topography, the gain in photon flux density envisaged for the ESRF-EBS would allow significant improvement in the spatio-temporal resolution and should make accessible more details of the dynamics around the propagating crack tip.

Focussing again on time resolution but this time for soft matter, users of the new Time-resolved USAXS/SAXS/WAXS Beamline, ID02, have discovered how sleeping muscles economise energy, resulting in a novel dual-filament concept for the regulation of contraction in skeletal muscle [9].

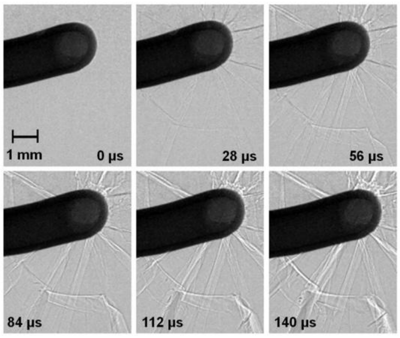

Figure 6. Time series recording crack propagation in a glass plate initiated by an accelerated bolt. Credit [7].

X-ray diffraction patterns were recorded from single muscle cells on a millisecond timescale while they were stimulated electrically. It was discovered that the majority of myosin proteins, which effectuate muscle contraction, remained in the resting state until a high stress causes a conformational change that activates them. The very high brilliance and X-ray collimation of this new beamline made these challenging experiments possible.

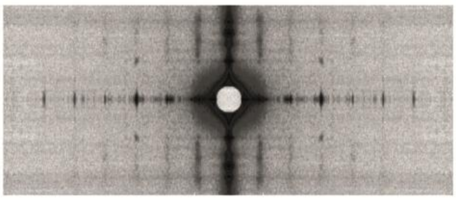

Figure 7. X-ray diffraction pattern from a resting muscle fibre. Credit: E. Brunello, [9].

Looking back over the last 21 years, since the start of user operation in 1994, the ESRF's users and staff have published a record 26,958 refereed publications in top scientific journals and four Nobel prizes have been awarded to laureates using the ESRF for their work. In 2010, for the first time ever, more than 1000 protein structures were deposited in a single year in the worldwide Protein Data Bank (PDB) from data collection at the ESRF [10], the total to date reaching 11,918 structures and accounting for over 40% of the European facility deposits [11].

The outlook for the next 20 years is that the users should be even more productive following the ESRF - EBS. The higher brilliance of the X-ray beams, faster detectors, increased automation and suitably-dimensioned data infrastructure will all contribute to making experiments faster. While the smaller X-ray source will permit a transition from the micrometre scale towards the nanometre scale for beamlines that privileges a small beam size. Furthermore, a significant increase in the coherence of the source holds promise for new experiments that have yet to be imagined.

---

[1] D. Einfeld *et al.*, in *Proceedings EPAC 1996*, Sitges 1996.
[2] J.C. Biasci *et al.*, *Synchrotron Radiation News*, **27** (2014) 8-12.
[3] C. Mueller-Dieckmann *et al.*, *Eur. Phys. J. Plus* **130** (2015) 70.
[4] M.W. Bowler *et al.*, *Crystallography Reviews* (2016), DOI: 10.1080/0889311X.2016.1155050.
[5] P. Nogly *et al.*, *IUCrJ* **2**, 168-176 (2015).
[6] U. Zander *et al.*, *Acta Cryst.* **D71** (2015) 2328–2343.
[7] A. Rack *et al.*, *Journal of Synchrotron Radiation* **21** (2014) 815-818.
[8] A. Rack *et al.*, *IUCrJ* (2016) 108-114.
[9] M. Linari *et al.*, *Nature* **528** (2015) 276-279.
[10] PDB: http://www.pdb.org/
[11] Data from BioSync: http://biosync.sbkb.org/

Membership of Poland in ESRF

K. Jablonska [1]

[1]*Institute of Physics, Polish Academy of Sciences, Warsaw, Poland*

*e-mail: jablo@ifpan.edu.pl

Starting from year 2004, Poland is an Associated Member of the European Synchrotron Radiation Facility (ESRF) in Grenoble, France. In the period from 2004-2006 with the contribution at the level of 0.6% of ESRF budget and in the period 2006-2011 at the level of 1%. Starting from October 2011 there was no a legal path to apply for paying the Polish contribution. Nevertheless, Polish government has declared that is working on solving this problem and the necessary changes in the low will be made but any agreement between Poland and ESRF was signed. In the absence of a valid agreement, securing the necessary funding was no longer possible. However, activities for the establishment of a new legal and financial mechanism enabling the renewal of the long-term arrangement have been actively ongoing since October 2011. Moreover, the Polish scientific community has continued to successfully use the ESRF at the same level as before and Polish post-docs and PhD students have continued to be welcomed in the ESRF staff complement, despite the fact that no formal arrangement has been in force between the Parties since October 2011 and that IF PAN (as representative of Poland) has not made any financial contribution to the ESRF during this period.

Figure 1. View of the ESRF synchrotron from above. *(Image courtesy ESRF)*

On 25 May 2015, an amended act on the financing of research in Poland entered into force and was published in the official bulletin of the Polish Government under the reference Dz. U z 2015 r. poz. 249. The appropriate regulation was published on 7 December 2015. These acts include the legal instruments enabling the Polish Ministry of Science and Higher Education to finance the participation of Polish institutions in international research infrastructures. The situation is now such that IF PAN has access to a formal procedure to renew its Scientific Association with the ESRF for a 5-year period and, additionally, make the financial contribution necessary to cover the period 01 October 2011 to 31 March 2016, in which the continued use of the ESRF by Poland took place. Therefore, the application for the funds to pay outstanding contribution and contribution up to 2020 was submitted to the Ministry of Science and High Education by IF PAN. This application was sent by IF PAN as the leader of the Consortium of Institutions Interested in the Use of ESRF. This Consortium was established on 16 March 2006 with 7 members. Next year two institutions were joined the Consortium and in this year 11 institutions have declared access to the Consortium. At the time of application Consortium was made up by 20 following institutions:

1. Instytut Fizyki PAN w Warszawie
2. Instytut Neurologii, Collegium Medium Uniwersytetu Jagiellońskiego w Krakowie
3. Wydział Fizyki i Informatyki Stosowanej Akademii Górniczo-Hutniczej w Krakowie
4. Wydział Fizyki Technicznej i Matematyki Stosowanej, Politechniki Gdańskiej
5. Instytut Chemii Fizycznej PAN w Warszawie
6. Instytut Fizyki Uniwersytet Śląski w Katowicach
7. Instytut Fizyki Doświadczalnej Uniwersytetu Warszawskiego
8. Wydział Chemii Uniwersytetu Warszawskiego
9. Instytut Paleobiologii PAN w Warszawie
10. Wydział Chemii Uniwersytet Adama Mickiewicza
11. Instytut Chemii i Techniki Jądrowej
12. Instytut Materiałów Inżynierskich i Biomedycznych, Politechnika Śląska
13. Instytut Wysokich Ciśnień PAN, Unipress
14. Wydział Fizyki, Uniwersytet w Białymstoku
15. Wydział Chemii, Politechniki Warszawskiej
16. Wydział Fizyki, Uniwersytet Adama Mickiewicza
17. Wydział Fizyki, Politechniki Warszawskiej
18. Instytut Fizyki Jądrowej Polskiej Akademii Nauk
19. Instytut Metalurgii i Inżynierii Materiałowej im Aleksandra Krupkowskiego Polskiej Akademii Nauk
20. Instytut Optoelektroniki, Wojskowa Akademia Techniczna w Warszawie

Nevertheless, each scientist affiliated in Polish scientific institution can apply for beamtime, regardless of being the member of Consortium.

More than 40 papers have been published per year by the scientists from Polish institutions performing experiments at the ESRF in the period when Poland was not paid the contribution (see Figure 2). It is only slightly lower than it has been when Poland paid contribution (50).

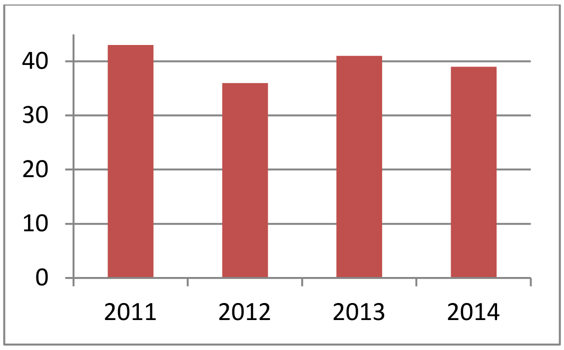

Figure 2. Polish papers with use of ESRF.

We do hope that application will be successful and soon Polish representatives will attend the meetings of the Council and the Financial and Administrative Committee at ESRF as it was before. Therefore, we strongly encourage all Polish scientists to submit the scientific proposals to ESRF. The next deadline is 10 September 2016. Moreover, have a look on the ESRF webpage, http://www.esrf.eu and check the possibility to apply for PhD and postdocs or technical positions. As soon as the IF PAN application will be approved the information about such possibilities you will find also at the updated page of the related project http://info.ifpan.edu.pl/esrf/Local_Publish/ .

In addition, everyone should be aware that paying the Polish contribution is a kind of scientific project. Therefore, the Ministry will be asked for various details concerning the use of ESRF. The IF PAN will be obligated to provide the list of institutions applying for and getting the beamtime and the corresponding numbers of applied and allocated shifts. Please be aware, that if you name is appearing in the approved international project and even you are not taking part in the performed experiment still the appropriate part of beamtime is counted for Poland (the number of shifts is divided by the number of countries in the project).

You will be asked also to send to IF PAN a short report from the performed experiment and later a list of publications resulting from performed experiments together with the corresponding journal impact factors as well as a list of conference presentations, doctoral theses *etc*. Therefore, I am taking this opportunity to ask all of ESRF Polish users to remember regularly visit the webpage of the project and systematically inform us about all papers, doctoral theses and conference presentations with contribution of data collected at ESRF. The appropriate acknowledge of the project should be also explicitly exposed in the papers and conference presentations. Following this way and providing all necessary data is crucial for the further access to ESRF. Realization of project will be evaluated each year and only after positive evaluation the project be continued. Moreover, please distinguish between the ESRF access which is paid by Polish Ministry of Science and High Education and access to European national synchrotrons e.g. Elettra, Soleil, Alba, Bessy or Petra which is supported by the European project paid by the European Commission. Starting from May 2015, there is no such project but Calipso-plus was submitted in March 2016 after 2 year fight of the European Synchrotron Users Organization (ESUO) with the EC for opening the appropriate call.

I wish you all success in getting the beamtime.

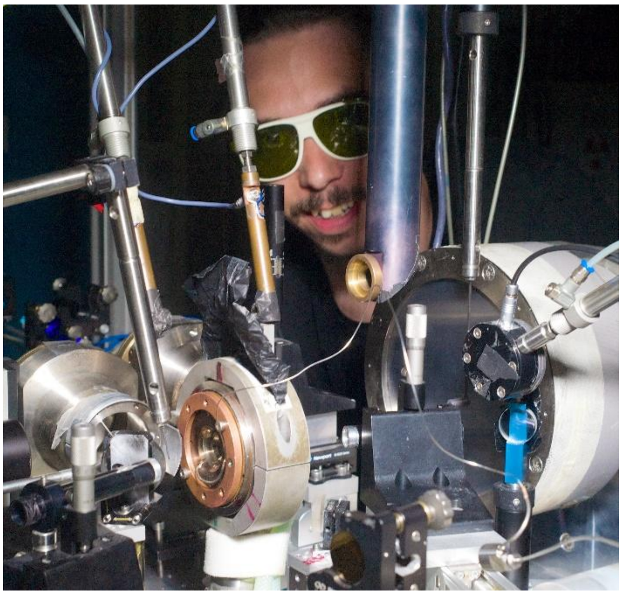

Figure 3. Experiment at one of ESRF beamlines (ID27). *(Credits ESRF/Blascha Faust)*

A-04 **News from European XFEL**

Bright Future for X-ray Science

W. Gawełda[1]* and R. Sobierajski[2]*

[1]*European XFEL GmbH, Holzkoppel 4, 22869 Schenefeld, Germany*
[2]*Institute of Physics Polish Academy of Sciences, Al. Lotników 32/46, 02-668 Warsaw, Poland*

Keywords: X-ray free-electron laser, femtosecond X-rays, self-amplified spontaneous emission (SASE)

*e-mail: wojciech.gawelda@xfel.eu, ryszard.sobierajski@ifpan.edu.pl

With the advent of X-ray free electron laser (XFEL) sources, entirely new scientific opportunities have become available across various fields of physics, chemistry and biology. One of the most unprecedented features is the ability to generate high-intensity X-ray pulses with durations well below 100 femtoseconds (1 fs=10^{-15} s). This property enables dynamical studies of light–matter interactions almost in any medium (from gaseous phase to complex strongly correlated solids, i.e. high-temperature superconductors, and biomolecules [1-2]) with temporal resolution down to the very fundamental timescales of atomic processes. Moreover, the unique properties of XFEL radiation enable a solution to the well-known radiation damage problem and to take the capture of snapshots of three-dimensional structures of nanometer-sized protein crystals before the ionization and electrostatic forces destroy the crystal [3]. The XFEL developments have led to emergence of new methods in structural biology, such as serial femtosecond crystallography [4]. In the near future, a new XFEL source will expand the research opportunities of the existing laboratories, i.e. Linac Coherent Light Source in Stanford, USA [5], and SACLA XFEL in Hyogo, Japan [6]. It will be the world's brightest source of ultrashort X-ray pulses: the European XFEL [7], a 3.4 km long X-ray laser facility in the Hamburg metropolitan area (Fig. 1). Due to its unprecedented photon beam properties (Table 1), the ultrashort and ultraintense flashes of X-rays generated by the European XFEL machine will enable researchers to map the atomic details of viruses, decipher the molecular compositions of cells, record three-dimensional images of the nanoworld, film chemical reactions and study processes such as those occurring deep inside planets.

Responsible for construction and operation is the European X-Ray Free-Electron Laser Facility GmbH, a limited liability non-profit company constituted under German law that was officially founded in 2009 in Hamburg, Germany [8].

Beam parameter	Value
Wavelength range [nm]	0.05–4.7
Photon flux/pulse	10^{11}–10^{13}
Peak brilliance [photons/s•mrad^2•mm^2•0.1% BW]	5x10^{33}
Number of pulses/second	27 000
Typical pulse widths [fs]	10–100

Table 1: Photon beam parameters of the European XFEL facility.

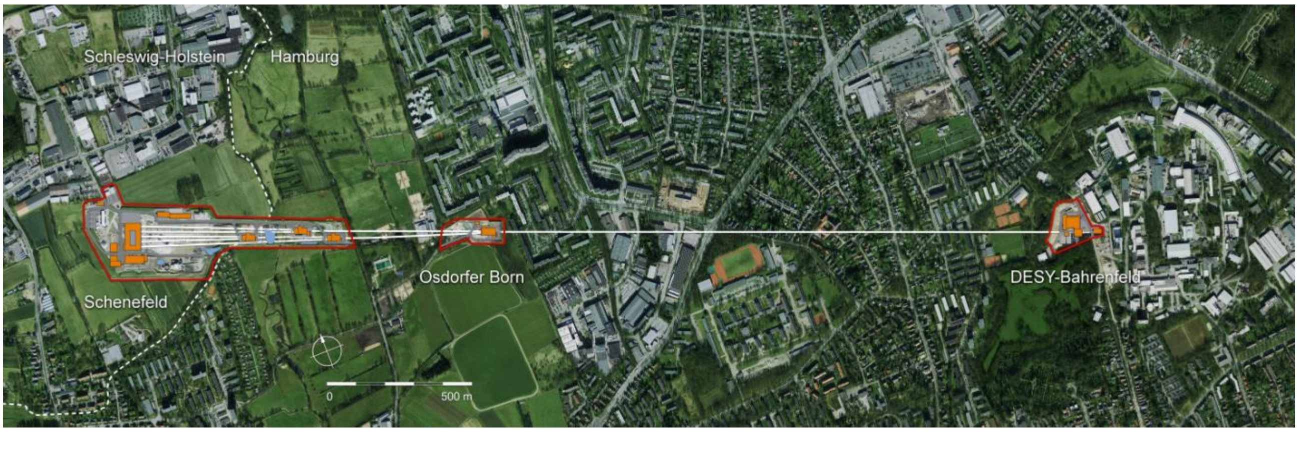

Figure 1. Aerial view of the European XFEL facility. The electron injector is located on the DESY campus in Hamburg, while the underground Experimental Hall hosting the scientific infrastructure dedicated to the user science program is located in nearby Schenefeld. Credit: European XFEL, aerial views: FHH, Landesbetrieb Geoinf. und Vermessung.

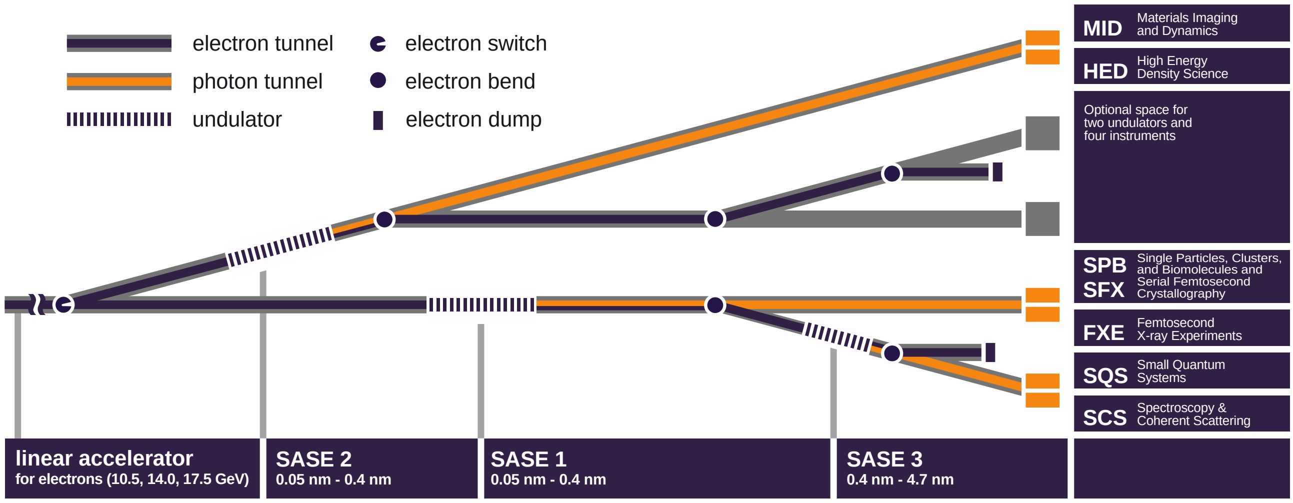

Figure 2: Schematic layout of the European XFEL facility, including the initial SASE undulators, the various beam distribution systems and the initial scientific instruments. Credit: European XFEL.

The construction work on the European XFEL started in 2009. The first electrons have been generated in the laser-driven electron gun, and commissioning of the injector started in late 2015. The installation of the main superconducting accelerator, provided through contributions by institutes from nearly all 11 partner countries, is in full swing and should be completed in late summer 2016. Soon afterwards, commissioning with electron beam will start at electron energies of 14–17.5 GeV. In early 2017, the electron beam and all undulator segments for the SASE1 XFEL source (Fig. 2), which is based on a principle of self-amplified spontaneous emission (SASE), will be ready for first generation of FEL radiation. The challenging X-ray optics and diagnostics components are currently being installed and prepared for commissioning. At the same time, the design of the initial six scientific instruments is largely complete, and the installation has started. The start of operation is foreseen in early summer 2017, which is when the first experiments on a scientific instrument will be performed. Shortly thereafter, the early first pilot user experiment program will start. Full performance of the accelerator, FEL radiation and scientific instruments will be reached in 2018. It is currently planned to increase the amount of accelerator operation dedicated to the user program from 1000 hours in 2017, to over 2000 hours in 2018, and to the final 4000 hours in 2019.

The European XFEL facility is being realized as a joint effort of many partners across Europe. Presently, 11 countries are participating in the European XFEL project: Denmark, France, Germany, Hungary, Italy, Poland, Russia, Slovakia, Spain, Sweden and Switzerland, while the UK will join the project in the near future. With its repetition rate of 27 000 pulses per second and a peak brilliance a billion times higher than that of the most conventional X-ray sources, the European XFEL will open up new research venues for scientists and industrial users across the world.

The new X-ray light generated by the European XFEL will provide unprecedented opportunities for Polish research groups. Poland has been part of the project from the very beginning and became one of the shareholders of the European XFEL GmbH with a 2% contribution, which includes both the construction and operation phases of the facility. The National Center for Nuclear Research (NCBJ) in Świerk has coordinated the Polish in-kind contributions realized during the construction phase of the machine. It also acts as the coordinator of a national consortium (XFEL-Polska), embracing various Polish universities and research institutions involved in this effort. Starting in 2017, Polish scientists can apply for user beamtime at any of the available scientific instruments [9]. It will be the role of a recently established User Office to coordinate the calls for user proposals (to be issued twice per year) and help the users to plan and carry out their proposed research while visiting the European XFEL facilities in Schenefeld. The entire beamtime application and travel arrangements will be provided digitally via a web-based portal called UPEX (User Portal for European XFEL).

The main criterion for obtaining beamtime for non-proprietary studies at the European XFEL will be the scientific excellence of the proposed research, which will be evaluated by panels of external experts. It is therefore extremely important to prepare and train the Polish scientific community, in particular the younger generation of Polish scientists, to enter this very competitive field of science and help them to exploit one of the most modern research tools in their scientific careers. In this context, it is essential to underline the efforts made by the existing consortium XFEL-Polska and its coordinator, NCBJ, to gather the interested research groups from all over Poland and support them in preparation and execution of scientific proposals at the European XFEL. We also point to the initiatives undertaken by the Polish Synchrotron Radiation Society (PTPS) in disseminating the scientific topics and research prospects that became available with the development of

XFEL sources. Each year, during either the National Symposium of Synchrotron Radiation Users (KSUPS) or the International Symposium and School on Synchrotron Radiation in Natural Science (ISSRNS), XFEL international and Polish researchers are invited to present their results to Polish scientific audience/community. The XFELs have also been remarkably present during the past 43rd Congress of Polish Physicists organized by the Polish Physical Society (PTF) in Kielce in September 2015. Last but not least, we would like to acknowledge our own effort, supported by European XFEL and Institute of Physics Polish Academy of Sciences via EAgLE grant, to organize meetings in Poland with XFEL scientists, in particular during the previous ISSRNS conference in 2014 and the Warsaw School on Science with FELs in 2015.

Further initiatives, beyond training activities, are needed in order for the new light sources to fully benefit the Polish scientific community. The XFEL science is a relatively young field, which still undergoes very rapid and constant development both on the technological and scientific sides and remains very competitive. This stems predominantly from a limited amount of beamtime provided by the only two hard X-ray XFELs currently operating worldwide. Writing competitive proposals requires the involved scientists to carry out detailed and thorough preparatory investigations and often engages them in large international collaborations that prepare jointly the experiments to be carried out at XFEL facilities.

It is therefore essential to gather now the potential Polish scientific users of the European XFEL and work jointly towards successful beamtime proposals and research activities in this field of science. Clearly, such initiatives can only become successful if dedicated funding can be provided. In that sense, the consortium XFEL-Polska, together with a number of Polish research institutes and universities, has commenced an effort to prepare a joint proposal to the Ministry of Science and Higher Education (MNiSzW) for financial support to Polish groups preparing for the operation phase of the European XFEL. Within this proposal, it is foreseen to focus the effort not only on preparatory research activities but also on training and educational aspects, which will allow preparation of younger generations of Polish scientists to take full advantage of this new light in the near future.

Acknowledgments: This work was supported by the European XFEL GmbH and EAGLE project (FP7-REGPOT-2012-2013-1, Project Number: 316014).

---

[1] W. Gawelda, J. Szlachetko and C. J. Milne, *X-Ray Spectroscopy at Free Electron Lasers*, (J. A. van Bokhoven and C. Lamberti, John Wiley & Sons, 2016), doi: 10.1002/9781118844243.ch22.

[2] C. Bostedt *et al.*, *Rev. Mod. Phys.* **88** (2016) 015007–59.

[3] R. Neutze, R. Wouts, D. van der Spoel, E. Weckert and J. Hajdu, *Nature* **406** (2000) 752–757.

[4] H. N. Chapman *et al.*, *Nature* **470** (2011) 73-77.

[5] P. Emma *et al.*, *Nature Photonics* **4** (2010) 641–647.

[6] H. Tanaka and M. Yabashi *et al.*, Nature Photonics **6** (2012) 540–544.

[7] M. Altarelli, *High Power Laser Science and Engineering* **3** (2015) e18.

[8] Official website of the European XFEL GmbH: http://www.xfel.eu/

[9] A summary of technical specifications of all scientific instruments to be available at the European XFEL: http://www.xfel.eu/events/users_meetings/2016_users_meeting

News

Synchrotron Light News

SOLARIS operational from 2017

In a few months the National Synchrotron Radiation Centre SOLARIS will be opened to the first users. This synchrotron light source was constructed in Krakow, Poland and the commissioning of the storage ring has started in May 2015. Currently both the efforts to improve the machine performance and steep progress towards the commissioning of the two experimental beamlines are realized.

Inauguration of MAX IV

On 21 June 2016 the first of the fourth generation of synchrotron light sources, namely MAX IV, will be opened in Lund. The biggest ever Swedish investment in research infrastructure is plan to host more than 2000 scientists from all over the world each year offering new opportunities for groundbreaking experiments in materials and life sciences.

SESAME – synchrotron light of unity in Middle East

In the heart of the Middle East, surrounded by political tensions and humanitarian disaster, scientists outdistance diplomats in efforts for stabilization and peace with SESAME – Synchrotron-Light for Experimental Science and Applications in the Middle East. In the project are involved countries such as: Bahrain, Cyprus, Egypt, Iran, Jordan, Pakistan, the Palestinian Authority, Turkey and Israel as well. Most member countries pay annual membership fees of some $500,000 each. This project also brings together European scientists, and it seeks to foster advanced research in the region and allow researchers to collaborate across the whole Middle East. The EU has by now contributed over €10 million for the construction of the facility. SESAME will be located in Jordan and is due to be commissioned in the middle of 2017 year.

Gregori Aminoff Prize 2016

The Royal Swedish Academy of Sciences has awarded the Gregori Aminoff Prize in crystallography 2016 to Professor Poul Nissen, Aarhus University, Denmark, and Professor Chikashi Toyoshima, University of Tokyo, Japan, “for their fundamental contributions to understanding the structural basis for ATP-driven translocation of ions across membranes”. The prize amount to in total 100.000SEK.

Innovation Award on Synchrotron Radiation 2015

The 2015 Innovation Award on Synchrotron Radiation has been given on December 10, 2015 in Berlin-Adlershof to Dr. Claudio Masciovecchio from the Elettra-Sincrotrone in Trieste. His work on "First transient grating experiment in the soft X-ray range at the FERMI free-electron laser by exploitation of the coherent and multi-wave nature of the four-wave mixing process" has impressively demonstrated the prospects of the worldwide first seeded free electron laser for soft X-rays FERMI. The Innovation Award on Synchrotron Radiation is sponsored by SPECS GmbH and BESTEC GmbH.

Kai Siegbahn Prize 2015

Giacomo Ghiringhelli from the Politecnico di Milano, Milan, Italy has been selected by an international committee of top researchers in the field of synchrotron radiation. Giacomo Ghiringhelli is being awarded the prize for his outstanding, innovative work in the experimental development and scientific exploitation of Resonant Inelastic X-ray Scattering in the soft X-ray regime as a new and key tool to understand magnetic and electronic excitations in highly correlated transition metal compounds. The award recognizes this incredible achievement with a cash prize, honoring Dr. Ghiringhelli with an award ceremony at Uppsala University.

Ernst Eckhard Koch Prize 2015

The Association of Friends of Helmholtz-Zentrum Berlin awarded during the Seventh Joint BER II and BESSY II User Meeting on 10 December 2015 the 25th Ernst Eckhard Koch Prize for outstanding doctoral theses in the field of research with synchrotron radiation. Dr. Robert Streubel was honored for his doctoral dissertation “Imaging Spin Textures on Curved Magnetic Surfaces” at Technische Universität Chemnitz that dealt with the investigation of three-dimensional magnetic structures by a new combination of X-ray absorption tomography and photoemission microscopy.

Spanish Synchrotron User Association Prize 2015

Prize to the best PhD thesis in Synchrotron Radiation awarded to Ignacio Martín-Fabiani. The board of directors of the AUSE (Spanish Synchrotron User Association) has awarded Dr. Ignacio Martín-Fabiani with the prize to the best PhD thesis 2015 for his dissertation on "Nanostructuring of Polymer Materials with controlled Morphology".

Helmholtz Prize 2015

For their high-precision measurements carried out at DESY’s free-electron laser FLASH, five research scientists from the Goethe University in Frankfurt am Main are to receive the Helmholtz Prize in Metrology. The team surrounding Reinhard Dörner used a special apparatus to study extremely weakly bound helium molecules. This excellent work is an outstanding example of high-precision metrology and demonstrates the enormous potential of free-electron laser. The Helmholtz Prize is endowed with 20,000 euros.

Infineum-Diamond Prize 2015

The Infineum-Diamond prize for innovative automotive research using synchrotron light has been awarded to Oxford University post-doctoral researcher, David Collins. Working in collaboration with BMW-MINI, David’s research looks at the ductility of sheet metal used in manufacturing. This research has the potential to create stronger, more streamlined and more geometrically complex steel structures.

IXAS Awards 2015

IXAS Awards were presented at XAFS16 conference in Karlsruhe. IXAS Young Scientist Awards, Dale Sayers Prize and Farrel Lytle Prize, have been granted to Narciso Souze-Neto (Brazilian Synchrotron Light Laboratory) and Amelie Juhin (French National Centre for Scientific Research, Paris), respectively. IXAS Outstanding Achievement Award, Ed Stern Prize, was presented to Majed Chergui (Ecole Polytechnique Federale de Lausanne) and Andrea Di Cicco (Università di Camerino).

ESRF Young Scientist of the Year 2016

The Young Scientist Award was presented to Andrew Cairns for his ground breaking studies of negative linear compressibility. The "Young Scientist of the Year" award is given every year by the Users Organisation for outstanding work done at the ESRF by a scientist 35 years of age or younger.

Carousel – synchrotron free time reading

24 hours at the X-ray factory

R. Van Noorden,
Nature **531**(7596) (2016) 564.

Reportage from visiting the ESRF synchrotron. *Nature* spent a day and a night at the European Synchrotron Radiation Facility to reveal the science that never sleeps.

Beamtime

P. Gambardella,
ETH MatBlatt **2015/1**, 4.

‘So what is beamtime?’ An attempt to answer this fundamental question has been published in the *Professoren Ecke* of the *Bulettin of Materials Division* of ETH Zurich. Must read par for anyone who wants to do synchrotron experiments.

Revealing letters in rolled Herculaneum papyri by X-ray phase-contrast imaging

V. Mocella, E. Brun, C. Ferrero, D. Delattre,
Nature communications **6** (2015) 5895.

The paper presents the opportunity to read the of Herculaneum papyrus rolls carbonized due to the eruption of Mount Vesuvius in 79 AD and belonging to the only library passed on from Antiquity. Due to carbonization, enrolling the rolls is impossible. The experimental readout method consists in X-ray phase-contrast imaging.

Mitigation strategies for radiation damage in the analysis of ancient materials

L. Bertrand, S. Schöeder, D. Anglos, M. B. Breese, K. Janssens, M. Moini, A. Simon,
TrAC Trends in Analytical Chemistry **66** (2015) 128-145.

A review of methodologies aiming for reducing the radiation damage when studying the Cultural heritage materials using the intense radiation sources.

Discovery and Structure Determination of an Unusual Sulfide Telluride through an Effective Combination of TEM and Synchrotron Microdiffraction

F. Fahrnbauer, T. Rosenthal, T. Schmutzler, G. Wagner, G. Vaughan, J. P. Wright, O. Oeckler,
Angewandte Chemie International Edition **54**(34) (2015) 10020-10023.

The authors report on the use of combined transmission electron microscopy and microfocused synchrotron in a study of a new sulfide telluride Pb8Sb8S15Te5 compound. The structure consists of chains of heterocubane-like units.

Handbook on Synchrotron Radiation: Vacuum Ultraviolet and Soft X-ray Processes

Marr, G. V. (Ed.) (Elsevier, 2013)

This valuable book focuses on the use of synchrotron radiation extending from about 10 eV to 3 keV photon energy.

X-Ray Absorption and X-Ray Emission Spectroscopy: Theory and Applications

J.A. van Bokhoven, C. Lamberti (Eds.) (Wiley, 2016)

Two-volume book features articles that explain the phenomena and describe examples of X–ray absorption and emission applications in chemistry, biochemistry, catalysis, amorphous and liquid systems, and surface science.

Hard X-ray Photoelectron Spectroscopy (HAXPES)

J.C. Woicik (Ed.) (Springer, 2016)

The first complete summary of the state of the art in HAXPES. Historical works, modern instrumentation, theory and applications, from physics to chemistry and materials science and engineering.

Combining In Situ Synchrotron X-Ray Diffraction and Absorption Techniques with Transmission Electron Microscopy to Study the Origin of Thermal Instability in Overcharged Cathode Materials for Lithium-Ion Batteries

K. W. Nam, S. M. Bak, E. Hu, X. Yu, Y. Zhou, X. Wang, L. Wu , Y. Zhu K-Y. Chung, X. Q. Yang,
Advanced Functional Materials, **23**(8) (2013) 1047-1063.

Thermal Instability in Overcharged Cathode Materials for Lithium- Ion Batteries is studied using combined experimental methods involving the synchrotron radiation.

Serial crystallography on in vivo grown microcrystals using synchrotron radiation

C. Gati, G. Bourenkov, M. Klinge, D. Rehders, F. Stellato, D. Oberthür,... & C.Betzel,
IUCrJ **1**(2) (2014) 87-94.

A strategy applicable in protein microcrystallography is presented. The strategy is found to be helpful in studies of micrometre size protein crystals.

Evidence for Degradation of the Chrome Yellows in Van Gogh's *Sunflowers*: A Study Using Noninvasive In Situ Methods and Synchrotron-Radiation-Based X-ray Techniques

L. Monico, K. Janssens, E. Hendriks, F. Vanmeert, G. Van der Snickt, M. Cotte, G. Falkenberg,, B. G. Brunetti, C. Miliani

Angewandte Chemie, **127**(47) (2015) 14129-14133

The study reveals definite changes in the least lightfast variety of the yellow pigments and thus opens questions about possible color alterations in this and other paintings. The authors stress the need for careful monitoring of paintings containing this pigments over time.

Subluminal Propagation of Narrow-band X-Ray Pulses

K.P. Heeg, J. Haber, D. Schumacher, L. Bocklage, H.-C. Wille, K.S. Schulze, R. Loetzsch, I. Uschmann, G.G. Paulus, R. Rüffer, R. Röhlsberger, and J. Evers

Physical Review Letters **114** (2015) 203601

X-ray beam has been made to travel 10,000 times slower than the speed of light by tuning the interaction of light with the nuclei of iron atoms. Controlling X-rays in this way could be useful for high-resolution imaging and other applications.

Revealing Complexity of Nanoparticle Synthesis in Solution by in Situ Hard X-ray Spectroscopy – Today and Beyond

D. Koziej

Chemistry of Materials **28**(8) (2016) 2478–2490

Perspective article within *Up-and-Coming* series presents how modern hard X-ray spectroscopic methods, far from merely providing new tools, are extending the way we study and understand synthesis of complex nanoparticles.

Spectroscopic Studies on Organic Matter from Triassic Reptile Bones, Upper Silesia, Poland

D. Surmik, A. Boczarowski, K. Balin, M. Dulski, J. Szade, B. Kremer, & R. Pawlicki

PloS one, **11**(3) (2016) e0151143

The authors report and discuss the unexpected discovery of molecular signals from proteins present in the blood vessels of triassic-reptile bones.

Interaction of bovine serum albumin (BSA) with novel gemini surfactants studied by synchrotron radiation scattering (SR-SAXS), circular dichroism (CD), and nuclear magnetic resonance (NMR)

W. Gospodarczyk, K. Szutkowski, & M. Kozak

J. Phys. Chem. B **118**(29) (2014) 8652-61

In this paper multiple synchrotron-based experimental techniques have been used in order to study an interaction of three dicationic (gemini) surfactants nad of their importance for the conformation of bovine serum albumin (BSA).

Three-dimensional visualization of fossil flowers, fruits, seeds, and other plant remains using synchrotron radiation X-ray tomographic microscopy (SRXTM): new insights into Cretaceous plant diversity

E.M. Friis, F. Marone, K.R. Pedersen, P.R. Crane, & M. Stampanoni,

Journal of Paleontology **88**(04) (2014) 684-701

The paper presents an application of synchrotron-radiation-based X-ray tomographic microscopy (SRXTM) to the study of mesofossils. The use of SRXTM is found to be essential for resolving critical structural details.

Determination of the electronic and structural configuration of coordination compounds by synchrotron-radiation techniques.

C. Garino, E. Borfecchia, R. Gobetto, J.A. van Bokhoven, & C. Lamberti,

Coordination Chemistry Reviews 277 (2014) 130-186

The authors present a survey of the potential of synchrotron radiation techniques applicable for understanding the structural and electronic properties of coordination compounds.

The most incompressible metal osmium at static pressures above 750 GPa

L. Dubrovinsky, N. Dubrovinskaia, E. Bykova, M. Bykov, V. Prakapenka, C. Prescher, K. Glazyrin, H.-P. Liermann, M. Hanfland, M. Ekholm, Q. Feng, L. V. Pourovskii, M. I. Katsnelson, J. M. Wills, and I. A. Abrikosov; *Nature* **525**(7568) (2015) 226-229.

An international team of scientists led by the University of Bayreuth has created the highest static pressure ever achieved in a lab. Using the double-stage diamond anvil cell the researchers investigated the behaviour of the metal osmium at pressures of up to 770 GPa, by about 130 GPa higher than the previous world record. The experiments were conducted on ID09A (ESRF), ECB (PETRA) and 13-IDD (APS).

Structural complexity of simple Fe_2O_3 at high pressures and temperatures

E. Bykova, L. Dubrovinsky, N. Dubrovinskaia, M. Bykov, C. McCammon, S.V. Ovsyannikov, H.-P. Liermann, I. Kupenko, A.I. Chumakov, R. Rüffer, M. Hanfland, V. Prakapenka *Nature communications* **7** (2016) 10661.

The authors used three synchrotron beamlines to conduct a systematic investigation of the behaviour of iron oxides at pressures over 100 GPa and temperatures above 2,500 K. They discovered some unusual mixed-valence iron oxides e.g. Fe_5O_7 and $Fe_{25}O_{32}$. The single-crystal X-ray diffraction experiments were conducted on ID09A (ESRF), 13-IDD (APS) and P02.2 (PETRA).

Future conferences & workshops

KSUPS'17

12th National Meeting of Synchrotron Radiation Users

Gdańsk (Poland), 4-7 September 2017

http://www.synchrotron.org.pl/

VUVX2016
39th International conference on Vacuum Ultraviolet and X-ray Physics
Zurich (Switzerland), 3-8 July 2016
www.psi.ch/vuvx2016

IWORID 2016
18th International Workshop on Radiation Imaging Detectors
Barcelona (Spain), 3-7 July 2016
iworid2016.com

SFR 2016
Synchrotron and Free electron laser Radiation: generation and application
Novosibirsk (Russia), 4-8 July 2016
indico.inp.nsk.su/event/3/

ICSXNS16
International Conference on Surface X-ray and Neutron Scattering
Stony Brook (USA), 10-14 July 2016
www.bnl.gov/sxns14/

ISSCG-16
16th International Summer School on Crystal Growth
Lake Biwa (Japan), 1-7 August 2016
www.iccge18.jp/isscg16/

ICCGE-18
18th International Conference on Crystal Growth and Epitaxy
Nagoya (Japan), 7-12 August 2016
iccge18.jp

XRM 2016
X-Ray Microscopy Conference 2016
Oxford (UK), 15-19 August 2016
xrm2016.com

BSR16
12th International Conference on Biology and Synchrotron Radiation
Stanford (USA), 21- 24 August 2016
conf-slac.stanford.edu/bsr-2016/

ECM-30
30th Meeting of the European Crystallographic Association
Basel (Switzerland), 28 August – 1 September 2016
ecm30.ecanews.org

SMARTER 5
Fifth Structure elucidation by combining Magnetic Resonance, Computational Modelling and Diffraction
Bayreuth (Germany), 4-8 September 2016
www.smarter5.uni-bayreuth.de

EHPRG -54
The 54th European High Pressure Research Group International Meeting on High Pressure Science and Technology
Bayreuth (Germany), 4-9 September 2016
ehprg2016.org

CMD26
EPS Condensed Matter Division Conference
Colloquium on X-ray spectroscopy of correlated oxides
Groningen (Holland), 4-9 September 2016
cmd26.eu

IBIC 2016
International Beam Instrumentation Conference
Barcelona (Spain), 11-15 September 2016
ibic2016.org

Fifteenth Ukrainian — Polish Symposium on Theoretical and Experimental Studies of Interface Phenomena and their Technological Applications
simultaneously with
Second NANOBIOMAT Conference Nanostructured Biocompatible/Bioactive Materials
Lviv (Ukraine), 12-15 September 2016
www.thomascat.info/Symposium.htm

ISMC2016
The 4th International Soft Matter Conference
Grenoble (France), 12-16 September 2016
ismc2016.org

2016 E-MRS Fall Meeting
European Materials Research Society Fall Meeting (Symposia A - Z, ZU)
Functional Oxides – Synthesis, Structure, Properties and Applications (Symposium Z)
Warsaw (Poland), 19-22 September 2016
www.european-mrs.com/meetings/2016-fall

Debye-Rietveld celebration
Amsterdam (Holland), 22 September 2016
debye-rietveld.nl

The regional ICDD Grant meeting
Lviv (Ukraine) 23-24 September 2016
Contact information: ihor.zavaliy@gmail.com

ECS3
3rd European Crystallography School
Bol (Croatia), 25 September – 2 October 2016
ecs3.ecanews.org

PCCr1
First Pan-African Conference in Crystallography
Dschang (Cameroun), 6-11 October 2016
pccr1-2016.univ-dschang.org

ICPSCG10
International Conference of Polish Society for Crystal Growth
Zakopane (Poland) 16-21 October 2016
icpscg10.pl

OMEE-2017
International Conference on Oxide Materials for Electronic Engineering will be held at Lviv Polytechnic National University (Lviv, Ukraine) on May 29 – Jun 02, 2017. Details will be available soon at http://science.lp.edu.ua/omee-2017, Contact information: crystal@lp.edu.ua

Gordon Research Conference on X-Ray Science
Easton (USA), 30 July – 4 August 2017
www.grc.org/programs.aspx?id=12236

EHPRG -55
55th European High Pressure Research Group Meeting on High Pressure Science and Technology
Poznan (Poland), 3-8 September 2017
www.ehprg.org/meetings.php

IUCR 2017
XXIV Congress & General Assembly of the International Union of Crystallography
Hyderabad (India), 21-28 August 2017
iucr2017.org

SRI2018
13th International Conference on Synchrotron Radiation Instrumentation
Taipei (Taiwan), 11-15 June 2018
www.nsrrc.org.tw/SRI_2018

XAFS18
17th International Conference on X-ray Absorption Fine Structure
Cracow (Poland), 22-27 July 2018
xafs2018.com

Find more at:
www.lightsources.org/events

Synchrotron classifieds

The webpage of PTPS (synchrotron.org.pl) was largely modified. The new structure enables easier navigation among the features. In particular we offer a space for PhD and PostDoc
(http://www.synchrotron.org.pl/index.php/en/announcements/phd-studies-in-synchrotron-science)
and other job position advertisements
(http://www.synchrotron.org.pl/index.php/en/announcements/job-opportunities).
Offers from Polish universities and research institutions are particularly welcome.

XII Krajowe Sympozjum
Użytkowników Promieniowania Synchrotronowego (KSUPS'17)
4-7 września 2017, Gdańsk

Organizatorzy
Polskie Towarzystwo Promieniowania Synchrotronowego
oraz
Wydział Fizyki Technicznej i Matematyki Stosowanej Politechniki Gdańskiej

KSUPS jest odbywającą się w cyklu dwuletnim krajową konferencją dedykowaną przeglądowi aktualnych osiągnięć naukowych, technologicznych oraz trendów rozwojowych z zakresu badań wykorzystujących promieniowanie synchrotronowe polskiego środowiska badawczego. Kolejna, już dwunasta, odsłona konferencji po raz pierwszy będzie miała miejsce w Gdańsku. Niezwykłe położenie, typowy dla miast hanzeatyckich styl w architekturze i ponad tysiącletnia historia Gdańska sprawiają, że jest to wyjątkowe i wyraziste miasto, które warto odwiedzić. Zwłaszcza, że będąc światową stolicą bursztynu jest niewątpliwą atrakcją turystyczną. Współczesny Gdańsk to również prężnie rozwijające się pomorskie centrum kultury, sportu i nauki, w którym Politechnika Gdańska, uczelnia techniczna łącząca nowoczesność z ponad stuletnią tradycją, pełni szczególną rolę. Dlatego też na KSUPS'17 zapraszamy na Wydział Fizyki Technicznej i Matematyki Stosowanej Politechniki Gdańskiej. Atmosfera miasta i uczelni na pewno będą sprzyjać wymianie wiedzy i doświadczeń, będą stymulować do ciekawych dyskusji naukowych oraz inspirować do podejmowania nowych wyzwań badawczych.

W trakcie KSUPS'17 planowane są sesje z plenarnymi wykładami zaproszonych naukowców, komunikatami ustnymi, sesje plakatowe oraz panele dyskusyjne. Tematyka Sympozjum skupiać się będzie głównie na:

- synchrotronowych i alternatywnych źródłach promieniowania
- spektroskopii emisyjnej i absorpcyjnej
- spektroskopii fotoelektronowej
- rozpraszaniu i dyfrakcji promieniowania synchrotronowego
- rentgenowskim dichroizmie magnetycznym
- badaniach materiałowych z wykorzystaniem promieniowania synchrotronowego
- zastosowaniu promieniowania synchrotronowego w nanotechnologii
- badaniach in situ z wykorzystaniem promieniowania synchrotronowego
- zastosowaniu promieniowania synchrotronowego w badaniach medycznych i biologicznych
- krystalografii białek
- badaniach strukturalnych polimerów.

Bardzo serdecznie zapraszamy do udziału w KSUPS'17. Będzie to wyjątkowa okazja do aktywizacji i integracji polskiego środowiska użytkowników promieniowania synchrotronowego. Nikt nie powinien jej przegapić.

Informacje i kontakt:
Agnieszka Witkowska
WFTiMS, Politechnika Gdańska
ul. Narutowicza 11/12, 80-233 Gdańsk
agnieszka@mif.pg.gda.pl, tel. (+48 58) 348 66 0

Presenting Author's Index